For Reference

NOT TO BE TAKEN FROM THIS ROOM

Ex libris
Universitatis
Albertaensis

QUAECUMQUE VERA

Digitized by the Internet Archive
in 2022 with funding from
University of Alberta Library

https://archive.org/details/Green1983

THE UNIVERSITY OF ALBERTA

REACTIONS OF SULFUR ATOMS WITH 1,2-BUTADIENE, DIMETHYLSULFIDE AND THIETANE

by

© MARTINA GREEN

A THESIS

SUBMITTED TO THE FACULTY OF GRADUATE STUDIES AND RESEARCH
IN PARTIAL FULFILMENT OF THE REQUIREMENTS FOR THE DEGREE
OF DOCTOR OF PHILOSOPHY

IN

CHEMISTRY

DEPARTMENT OF CHEMISTRY

EDMONTON, ALBERTA

SPRING, 1983

To Kirk

ABSTRACT

$S(^1D_2)$ atoms, generated by the gas phase photolysis of COS (λ>240 nm), react with 1,2-butadiene to yield three unsaturated thiiranes and two doubly unsaturated thiols, which have not been previously characterized. The thiiranes, products of 2,3 and cis and trans 1,2-additions, constitute the bulk of the products. The extrapolated zero time thiirane yields indicate that 2,3-addition is slightly preferred, $k_{2,3}/k_{1,2} \sim 1.3$, and that for 1,2-addition, the trans product is favoured over the cis by a factor of $\sim$1.4

The thiols are minor products. One results from direct insertion into the methyl C-H bonds, and the other, 1,3-butadiene-2-thiol, is postulated to arise indirectly from insertion into the C-H bond of the alkyl-substituted vinylic carbon.

The $S(^3P) + 1,2\text{-}C_4H_6$ reaction affords only the thiiranes, and a higher selectivity is observed, $k_{2,3}/k_{1,2} \sim 2$. The 1,2-addition features a surprisingly high trans/cis product ratio of $\sim$ 6.

Rate parameters for the $S(^3P) + 1,2\text{-}C_4H_6$ reaction were determined in competition with the $S(^3P) + 1\text{-}C_4H_8$ reaction. The former reaction exhibits a relatively high A factor and activation energy, with the 2,3 and 1,2-additions having similar E_a's. Accordingly,

$$k_{2,3} = (2.96\pm0.80) \times 10^{10}\exp[-(1455\pm225)/RT]\ M^{-1}s^{-1}$$

$$k_{1,2} = (1.41\pm0.38) \times 10^{10}\exp[-(1455\pm225)/RT]\ M^{-1}s^{-1}$$

The reactions of $S(^1D_2,{}^3P)$ with CH_3SCH_3 and $\overline{\mathrm{CH_2(CH_2)_2S}}$ yield the corresponding disulfides as the only S addition products. In the $S(^1D_2)$ + CH_3SCH_3 reaction, CH_3SSCH_3 and small amounts of C_2H_6 are produced in low overall yields, less than 30% in terms of the sulfur atoms consumed, and large quantities of elemental sulfur are formed. In contrast, the $S(^1D_2)$ + $\overline{\mathrm{CH_2(CH_2)_2S}}$ reaction affords similar amounts of 1,2-dithiolane ($\overline{\mathrm{CH_2(CH_2)_2SS}}$) and C_2H_4 in high yields, up to ~85%. With CH_3SCH_3, the $S(^3P)$ reaction results in a substantial decrease in the CH_3SSCH_3 and C_2H_6 yields, while with $\overline{\mathrm{CH_2(CH_2)_2S}}$, only the C_2H_4 yield is reduced.

Based on the observed products, and the effects of pressure and added gases, it is proposed that for both thioethers, the sole primary reaction is attack by S atoms on the non-bonding p orbitals of the sulfur site to form an unstable excited thiosulfoxide adduct. This adduct then undergoes isomerization yielding the corresponding disulfide, fragmentation leading to hydrocarbon products or deactivation to the ground state.Bimolecular reaction between two ground state thiosulfoxide molecules leads to regeneration of the substrate. Deactivation is the major process for both S_0 and T_1 dimethylthiosulfoxides, but appears to be important only for the T_1 thietanethiosulfoxide.

The rate parameters for the reactions of $S(^3P)$ atoms with CH_3SCH_3 and $\overline{\mathrm{CH_2(CH_2)_2S}}$ have been measured in competition with the $S(^3P)$ + C_3H_6 reaction:

$$k_{CH_3SCH_3} = (3.19 \pm 1.21) \times 10^{10} \exp[(900 \pm 237)/RT]\ M^{-1}s^{-1}$$

$$k_{\overline{CH_2(CH_2)_2S}} = (5.23 \pm 1.94) \times 10^{10} \exp[(810 \pm 220)/RT]\ M^{-1}s^{-1}$$

Both reactions feature large A factors and negative activation energies. Consequently, they proceed at extremely high rates, having room temperature rate constants approaching the collision frequencies.

It has also been shown that $S(^3P)$ atoms are not produced in the $\lambda > 240$ nm photolysis of thiirane. Additionally, it has been demonstrated that the role of CO_2 in effecting a decrease in the CO yield in the $\lambda > 240$ nm photolysis of COS is to act as a chaperon for the recombination of $S(^3P)$ atoms.

ACKNOWLEDGMENTS

The author wishes to express her sincere appreciation to Professor O. P. Strausz for his supervision, constant support and patience throughout the course of this investigation.

I am especially indebted to Dr. F. C. James, whose enthusiam, invaluable advice and unceasing encouragement have made this work possible.

The author is grateful to Dr. E. M. Lown for her many suggestions and guidance in this study and her assistance in the preparation of this manuscript.

It is a pleasure to thank the members of the Photochemistry group, particularly Dr. I. Safarik for his patient and illuminating instructional assistance, Drs. M. Torres and R. K. Gosavi for their helpful discussions and Mr. A. Jodhan for his technical advice and assistance. My special appreciation is extended to Mr. A. Clement, whose humorous and cheerful demeanor has lightened those tense and frustrating moments in research.

The generosity of Dr. B. Verkoczy in sharing his research experience is also greatly appreciated.

The author thankfully acknowledges the cooperation and efficient service provided by the technical staff of the Chemistry Department, especially Messrs. J. Olekszyk, E. Feschuk, G. Streefkerk, T. Van Esch and H. Hofmann.

I am also grateful to Mrs. L. Eastman and Ms. A. Morris

for their kindness and generous assistance during the typing of this thesis.

My special thanks go to Professor J.R. Bolton for inspiring my interest in research.

Finally, the author wishes to express her profound gratitude to her husband, Kirk, who in spite of the difficult times, remained devoted and provided moral support to the end.

TABLE OF CONTENTS

PAGE

ABSTRACT.. v

ACKNOWLEDGMENTS... viii

LIST OF TABLES.. xiv

LIST OF FIGURES... xvii

CHAPTER I: INTRODUCTION................................... 1

A. Spectroscopic States of Group VI A Atoms........ 2

B. Sources of Sulfur Atoms.......................... 2

C. Reactions of Group VI A Atoms with Hydrocarbons. 9

1) Reactions of S and O Atoms..................... 9

(a) with alkanes................................. 9

(i) S($^1D_2$, ^3P) Atoms..................... 9

(ii) O($^1D_2$, ^3P) Atoms.................... 11

(b) with alkenes................................. 13

(i) S($^1D_2$) and O($^1D_2$) Atoms............. 13

(ii) S(^3P) and O(^3P) Atoms................ 16

(c) with alkynes................................. 24

(i) S($^1D_2$) and O($^1D_2$) Atoms............. 24

(ii) S(^3P) and O(^3P) Atoms................ 27

2) Reactions of Se Atoms.......................... 28

3) Reactions of Te Atoms.......................... 29

D. Reactions of S and O Atoms with Polyunsaturated Hydrocarbons..................................... 29

1) with aromatics................................. 29

(a) S($^1D_2$, ^3P) Atoms...................... 29

(b) $O(^1D_2, ^3P)$ Atoms.......................... 30

2) with dienes................................ 32

(a) $S(^1D_2, ^3P)$ Atoms......................... 32

(b) $O(^1D_2, ^3P)$ Atoms......................... 34

E. Reactions of S and O Atoms with Carbonylsulfide and Thioethers.......................... 37

1) Reactions with COS......................... 37

(a) $S(^1D_2, ^3P)$ Atoms......................... 37

(b) $O(^1D_2, ^3P)$ Atoms......................... 38

2) Reactions with Cyclic Thioethers........... 39

(a) $S(^1D_2, ^3P)$ Atoms......................... 39

(b) $O(^1D_2, ^3P)$ Atoms......................... 39

3) Reactions wtih Acyclic Thioethers.......... 41

(a) $S(^1D_2, ^3P)$ Atoms......................... 41

(b) $O(^1D_2, ^3P)$ Atoms......................... 41

F. Aim of the Present Investigation............... 44

CHAPTER II: EXPERIMENTAL.............................. 48

A. The High Vacuum System......................... 48

B. Photolytic Assembly............................ 50

C. Materials and Purification..................... 51

D. Analytical Techniques.......................... 53

E. Operating Procedures........................... 60

F. Microwave Discharge Experiments for the $COS - CH_3SCH_3$ System............................ 62

CHAPTER III: REACTIONS OF SULFUR ATOMS WITH 1,2-BUTADIENE............................ 63

A. Results.................................. 63
1) Reaction Products.......................... 63
(a) Identifications........................ 65
(b) Properties............................. 87
2) Effects of Exposure Time, Total Pressure and Added CO_2 on Product Yields............. 91
3) Relative Rate Parameters................... 95
B. Discussion................................. 109

CHAPTER IV: REACTIONS OF SULFUR ATOMS WITH ACYCLIC AND CYCLIC THIOETHERS

CHAPTER IV: REACTIONS OF SULFUR ATOMS WITH ACYCLIC AND CYCLIC THIOETHERS...................... 142
A. Results.................................. 142
1) $S(^1D_2, ^3P)$ + Dimethylsulfide - An Acyclic Thioether................................. 142
(a) UV Absorption of Dimethylsulfide........ 142
(b) Reaction Products....................... 142
(c) Effects of Exposure Time, Total Pressure and Added CO_2 and NO in the COS - CH_3SCH_3 System............................ 146
(d) Relative Rate Parameters................ 152
2) $S(^1D_2, ^3P)$ + Thietane - A Cyclic Thioether.. 161
(a) UV Absorption of Thietane.............. 161
(b) Reaction Products....................... 163
(i) Identifications..................... 163
(ii) Properties of 1,2-Dithiolane....... 166
(c) Effects of Exposure Time, Total Pressure and Added CO_2 in the COS - Thietane System................................ 168

(d) Relative Rate Parameters.............. 171

B. Discussion.............................. 177

1) $S(^1D_2,^3P) + CH_3SCH_3$ Reactions............... 186

2) $S(^1D_2,^3P) + \overline{CH_2(CH_2)_2S}$ Reactions............ 207

3) Rate Parameters for $S(^3P) + CH_3SCH_3$/ $\overline{CH_2(CH_2)_2S}$ Reactions......................... 217

CHAPTER V: SUMMARY AND CONCLUSIONS.................... 227

BIBLIOGRAPHY...................................... 236

APPENDIX

A 1. Mass Spectral Data of the C_4H_6S Isomers....... 250

2. Mass Spectral Data of $C_3H_6S_2$................. 251

B Calculations of the Nuclear Overhauser Effect (nOe) for cis and trans Ethylidenethiirane.... 252

C 1. Estimation of the Ratios, $k_{2,3}/k_{1,2}$ at t=0, P=1200 and 250 torr, and trans $(\underset{\sim}{4})$/cis $(\underset{\sim}{3})$ at t=0, P=1200 torr for $S(^1D_2)$ Addition to 1,2-C_4H_6................................ 256

2. Estimations of the % Recovery of Disulfides and the Deactivation/Isomerization Ratio for $S(^1D_2)$ and $S(^3P)$ Addition to CH_3SCH_3 and $\overline{CH_2(CH_2)_2S}$................................ 262

D The Role of CO_2 in the COS-CO_2 System......... 268

E The Intermediacy of $S(^3P)$ Atoms in the Photolysis of Thiirane......................... 271

LIST OF TABLES

TABLE PAGE

I-1 Energy levels of the atoms of the group VI A elements.......... 3

I-2 Sources of S atoms.......... 5

I-3 Rate constants and Arrhenius parameters for $S(^3P)$ and $O(^3P)$ atom reactions with alkenes.......... 19

II-1 Columns used.......... 54

II-2 GC operating conditions and retention times.......... 55

III-1 Calculated and observed nOe for the *cis* and *trans* isomers of ethylidenethiirane.......... 81

III-2 Effect of exposure time on the product yields in the COS-1,2-C_4H_6 system.......... 92

III-3 Effect of total pressure on product yields in the COS-1,2-C_4H_6 system.......... 96

III-4 Effect of added CO_2 on the distribution of 1,2-C_4H_6S isomers.......... 98

III-5 Product yields as a function of the [1,2-C_4H_6]/[1-C_4H_8] ratio at 300 K.......... 101

III-6 Product yields as a function of the [1,2-C_4H_6]/[1-C_4H_8] ratio at 333 K.......... 102

III-7 Product yields as a function of the [1,2-C_4H_6]/[1-C_4H_8] ratio at 363 K.......... 103

III-8 Product yields as a function of the [1,2-C_6H_6]/[1-C_4H_8] ratio at 393 K.......... 104

III-9 Product yields as a function of the [1,2-C_4H_6]/[1-C_4H_8] ratio at 423 K.......... 105

III-10 Slopes and intercepts of the plots in figure III-16.................................... 107
III-11 Product distributions for the COS-alkene systems. 118
III-12 Atom and radical reactions with terminal allenes.. 130
III-13 Arrhenius parameters for $S(^3P)$, $O(^3P)$ and $OH(^2\Pi)$ in reactions with alkenes and dienes...... 133
III-14 Effect of temperature on the yields of 2,3 and 1,2 - $S(^3P)$ addition products................ 139
IV-1 Effect of exposure time on the product yields in the $COS-CH_3SCH_3$ system........................ 144
IV-2 Effect of total pressure on the rate of product formation in the $COS-CH_3SCH_3$ system.............. 149
IV-3 Effect of added CO_2 and NO on product formation in the $COS-CH_3SCH_3$ system........................ 151
IV-4 Product yields as a function of the $[CH_3SCH_3]/[C_3H_6]$ ratio at 300 K.................. 153
IV-5 Product yields as a function of the $[CH_3SCH_3]/[C_3H_6]$ ratio at 330 K.................. 154
IV-6 Product yields as a function of the $[CH_3SCH_3]/[C_3H_6]$ ratio at 360 K.................. 155
IV-7 Product yields as a function of the $[CH_3SCH_3]/[C_3H_6]$ ratio at 392 K.................. 156
IV-8 Product yields as a function of the $[CH_3SCH_3]/[C_3H_6]$ ratio at 423 K...................157
IV-9 Slopes and intercepts of the plots in figure IV-4..159
IV-10 Effect of exposure time on product formation

in the COS-$\overline{CH_2(CH_2)_2S}$ system.................. 169

IV-11 Effect of total pressure on product yields in the COS-$\overline{CH_2(CH_2)_2S}$ system...................... 173

IV-12 Effect of CO_2 pressure on product yields in the COS-$\overline{CH_2(CH_2)_2S}$ system...................... 175

IV-13 Product yields as a function of the [$\overline{CH_2(CH_2)_2S}$]/[C_3H_6] ratio at 303 K............. 178

I -14 Product yields as a function of the [$\overline{CH_2(CH_2)_2S}$]/[C_3H_6] ratio at 333 K............. 179

IV-15 Product yields as a function of the [$\overline{CH_2(CH_2)_2S}$]/[C_3H_6] ratio at 363 K............. 180

IV-16 Product yields as a function of the [$\overline{CH_2(CH_2)_2S}$]/[C_3H_6] ratio at 393 K............. 181

IV-17 Product yields as a function of the [$\overline{CH_2(CH_2)_2S}$]/[C_3H_6] ratio at 423 K............. 182

IV-18 Slopes and intercepts of the plots in figure IV-13................................... 184

IV-19 Rate parameters for the reactions of some atomic and radical species wtih CH_3SCH_3 and $\overline{CH_2(CH_2)_2S}$.............................. 225

LIST OF FIGURES

FIGURE PAGE

I-1 Ionization potential *versus* E_a for the addition of S(^{3}P) atoms to alkenes.................... 20

II-1 The high vacuum system........................... 49

III-1 Mass (m/e) = 86 cross scan.......................... 64

III-2 NMR spectrum of 2-methyl-3-methylenethiirane (1).. 66

III-3 The gas phase FTIR spectrum of 2-methyl-3-methylenethiirane (1) 69

III-4 NMR spectrum of 1,3-butadiene-2-thiol (2)........ 71

III-5 NMR spectrum of *cis* ethylidenethiirane (3)....... 74

III-6 NMR spectrum of *trans* ethylidenethiirane (4)..... 76

III-7 The gas phase FTIR spectrum of *trans* ethylidenethiirane (4)........................... 82

III-8 NMR spectrum of 2,3-butadiene-1-thiol (5)....... 84

III-9 The gas phase FTIR spectrum of 2,3-butadiene-1-thiol (5)....................... 86

III-10 The gas phase UV spectrum of 2-methyl-3-methylenethiirane (1) at low and high concentrations................................ 88

III-11 The gas phase UV spectrum of *trans* ethylidenethiirane (4) at low and high concentrations...... 89

III-12 The gas phase UV spectrum of 2,3-butadiene-1-thiol (5).................................. 90

III-13 S product yields as a function of CO in the COS - 1,2-C_4H_6 system............................ 93

III-14 Rates of S product formation *versus* CO yield

in COS - 1,2-C_4H_6 system.......................... 94

III-15 Rates of S product formation *versus* total pressure in the COS - 1,2-C_4H_6 system.......... 97

III-16 Plots of $(A_o-A)/A$ *versus* [1,2-C_4H_6]/[1-C_4H_8]... 106

III-17 Arrhenius plot for the $S(^3P)$ + 1,2-C_4H_6 and 1-C_4H_8 system.................................. 108

III-18 Plots of E_a *versus* ionization potential for the $S(^3P)$ + alkenes, alkynes and diene systems, and $O(^3P)$ + alkenes................................ 137

IV-1 Product yields as function of CO yield in the COS-CH_3SCH_3 system............................. 147

IV-2 Rates of product formation *versus* CO yield in the COS-CH_3SCH_3 system......................... 148

IV-3 Rates of product formation *versus* total pressure in the COS-CH_3SCH_3 system............. 150

IV-4 Plots of $(A_o-A)/A$ *versus* $[CH_3SCH_3]/[C_3H_6]$...... 158

IV-5 Arrhenius plot for the $S(^3P)$ + CH_3SCH_3 and C_3H_6 system.................................... 160

IV-6 Absorption spectra of COS, $\overline{CH_2(CH_2)_2S}$ and 1 mm Vycor 791 + 240 nm interference filters... 162

IV-7 NMR spectrum of $\overline{CH_2(CH_2)_2SS}$.................... 164

IV-8 Comparison NMR spectra of $\overline{CH_2(CH_2)_2S}$, $\overline{CH_2(CH_2)_2SS}$ and $\overline{CH_2(CH_2)_3S}$.................... 167

IV-9 Product yields as a function of CO in the COS-$\overline{CH_2(CH_2)_2S}$ system......................... 170

IV-10 Rates of product formation *versus* CO yield in the COS-$\overline{CH_2(CH_2)_2S}$ system.................. 172

IV-11 Rates of product formation *versus* total pressure in the COS-$\overline{CH_2(CH_2)_2S}$ system.......... 174

IV-12 Product yields as a function of CO_2 pressure... 176

IV-13 Plots of $(A_o-A)/A$ *versus* $[\overline{CH_2(CH_2)_2S}]/[C_3H_6]$... 183

IV-14 Arrhenius plot for the $S(^3P)$ + $\overline{CH_2(CH_2)_2S}$ and C_3H_6 system.................................. 185

IV-15 Plots of E_a *versus* ionization potential for $S(^3P)$ + alkenes, $\overline{CH_2(CH_2)_2S}$ and CH_3SCH_3........ 221

CHAPTER 1

INTRODUCTION

Over the past two decades, the chemistry of divalent atoms, particularly the Group VI A atoms, has been the subject of increasing interest. This trend can be explained by several factors:

Air pollution, especially in industrial regions , has become a matter of increasing concern. Oxygen atoms play an important role in atmospheric chemistry, and thus their reactions, especially those with common pollutants such as hydrocarbons and organosulfides, have received considerable attention. The great similarity in the chemistry of atomic sulfur and oxygen has motivated interest in S atom reactions.

Prior to the discovery of negative activation energies in the reactions of Group VI A atoms with branched alkenes in the 1970's, all addition reactions were thought to proceed with positive activation energies or with no temperature dependence in the high pressure region. Due to this finding, these reactions have attracted additional interest from the kinetic and mechanistic point of view.

Finally, divalent atoms are the simplest divalent species. Thus, the reactions of these atoms can also be used to elucidate the reaction mechanisms of other divalent chemical reagents such as carbenes and nitrenes.

Before discussing the reactions of atomic S and O, let us first review the spectroscopic states of the group VI A atoms.

A. Spectroscopic States of Group VI A Atoms

Atoms of this group have two unpaired valence electrons. This allows the possibility of at least two low lying electronic states with different multiplicities and energies. If the electron spin vectors are antiparallel, the electronic state is designated a singlet; if the spin vectors are parallel, then a triplet state results, with three components lying close in energy. The electronic configuration of these atoms is ns^2p^4 , thus giving rise to five spectroscopic states, which are designated as $^3P_{2,1,0}$, $^1D_2$ and $^1S_0$. The energy spacing of these states is shown in Table I-1.[1] $^3P_2$ is the ground state, and for O and S atoms, this state lies very close in energy to the other triplet components, $^3P_0$ and $^3P_1$. These small energy differences are usually not observable by chemical means, and so for convenience the ground state is simply designated as ^3P. $^1D_2$ and $^1S_0$ are the first and second excited states, respectively. Both are metastable, with transitions to the ground state being forbidden by rigid selection rules. Consequently, they both have long lifetimes with respect to radiative decay.

B. Sources of Sulfur Atoms

Since the present study is concerned with the reactions of S atoms, it is desirable to give a brief review of the methods of generation of these species. A good source compound must:

TABLE I-1

Energy Levels of the Atoms of the Group VI A Elements[1].

Term	Energy (kcal/mole)			
	O	S	Se	Te
$^3P_2$	0	0	0	0
$^3P_1$	0.45	1.14	5.69	13.5
$^3P_0$	0.65	1.64	7.25	13.6
$^1D_2$	45.4	26.4	27.4	30.2
$^1S_0$	96.6	63.4	64.2	66.3

1) absorb in a convenient region of the spectrum
2) be readily available in a stable form
3) produce sulfur atoms in clearly defined spectroscopic states

Moreover, the remaining photofragments should be inert under the reaction conditions.

The currently available kinetically and synthetically useful sources of S atoms are all based on photochemical processes. A summary of these is given in Table I-2, and only the most often employed source, the photolysis of carbonyl sulfide (COS), will be discussed here in some detail.

COS is a gas, readily available in high purity. Its absorption spectrum has been reported to feature three distinct transitions.[9,26] The first long wavelength UV absorption band of COS, which shows superimposed vibrational structure , extends from ca. 260 nm to the vacuum region (180 nm), and has a rather low absorption coefficient ($\varepsilon_{max} \simeq 80$ l mole^{-1}cm^{-1}, λ_{max}=224 nm).[7] Absorption increases substantially with increasing temperature at the long wavelength end of this band.[11-13] The radiative lifetime of the first excited state has been calculated to be $\sim 3 \times 10^{-7}$s.[14] M.O. calculations indicate that the lowest lying electronic state corresponds to a $\pi \rightarrow \pi^*$ transition.[7]

Since D(OC=S) = 72.4 kcal mole^{-1}, the spin and symmetry-allowed primary photolytic step,

$$COS(^1\Sigma^+) + h\nu \longrightarrow CO(^1\Sigma^+) + S(^1D_2) \qquad [1]$$

becomes energetically feasible at 72.4 + 26.4 = 98.8 kcal

TABLE I-2

Sources of S Atoms

PROCESS	QUANTUM YIELD	λ,nm	REFERENCES
$SPF_3 + h\nu \longrightarrow PF_3 + S(^1D_2)$	-	<230	2
$\overline{C_2H_4S} + h\nu \longrightarrow C_2H_4 + S(^3P)$	-	<210	3
$CS_2 + h\nu \longrightarrow CS + S(^1D_2, {}^3P)$	-	<210	4.5
$S_8(s) + h\nu \rightarrow S_8(g) + h\nu \rightarrow 8S(^3P)$	-	240 (Kr laser)	6
$COS + Hg(^3P) \longrightarrow CO + S(^3P)$	0.9	254	7
$COS + h\nu \longrightarrow CO + S(^1S_o)$	0.8-0.9	140-160	8,9
$\longrightarrow CO + S(^1S_o, {}^1D_2)$	-	<200	10
$\longrightarrow CO + S(^1D_2, {}^3P)$	0.9	210-260	7
$COS + M + h\nu \longrightarrow CO + S(^3P) + M$	0.9	210-260	7

mole^{-1}, corresponding to $\lambda<290$ nm. For $S(^3P)$, the wavelength threshold is only $\sim$ 400 nm[9], and it has been suggested that $S(^3P)$ atoms may also be produced in the spin forbidden process:[7,11]

$$COS(^1\Sigma^+) + h\nu \rightarrow CO(^1\Sigma^+) + S(^3P) \qquad [2]$$

The possible occurrence of step [2] is based upon the fact that about 25% of the S atoms produced in the photolysis cannot be scavenged by added paraffins (which are inert towards $S(^3P)$ atoms, vide infra)[14] and also on kinetic analysis of COS-alkene systems.[15] The results concordantly suggest that 25-30% of the sulfur atoms are initially produced in the ^3P state.

It has been shown that the quantum yield (Φ) of the primary steps [1] + [2] at 229 nm and 253 nm is 0.9 for $P(COS)>100$ torr,[7] or in solution.[16] The slight inefficiency is probably due to non-radiative transitions to the ground state.[17]

Secondary reactions which may occur in the photolysis of pure COS are[14]:

$$S(^1D_2) + COS(^1\Sigma^+) \rightarrow CO(^1\Sigma^+) + S_2(^1\Delta_g) \qquad [3]$$

$$\rightarrow COS(^1\Sigma^+) + S(^3P) \qquad [4]$$

$$S(^3P) + COS(^1\Sigma^+) \rightarrow CO(^1\Sigma^+) + S_2(\tilde{X}^3\Sigma_g^-) \qquad [5]$$

$$S_2(^1\Delta_g) + M \rightarrow S_2(\tilde{X}^3\Sigma_g^-) \qquad [6]$$

$$S(^3P) + S_{2-7} \rightarrow S_{3-8} \qquad [7]$$

The quantum yield of CO formation for the photolysis is 1.8[7], however, indicating that step [7] is unimportant. From examination of steps [1] - [5] it is apparent that for each S atom generated in the primary steps, two molecules of CO are produced. Thus, if R°_{CO} is the rate of CO formation in the absence of substrate, then the rate of S atom formation is $R^{\circ}_{CO}/2$. If a substrate is present, it will compete with COS for the S atoms,

$$S(^1D_2, {}^3P) + \text{Substrate} \longrightarrow \text{Products} \qquad [8]$$

decreasing the CO yield from abstraction steps [3] and [5]. Therefore if R_{CO} is the rate of CO formation in the presence of a substrate, then the total rate of S atom abstraction, steps [3] and [5], is given by,

$$R_{abstraction} = R_{CO} - R^{\circ}_{CO}/2 \qquad [I]$$

and the rate of S atom reaction with a substrate is

$$R_{reaction} = R^{\circ}_{CO} - R_{CO} \qquad [II]$$

Hence, the total rate of S atom production is,

$$R_{abstraction} + R_{reaction} = R^{\circ}_{CO}/2 \qquad [III]$$

Therefore, it is apparent that the CO produced can serve as a useful internal actinometer for the amount of sulfur atoms produced and scavenged in the presence of a reactive substrate.

Absolute rate constants have been determined for the abstraction steps [3] and [5]. Donovan et al.,[18] by monitoring the growth of the S_2 $(g^1\Delta_u \leftarrow a^1\Delta_g)$ spectrum, determined the

rate constant for step [3] to be $k_3 \geqslant 4 \times 10^{10}\ M^{-1}s^{-1}$. The combined(abstraction + deactivation) rate constant $k_3 + k_4 \simeq 7 \times 10^{10}\ M^{-1}s^{-1}$ has been obtained by monitoring the decay of $S(^1D_2)$ atoms directly[5]. Using this value and the ratio of $k_3/k_4 \simeq 2$ estimated by Sherwood et al.[19], k_3 and k_4 are 4×10^{10} and $2 \times 10^{10}\ M^{-1}s^{-1}$ respectively. A more recent direct measurement of $k_3 + k_4$ is reported to be $\sim 2 \times 10^{11}\ M^{-1}s^{-1}$. This value was claimed to be more reliable.[20] For the abstraction by $S(^3P)$, step [5], Klemm and Davis[21] obtained $k_5 = 2 \times 10^6\ M^{-1}s^{-1}$ and $E_5 = 3.6$ kcal mole^{-1}. Thus COS is expected to compete with a reactive substrate for $S(^1D_2)$ atoms much more efficiently than for $S(^3P)$ atoms.

In the presence of a large excess of inert gas such as CO_2, the $S(^1D_2)$ atoms will be collisionally deactivated to the ground state.[18,22-24] CO_2, Xe and Ar have been demonstrated to be efficient quenchers of $S(^1D_2)$ atoms.[22,23] The values of

$$S(^1D_2) + M \longrightarrow S(^3P) + M \qquad [9]$$

k_9 are $> 1 \times 10^{10}$, $>4 \times 10^9$, and $> 6 \times 10^8\ M^{-1}s^{-1}$ for CO_2, Xe, and Ar, respectively.[18,24] Since the rate of quenching of $S(^1D_2)$ by CO_2 is comparable to the rate of reaction of $S(^1D_2)$ atoms with hydrocarbons or COS, the introduction of a large excess of CO_2 will result in virtually complete deactivation of $S(^1D_2)$ atoms to the ground (^3P) state.[23] For example, a CO_2/COS ratio $\simeq 40$ affords 95% deactivation.[25] Thus the CO_2-COS system is a clean source of $S(^3P)$ atoms.

Alternatively, $S(^3P)$ atoms can also be produced directly by the triplet mercury photosensitization of COS.[7]

$$COS + Hg(6^3P) \longrightarrow CO + S(^3P) + Hg(6^1S_o) \qquad [10]$$

A recent study of the photolysis of pure COS at low pressures (2.5 - 10.5 torr) reported a primary quantum yield of 0.7 over the wavelength range 215 - 254 nm. This low value may reflect a true drop-off in the quantum yield at low pressures, or alternatively, under these conditions $S(^3P)$ atoms may diffuse to the wall and recombine there.

The second and third absorption bands of COS lie in the vacuum UV, with maxima at 167 and 153 nm, respectively. The second band is a continuum with superimposed vibrational structure and the third one consists of several diffuse bands.[26] Photolysis of COS in these bands produces $S(^1S_o)$ atoms and vibrationally excited CO.[9,10,26] Only $S(^1S_o)$ atoms

$$COS \xrightarrow{\lambda < 180nm} CO^\dagger + S(^1S_o, ^1D_2) \qquad [11]$$

$$\xrightarrow{\lambda \simeq 140\text{-}160nm} CO^\dagger + S(^1S_o) \qquad [12]$$

are produced in the third band, and the primary quantum yield of $S(^1S_o)$ at 153 nm has been reported to be 0.8 - 0.9.[8] Therefore photolysis of COS in this band is a clean source of $S(^1S_o)$ atoms. Since transitions from $S(^1S_o)$ to $S(^1D_2)$ and $S(^3P)$ are forbidden by symmetry and spin rules, respectively, the $S(^1S_o)$ state has a relatively long lifetime (∿100 μs).[10]

C. Reactions of Group VI A Atoms with Hydrocarbons.

1) Reactions of S and O Atoms.

(a) with alkanes

(i) $S(^1D_2, ^3P)$ Atoms.

Only $S(^1D_2)$ atoms are reactive.[14] The major reaction with alkanes is direct insertive type attack on the aliphatic C-H bonds to give isomeric thiols.[22,28]

$$S(^1D_2) + RH \xrightarrow{\qquad\qquad} RSH^{\dagger} \qquad [13]$$

In the gas phase the insertion reaction is indiscriminate with respect to bond order, but in solution some preference for weaker secondary and tertiary C-H bonds has been observed.[16,17] At 254 nm the $S(^1D_2)$ atoms may contain up to 6 kcal $mole^{-1}$ excess translational energy, thus rendering them kinetically "hot". Even at high alkane pressures (RH/COS > 5/1) the yield of isomeric thiols reaches a limiting value of only 73% of the sulfur atoms available for reaction. This observation indicates the presence of $S(^3P)$ atoms in the system, which are incapable of inserting.[28] These are likely formed in a primary step (*vide supra*) although the occurrence of the deactivation step [14] cannot be discounted.

$$S(^1D_2) + RH \xrightarrow{\qquad\qquad} RH + S(^3P) \qquad [14]$$

In contrast to the higher alkanes, the reaction of $S(^1D_2)$ atoms with methane is characterized by extensive fragmentation at pressures less than ≃2 atm.[14] This is because the adduct has an insufficient number of degrees of freedom to dissipate the energy released by the reaction ($\Delta H \sim -83$ kcal $mole^{-1}$).[14,28] The final products of the reaction are CH_3SH, H_2S, CH_3SSCH_3, CH_3SCH_3, CS_2, C_2H_6, H_2 and elemental sulfur. The fragmentation process can be envisioned by the following mechanism:

$$S(^1D_2) + CH_4 \longrightarrow CH_3SH^{\dagger} \qquad [15]$$

$$CH_3SH^{\dagger} \longrightarrow \cdot CH_3 + \cdot SH \qquad [16a]$$

$$\longrightarrow :CH_2 + H_2S \qquad [16b]$$

$$\longrightarrow CS + 2H_2 \qquad [16c]$$

$$\xrightarrow{M} CH_3SH \qquad [16d]$$

The nature of the transition state for the insertion reaction with alkanes has not been fully elucidated. However, it has been suggested that the transition state is similar to a H-bonded radical pair (C····H····S) in which rotation of the HS moiety can lead to insertion[14].

The rate of insertion is similar for all alkanes, and the estimated rate constants lie in the range ($>$0.3 - 1.2) x $10^{10}M^{-1}s^{-1}$. The upper limit of the activation energy is believed to be $\sim$3 kcal mole^{-1}. No direct kinetic measurements for the $S(^1D_2)$ + alkane reactions have been reported.

(ii) $O(^1D_2, {}^3P)$ Atoms.

$O(^1D_2)$ atoms also insert directly into the C-H bonds of alkanes, giving vibrationally excited alcohols[29,30]. Unlike the $S(^1D_2)$ reactions, the hot adduct can only be stabilized at very high pressures, e.g. >100 atm. for C_2H_6[31].

$$O(^1D_2) + RH \longrightarrow ROH^{\dagger} \qquad [17]$$

$$ROH^{\dagger} \longrightarrow \text{fragmentation} \qquad [18a]$$

$$\longrightarrow R\cdot + \cdot OH \qquad [18b]$$

$$\xrightarrow{M} ROH \qquad [18c]$$

In addition to insertion, abstraction of H is also significant (20 - 30%).[29]

$$O(^1D_2) + C_2H_6 \rightarrow \cdot C_2H_5 + \cdot OH \quad \Delta H = -48.9 \text{ kcal mole}^{-1} \qquad [19]$$

$$S(^1D_2) + C_2H_6 \nrightarrow \cdot C_2H_5 + \cdot SH \quad \Delta H = -11.6 \text{ kcal mole}^{-1} \qquad [20]$$

The absence of this process in the $S(^1D_2)$ - alkane systems can be explained by the small exothermicity of reaction [20].

Recently, Luntz[32] suggested that insertion results from a perpendicular approach of the $O(^1D_2)$ atom to the C-H bond, and that abstraction results from a collinear approach.

In general, the products of the $O(^1D_2)$ + alkane reactions include alcohols, carbonyls, water, CO, CH_4, higher alkanes and H_2.[34] The small amounts of H_2 produced in the reaction have been postulated to arise from a third pathway, but the detailed mechanism of its formation is still controversial.[29,35,36]

A few combined rates of insertion + abstraction for some alkanes have recently been compiled by Schofield and are in the range (1 - 4) x 10^{11} $M^{-1}s^{-1}$ on going from CH_4 to $n\text{-}C_5H_{12}$.[33] The $O(^1D)$ + alkane reactions have been proposed to be nearly temperature independent.[32]

In sharp contrast to $S(^3P)$ atoms, which do not react with alkanes, $O(^3P)$ atoms react by H abstraction.[37-39]

$$O(^3P) + R\text{-}H \longrightarrow R\cdot + \cdot OH \qquad [21]$$

Recently, Paraskevopoulos and Cvetanovic[37] studied the reaction of $O(^3P)$ with iso-C_4H_{10} using NO_2 as the source of $O(^3P)$ as well as a trap for the radicals formed in the reaction. Based on product analysis the following overall mechanism was proposed:

$$O(^3P) + (CH_3)_3CH \rightarrow \cdot OH + (CH_3)_3C\cdot\ ,\ (CH_3)_2CHCH_2^{\cdot} \qquad [22]$$

$$\cdot OH + (CH_3)_3CH \rightarrow H_2O + (CH_3)_3C\cdot\ ,\ (CH_3)_2CHCH_2^{\cdot} \qquad [23]$$

$$(CH_3)_3C\cdot + NO_2 \rightarrow (CH_3)_3CNO_2 \qquad [24]$$

$$\rightarrow (CH_3)_3CO\cdot + NO \qquad [25]$$

$$(CH_3)_3CO\cdot + NO \rightarrow (CH_3)_3CONO \qquad [26]$$

$$+ NO_2 \rightarrow (CH_3)_3CONO_2 \qquad [27]$$

The observation of $(CH_3)_3CNO_2$, $(CH_3)_3CONO$ and $(CH_3)_3CONO_2$ formed in steps [24], [26] and [27], respectively, supports H abstraction as the primary step in $O(^3P)$ - alkane systems. Kinetic data indicate that this reaction is quite slow ($k_{21} = 10^4\text{-}10^8\ M^{-1}s^{-1}$, on going from CH_4 to $(CH_3)_2(CH)_2(CH_3)_2$).[39,40] This can be attributed to the presence of an appreciable activation energy,[38] which depends on the nature of the C-H bond (∿5.8,∿4.5 and ∿3.3 kcal $mole^{-1}$ for 1°, 2° and 3° C-H bonds, respectively).[39] It has been suggested that the reaction occurs when the approach of the $O(^3P)$ atom is collinear to the C-H bond.[38]

(b) with alkenes.

(i) $S(^1D_2)$ and $O(^1D_2)$ Atoms.

Two processes are operative in the $S(^1D_2)$ - alkene systems.One is stereospecific cycloaddition to the double bond to form a hot thiirane,

$S(^1D_2) + H_2C{=}CH_2 \longrightarrow$ 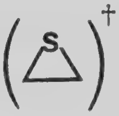 [28]

which for the case of $\overline{C_2H_4S}$, has an energy content of ∿85 kcal mole^{-1}. The hot adduct can be collisionally stabilized

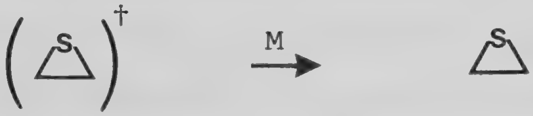 [29a]

(step [29a]), or can isomerize to vinylthiol (step [29b]).[19,41]

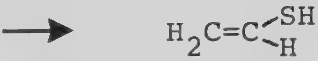 [29b]

$$\longrightarrow \quad H_2C{=}C\begin{smallmatrix}SH\\ H\end{smallmatrix}$$

With higher alkenes ($\geqslant C_4$), isomerization does not occur,due to the presence of more internal degrees of freedom to dissipate the excess energy of the hot adduct.[14]

The other reaction is direct insertion into the C-H bonds, by analogy with the $S(^1D_2)$ - alkane systems,to form isomeric thiols. The rate of insertion into the aliphatic C-H bonds is nearly statistical.[14] Vinylthiols arise only if a terminal methylene group is present in the alkene.[14] To date, no alkyl substituted vinylthiols have been observed.[14,42]

Sparse kinetic data are available for the $S(^1D_2)$ - alkene systems. Earlier work[41] estimated the total reaction rate constants for C_2H_4, C_3H_6 and i-C_4H_8 to be ∿2×10^{10}, ∿6×10^{10} and ∿1.5×10^{11} $M^{-1}s^{-1}$, respectively. A more recent estimate [19] places the rate constant for the $S(^1D_2) + C_2H_4$ reaction at 8×10^{10} $M^{-1}s^{-1}$, with insertion and addition

proceeding at nearly equal rates (4.2×10^{10} and 3.8×10^{10} $M^{-1}s^{-1}$, respectively). In general, the rate of reaction increases slightly with alkyl substitution, and insertion has a slightly higher activation energy than addition. (e.g. $E_{a(\text{vinylthiol})} - E_{a(\text{thiirane})} \sim 0.5$ kcal mole^{-1} for C_2H_4).[14]

Little work has been done on the reactions of $O(^1D_2)$ atoms with alkenes. Unlike the case of $S(^1D_2)$ + alkene reactions, these studies are complicated by the high exothermicity of the reaction (e.g. $\Delta H = -130$ kcal mole^{-1} for C_2H_4),[41] which leads to extensive fragmentation. Kajamoto _et al._[44] studied the reaction of $O(^1D_2)$ with C_3H_6 at high pressures (_ca_. 20-150 atm. He), and confirmed that two main process were operative. Analogous to the $S(^1D_2)$ - alkene system, one is addition to the double bond forming a hot epoxide (reaction [30a]),

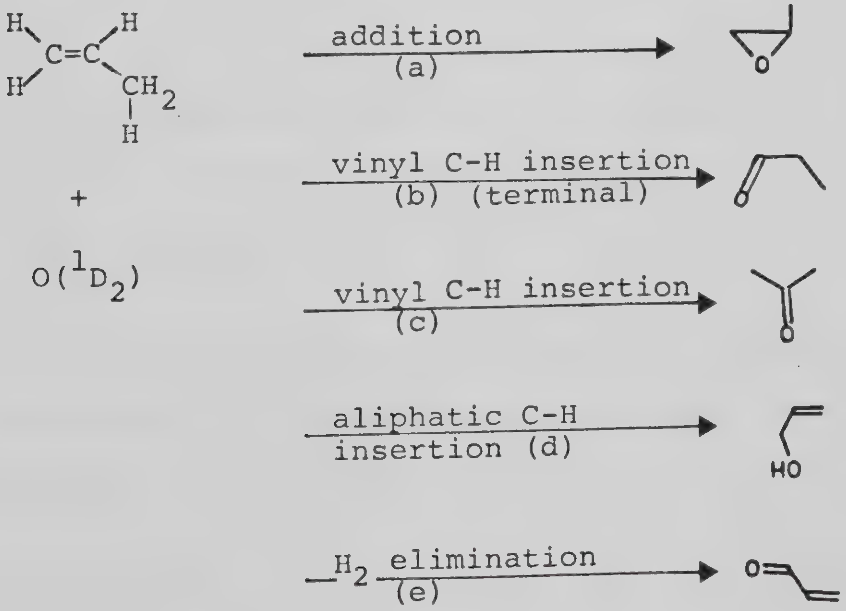
H
H
C=C
H
CH2
H
+
O(1D2)
addition
(a)
vinyl C-H insertion
(b) (terminal)
vinyl C-H insertion
(c)
aliphatic C-H
insertion (d)
HO
H2 elimination
(e)
O

[30]

and the other is insertion into vinylic and aliphatic C-H bonds yielding carbonyls and alcohols, respectively (reactions [30b-d]). A minor pathway (*ca.* 2%) involves the elimination of H_2 (step [30e]). These results are consistent with an earlier study of the reaction of $O(^1D_2)$ atoms with C_2H_4 in liquid Ar where a similar distribution of the corresponding products was observed.[43] The addition process (step [30a]) has been shown to be stereospecific. Recent *ab initio* calculations for the $O(^1D_2)$ - C_2H_4 system indicate that the lowest energy reaction path corresponds to a symmetric concerted addition,[46] which is consistent with the observed stereospecificity.

There are few kinetic data available for these systems. However, a recent competitive rate study[47] involving several alkenes indicated that rate constants are extremely high and lie in the range of $(1 - 6) \times 10^{11}\ M^{-1}s^{-1}$ on going from C_2H_4 to $(CH_3)_2C{=}C(CH_3)_2$. These observations are consistent with earlier estimates[33] and follow the same trend as observed in the $S(^1D_2)$ - alkene systems (*vide infra*).

(ii) $S(^3P)$ and $O(^3P)$ Atoms.

The only reaction observed in the $S(^3P)$-alkene systems is the cycloaddition to the double bond yielding the corresponding thiirane as the sole product:[41]

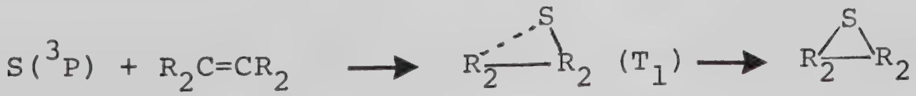

[31]

A unique feature of this reaction is its compulsion to follow a stereospecific path, as illustrated by the reaction of S(^{3}P) with cis and trans 2-butene,[42,48,49]

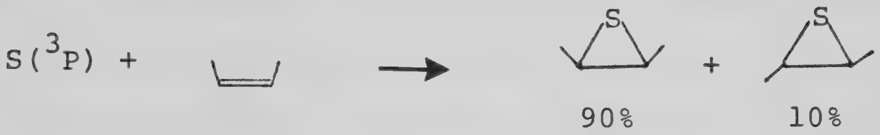

[32]

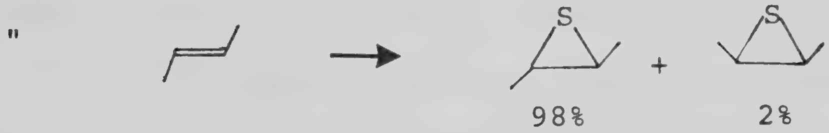

[33]

The S(^{3}P) + alkene reaction provided the first example of a stereospecific cycloaddition involving a divalent triplet state reagent.[41] Subsequent EHMO calculations indicated that the triplet (T_1) thiirane formed in reaction [31] lies ∿40 kcal mole^{-1} above the ground (S_o) state and possesses a ring distorted geometry with a rotational energy barrier of ∿23 kcal mole^{-1}.[50,51] This high energy barrier can explain the observed high stereospecificity of the S(^{3}P) + alkene reactions.

(T_1) thiirane has a very long lifetime and has been shown to be an efficient reagent for inducing cis - trans isomerization in alkenes.[3] This observation may account for some of the isomerized products observed in reactions [32] and [33].

Rate constants and Arrhenius parameters have been determined for a series of alkenes.[40,41] A few of them are

listed in Table I-3 to illustrate the general trend of these reactions. From this Table, it is apparent that the rate constants increase with alkyl substitution on the vinylic carbon of the alkene but decrease with halogen substitution. The A factors do not seem to show particularly strong trends, and consequently the variations in the rate constants are mainly due to changes in the activation energy. Increasing alkyl substitution on the vinylic carbon has a diminishing effect on E_a, while substitution of electron-withdrawing groups such as fluorine has an increasing effect. This behaviour illustrates the electrophilic character of $S(^3P)$, which is further substantiated by the linear relationship between E_a and ionization potential of the alkene, as illustrated in Figure I-1.[52,53] Of particular interest are the predicted negative activation energies for reactions with alkenes having low ($\leqslant$9.3 eV) ionization potentials. In order to account for this phenomenon, it has been proposed that E_a is dependent upon the location of the crossing point of the reactant surface and the product surface:[54]

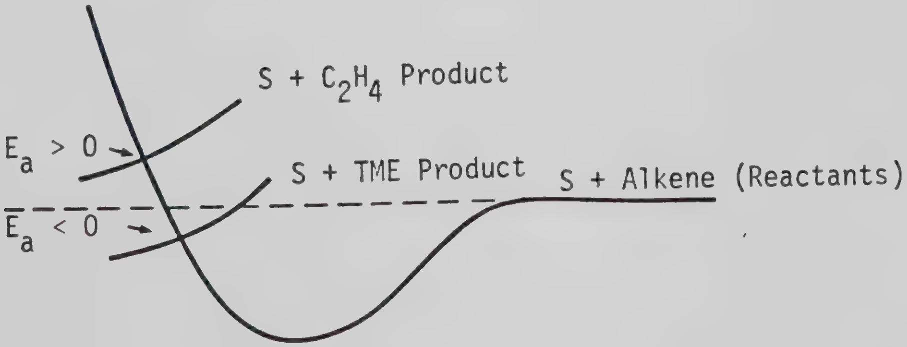

TABLE I-3

Rate Constants[a] and Arrhenius Parameters for $S(^3P)$ and $O(^3P)$ Atom Reactions with Selected Alkenes

Alkenes	$S(^3P)$			$O(^3P)$		
	$k\times10^{-9}$ $(M^{-1}s^{-1})$	E_a (kcal mole^{-1})	$A\times10^{-10}$ $(M^{-1}s^{-1})$	$k\times10^{-9}$ $(M^{-1}s^{-1})$	E_a (kcal mole^{-1})	$A\times10^{-10}$ $(M^{-1}s^{-1})$
C_2H_4	0.9[b]	1.5	1.2	0.4[d]	1.7	0.7
C_3H_6	5.4[b]	0.5	1.3	2.3[d]	0.7	0.8
1-C_4H_6	8.2[b]	0.2	1.2	2.4[d]	0.7	0.7
cis-C_4H_8	12[c]	-0.1	1.0	10.0[d]	-0.3	0.7
iso-C_4H_8	29[c]	-0.4	1.5	10.0[d]	-0.1	0.9
$(CH_3)_2C{=}CHCH_3$	50[c]	-1.1	0.8	38.0[e]	-1.3	0.4
$(CH_3)_2C{=}C(CH_3)_2$	60[b]	-1.3	0.7	48.0[e]	-1.6	0.3
$H_2C{=}CHF$	0.3[c]	2.6	2.2	0.3[e]	-	-
cis-HFC=CHF	0.01[c]	4.6	2.7	0.3[e]	-	-

[a] 298°K., [b] Reference 53., [c] calculated from relative data of Reference 96 using absolute data for 1-C_4H_8 from Reference 53., [d] Reference 55., [e] Reference 40.

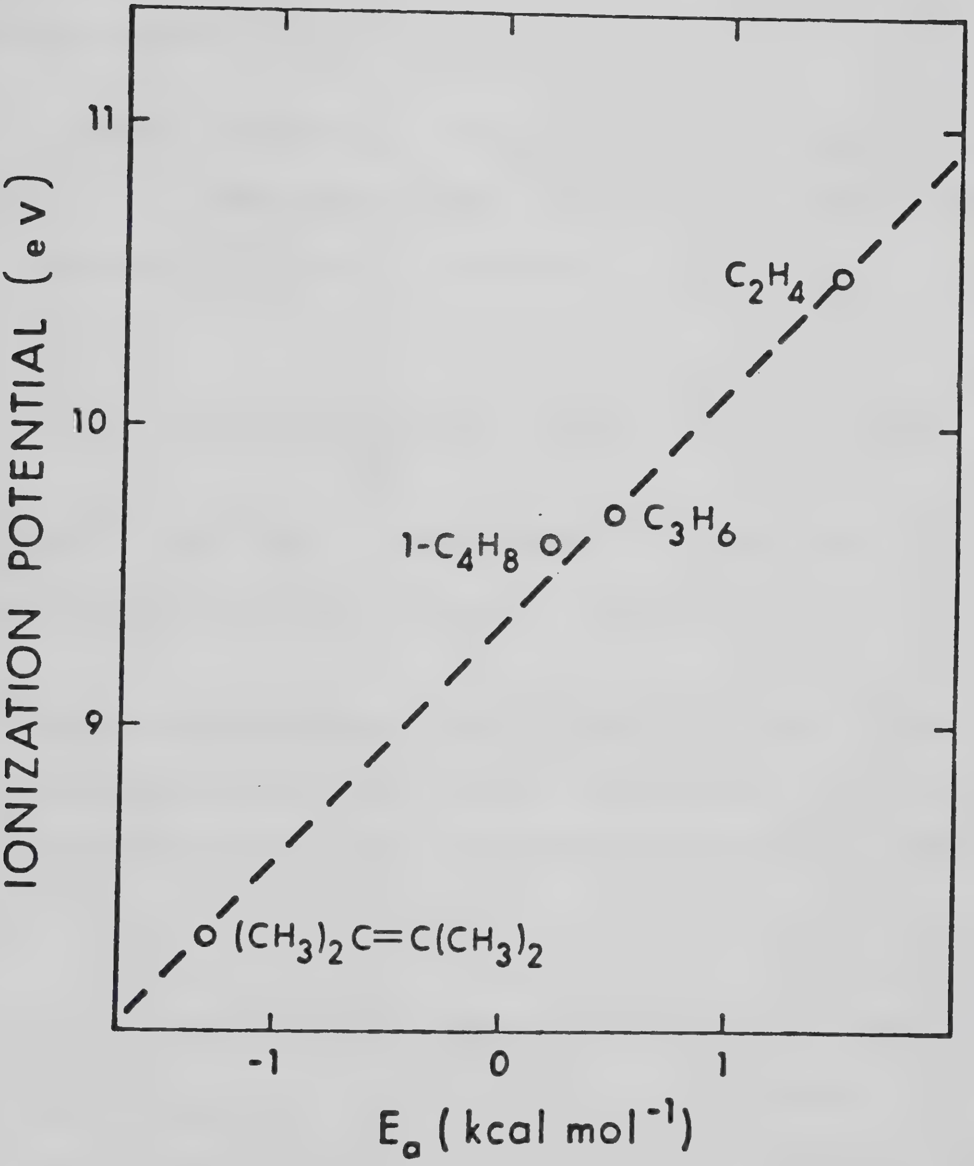

FIGURE I-1: Ionization potential versus E_a for the addition of $S(^3P)$ atoms to alkenes[53].

The crossing point may lie above or below the energy of the separate reactants. The former case corresponds to a positive temperature dependence, while the latter corresponds to a negative temperature dependence.

The model proposed by Cvetanovic and co-workers[55] to account for similar observations in the $O(^3P)$ case assumes the formation of a loose π complex:

$$O(^3P) + \text{Alkene} \underset{E_{a_{-1}}}{\overset{E_{a_1}}{\rightleftarrows}} \text{Complex}^{\ddagger} \xrightarrow{E_{a_2}} \text{Product} \qquad [34]$$

This complex can either decompose back to the reactants or evolve to products. E_a is negative when $E_{a_{-1}} > (E_{a_1} + E_{a_2})$.

The two models are not in conflict, and their application in the interpretation of other systems having a negative temperature dependence will be discussed in detail (*vide infra*).

For the $O(^3P)$ + alkene reactions, the basic kinetic features are very similar to those for $S(^3P)$ atoms. The reactions proceed at comparable rates, as is apparent from examination of the rate parameters listed in Table I-3. The activation energies also decrease with increasing alkyl substitution and eventually become negative, which illustrates the electrophilic nature of $O(^3P)$.

As for the nature of the reaction, $O(^3P)$ also adds to the double bond:

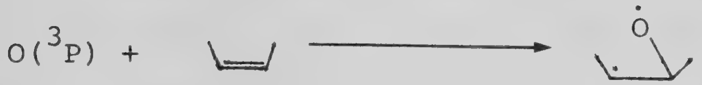

[35]

However, the triplet biradical primary adduct contains a great deal of excess energy, and in addition to ring closure to form epoxide (step [36a]):[14,56-59]

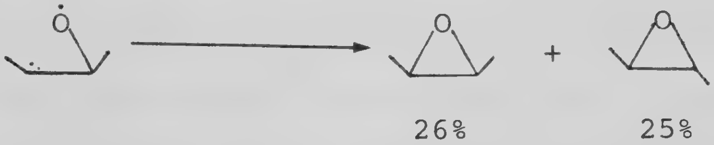

[36a]

can undergo either intramolecular hydrogen or alkyl migration to yield carbonyls (step [36b]), or fragmentation (step [36c]).

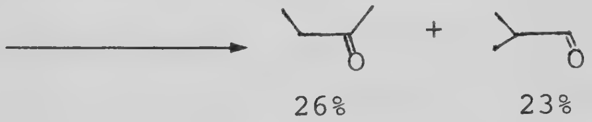

[36b]

$$\xrightarrow{P<50\ \text{torr}} \text{CO + Low M.W. Hydrocarbons}$$

[36c]

In contrast to $S(^3P)$, $O(^3P)$ addition to the double bond is non-stereospecific, as illustrated by the product distribution of step [36a]. This observation has been cited as evidence for the existence of a freely rotating triplet biradical intermediate.[45,56] Indeed, a recent theoretical conformational study has shown that the ring-opened triplet isomers of methyloxirane are lower in energy than the ring-closed structure. The rotational barriers about the $\dot{C}HR-C\dot{O}$

bond of these isomers were found to lie in the range 0.8 - 1.2 kcal $mole^{-1}$, indicating freely rotating species[60].

M.O. calculations on the possible intermediates of the $O(^3P)$ + $CH_3CH{=}CH_2$ reaction reveal that four isomeric triplet states are energetically accessible[61]:

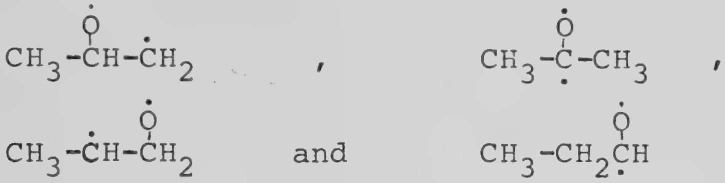

$CH_3-\overset{\dot{O}}{C}H-\dot{C}H_2$, $CH_3-\underset{\bullet}{\overset{\dot{O}}{C}}-CH_3$,

$CH_3-\dot{C}H-\overset{\dot{O}}{C}H_2$ and $CH_3-CH_2\underset{\bullet}{\overset{\dot{O}}{C}}H$

These biradicals may evolve into the observed products, methyloxirane, propionaldehyde and acetone. The product distribution of this reaction is temperature dependent, and this was explained in terms of the differences in the thermodynamic stabilities of the adducts involved.

The fragmentation process, which is absent in the $S(^3P)$-alkene systems,is attributed to the higher exothermicity of the $O(^3P)$ addition (25-30 kcal $mole^{-1}$ higher for $O(^3P)$).The presence of carbonyl products in these systems can be explained by the greater difference in bond strengths between the C=O and C-O bonds as compared to the difference between the corresponding S bonds[14]. The distribution of carbonyl products, for example:

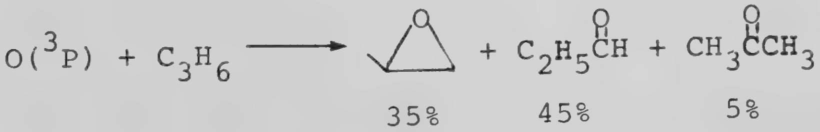

$O(^3P) + C_3H_6 \longrightarrow$ methyloxirane $+ C_2H_5\overset{O}{\overset{\|}{C}}H + CH_3\overset{O}{\overset{\|}{C}}CH_3$ [37]

indicates that $O(^3P)$ adds predominantly to the less substituted vinylic carbon[45,62].

(c) with alkynes

(i) $S(^1D_2)$ and $O(^1D_2)$ Atoms.

Only a limited number of $S(^1D_2)$ + alkyne reactions have been studied. In general the reactions are characterized by low product recoveries and extensive polymerization at room temperature. The end products are usually thiophene, benzene, polymer and, in some cases, CS_2.[14,63,64] Volatile product

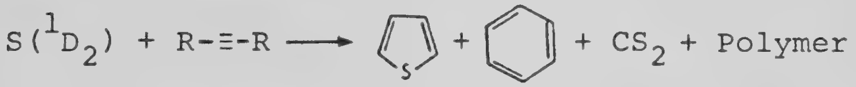

[38]

yields are low for the parent acetylene, but increase with reaction temperature and fluoromethyl substitution[63].

It is generally accepted that the reaction of $S(^1D_2)$ with alkynes is addition to the triple bond, forming an unstable adduct, presumably the thiirene[63-66].

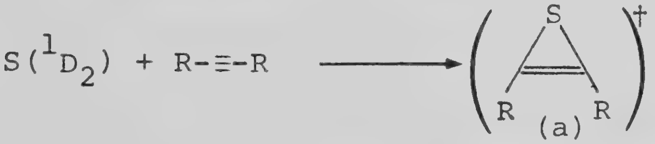

[39]

There is a possibility that a minor pathway, insertion into the alkynyl C-H bonds to form the ethynylthiol, exists. However this cannot be verified due to instability of the product.[63] Several other isomers of C_2R_2S have also been considered as the intermediate:

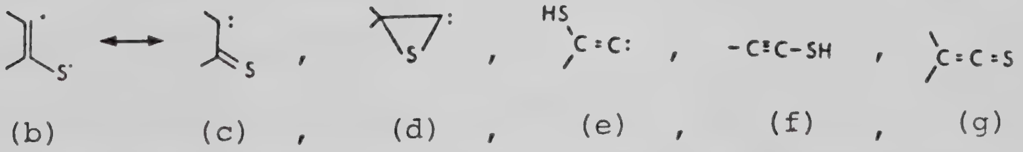

However, the transient existence of thiirene is supported by the following experimental observations[64-66]. Flash photolysis

studies of COS-alkyne systems employing kinetic mass spectrometry revealed the presence of transient species corresponding to the molecular weight of the adduct[66]. The lifetimes of these transients were unusually long (>0.1 - 7 s), which militates against excited or radical species (b) - (e) as the intermediate[14,65]. Moreover, thiophenes are among the end products, and are postulated to be formed via addition of the adduct to a substrate molecule[63-65], for example in the case of S + $F_3CC{\equiv}CCF_3$,

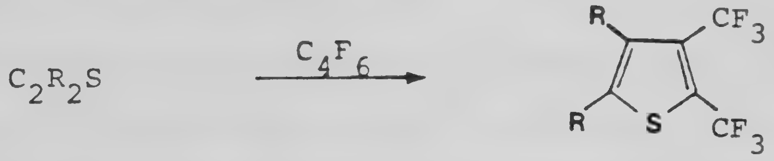

[40]

Ethynylthiol (f) cannot be formed in the case of disubstituted alkynes, yet the thiophene yields are highest for the S + $F_3CC{\equiv}CCF_3$ reaction[63,64]. Hence its intermediacy can be discounted. This leaves only the thioketene (g) and thiirene (a) as reasonable alternatives. For this ketene (g) to be implicated in the thiophene forming reaction, two intramolecular H, CH_3 or CF_3 shifts would be required. These processes should be least likely for the case of $F_3CC{\equiv}CCF_3$, which is inconsistent with the observed high thiophene yield. On the basis of these considerations, it has been concluded that the primary adduct of the $S(^1D_2)$ + alkyne reaction is the corresponding thiirene[65,66].

Direct evidence for the existence of thiirenes has been obtained from the Ar-matrix photolysis of 1,2,3-thiadiazole,

which affords thiirene, thioketene and ethynylthiol.[67,68]

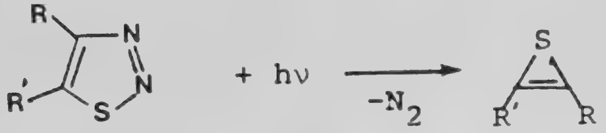

+ Rearrangement Products. [41]

The thermodynamic and kinetic properties of the products are consistent with the theoretically predicted stabilities of the C_2R_2S isomers.[69]

Recently, Verkoczy[63] has studied the $F_3CC{\equiv}CH$ - COS and $F_3CC{\equiv}CCF_3$ - COS systems. Small amounts of $S{=}C{=}CH{-}CF_3$ and CS_2, along with CF_3-substituted benzene and CF_3-substituted thiophenes, were observed in the former system. For the latter, at low conversion, only perfluorotetramethylthiophene (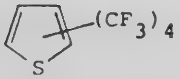) was obtained. At high conversion, however, unique products arising from S atom addition to the double bonds of thiophene were observed, along with dimers and trimers of the initial adduct, C_4F_6S; some aspects of this will be discussed later (vide infra).

Only limited kinetic data are available for S + alkyne reactions; rate constants for $HC{\equiv}CH$ and $F_3CC{\equiv}CCF_3$ are estimated to be in the range (3-9) x 10^{10} $M^{-1}s^{-1}$.[63,70]

To date, only two experimental investigations on $O(^1D_2)$ + alkyne reactions have been reported[71,72]. Ogi and Strausz investigated the 2-butyne reaction and found a number of non-condensable products, but were unable to characterize the oxygen containing products. A recent study[72] of the $O(^1D_2)$ + $HC{\equiv}CH$ system showed that vibrationally excited CO is produced in the reaction, and it was postulated that most of the CO comes from

the process:

$$O(^1D_2) + HC{\equiv}CH \longrightarrow C_2H_2O \longrightarrow :CH_2(\tilde{a}\,^1A_1) + CO^{\dagger} \qquad [42]$$

$$\Delta H = -\,86 \text{ kcal mole}^{-1}$$

Recent ab initio calculations suggest that the most probable primary process is spin and symmetry allowed addition to the triple bond to form an unstable oxirene.[73,74]

$O(^1D_2) + HC{\equiv}CH \longrightarrow$ 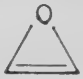 $(S_0)^{\dagger}$ [43]

Unlike thiirene, oxirene has never been observed. However there is compelling evidence for its transient existence as an intermediate in some photochemical Wolff rearrangements, for example those of α-diazoketones and esters.[75]

(ii) $S(^3P)$ and $O(^3P)$ Atoms.

For $S(^3P)$ + alkyne reactions, the nature and yields of the products are similar to those for the case of $S(^1D_2)$.[63,64] However, the primary adduct is the vibrationally excited ground state triplet thioketocarbene:[63,69,76]

$S(^3P) + R{-}{\equiv}{-}R \longrightarrow$ 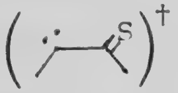 $\longrightarrow$ Products [44]

Rate constants have been measured for a few alkynes, and lie in the range $10^8 - 10^{10}\ M^{-1}s^{-1}$.[76] The activation energies are slightly higher than those for the corresponding alkene reactions (-1 to +3 kcal mole^{-1}), but follow the same general trend.[76] As in the case of alkenes, fluorination of the substrate drastically reduces the rate of addition: the rate constant for $S(^3P) + F_3CC{\equiv}CCF_3$ is $2.1 \times 10^8\ M^{-1}s^{-1}$.[53]

It has been postulated that analogous to the $S(^3P)$-alkyne systems, $O(^3P)$ adds to the triple bond giving the triplet ketocarbene intermediate,

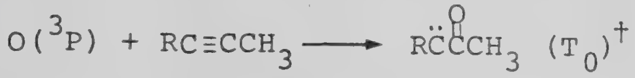

$$O(^3P) + RC\equiv CCH_3 \longrightarrow R\ddot{C}\overset{O}{\overset{\|}{C}}CH_3\ (T_0)^{\dagger} \qquad [45]$$

In addition to this process, H abstraction has been suggested as a minor pathway (< 5%) in the case of acetylene[78].

A distinct difference between the $S(^3P)$ and $O(^3P)$ atom reactions with alkynes is the occurrence of significant amounts of fragmentation products in the latter system, resulting from decomposition of the primary adduct. In general, the end products are polymer, CO, alkenes and unsaturated ketones[71,79].

2) Reactions of Se Atoms.

Although limited in scope, the data available on the reactions of Se atoms complement the general trends already established for S and O atoms. Thus $Se(^1D_2)$ inserts into the C-H bonds of alkanes indiscriminately, yielding selenomercaptans[81,82]. With alkenes, the only reaction observed for both $Se(^1D_2)$ and $Se(^3P)$ is addition to the double bond, which leads to the formation of unstable episelenides:[82]

$Se(^1D_2, ^3P) + R_2C=CR_2 \longrightarrow$

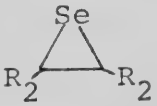

[46]

The rate of $Se(^3P)$ addition varies from $\sim 10^8\ M^{-1}s^{-1}$ for C_2H_4 to $\sim 10^{10}\ M^{-1}s^{-1}$ for $i\text{-}C_4H_8$[83]. The trend in E_a (2.8 - 1.0 kcal mole^{-1})[83] with alkyl substitution parallels that observed in the $S(^3P)$ and $O(^3P)$ systems (vide supra).

3) Reactions of Te Atoms.

Only Te(^{3}P) + alkene reactions have been examined. The adducts are unstable epitellurides[84]:

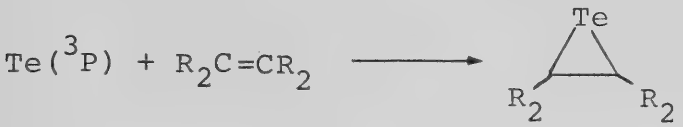

[47]

Arrhenius parameters have been determined for C_2H_4, C_3H_6 and $(CH_3)_2C{=}C(CH_3)_2$ and the rate constants are in the order of $10^7 - 10^9\ M^{-1}s^{-1}$ [54]. The trend in E_a is consistent with other Group VI A atoms. In fact, the E_a observed for the reaction of Te(^{3}P) with $(CH_3)_2C{=}C(CH_3)_2$ was the first negative E_a reported for an addition reaction.

D. Reactions of S and O Atoms with Polyunsaturated Hydrocarbons

1) with aromatics

(a) S($^1D_2$, ^{3}P) Atoms.

Until recently, the only S + aromatic reaction investigated was the benzene system, and no retrievable products were observed[85]. However, direct evidence for the occurrence of a reaction between S atoms and an aromatic ring was obtained from a study of the S($^1D_2$, ^{3}P) - $F_3CC{\equiv}CCF_3$ system[63]. One of the products observed at high conversion, (i), was postulated to arise from the addition of two S atoms to perfluorotetramethylthiophene (PFTMT), steps [48] and [49]:

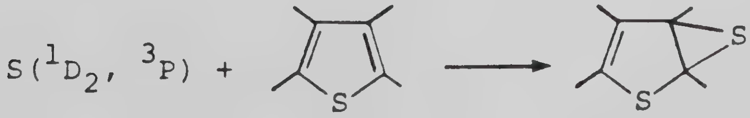

[48]

(h)

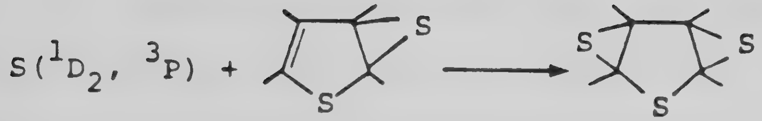
(i) [49]

The hypothetical $C_8F_{12}S_2$ species (h) was not detected, but it was also assumed to be the precursor of the observed species (j) and (k):

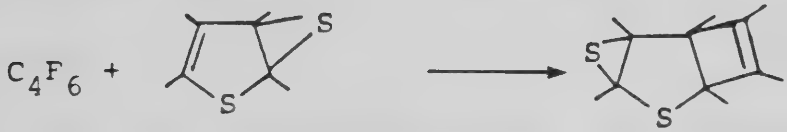
(j) [50]

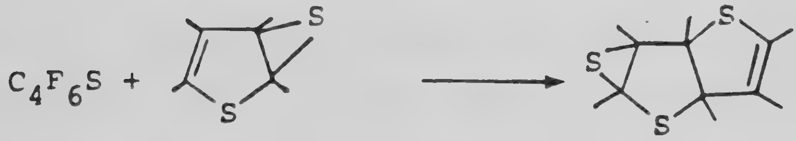
(k) [51]

(b) $O(^1D_2, ^3P)$ Atoms.

To date no $O(^1D_2)$ + aromatic reactions have been reported. However, $O(^3P)$ - aromatic systems have received considerable attention, particularly in the last decade. In an early study of the reactions of $O(^3P)$ atoms with benzene and toluene, Cvetanovic and co-workers found that these reactions were characterized by extensive polymerization (>75%).[86] Volatile products consisted mainly of phenols, with small amounts of CO and H_2O. Based on the absence of aromatic ring H abstraction products, a mechanism similar to that for $O(^3P)$ - alkene systems was postulated:

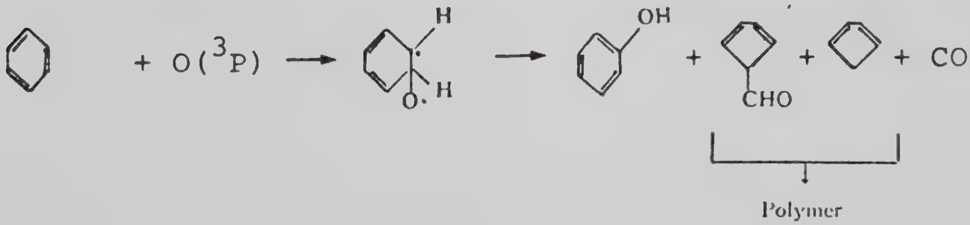
[52]

The O atom adds to the aromatic ring to form a triplet biradical which either rearranges to a phenol or undergoes ring rupture yielding unstable products which decompose or polymerize. Subsequent studies[87,88] of these systems were in agreement. A more recent study[89] on deuterated aromatics showed no evidence of a primary kinetic isotope effect at temperatures below 600 K, which lends support to the addition mechanism.

Absolute rate parameters have been measured by several techniques and are in reasonable agreement[89-92]. The trends observed for both the rate constants and the activation energies parallel those already established for $O(^3P)$ and $S(^3P)$ - alkene systems. Rate constants vary from 10^7 $M^{-1}s^{-1}$ for benzene to 10^9 $M^{-1}s^{-1}$ for 1,3,5 - trimethylbenzene, while the activation energies drop from ~ 4 kcal $mole^{-1}$ to ~ 1 kcal $mole^{-1}$ along the same series.

Rate parameters for the $O(^3P)$ reaction with a heteroatomic aromatic, thiophene, have been determined only recently using a discharge flow-resonance fluorescence technique[93]. The rate constant over the temperature range 262 - 448 K was well represented by the Arrhenius expression,

$$k = 2 \times 10^{10} \exp(-1100/RT)\ M^{-1}s^{-1}.$$

However, below 262 K, a large negative E_a of -2.6 kcal $mole^{-1}$ was observed. The discontinuity in the Arrhenius plot was explained in terms of two reaction pathways: addition of $O(^3P)$

to the S atom, step [53], and addition to the double

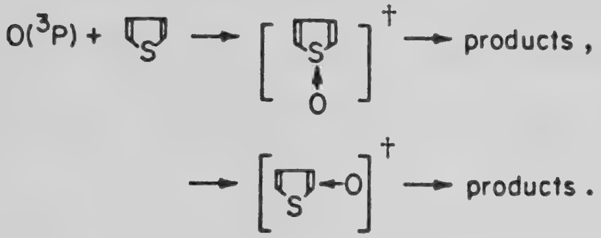

[53]

[54]

bonds of the aromatic ring (step [54]). Benzene and thiophene have comparable resonance energies and because the room temperature rate constant for the O + thiophene reaction was two orders of magnitude greater than for reaction with benzene, but similar in magnitude to those of other organosulfides (vide infra), it was suggested that above 262 K the predominant reaction involves the S atom. Based on the known negative E_a (-0.4 kcal mole^{-1}) of the O + reaction,[94] it was tentatively proposed that the low temperature reaction pathway is addition to the double bond, step [54].

2) with dienes

(a) $S(^1D_2, {}^3P)$ Atoms.

The reactions of S atoms with dienes have not been studied as extensively as those with alkenes. To date, only the reactions with 1,3-C_4H_6 and allene (C_3H_4) have been investigated. The photolysis of COS in the presence of 1,3-C_4H_6 led to the formation of only one S addition product, vinylthiirane, along with some thiophene, trace amounts of H_2 and an

$S(^1D_2, {}^3P)$ +

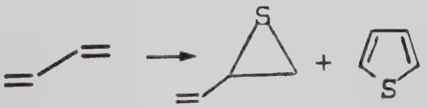

+ H_2 [55]

60-80% 20-30% <1%

unidentified product of molecular weight 88.[25,95] The vinylthiirane yield was found to increase with decreasing substrate pressure, and in the presence of CO_2. These observations were explained in terms of a hot vinylthiirane,

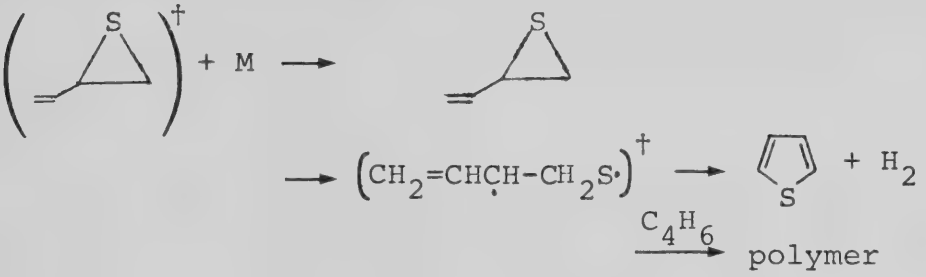

[56a]

[56b]

[56c]

which can be collisionally stabilized, or undergo ring rupture to form a biradical. This biradical can either react with the substrate,yielding polymer or rearrange to form thiophene via H_2 elimination. Some of the thiophene can also arise from secondary photolysis of vinylthiirane. Unlike the S + alkene systems, no insertion products were observed.

Relative rate parameters for $S(^3P)$ addition to 1,3-C_4H_6 have been measured,[96] and based on the data for C_2H_4,[97] $k_{(298)} = 2.2 \times 10^{10}\ M^{-1}s^{-1}$, and $E_a = 0.5$ kcal $mole^{-1}$; these values are comparable to those of the $S(^3P)$-alkene systems.

The $S(^1D_2, {}^3P)$ + allene reaction has been briefly examined. As in the case of 1,3-C_4H_6, only cycloaddition to one of the double bonds was observed.[63] The product, methylenethiirane,was obtained in nearly quantitative yields at low conversions and therefore insertion seems unlikely.

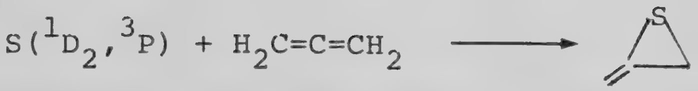

$$S(^1D_2,^3P) + H_2C=C=CH_2 \longrightarrow \quad [57]$$

No kinetic measurements were reported. However, based on the known rate parameters for the $O(^3P) + CH_2=C=CH_2$ reaction, it was suggested that the room temperature rate constant should be $\sim(2-4) \times 10^9\ M^{-1}s^{-1}$ with an E_a $\sim$0-1 kcal mole^{-1}.

(b) $O(^1D_2,\ ^3P)$ Atoms.

Only $O(^3P)$ + diene reactions have been investigated. Cvetanovic and Doyle[98] studied the reaction of $O(^3P)$ atoms with 1,3-C_4H_6 and observed the major products to be 3,4-epoxy-1-butene, 3-butanal and CO. Small amounts of fragmentation products and polymer were also observed. Based on these observations it was suggested that, similar to the case of alkenes, the sole primary process is 1,2-addition of $O(^3P)$ to one of the double bonds, producing a biradical intermediate.

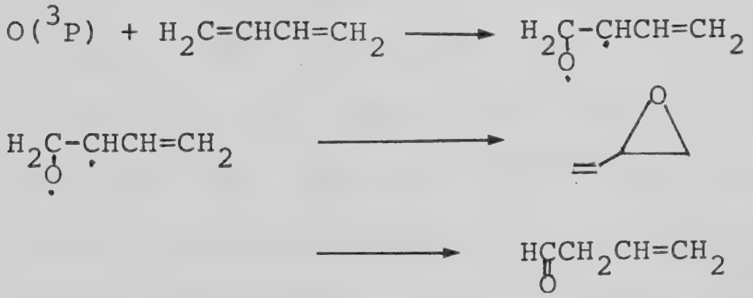

$$O(^3P) + H_2C=CHCH=CH_2 \longrightarrow H_2\underset{\dot{O}}{C}-\dot{C}HCH=CH_2 \quad [58]$$

$$H_2\underset{\dot{O}}{C}-\dot{C}HCH=CH_2 \longrightarrow \quad [59a]$$

$$\longrightarrow H\underset{\overset{\|}{O}}{C}CH_2CH=CH_2 \quad [59b]$$

This intermediate can then undergo either ring closure to form the corresponding epoxide, or 1,2-H shift to form the aldehyde. CO was thought to be a fragmentation product of the aldehyde. A later product analysis study[99] reported small amounts of 3-butene-2-one and vinylether in addition to the aldehyde and epoxide. This observation led to the proposal

that an additional isomeric biradical intermediate, 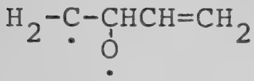 $H_2\text{-}\underset{\cdot}{C}\text{-}\underset{\underset{\cdot}{O}}{C}HCH{=}CH_2$, was also formed in the primary step.

It is apparent that both $S(^3P)$ and $O(^3P)$ atoms react with 1,3-C_4H_6 by electrophilic addition to one of the double bonds. As in the alkene systems, thiocarbonyls are absent in the $S(^3P)$ + 1,3-C_4H_6 reaction (vide supra). Furthermore, H_2 elimination to form furan, the oxygen analogue of thiophene, does not occur in the $O(^3P)$ case.

Absolute rate parameters for the $O(^3P)$ + 1,3-C_4H_6 reaction have been determined in two separate laboratories.[100,101] The results are in excellent agreement, with $k_{(298)} = 1.2 \times 10^{10} M^{-1}s^{-1}$ and $E_a \sim 0$. These results are also comparable to those measured for the $S(^3P)$ reaction.

The only other conjugated diene which has been studied is c-C_5H_6.[102] The reaction is characterized by extensive fragmentation and the absence of O - containing products.

To date only two product analyses on the $O(^3P)$ + allene reactions have been reported.[103,104] At high pressures (∿600 torr) in a static system,[103] the products observed for a series of allenes were, in general, CO, alkenes and α,β-unsaturated carbonyl compounds. The mechanism proposed to explain the formation of these products for the specific case of allene is as shown:

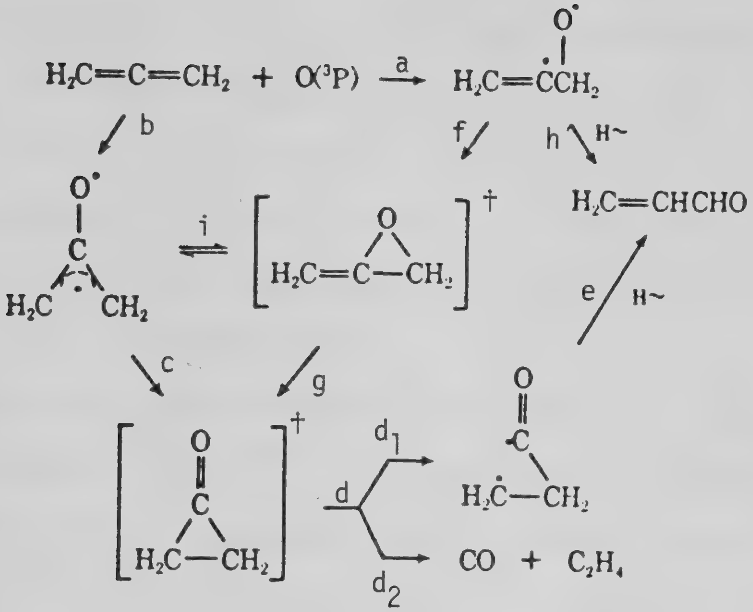

[60]

The carbonyl product distributions indicated that the O(^{3}P) atom could attack at any of the vinylic carbons at rates determined by the substituents. It was proposed that CO and alkene are formed by decarboxylation of an excited cyclopropanone (step [60d$_2$]),while carbonyls are produced by rearrangement, either of the excited cyclopropanone ([60d] + [60e]), or of the initially formed biradicals, [60h]. For every allene studied, the CO yield accounted for more than 50% of the O(^{3}P) atoms produced,indicating that decarboxylation is the major step. Evidence for the transient existence of cyclopropanone was obtained by chemical trapping with methanol to form a hemiketal. In a later study[104] of the parent allene in a low pressure flow system, Lin and co-workers failed to observe any carbonyls. Instead, significant quantities of acetylene and methyl acetylene were found. The inconsistency

in the products observed in the two studies may be attributed to the different reaction conditions employed. However Lin *et al.*'s results also support the intermediacy of an excited cyclopropanone; thus the observed CO vibrational distribution was consistent with that predicted for the decomposition of the excited cyclopropanone.

Absolute rate parameters are available only for the parent allene[100,101,105]. Values from different co-workers are in reasonable agreement, with average values $k_{(298)}$ ∿6 x 10^{10} $M^{-1}s^{-1}$ and E_a ∿1.8 kcal $mole^{-1}$. Relative rate constant measurements for a series of allenes indicate that the rate of $O(^3P)$ addition increases with alkyl substitution[103]. This behaviour parallels that of $O(^3P)$ and $S(^3P)$ + alkene reactions (*vide supra*).

E. Reactions of S and O Atoms with Carbonylsulfide and Thioethers.

1) Reaction with COS.

(a) $S(^1D_2, {}^3P)$ Atoms.

The reactions of $S(^1D_2, {}^3P)$ with COS have already been discussed in considerable detail (*vide supra*). To summarize briefly, both $S(^1D_2)$ and $S(^3P)$ abstract S from COS. The

$$S(^1D_2) + COS \longrightarrow CO + S_2 \qquad [3]$$

$$S(^3P) + COS \longrightarrow CO + S_2 \qquad [5]$$

room temperature rate constants and activation energies are:

$k_3 = 4 \times 10^{10}\ M^{-1}s^{-1}$ [5,19], $E_a < 2$ kcal mole^{-1} [14] and

$k_5 = 2 \times 10^{6}\ M^{-1}s^{-1}$, $E_a = 3.6$ kcal mole^{-1} [21]

(b) $O(^1D_2,\ ^3P)$ Atoms.

Very little data are available for the $O(^1D_2) + COS$ reaction. However, two processes have been shown to occur under low temperature (15 - 60 K) matrix conditions.[106]

$$O(^1D_2) + COS \longrightarrow CO + SO \qquad [61]$$

$$O(^1D_2) + COS \longrightarrow CO_2 + S \qquad [62]$$

In these experiments, reaction [62] was the dominant step. The estimated gas phase room temperature total rate constant is very large, $k_{298} \sim 9 \times 10^{10}\ M^{-1}s^{-1}$ [33], and is comparable to that for the $S(^1D) + COS$ reaction.

Several studies have been reported on the reaction of $O(^3P)$ with COS[107-110]. The only process operative at temperatures below 800 K is thought to be abstraction of S from COS,

$$O(^3P) + COS \longrightarrow CO + SO \qquad [63]$$

and at higher temperatures, elimination of atomic S may become important[107].

$$O(^3P) + COS \longrightarrow CO_2 + S \qquad [64]$$

Rate parameters have been determined by several techniques. The average room temperature rate constant is $\sim 8 \times 10^{6}\ M^{-1}s^{-1}$, similar to that observed for $S(^3P)$[107-110]. However the E_a is somewhat larger, ~ 5 kcal mole^{-1}.

2) Reactions with Cyclic Thioethers (Sulfides)

(a) $S(^1D_2, {}^3P)$ Atoms.

Thiiranes are the only cyclic sulfides which have been studied. Investigations have been limited to $S(^3P)$ atoms and the sole reaction is thought to be desulfurization via a single step, concerted process; for $\overline{C_2H_4S}$, the reaction products are C_2H_4 and S_2.[4,111]

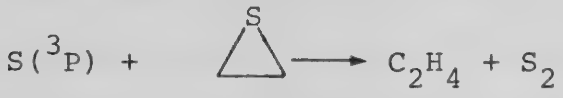

[65]

The absolute rate constant for the $S(^3P)$ + thiirane reaction has been determined by flash photolysis techniques and is temperature independent[112] with a value of $k_{65} = 2 \times 10^{10} M^{-1}s^{-1}$.[4,53,112] The rate constants for a series of thiiranes have been measured, and were found to increase with alkyl substitution.[53] This behaviour is analogous to that of the $S(^3P)$ - alkene systems (vide supra).

(b) $O(^1D_2, {}^3P)$ Atoms.

No studies on $O(^1D_2)$ + cyclic sulfide reactions have been reported. To date, only a few reactions of $O(^3P)$ atoms with cyclic sulfides have been studied.[113-115] A study of the reaction with thiirane in a fast flow - mass spectrometric system indicated that ethylene and SO were the major products[113] ([66]). These products, analogous to those of the

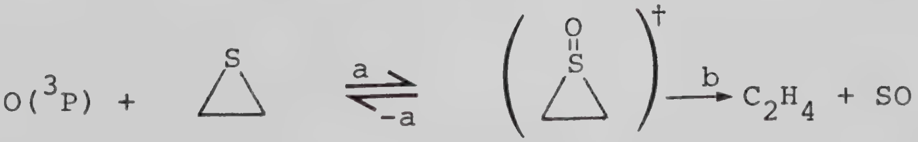

[66]

$S(^3P)$ + thiirane reactions, were postulated to arise from $O(^3P)$ attack on the S site of thiirane to form an excited sulfoxide intermediate ([66a]), which then decomposes to C_2H_4 and SO. The SO was observed as SO_2, produced by the reaction:

$$O + SO \longrightarrow SO_2 \qquad [67]$$

It is apparent that reaction [66] is analogous to S abstraction from thiirane by $S(^3P)$.

The rate constant of $O(^3P)$ addition to thiirane was determined to be $k_{66} \sim 8 \times 10^9\ M^{-1}s^{-1}$ and, as in the case of $S(^3P)$, showed no temperature dependence.

In a very recent study on the $O(^3P) + \overline{CH_2(CH_2)_2S}$ (thietane) reaction, Singleton reported that the products are C_2H_4 and $c\text{-}C_3H_6$ in a total yield of $\sim 90\%$[114]. It was suggested that the primary step was addition of the $O(^3P)$ atom to the S site, followed by C-S bond scission to form a ring opened triplet biradical. The reaction channels can be described as:

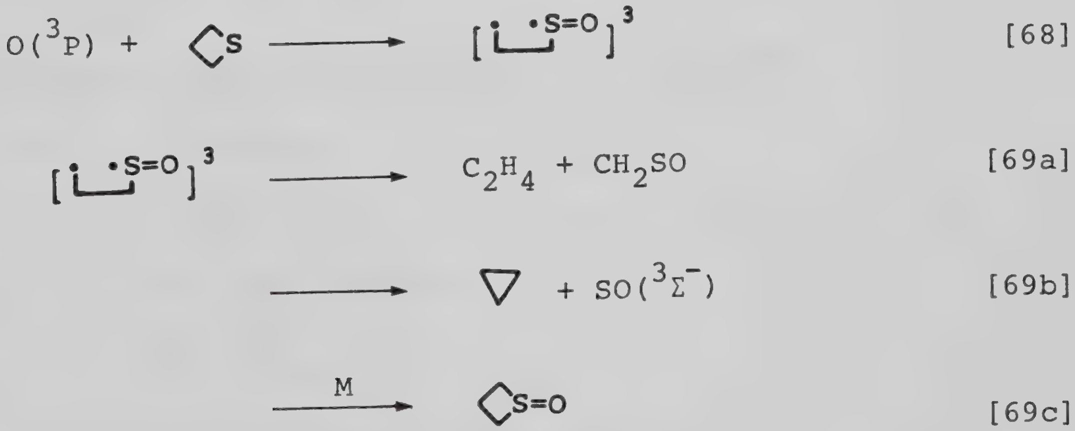

The sulfoxide which may have been formed in step [69c] was not observed, even at pressures up to 800 torr. A trace amount of C_3H_6 was also found, but it was thought to arise mostly from secondary reactions.

Relative rate measurements with 1-butene gave a room temperature rate constant of 1 x $10^{11} M^{-1}s^{-1}$, much faster than the corresponding reaction with thiirane.

The reaction of $O(^3P)$ atoms with tetrafluoro-1,3-dithietane ($\overline{CF_2SCF_2S}$) has also been studied.[119] The products observed were consistent with a primary reaction mechanism involving $O(^3P)$ addition to one of the S sites,

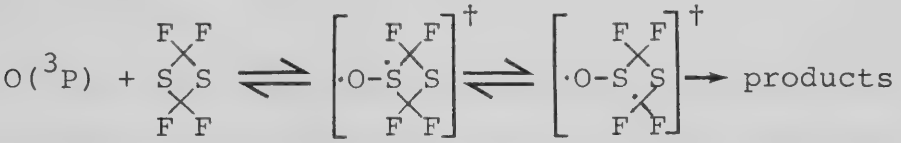

[70]

followed by decomposition via C-S bond cleavage. The rate constant measured is:[119]

$$k_{70} = 1.4 \times 10^{10} \exp(-1700/RT)\ M^{-1}s^{-1}$$

3) Reactions with Acyclic Thioethers (Sulfides)

(a) $S(^1D_2, {}^3P)$ Atoms.

To date, the reactions of S atoms with acyclic thioethers have not been reported.

(b) $O(^1D_2, {}^3P)$ Atoms.

Of the acyclic monosulfides, only CH_3SCH_3 has been studied extensively. A fast flow mass spectrometric study

of the $O(^3P) + CH_3SCH_3$ reaction detected the formation of large amounts of CH_3SO along with trace quantities of CH_3S and CH_3O[116]. It was proposed that $O(^3P)$ attacks the S site of CH_3SCH_3, forming an excited dimethylsulfoxide intermediate. This excited adduct is formed with 85-88 kcal $mole^{-1}$

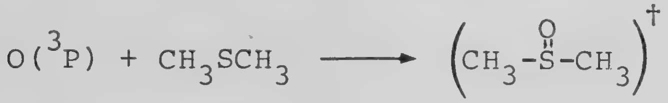

$$O(^3P) + CH_3SCH_3 \longrightarrow \left(CH_3-\overset{O}{\overset{\|}{S}}-CH_3\right)^{\dagger} \qquad [71]$$

of excess energy, exceeding the energy required for C-S bond cleavage by 23 kcal $mole^{-1}$. Therefore at low pressures the excited adduct decomposes rapidly, releasing CH_3 and CH_3SO.

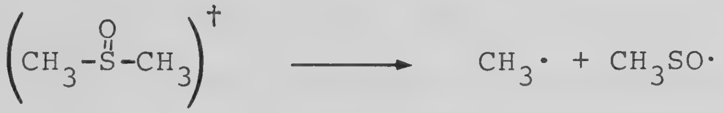

$$\left(CH_3-\overset{O}{\overset{\|}{S}}-CH_3\right)^{\dagger} \longrightarrow CH_3\cdot + CH_3SO\cdot \qquad [72a]$$

The CH_3S and CH_3O products are probably the result of rearrangement in the excited adduct followed by decomposition, although this appears to be a minor pathway.

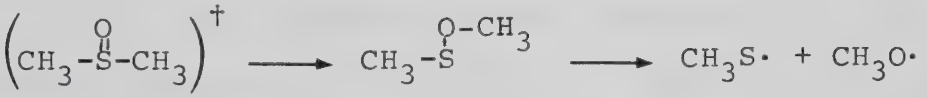

$$\left(CH_3-\overset{O}{\overset{\|}{S}}-CH_3\right)^{\dagger} \longrightarrow CH_3-\overset{O-CH_3}{\overset{|}{S}} \longrightarrow CH_3S\cdot + CH_3O\cdot \qquad [72b]$$

It was suggested that the excited adduct could also be collisionally stabilized. A second study[113] using the same technique arrived at similar conclusions regarding the reaction mechanism.

Recently, Cvetanovic and co-workers re-examined the $O(^3P) + CH_3SCH_3$ reaction in a static system[117]. End product analysis revealed two products, C_2H_6 and $(CH_3)_2S=O$. The following additional steps were considered:

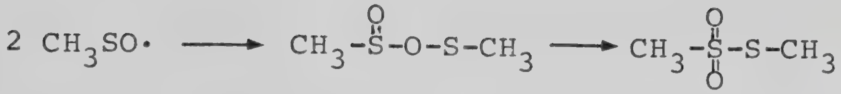

$$2\ CH_3SO\cdot \longrightarrow CH_3\text{-}\overset{O}{\overset{\|}{S}}\text{-}O\text{-}S\text{-}CH_3 \longrightarrow CH_3\text{-}\underset{\overset{\|}{O}}{\overset{O}{\overset{\|}{S}}}\text{-}S\text{-}CH_3 \qquad [73]$$

$$2\ CH_3\cdot \longrightarrow C_2H_6 \qquad [74]$$

$$CH_3\cdot + CH_3SO\cdot \rightarrow (CH_3)_2S{=}O \qquad [75]$$

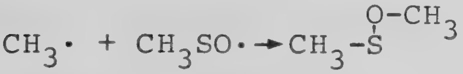

$$CH_3\cdot + CH_3SO\cdot \rightarrow CH_3\text{-}\overset{O\text{-}CH_3}{S} \qquad [76]$$

Although products formed in steps [73] and [76] were not observed, $(CH_3)_2S{=}O$ was shown to result entirely from step [75], and not from pressure stabilization of the adduct.

In a recent study[118], O_3 was photolyzed with CH_3SCH_3 in an Ar matrix. $(CH_3)_2S{=}O$ was observed, substantiating the intermediacy of $(CH_3)_2S{=}O$ proposed by other workers.

All of these observations unequivocally point to the attack of $O(^3P)$ on CH_3SCH_3 as taking place exclusively on the S atom to form an excited sulfoxide intermediate.

Absolute rate parameters measured by several techniques [113,119-121] are in good agreement. Averaging all the data available gives $k_{298} \sim 3 \times 10^{10}\ M^{-1}s^{-1}$ with $E_a \sim -0.8$ kcal mole^{-1}. These parameters also have been shown to fit the ionization potential correlations already established for alkenes.

For the case of disulfides, the $O(^3P) + CH_3SSCH_3$ reaction has been studied recently[117]. No volatile products were observed, which was explained in terms of a mechanism involving regeneration of the substrate and production of heavy and unstable compounds. It was proposed that the O atom attacks one of the S atoms of the disulfide, forming a vibrationally excited thiosulfonate,

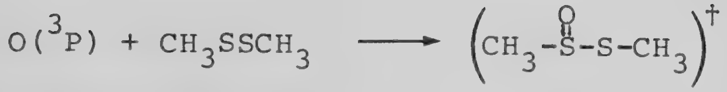

$$O(^3P) + CH_3SSCH_3 \longrightarrow \left(CH_3-\overset{O}{\overset{\|}{S}}-S-CH_3\right)^{\dagger}$$

[77]

which then decomposes via S-S bond scission.

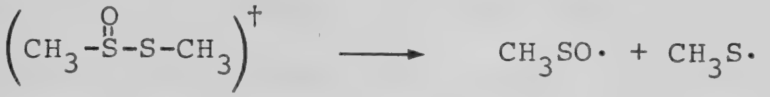

$$\left(CH_3-\overset{O}{\overset{\|}{S}}-S-CH_3\right)^{\dagger} \longrightarrow CH_3SO\cdot + CH_3S\cdot$$

[78]

Rate parameters measured by flash photolysis-resonance fluorescence[122] were $k_{(298)} = 1.2 \times 10^{11}\ M^{-1}s^{-1}$ and $E_a = 0$. On the other hand, values of $k_{(298)} = 6 \times 10^{10}\ M^{-1}s^{-1}$ and $E_a = -0.5$ kcal mole^{-1} were obtained using the phase shift technique. Nonetheless, the rate of this reaction is among the fastest of the known $O(^3P)$ reactions.

No data on the $O(^1D)$ + acyclic thioether reactions have been reported.

F. Aim of the Present Investigation

As is apparent from the foregoing discussion, studies on sulfur atom chemistry have been confined mainly to aliphatic hydrocarbons and the gross features of the reactions of $S(^1D_2, {}^3P)$ with COS, alkanes, alkenes and alkynes have been quite well defined, and a great deal of rate data are available. The reactions with dienes, however, are less well known; for allene and 1,3-butadiene, addition was the only observable reaction and no rate data are available for the former molecule. It was therefore decided to investigate the reactions of S atoms with 1,2-butadiene, for the following reasons:

- there are two distinct addition sites in this molecule, as a result of different electron densities: the relative product yields should therefore reflect the well established

electrophilic nature of $S(^3P)$ atoms.

- the presence of a methyl group allows the possibility of insertion, in competition with addition.
- insertion into vinylic C-H bonds of alkenes has been shown to take place, yet it is peculiar that insertion products were not detected in the $S(^1D_2)$ + 1,3-C_4H_6 and allene reactions; obviously, a meticulous search for insertion products is warranted.
- none of the possible unsaturated thiiranes and thiol products has been reported in the literature and they are expected to possess unusual and high reactivity.
- the availability of rate parameters for the $S(^3P)$ reaction would further extend the remarkable correlation between rate parameters and ionization potentials already delineated for S + alkene and alkyne reactions.

The reactions of sulfur atoms with COS and thiirane proceed by way of desulfurization,but other sulfur containing compounds,such as acyclic thioethers,have not been examined. It was therefore decided to first investigate the reactions of $S(^1D_2, {}^3P)$ atoms with dimethylsulfide, from the kinetic and mechanistic point of view. By analogy with the $O(^3P)$ + CH_3SCH_3 reaction it was anticipated that sulfur atoms would attack the sulfur site leading to the formation of dimethylthiosulfoxide, in which case some of the properties of this elusive molecule might be elucidated. The results would also allow useful reactivity correlations with other known

atom and radical reactions with dimethylsulfide. The S + thietane reaction was studied in order to examine the effect of adding one C atom to the thiirane ring on the nature of the primary process and the products. Also, there are more sites available for insertive attack in $\overline{CH_2(CH_2)_2S}$ as compared to $\overline{CH_2CH_2S}$, allowing some insight into the reactivity of the sulfur moiety in this molecule. It was also anticipated that this study would provide some insight into any differences between cyclic and acyclic thioether reactions.

Finally, two small projects were undertaken: when COS is photolyzed in the presence of CO_2, the CO yields have been reported to undergo a small but measurable decrease[42]. This could be due either to catalyzed recombination of $S(^3P)$ atoms, or to collisional deactivation of electronically excited COS. In order to elucidate the role of CO_2 in the photolysis of COS, it appeared desirable to reinvestigate the $COS\text{-}CO_2$ system.

The photolysis ($\lambda = 240$ nm) of thiirane generates C_2H_4 and elemental sulfur[4,111]. Although kinetic and mechanistic arguments point to the non-involvement of sulfur atoms in the photolysis, more direct evidence in this regard was warranted. Therefore, it was decided to study the vacuum flash photolysis using the same instrument as was previously employed[53] to measure rate constants for $S(^3P)$ atom reactions, and to monitor the 180.7 nm absorption line, corresponding to the $S(^3P_2 \rightarrow {}^3S_1)$ transition.

The results of these investigations are described in Appendices D and E.

CHAPTER II

EXPERIMENTAL

A. The High Vacuum System

A conventional high vacuum system constructed of Pyrex tubing was employed. The system, consisting of the photolytic assembly, two distillation units (one for purification of substrates, the other for separation of products), a storage system, and a Toepler pump-gas burette arrangement, is illustrated in Figure II-1. Rotaflo teflon plug stopcocks were used for the GC injection system and Delmar mercury float valves, Springham and Hoke helium-tested valves were used throughout to minimize the loss of products in stopcock grease. Evacuation to 10^{-6} torr was achieved by a two-stage mercury diffusion pump backed by a Welch Duoseal oil mechanical pump. Pirani tubes (Consolidated Vacuum Corporation Catalogue No. GP-001), conveniently located in the system, were used to monitor distillation and gas transferences. The McLeod gauge was used to calibrate the Pirani gauges (Type G-140). The analytical distillation unit consisted of two U-traps, a coil trap, and a solid nitrogen trap interconnected by mercury float valves. The gas chromatograph inlet system

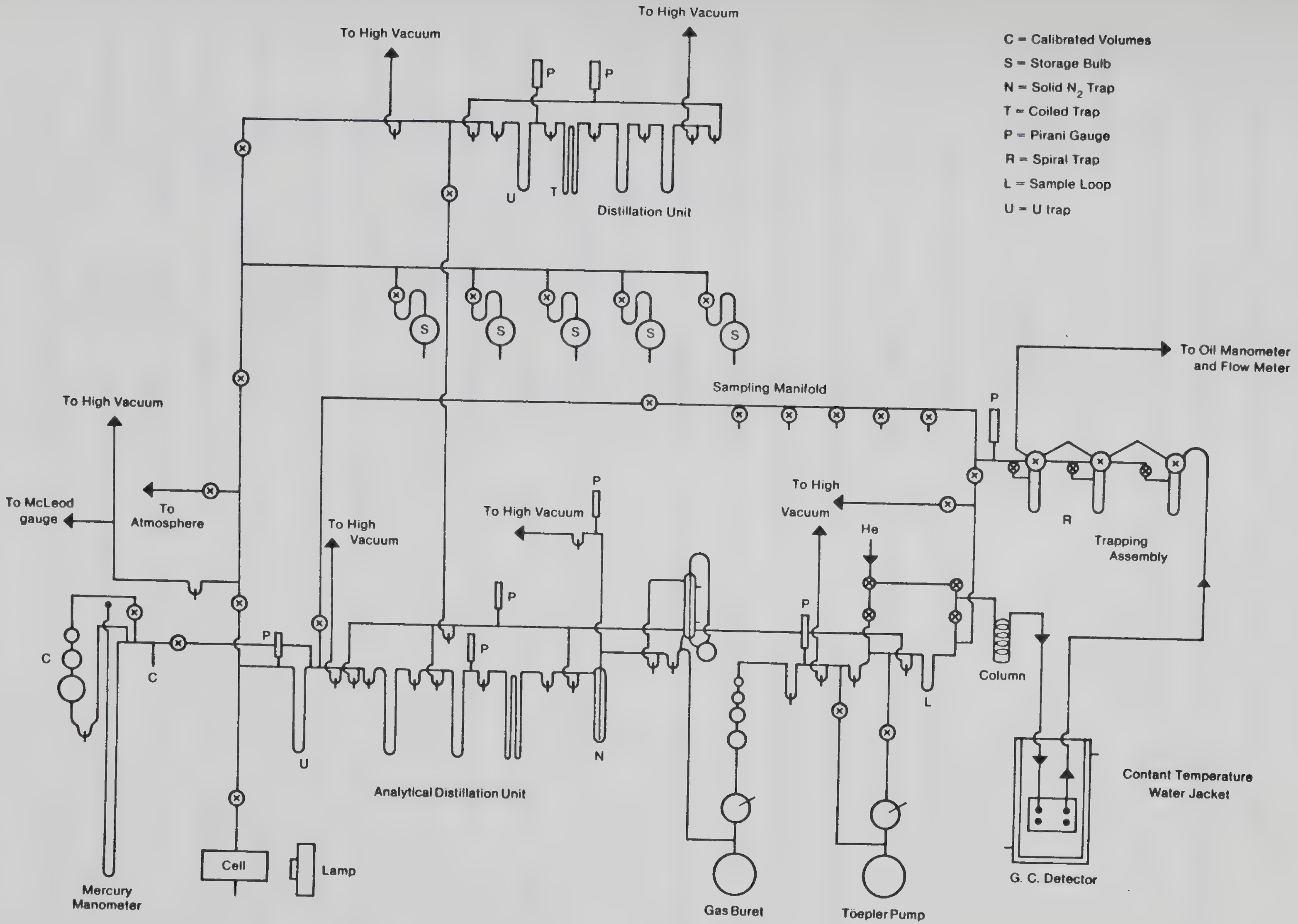
To High Vacuum
To High Vacuum
C = Calibrated Volumes
S = Storage Bulb
N = Solid N_2 Trap
T = Coiled Trap
P = Pirani Gauge
R = Spiral Trap
L = Sample Loop
U = U trap
P
P
U
T
Distillation Unit
S
S
S
S
S
To Oil Manometer and Flow Meter
Sampling Manifold
P
To High Vacuum
To McLeod gauge
To Atmosphere
To High Vacuum
To High Vacuum
P
To High Vacuum
He
R
Trapping Assembly
P
P
P
C
C
P
Column
L
U
N
Analytical Distillation Unit
Contant Temperature Water Jacket
Cell
Lamp
Mercury Manometer
Gas Buret
Töepler Pump
G. C. Detector

FIGURE II-1: The high vacuum system.

was connected directly to both the gas burette and the distillation train, thus enabling the condensable products to by-pass the Toepler pump and gas burette into the GC sampler.

B. Photolytic Assembly

A cylindrical quartz cell equipped with a cold finger (10 cm in length and 5 cm in diameter) and suprasil windows was used as the reaction vessel. A graded quartz-to-Pyrex seal attached to a high temperature Hoke valve (model 421306y) connected the cell to the high vacuum system. The reaction cell and lamp (~ 5 cm apart) were held in position by 3-pronged clamps.

The radiation source was a Hanovia medium-pressure mercury arc (model 30620). For the cases of CH_3SCH_3 and 1,2-C_4H_6, it was operated in conjunction with three 2 mm thick Vycor 7910 cut-off filters, which limited the effective radiation to > 220 nm. Because of the presence of a long wavelength absorption band (λ_{max} ~ 265 nm) in the spectrum of $\overline{CH_2(CH_2)_2S}$ (trimethylene sulfide), a 2 mm thick Vycor 7910 filter coupled with a 240 nm interference filter was required. This limited the effective radiation to ~ 240-260 nm, with the most intense radiation centered at ~ 250 nm. The lamp was allowed to warm up for an hour before

irradiation.

For temperature studies, the cell was placed in a hollowed-out cylindrical aluminum block furnace measuring 16 cm in length, 12.5 cm in external diameter and 6 cm in internal diameter. The open ends of the furnace were covered with 2 mm thick quartz plates to prevent cooling of cell faces by air currents. Surrounding the aluminum block was a one inch thick layer of fibreglass insulation. The furnace was heated by means of four 10 cm long 150 watt pencil heaters, inserted axially in the two halves of the block. Desired temperatures were maintained by an API 2-mode temperature controller. Cell temperatures (± 1°C) were measured by standard iron-constantan thermocouples and a thermometer placed in an axial hole located at the face of the block furnace.

C. Materials and Purification

1. Carbonyl sulfide (Matheson) was purified to remove CO_2 and H_2S impurities by passage through two washing bottles of saturated sodium hydroxide solutions in series with two bottles of saturated lead acetate solution. The gas was then distilled in vacuo at -139° (ethyl chloride slush) and degassed at -160° (isopentane slush).

2. Dimethyl sulfide (Terochem) was distilled in vacuo at -98°C (methanol slush). Prior to each experiment, further purification was achieved by GC on a 6 ft × 4 mm (I.D.) glass column packed with 12% tricresylphosphate on chromosorb WAW-DMCS (80/100 mesh), then degassed at -115° (ethanol slush) three times to remove any CO_2 which may have condensed during transference and storage in the GC train.
3. NO (Matheson CP grade) was distilled in vacuo at -183° (liquid argon) and degassed at -196°.
4. Propylene (Matheson, 99.7%) was distilled in vacuo at -139° and degassed at -160°.
5. O_2, CO_2 (Airco assayed reagents) were used as such.
6. 1,2-Butadiene (Chemical Sample Co., 99%) was distilled at -105° (methanol slush with traces of water) and degassed at -139° (ethyl chloride slush).
7. 1-Butene (Linde, research grade) was distilled at -115° (ethanol slush) and degassed at -196°.
8. Thietane (trimethylene sulfide, API-USBM standard sample, 99.95%) was purified prior to each measurement by GC on a 3 ft × 4 mm (I.D.) column packed with 10% squalane on chromosorb W, HP (80/100 mesh) then degassed at -105° (methanol slush with traces of water) to remove CO_2.

D. Analytical Techniques

1. Gas chromatography was used for the quantitative analysis of products and for purification of substrates. The unit consisted of a Gow-Mac power supply model 24-500 and a home made micro volume cell detector fitted with a pair of Gow-Mac 13-502 thermistors, operated at 30° with a bridge current of 8 mA. The temperature of the detector was kept constant by a Colora circulation bath connected to a water jacket, which housed the detector block. Signals were fed into a Hewlett-Packard model 7101 B strip chart recorder.

   The carrier gas was helium (Linde), purified by passage through a trap of molecular sieve 5A (1/16" pellets) at -196°. Flow control was attained by an NRS needle control valve (model A-12) and the flow rate was measured on a bubble flow meter.

   GC columns were constructed of Pyrex or quartz glass or teflon tubing and were connected to the apparatus by means of Beckman teflon tube fittings No. 404. Column temperature was maintained by a water bath. Tables II-1 and 2 summarize the columns used, the retention times and operating conditions for all the analyses and purifications reported in this work.

TABLE II-1

Columns Used

Column No.	Description
I	3 ft × 2 mm I.D. glass column packed with 80/100 mesh molecular sieve 5A.
II	6 ft × 2 mm I.D. glass column packed with 80/100 mesh porapak N.
III	6 ft × 2 mm I.D. glass column packed with 45/60 mesh molecular sieve 13X.
IV	4 ft × 4 mm I.D. glass column packed with 10% tricresylphosphate on 80/100 mesh chromosorb W,AW-DMCS.
V	2 ft × 2.5 mm I.D. teflon column packed with 3% OV-101 on 80/100 mesh chromosorb W,HP (Chromatographic Specialties Ltd.).
VI	6 ft × 4 mm I.D. glass column packed with 12% tricresylphosphate on 80/100 mesh chromosorb W,AW-DMCS.
VII	5 ft × 2.5 mm I.D. teflon column packed with 80/100 mesh porapak QS.
VIII	7 ft × 2 mm I.D. quartz column packed with 5% Ucon polar 50 HB 2000 on 80/100 mesh chromosorb P,AW-DMCS (Chromatographic Specialties Ltd.).
IX	3 ft × 4 mm I.D. glass column packed with 10% squalane on 80/100 mesh chromosorb W,HP.
X	6 ft × 2 mm I.D. glass column packed with 5% SP-300 on 100/120 mesh Supelcoport (Supelco Inc.).

TABLE II-2

G.C. Operating Conditions and Retention Times[a]

Compound	Structure	Column	Column Temperature (°C)	Retention Time (min.)
Methane	CH_4	I	27	2.9
Ethane	C_2H_6	II III[b]	27 27	9.5 15.0
Dimethyldisulfide	CH_3SSCH_3	IV V[c]	32 35	35.0 2.5
Methylthiirane	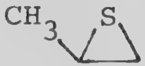	VI	32	21.0
Carbon dioxide	CO_2	VII	40	1.8
Water	H_2O	VII	40	14.0
Sulfur dioxide	SO_2	VII	40	25.4
Ethylthiirane	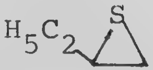	VIII	14	34.6
2-Methyl-3-methylenethiirane (1)	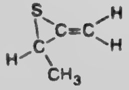	VIII X[d]	14 10	24.5 5.0

(continued)

TABLE II-2 (Continued)

Compound	Structure	Column	Column Temperature (°C)	Retention Time (min.)
1,3-Butadiene-2-Thiol (2)	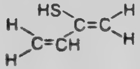	VIII	14	42.4
cis-Ethylidenethiirane (3)	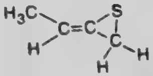	VIII	14	50.7
trans-Ethylidenethiirane (4)	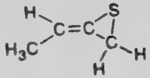	VIII	14	68.2
2,3-Butadiene-1-thiol (5)	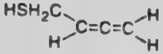	VIII	14	78.6
1,2-Dithiolane	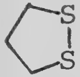	IX	50	45
Dimethylsulfide	CH_3-S-CH_3	IV VI	32 32	4.0 6.0
Thietane (Trimethylene Sulfide)	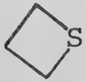	IX	50	6.0

[a] He flow rate, 25 ml min^{-1}.

[b] Used only when a large amount of CO_2 was present as an additive.

[c] Used only in the search for $CH_3(S)_4CH_3$.

[d] Used for the attempted separation of the optical isomers of 1.

Coated column packings were prepared by the "funnel coating method" as described by McNair and Bonelli[123], and the % coating was checked after the preparation. Occasionally, commercially coated supports were used.

GC effluents could be directed through a series of coiled traps at -196° (Figure II-1) in which the desired compounds could be trapped for further analysis and identification. Product identification was achieved initially by comparing the GC retention times with those of authentic samples, whenever possible, followed by spectral analysis.

A direct calibration for the detector response was made for nearly all the products. Standard samples of methane, ethane, ethylene, dimethylsulfide, dimethyldisulfide, methylthiirane and thietane (trimethylene sulfide) were available and others were obtained in vacuo by collecting the reaction products individually. Samples purified by GC were measured in the gas burette and the resulting peak areas were measured with an Ott planimeter. The response was always linear over the range of yields obtained from typical experiments and the calibrations were reproducible to better than $\sim$5%. In the case of 1,2-dithiolane ($\overline{\mathrm{CH_2(CH_2)_2SS}}$), the molar response was

estimated indirectly by assuming that the addition of a sulfur atom to thietane causes the same molar response change as in the case of dimethylsulfide. Therefore the molar response, R of 1,2-dithiolane was calculated from the relationship:

$$R_{(1,2\text{-dithiolane})} = \frac{R_{(\text{dimethyldisulfide})}}{R_{(\text{dimethylsulfide})}} \times R_{(\text{thietane})}$$

2. UV, NMR, IR and mass spectral analyses were used for qualitative identification of products.
   (a) For mass spectral analysis, samples from the GC effluent were distilled into GC/MS tubes, sealed in vacuo and stored at -196° until use. Mass spectra were obtained on an AEI MS-12 instrument with the ion source operating at 70 eV and the temperature of the ionization chamber was kept at ca 50°. Samples were analyzed on an appropriate GC column adapted to the MS-12 chromatograph (Varian Aerograph series 1400). In the case of solid samples, analyses were done individually by the direct probe method.
   (b) NMR spectra were generally obtained on a Bruker WH-400 spectrometer and occasionally on a WH-200 spectrometer. For volatile compounds, spectral

grade $CDCl_3$, used as a solvent, was degassed in pyrex medium wall NMR tubes. The trace quantity of $CHCl_3$ present in $CDCl_3$ also served as an internal standard. GC purified samples were then condensed into the tubes, which were then sealed under vacuum. For solid compounds, thin wall NMR tubes were used and the solutions were prepared by simply dissolving the solid samples in $CDCl_3$. Analyses were generally done at -30° or at room temperature, depending on the stability of the compound being analyzed.

(c) Infrared spectra were obtained in the gas phase or in Ar-matrix on a Nicolet 7199 FTIR spectrometer. Samples were purified by GC and distilled into a 10 cm × 1.9 cm cylindrical quartz cell fitted with Kodak ZnS polycrystal windows, or into an ordinary Pyrex tube fitted with a grease stopcock for later deposition of the sample into an Ar-matrix.

(d) UV spectra were obtained in the gas phase on a Unicam SP-1700 spectrometer using a 10 cm × 1.9 cm quartz cell fitted with suprasil windows. A UV spectrum of 1,2-dithiolane in methanol was also obtained on the same instrument.

E. Operating Procedures

Reactant pressures above 50 torr were measured on the manometer with the aid of a cathetometer (Guffin and George Ltd.). Calibrated volumes of various sizes (see Figure II-1) were used to prepare substrate pressures below 50 torr. The reactant mixtures were distilled into the cell through the U trap at the lowest temperature allowed by the vapour pressure of the substrates and allowed to mix overnight prior to irradiation. In those cases where there was only one substrate, at least one hour was allowed for equilibration.

In determining R°_{CO}, the rate of carbon monoxide formation from pure COS, short conversion runs producing less than 3 μmoles of CO were generally used to minimize the amount of deposition of elemental sulfur on the cell window.

After irradiation, the cell contents were frozen into the cell cold finger at -196° and non-condensable products, such as carbon monoxide and methane, were transferred through a series of traps at -196° via the Toepler pump in conjunction with the single stage mercury diffusion pump to the gas burette. To ensure complete removal of all non-condensable products, the condensable materials were alternately thawed and refrozen at least twice with the non-condensable gases being removed each time. In the cases

where NO or C_2H_4 was present, a solid nitrogen trap (-210°) was used. After being measured in the gas burette, the non-condensable products were transferred to the GC inlet where the amount of CH_4 could be determined chromatographically. This was then subtracted from the gas burette measurement, thus enabling quantitative determination of CO.

NO in the solid nitrogen trap was removed at -183° (liquid Ar). Other light hydrocarbon products and the excess reactants were separated from the sulfur products by distillation through three traps at appropriate low temperatures, as indicated below:

1) ethylene, at -183° (liquid Ar), collected in the gas burette and analyzed by GC.
2) ethane, at -160° (isopentane slush), and measured chromatographically.
3) COS, CO_2, and propylene at -139° (ethyl chloride slush).
4) 1,2-butadiene and 1-butene at -115° (ethanol slush)

The remaining condensable fraction, which contained the sulfur product(s), was distilled into the GC sample inlet for analysis. In the cases where dimethylsulfide, or $\overline{CH_2(CH_2)_2S}$ was the substrate, the substrate was transferred together with the sulfur products directly into the GC sampler and separated chromatographically.

After each experiment, the cell was cleaned by

admitting air and heating with an oxygen flame to remove elemental sulfur and/or polymer which deposited on the cell windows during irradiation, thereby reducing the effective light intensity.

F. Microwave Discharge Experiments for the COS-CH_3SCH_3 System

O_2 was used as an oxidant for the solid cell residue remaining after high conversion experiments. Complete oxidation was achieved by microwave discharge for 2 hours. After the discharge, the O_2 was separated from the oxidation products by careful distillation through three traps at -183° (liquid Ar). The oxidized cell contents were then subjected to GC analysis. The microwave discharge unit was a Baird Atomic Inc. Hg-Microwave Exciter Series No. EY-55.

CHAPTER III

REACTIONS OF SULFUR ATOMS WITH 1,2-BUTADIENE

A. Results

The U.V. absorption spectrum of 1,2-butadiene indicates that it has significant absorption in the region used for COS photolysis. The extinction coefficients at 298 K for 1,2-C_4H_6 at 240 and 254 nm are 9.71 and 0.724 l mole^{-1}cm^{-1}, respectively. The corresponding coefficients for COS are 31.8 and 13.6 l mole^{-1}cm^{-1}. A COS/1,2-C_4H_6 ratio of 4:1 was chosen in most cases, which ensured that >93% of the incident radiation was absorbed by COS at 240 nm and >99% at 254 nm. Even at the lowest COS/1,2-C_4H_6 ratio (2:1) used, >90% and >97% of the radiation was absorbed by COS at 240 and 254 nm, respectively.

1. Reaction Products

The photolysis of COS in the presence of 1,2-C_4H_6 led to the formation of five chromatographically separable sulfur addition products (**1**, **2**, **3**, **4** and **5**). The mass spectra indicated that all five products were of molecular weight 86, corresponding to the molecular formula C_4H_6S. A GC/MS study with a mass 86 cross-scan showed the presence of two additional mass 86 peaks, **6** and **7** (Figure III-1). Unfortunately, these two products were formed in very minute quantities, so that further spectral analyses were not possible. The possibility that either of these compounds is vinylthiirane

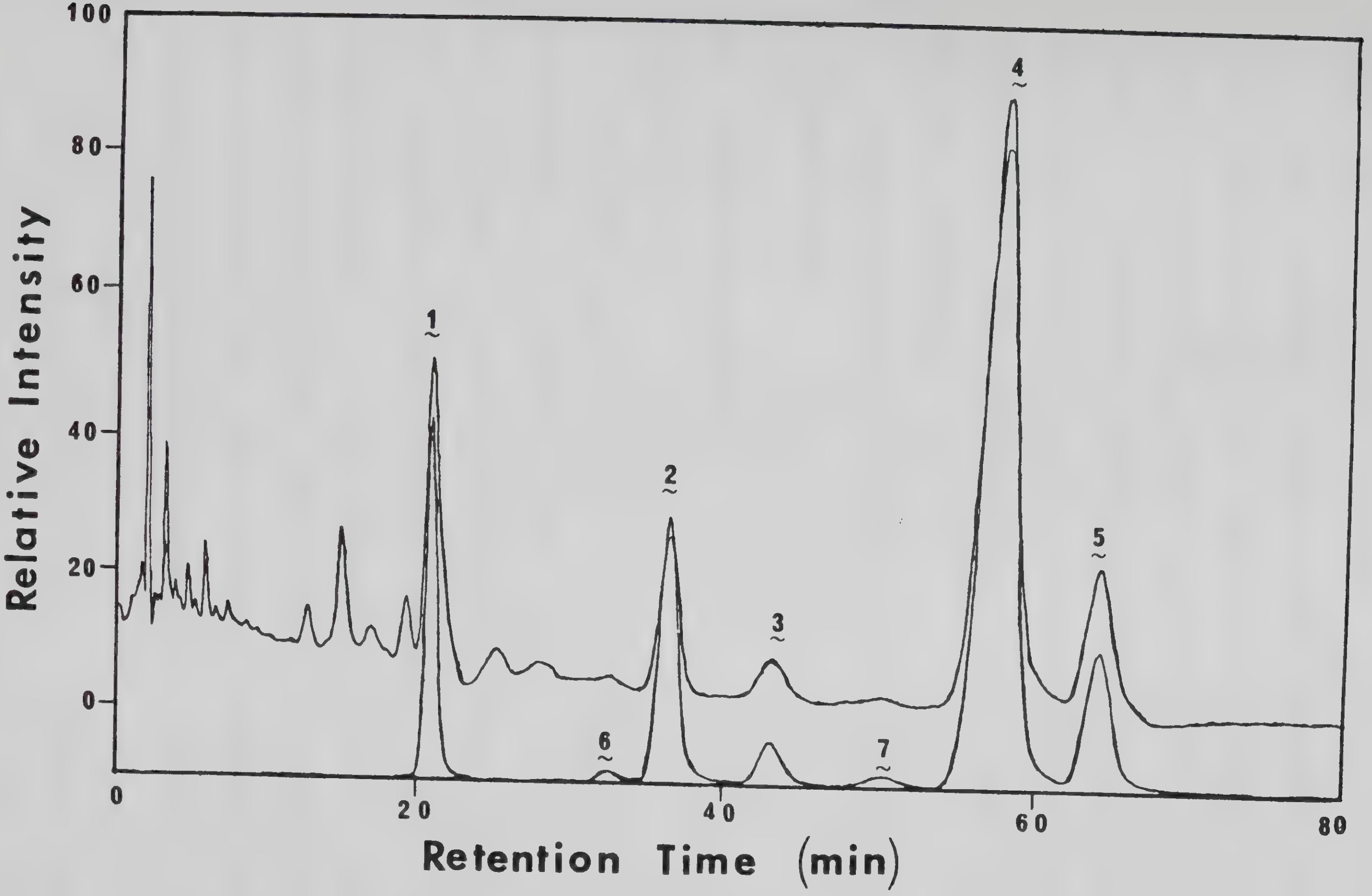

FIGURE III-1: G.C./M.S. (m/e = 86) cross scan.

(a product of the reaction of S atoms with 1,3-butadiene, which may be present as an impurity)[25] was ruled out by comparison of the mass spectra.

The five major products could be collected in sufficient quantities for NMR analysis at 400 MHz. Gas phase IR and UV analyses were also performed for products **1**, **4** and **5**. Ar matrix IR and gas phase IR analyses performed on **2** and **3**, respectively, were unsuccessful due to their small yields and low stability. UV analysis of **2** and **3** was not attempted.

The mass spectra of the seven S products are tabulated in Appendix A-1.

a) Indentifications:

Product **1**

The NMR spectrum of product **1** (Figure III-2) shows four resonances of relative intensities 1:1:1:3 (H_A:H_B:H_C:H_D). Two of these (H_A and H_B) are in the vinylic region, at δ= 5.62 and δ=5.21 respectively. Proton H_A is a triplet with a splitting of 1.6 Hz and proton H_B is also a triplet, with a splitting of 1.8 Hz. Proton H_C, at δ=3.26, shows a triplet splitting of 1.7 Hz and a quartet splitting of 5.8 Hz. This latter splitting is the same as that of protons H_D, which is a doublet at δ=1.55 (methyl region).

The relative area and chemical shifts of protons H_D correspond to a methyl group. The relatively large coupling of 5.8 Hz between H_D and H_C implies that they are close to

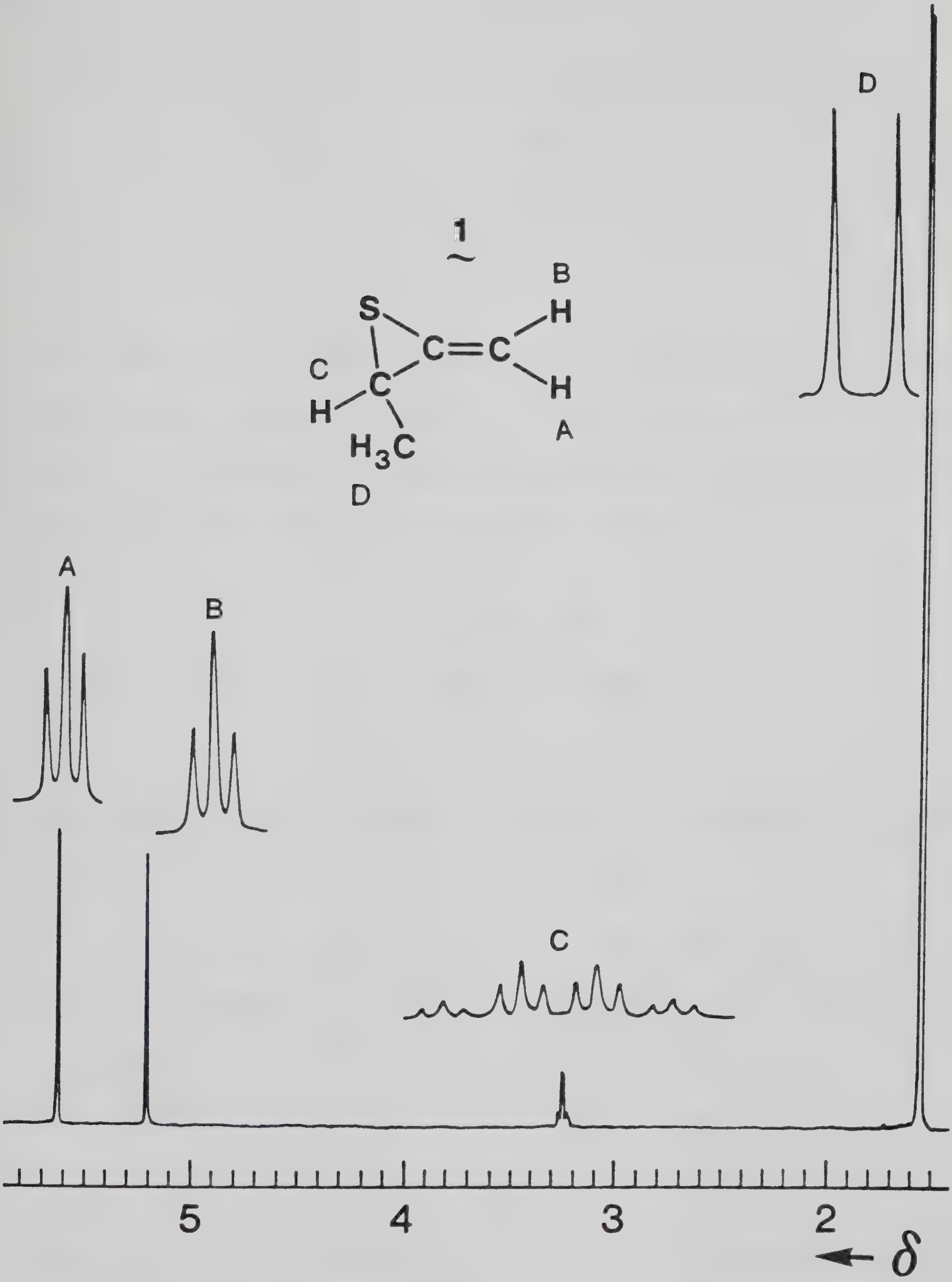

FIGURE III-2: NMR spectrum of 2-methyl-3-methylenethiirane (1). Note that the purpose of the expanded resonance lines is to show the splittings qualitatively.

each other (not more than three bonds apart) as shown:

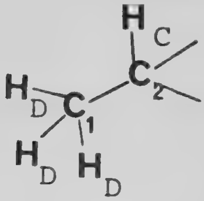
H C
C 2
H D
C 1
H D
H D

The fact that H_A and H_B are vinylic means that the other two carbon atoms (C_3 and C_4) of the molecule form a vinyl group. Consequently the fourth bond of the second carbon atom, C_2, must be to the S atom as shown:

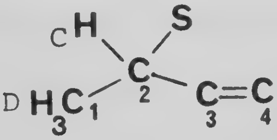
C H
S
C 2
D H3C 1
C=C
3 4

According to the molecular formula, a ring must be present. Hence only two structures are possible:

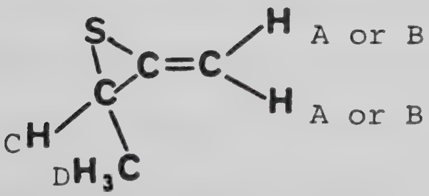
S
C=C
H A or B
H A or B
C
C H
D H3C

(I)

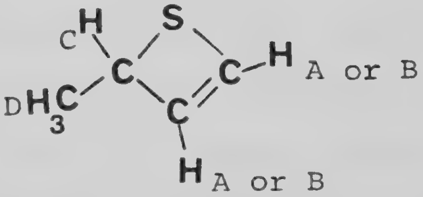
C H
S
C
C-H A or B
D H3C
C
H A or B

(II)

The cis vinylic protons (H_A and H_B) in structure (II) would have a coupling constant of at least 5 Hz (generally 7-10 Hz). However, from the spectrum, $J_{AB} \simeq 1.6-1.8$ Hz, which is a typical geminal vinylic coupling constant. This is consistent with structure (I). Finally, an -SR group on

a substituted ethylene will shift a proton cis to it to higher field (lower δ) than one trans to it. Since H_A is at δ=5.62 and H_B is at δ=5.21, H_B is assigned to be cis to the S atom. Thus 1 is 2-methyl-3-methylenethiirane, with the structure:

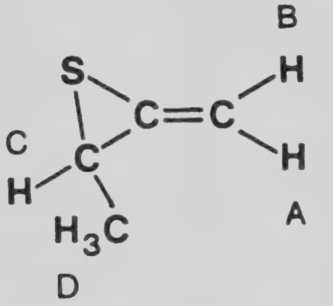

The IR spectrum of 1 (Figure III-3) is consistent with this assignment. Thus the strong absorption at ∿840 cm^{-1} corresponds to the out of plane C-H deformation of a disubstituted ethylene of the type $R_1R_2C=CH_2$ shifted from its normal value of ∿900 cm^{-1} to lower frequency due to the presence of an adjacent oxygen or sulfur atom.[125] The medium absorption at 1715 cm^{-1} corresponds to the C=C bond stretching. The C-H stretching frequencies at ∿3008 and ∿2970 cm^{-1} probably correspond to those of ring C-H stretch reported for vinylthiirane.[25] Also, the vinyl C-H stretch region of this spectrum bears a strong resemblance to that reported for methylenethiirane.[63]

As is apparent from the structure derived, 1 possesses a chiral center at C_2:

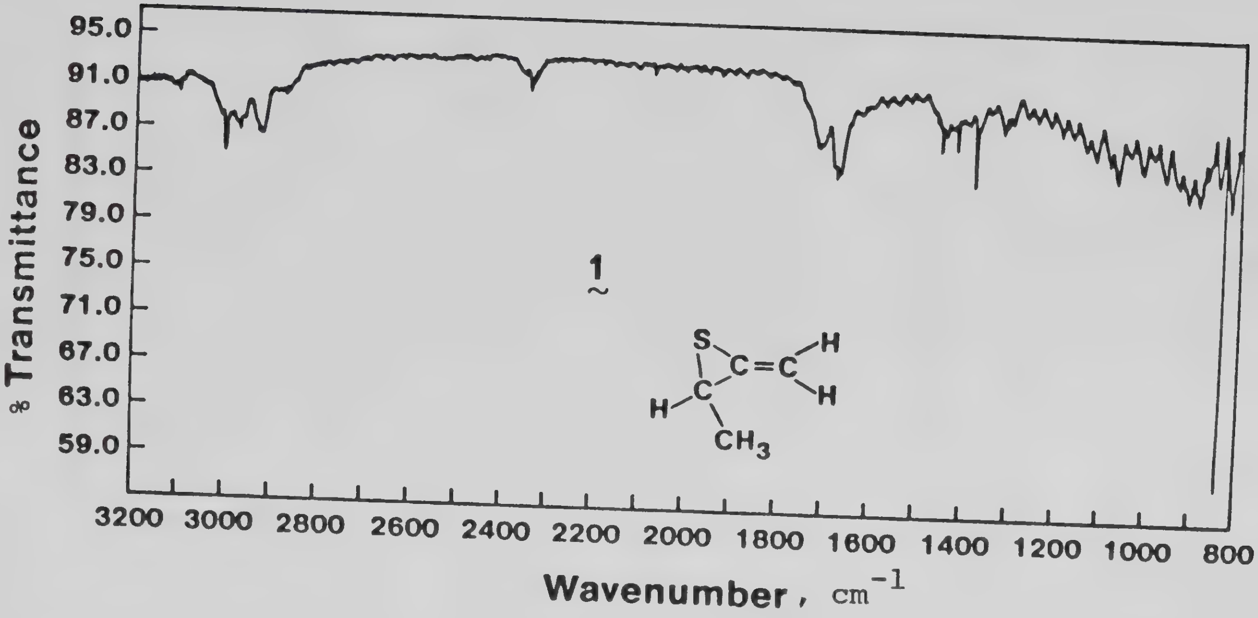

FIGURE III-3: The gas phase FTIR spectrum of 2-methyl-3-methylenethiirane (1).

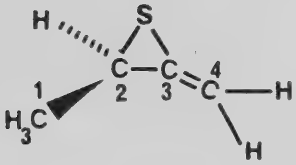

1

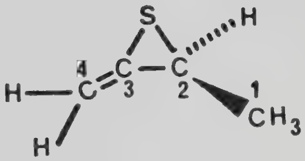

1

Attempts to separate the optical isomers of 1 by G.C. using a chiral stationary phase[126] proved unsuccessful.

Product 2

The NMR spectrum of product 2 (Figure III-4) shows five resonances of roughly equal areas in the vinylic region: proton H_A at $\delta=6.48$, which shows doublet splittings of 16.8 Hz and 10.4 Hz; proton H_B, with a doublet splitting of 16.8 Hz, at $\delta=5.41$; proton H_C, with a doublet splitting of 10.4 Hz at $\delta=5.26$; proton H_D, a broad singlet at $\delta=5.36$; and proton H_E, at $\delta=5.31$, with a doublet splitting of 0.5 Hz. Resonances H_A, H_C and H_B show additional unresolved splittings. A sixth resonance, due to proton H_F, occurring in the vinylic -SH region, is a singlet at $\delta=2.96$.

Proton H_A has common splittings with H_B ($J_{AB}=16.8$ Hz) and with proton H_C ($J_{AC}=10.4$ Hz), indicating that H_A is coupled to these two protons. Furthermore, $J_{AB}=16.8$ Hz is a typical coupling constant for protons trans across a double bond, and $J_{AC}=10.4$ Hz is typical of a cis coupling. Therefore protons H_A, H_B and H_C all belong to the same

2

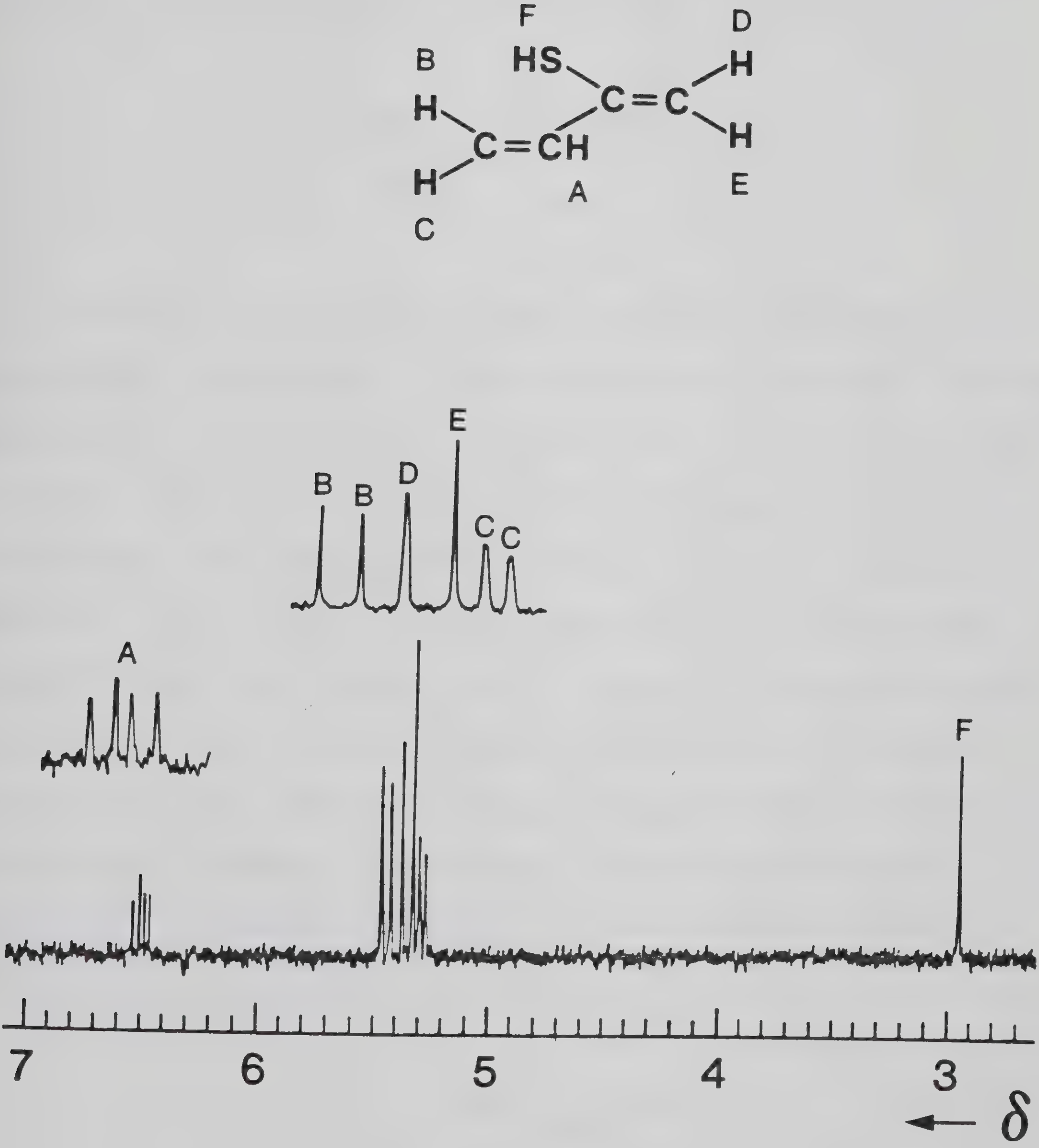

FIGURE III-4: NMR spectrum of 1,3-butadiene-2-thiol (2).

vinyl group. Protons H_D and H_E are also vinylic, indicating the presence of a second vinyl group in the molecule. The molecular formula (C_4H_6S) requires that these two vinyl groups must be conjugated to each other as shown:

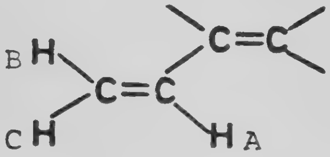

Some of the unresolved splittings were determined by decoupling experiments. The results show additional coupling constants: $0<J_{AD}<0.5$ Hz, $0<J_{DE}<0.5$ Hz, $J_{AE}=0.5$ Hz and $J_{CD}=$ 1.2 Hz. The small coupling constant between H_D and H_E is consistent only with a geminal configuration for these two protons. Thus they are on the terminal end of the second double bond. This leaves the -SH group on the substituted end of the double bond. Finally, the relation of protons H_D and H_E to the -SH group (cis or trans) still needs to be determined. However, additional information can still be obtained by comparing the coupling constants of product 2 with those of 2-chloro-1,3-butadiene.[127]

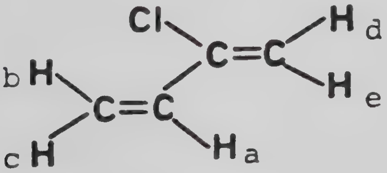

For 2-chloro-1,3 butadiene, the coupling constants are:

J_{ae}=0.60 Hz J_{cd}=1.4 Hz

J_{ad}=0.20 Hz J_{ce}=0.5 Hz

For product 2 the corresponding coupling constants are:

J_{AE}=0.5 Hz J_{CD}=1.2 Hz

$J_{AD}<0.5$ Hz $J_{CE}<0.5$ Hz

These similarities in the coupling constants (J_{ae} & J_{AE}, J_{ad} & J_{AD}, J_{cd} & J_{CD}, and J_{ce} & J_{CE}) strongly support the assignment of H_D as the proton cis to the -SH group. Therefore 2 is 1,3-butadiene-2-thiol, with the following structure:

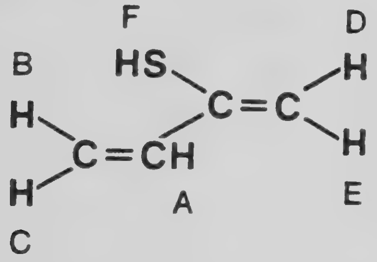

Product 3

The NMR spectrum of product 3 (Figure III-5) shows only three resonances, with relative intensities 1:2:3 (H_A:H_B:H_C). There is only one vinylic proton, H_A, occurring at δ=6.05, with a quartet splitting of 6.5 Hz and a triplet splitting of 1.6 Hz. Protons H_B, located at δ=2.77, show an apparent quintet splitting of 1.5 Hz. The third resonance, located at δ=1.89 (methyl region) is due to protons H_C. This shows a doublet splitting of 6.6 Hz and a triplet splitting of 1.5 Hz.

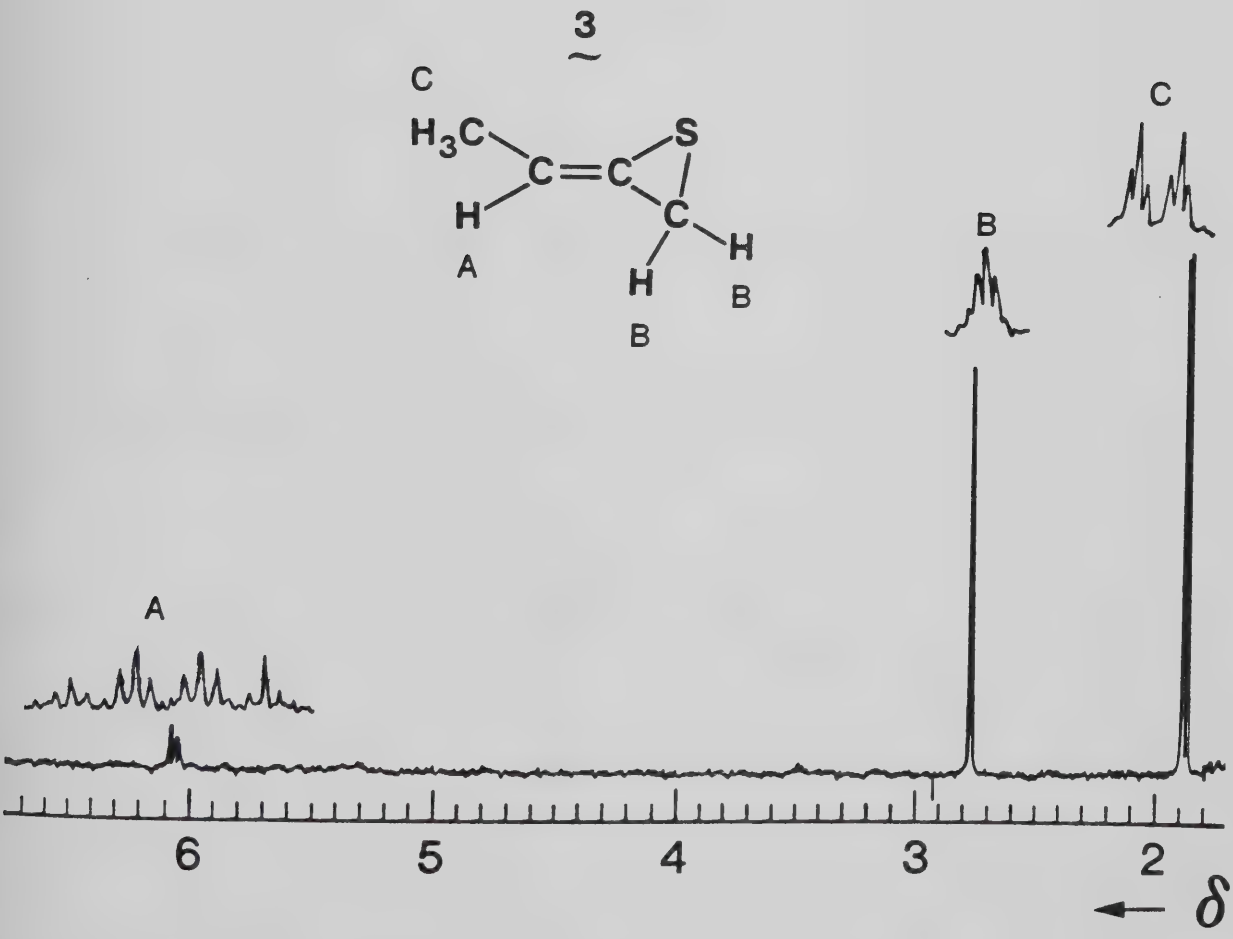

FIGURE III-5: NMR spectrum of cis ethylidenethiirane (3).

The area and location of H_C indicate that this signal is due to a $-CH_3$ group. The relatively large coupling constant between protons H_C and the vinylic proton H_A (J_{AC} = 6.5 Hz) implies that they are separated by three bonds at the most:

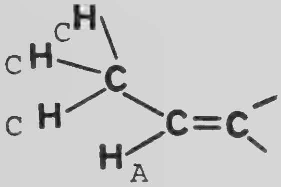

As protons H_B are not vinylic, the molecular formula requires that product 3 contain a ring. The only ring containing structure that is consistent with the partial structure shown above is either cis or trans ethylidenethiirane.

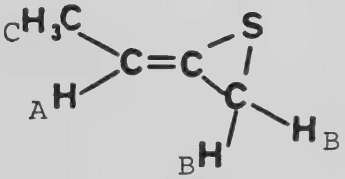

cis OR trans

The question of the isomeric identity of product 3 will be discussed together with that of product 4.

Product 4

Similar to product 3, the NMR spectrum of product 4 (Figure III-6) shows three resonances of relative intensities 1:2:3 (H_A:H_B:H_C). The single vinylic proton, H_A, located

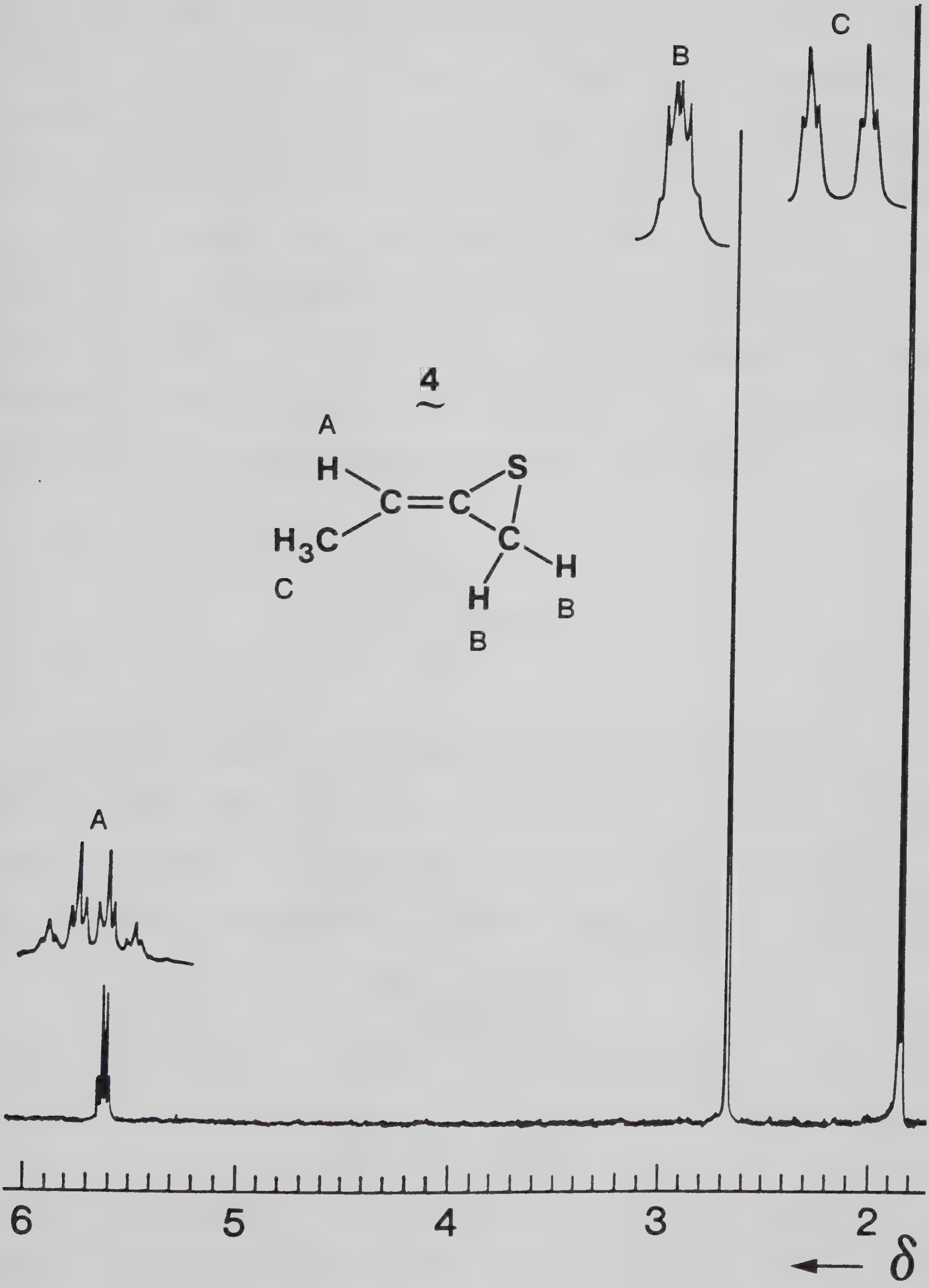

FIGURE III-6: NMR spectrum of trans ethylidenethiirane (4).

at δ=5.62, has a quartet splitting of 6.8 Hz and a triplet splitting of 1.8 Hz. Protons H_B appear as a multiplet at δ=2.66. Protons H_C, at δ=1.82 ($-CH_3$ region), show a doublet splitting of 6.9 Hz and a triplet splitting of 1.0 Hz.

The relative area and chemical shift of protons H_C indicate that they form a methyl group, as in the case of product 3. The relatively large coupling constant between protons H_C and H_A (J_{AC}=6.8 Hz) implies that these two protons are at the most three bonds apart as shown:

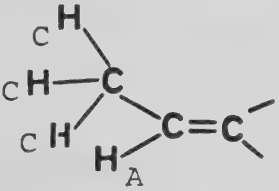

Since protons H_B are not vinylic, the molecular formula requires that product 4 must contain a ring, as in the case of product 3. Therefore, product 4 must be the geometric isomer of product 3, cis or trans ethylidenethiirane:

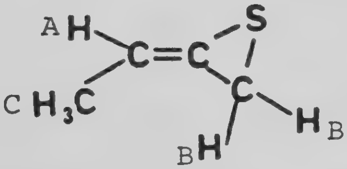

cis OR trans

The question of the assignment of cis and trans geometry to products 3 and 4 was resolved by examination of chemical shifts. Additional evidence, though not compelling, was obtained from an nOe (nuclear Overhauser effect) experiment on product 4.

Assignment of cis and trans geometry to products 3 and 4:

a) Chemical shift assignment

Chemical shift tables[123] indicate that in substituted ethylenes (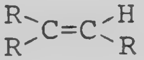 $R_2C=CHR$) , an -SR group shifts a proton cis to it by about 0.24 ppm to higher field (lower δ) relative to the unsubstituted ethylene, and a trans proton will be shifted by only 0.04 ppm to higher field as shown:

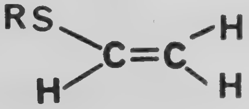

(cis) -0.24 ppm.
(trans) -0.04 ppm.

Therefore it should be possible to assign the geometry of isomers 3 and 4 by examining the relative chemical shifts of protons H_A for these two compounds. In the trans isomer,

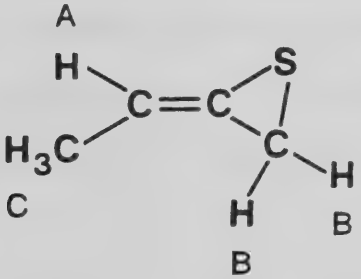

trans isomer

proton H_A is cis to the S atom. Therefore in this case, the H_A resonance is roughly 0.2 ppm to higher field than the H_A resonance in the cis isomer (H_A is trans to the S atom).

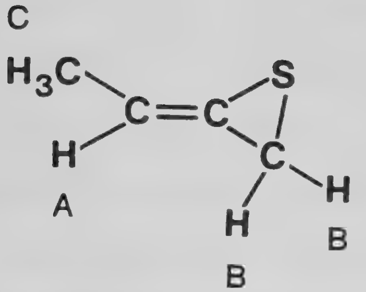

cis isomer

Since the H_A resonance in product **4** is 0.43 ppm to higher field than the H_A resonance of product **3** (6.05 ppm-5.62 ppm; H_A of **3** at $\delta=6.05$, H_A of **4** at $\delta=5.62$), it is reasonable to conclude that **4** is the *trans* isomer, and **3** is the *cis* isomer. The chemical shift difference obtained experimentally is larger than that predicted (0.43 *versus* 0.2 ppm). However, this is not surprising since the chemical shift quoted from the literature represents an average value only. Moreover, the shift caused by an S atom in a small ring is not necessarily identical to that caused by an -SR group. In fact, this chemical shift difference for the *cis* and *trans* (to the S atom) H_A protons of 0.43 ppm is in excellent agreement with that of product **1** (H_A, *trans* at $\delta=5.62$, H_B, *cis* at $\delta=5.21$).

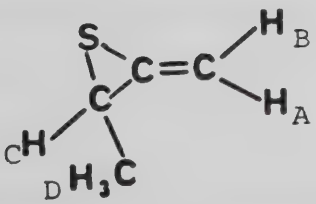

, *cis* $\delta=5.21$

, *trans* $\delta=5.62$

b. Nuclear Overhauser effect (nOe) evidence:

In an attempt to further confirm the isoméric assignment of **3** and **4**, a nuclear Overhauser effect (nOe) experiment

was performed on product 4. (It was not possible to collect sufficient quantities of 3 to perform a similar study.)

Basically, the nOe is a change in intensity of one NMR signal when another one is saturated. In simple cases, the nOe between two protons in a molecule can be calculated from the geometry of the molecule. Therefore it should be possible to predict nOe's for the *cis* and *trans* isomers 3 and 4. Using literature values of bond lengths and angles for methylenethiirane,[128] nOe's were calculated for the *cis* and *trans* isomers (Appendix B). These values were compared with the experimental ones obtained for 4 (Table III-1).

As shown in Table III-1, the signal for the H_B protons increased by a factor of 0.013 when the resonance of the methyl protons H_C was saturated. The predicted enhancements are 0.001 for the *cis* isomer and 0.069 for the *trans* isomer. Therefore the observation of a non-zero nOe (0.013 *versus* 0.069 predicted) at the H_B resonance when the H_C resonance was saturated can be taken as supporting evidence for the *trans* assignment of 4. However, the observation of such a small nOe is not very convincing, and the strongest arguments in favour of the geometric assignments are based on chemical shift data.

The IR spectrum of 4 (Figure III-7) is, as expected, similar to that of 1. Evidence for the presence of a vinyl group comes from the characteristic absorption at ∿3060 cm^{-1} (=CH), and the out of plane deformation at ∿895 cm^{-1}.

TABLE III-1

Calculated and Observed Nuclear Overhauser Effect (nOe) for the *cis* and *trans* Isomers of Ethylidenethiirane.

Proton(s) saturated	Proton(s) observed	Calculated nOe		Observed nOe (*trans* isomer, 4)
		cis	*trans*	
CH_2(B)	H(A)	0.019	0.006	0
CH_3(C)	H(A)	0.481	0.488	0.42
CH_3(C)	CH_2(B)	0.001	0.069	0.013
H(A)	CH_2(B)	0.004	0.0001	not done
H(A)	CH_3(C)	0.023	0.024	not done
CH_2(B)	CH_3(C)	0.0003	0.047	0[a]

[a] Spin-rotation relaxation of the CH_3 group may have decreased the nOe that would have been observed in this case.[129]

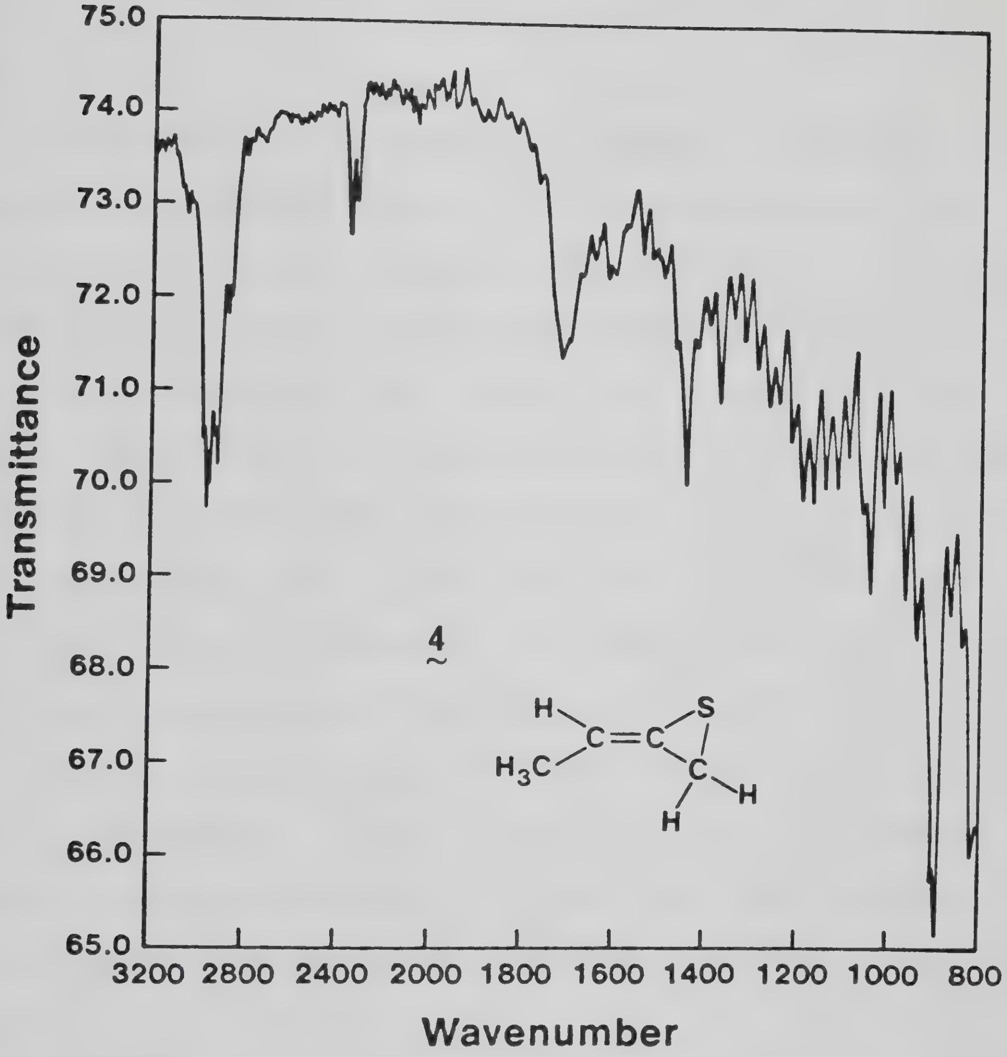

FIGURE III-7: The gas phase FTIR spectrum of trans ethylidenethiirane (4).

The C=C absorption evidently occurs at $\sim$1700 cm^{-1}. As in the case of 1, the absorption at $\sim$2990 cm^{-1} corresponds to the C-H stretching frequency of the thiirane ring.

Product 5

The NMR spectrum of product 5 (Figure III-8) shows four resonances of relative areas 1:2:2:1 corresponding to protons H_A, H_B, H_C and H_D, respectively. Proton H_A, located at $\delta=5.28$ (vinylic region), shows two triplet splittings of 7.4 and 6.6 Hz. Protons H_B, at $\delta=4.80$, are also in the vinylic region. They show a triplet splitting of 2.7 Hz and a doublet splitting of 6.6 Hz. Protons H_C, at $\delta=3.10$, show two doublet splittings of 7.4 and 7.9 Hz and a triplet splitting of 2.7 Hz. Finally, proton H_D is a triplet with a splitting of 7.9 Hz, occurring at $\delta=1.58$ (aliphatic -SH region).

From the chemical shift ($\delta=1.58$), proton H_D is apparently an -SH proton. It has a large splitting in common with the aliphatic protons H_C ($J_{CD}=7.9$ Hz). This implies that protons H_D and H_C are at most three bonds apart as shown:

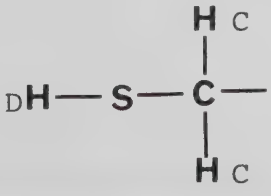

Protons H_C and H_A also have a large common splitting ($J_{AC}=$ 7.4 Hz). This again implies that they are separated by not more than three bonds:

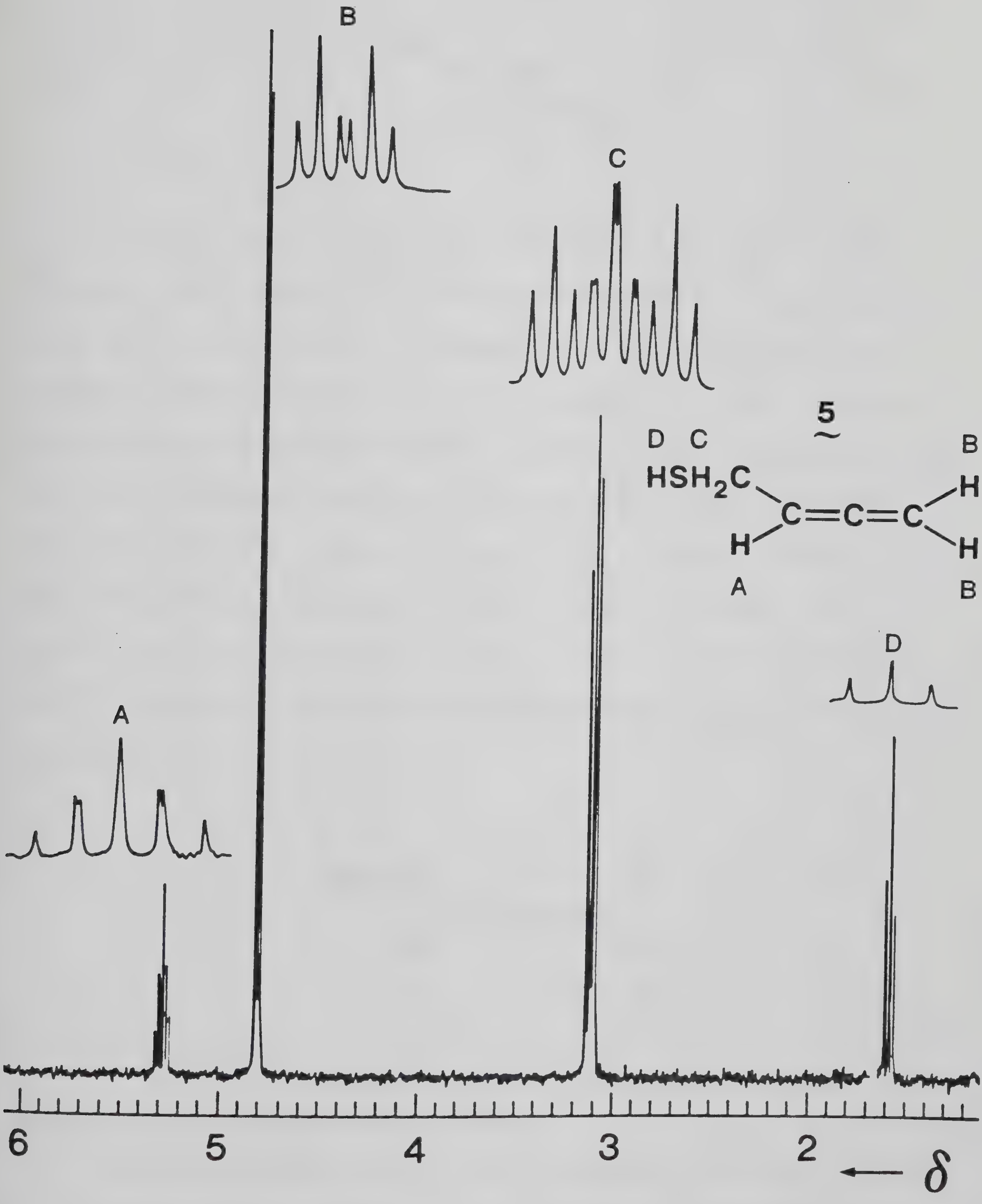

FIGURE III-8: NMR spectrum of 2,3-butadiene-1-thiol (5).

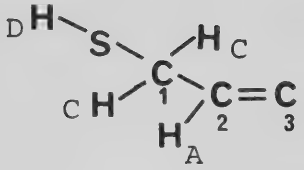

As mentioned earlier, protons H_A and H_B are vinylic. However, they cannot be on the same C=C bond, because protons H_B are equivalent. Consequently, there must be two double bonds in the molecule, in keeping with the requirement of the molecular formula. Furthermore, the equivalence of two H_B protons requires that the rest of the molecule be symmetric with respect to the $=C(H_B)_2$ plane. This is only possible if the second vinyl group is joined orthogonally to that of the H_B protons, thus putting the other half of the molecule perpendicular to the $=C(H_B)_2$ plane as shown:

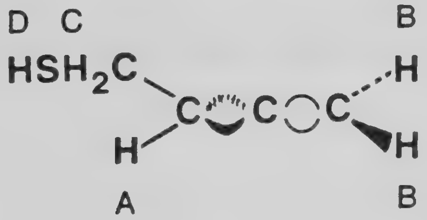

Hence 5 is 2,3-butadiene-1-thiol.

Further confirmation of this proposed structure is seen in the IR spectrum shown in Figure III-9. Conclusive evidence for a monosubstituted allene structure comes from the

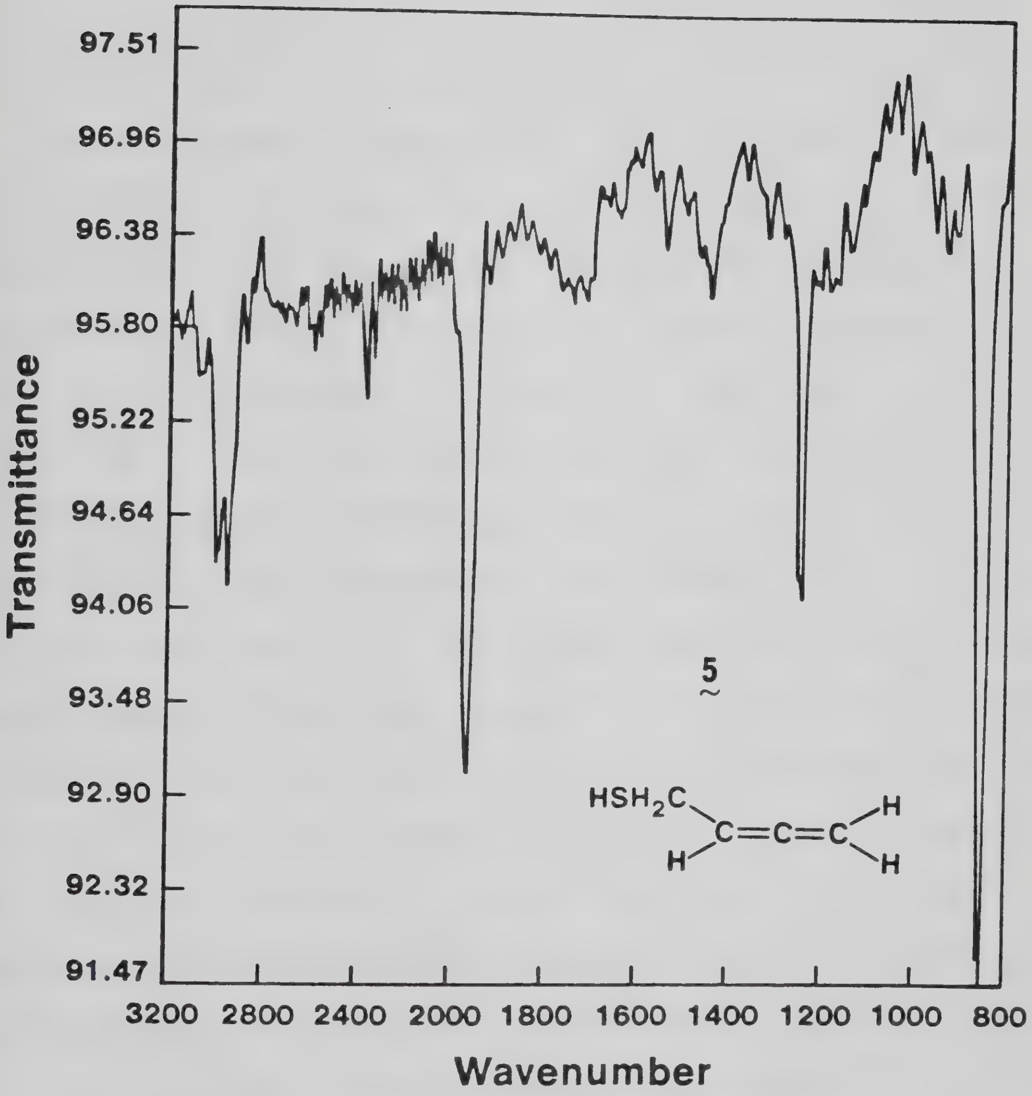

FIGURE III-9: The gas phase FTIR spectrum of 2,3-butadiene-1-thiol (5).

characteristic absorptions at 1960 cm^{-1} (C=C=C). The weak absorption at ∿2500 cm^{-1} is characteristic of an -SH group.

b) Properties of **1**, **2**, **3**, **4** and **5**

The gas phase UV spectra of **1** and **4**, shown in Figures III-10 and III-11, are quite similar in that both show three absorption maxima. For product **1**, the three maxima are located at λ_1=200, λ_2=235 and λ_3=275 nm with corresponding extinction coefficients $\varepsilon_1 \simeq 2x10^3$, $\varepsilon_2 \simeq 7x10^3$ and $\varepsilon_3 \simeq 2x10^2$ l $mole^{-1}cm^{-1}$. The three maxima of **4** are located at λ_4=195, λ_5=230, and λ_6=285 nm with $\varepsilon_4 \simeq 8x10^2$, $\varepsilon_5 \simeq 3x10^3$ and $\varepsilon_6 \simeq 2x10^2$ l $mole^{-1}cm^{-1}$. The UV spectrum of **5** (Figure III-12) is quite different from that of **1** and **4**; the long wavelength transition is absent. The first absorption maximum with $\varepsilon_7 \simeq 3x10^3$ l $mole^{-1}cm^{-1}$ is centered at $\lambda_7 \simeq 205$ nm. A weak shoulder with $\varepsilon_8 \simeq 1x10^3$ l $mole^{-1}cm^{-1}$ lies at $\lambda_8 \simeq 230$ nm. It is apparent that both the thiiranes (**1** and **4**) and the thiol (**5**) are photochemically quite unstable, due to their large extinction coefficients in the near UV. By analogy, products **2** and **3** are also expected to be photochemically unstable.

In the present investigation, it was noted that these compounds are very sensitive to Pyrex surfaces: leaving a gaseous mixture of the products at room temperature in a Pyrex trap overnight resulted in > 95% product loss. However, when the products were left in a quartz cell under the same conditions, more than 50% was recovered. At -196°, the products are relatively more stable. The products

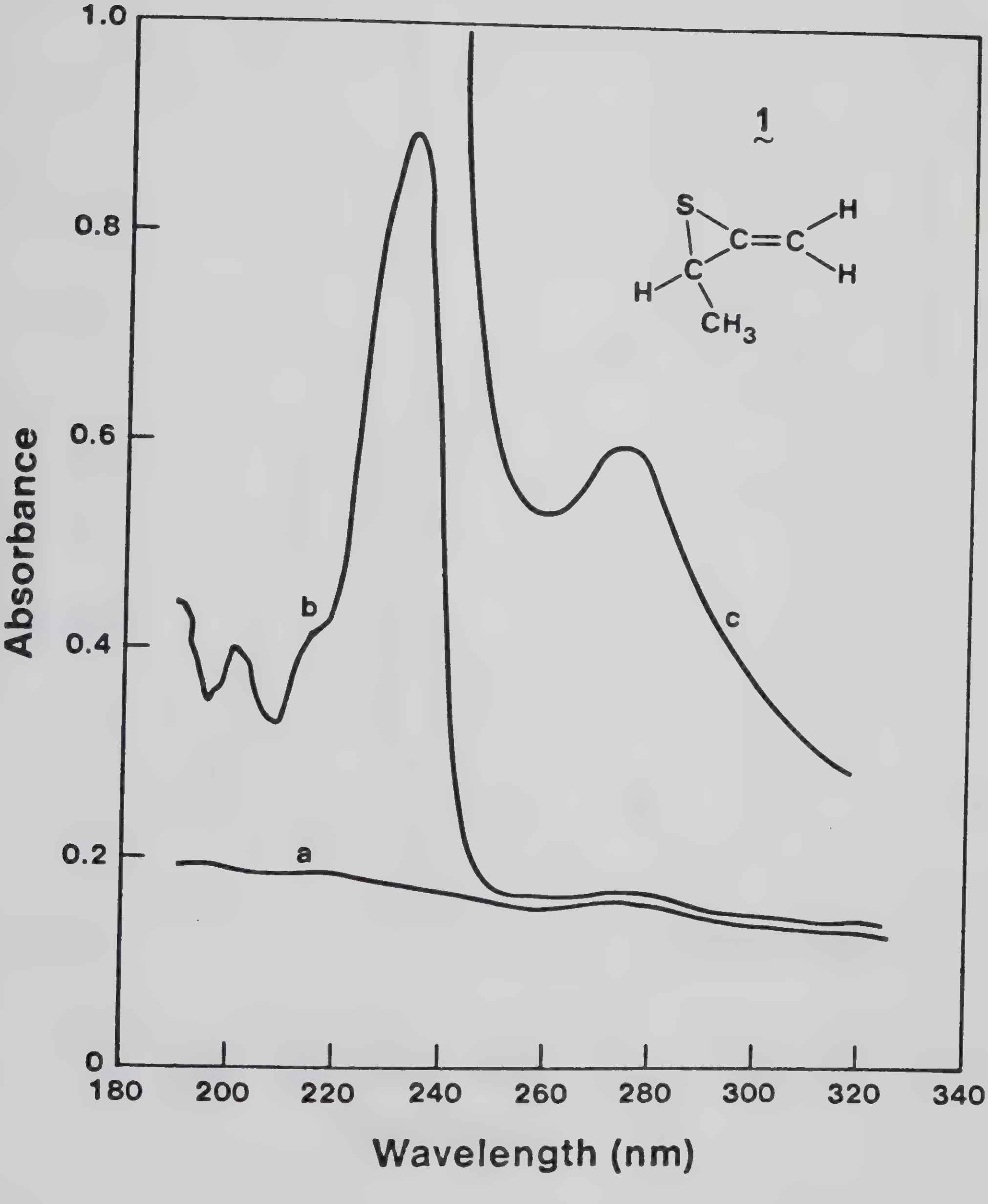

FIGURE III-10: The gas phase UV spectrum of 2-methyl-3-methylene-thiirane (1) at low and high concentrations. a=base line of 30 ml, 10 cm path length quartz cell, b=low concentration, P~0.2 torr, c=high concentration, P~4 torr.

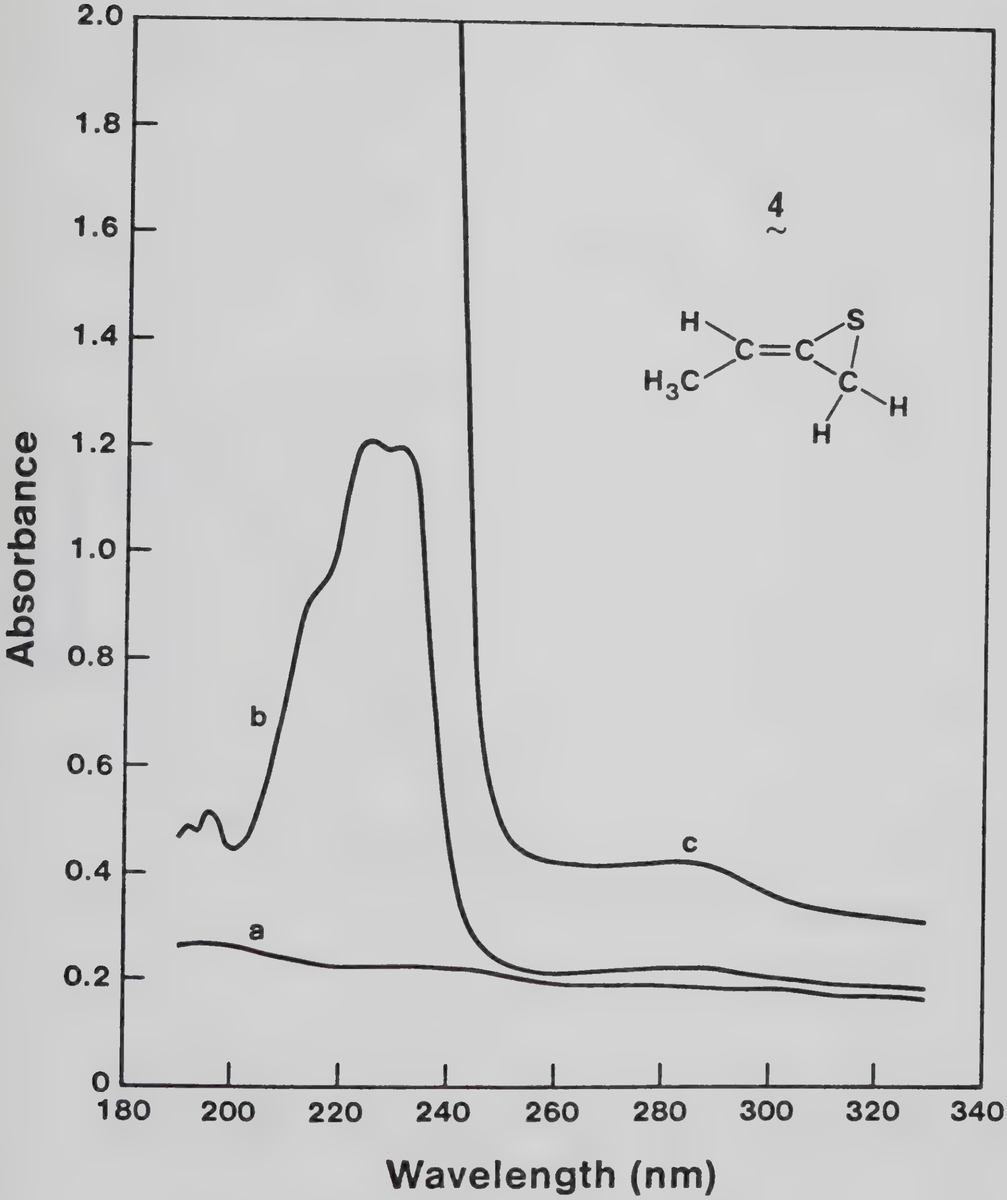

FIGURE III-11: The gas phase UV spectrum of trans ethylidenethiirane (4) at low and high concentrations. a=base line of 30 ml, 10 cm path length quartz cell, b=low concentration, P~0.6 torr, c=high concentration, P~1 torr.

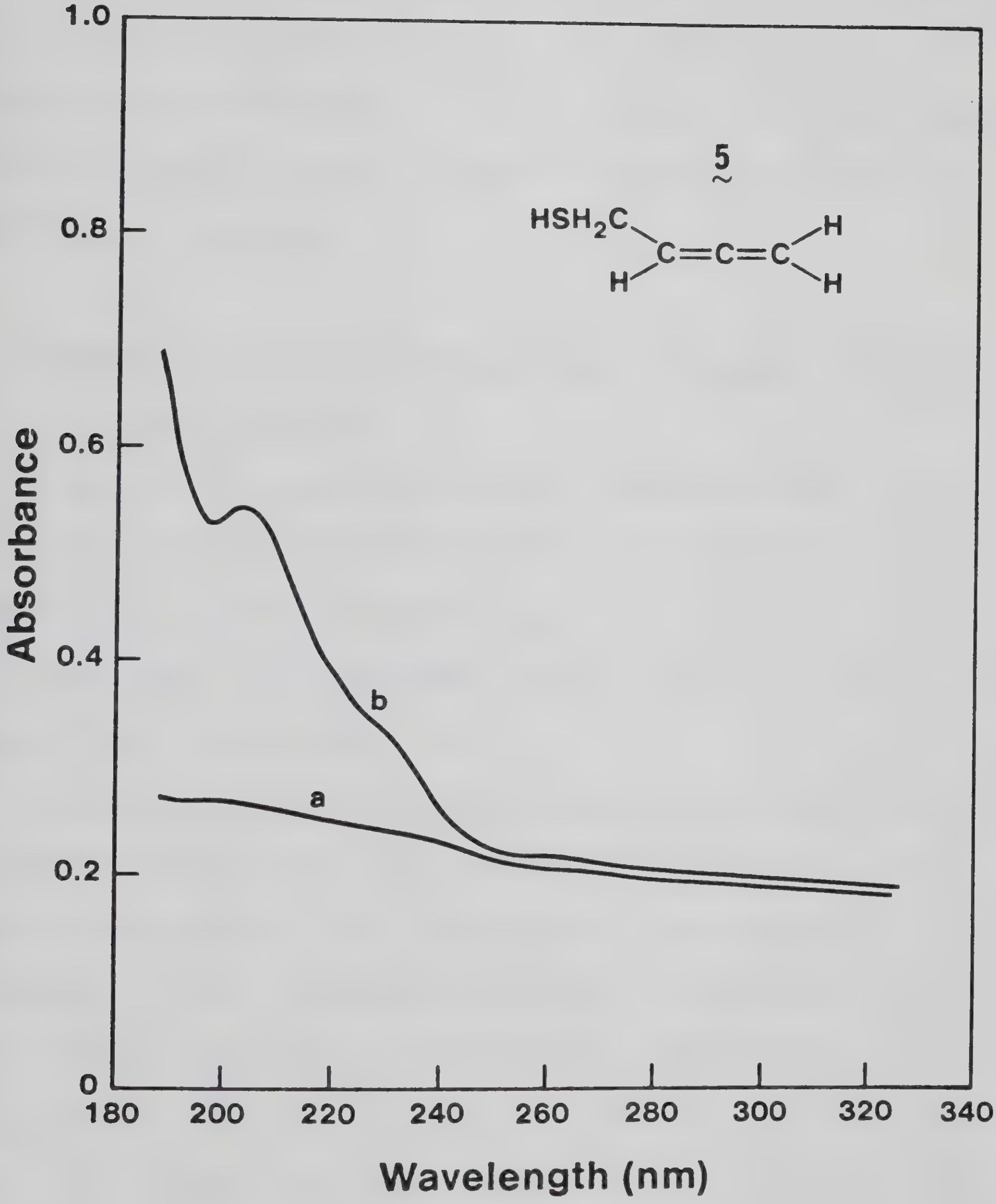

FIGURE III-12: The gas phase UV spectrum of 2,3 -butadiene-1-thiol. a=base line of 30 ml, 10 cm path length quartz cell, b=P~0.2 torr.

exhibit greatest stability in dilute $CDCl_3$ solution at -4^{o} in sealed NMR tubes covered with aluminum foil.

It was also noted that the S products are extremely sensitive to mercury surfaces: more than 50% of **1** was lost after being transferred to the GC sampler via the Töepler pump-gas burette system, where a large surface area of mercury is available.

2. Effects of Exposure Time, Total Pressure and Added CO_2 on Product Yields

Due to fluctuations in the intensity output of the lamp and to sulfur deposition on the cell window, along with changes in the COS absorbtivity with temperature, the amount of conversion was determined relative to the yield of CO rather than to exposure time.

The variations in product yields with exposure time are listed in Table III-2 and illustrated in Figure III-13. The product recoveries are low, even at low conversions. In addition to the S addition products, a very small amount of CS_2, which could not be determined quantitatively by GC or by distillation, was formed along with trace quantities of CH_4. As is apparent from Table III-2, the rate of CH_4 formation increases with time, indicating that at least part of it is formed in a secondary process. The variations in the product rates of S products are illustrated in Figure III-14, where it is seen that the rates of the formation of **1** and

TABLE III-2

Effect of Exposure Time on the Product Yields in the COS-1,2-C_4H_6 System[a]

Time	Products, μmoles; (Rates, μmoles/μmole CO)							
(min.)	CO	$\underset{\sim}{1}$[c]	$\underset{\sim}{2}$	$\underset{\sim}{3}$	$\underset{\sim}{4}$[c]	$\underset{\sim}{5}$	CH_4	% Recovery[b]
3.5	1.23	0.255 (0.207)	0.020 (0.016)	0.016 (0.013)	0.119 (0.097)	0.020 (0.016)	0.006 (0.005)	57
5.0	1.79	0.334 (0.187)	0.036 (0.020)	0.036 (0.020)	0.152 (0.085)	0.015 (0.009)	0.010 (0.006)	55
10	3.42	0.600 (0.175)	0.052 (0.015)	0.065 (0.019)	0.255 (0.074)	0.061 (0.018)	0.024 (0.007)	46
15	5.13	0.788 (0.154)	0.083 (0.016)	0.081 (0.016)	0.350 (0.068)	0.075 (0.015)	0.037 (0.007)	42
20	6.54	0.911 (0.139)	0.096 (0.015)	0.115 (0.018)	0.400 (0.061)	0.108 (0.016)	0.077 (0.012)	35

[a] $P(1,2\text{-}C_4H_8) = 51$ torr, $P(COS) = 200$ torr.

[b] % Recovery = $R(\underset{\sim}{1} + \underset{\sim}{2} + \underset{\sim}{3} + \underset{\sim}{4} + \underset{\sim}{5} + CH_4)/R(CO°-CO)$ where $R^{\circ}_{CO} = 0.569$ μmole min^{-1}.

[c] Extrapolated zero time rates for $\underset{\sim}{1}$ and $\underset{\sim}{4}$ (Figure III-2) are 0.235 and 0.115 μmole min^{-1}, respectively.

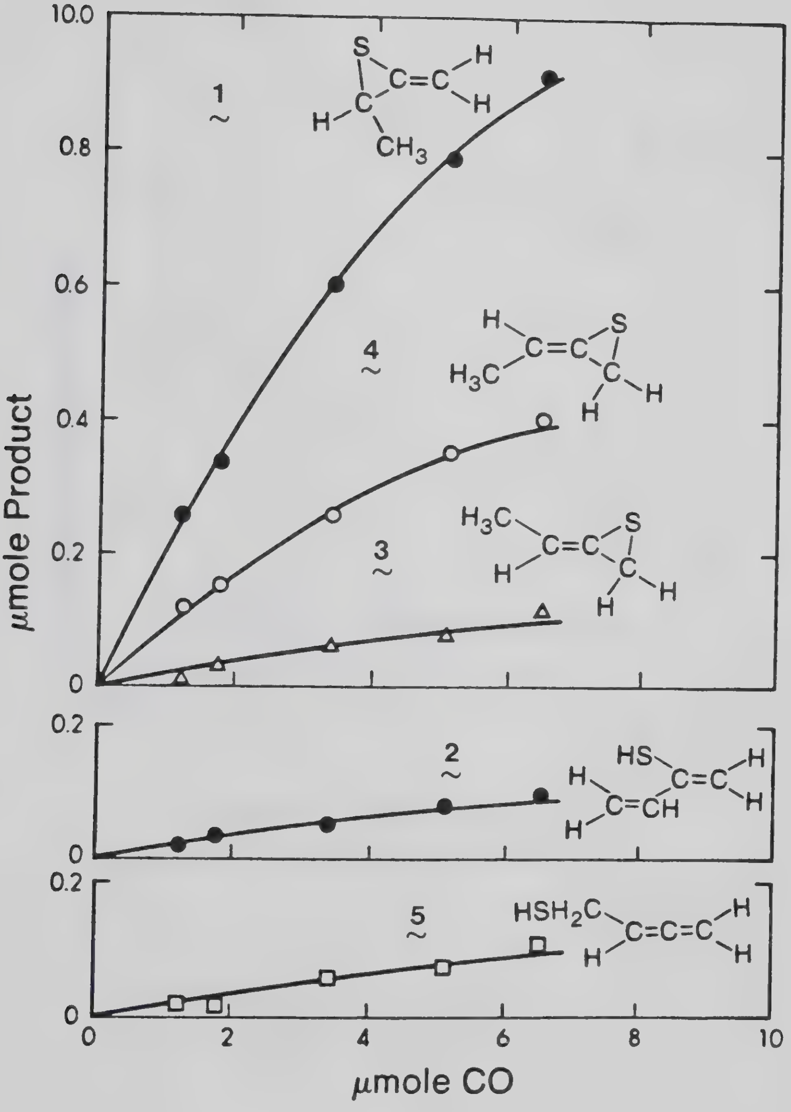

FIGURE III-13: S product yields as a function of CO yield in the COS - 1,2-C_4H_6 system. P(COS) = 200 torr, P(1,2-C_4H_6) = 50 torr.

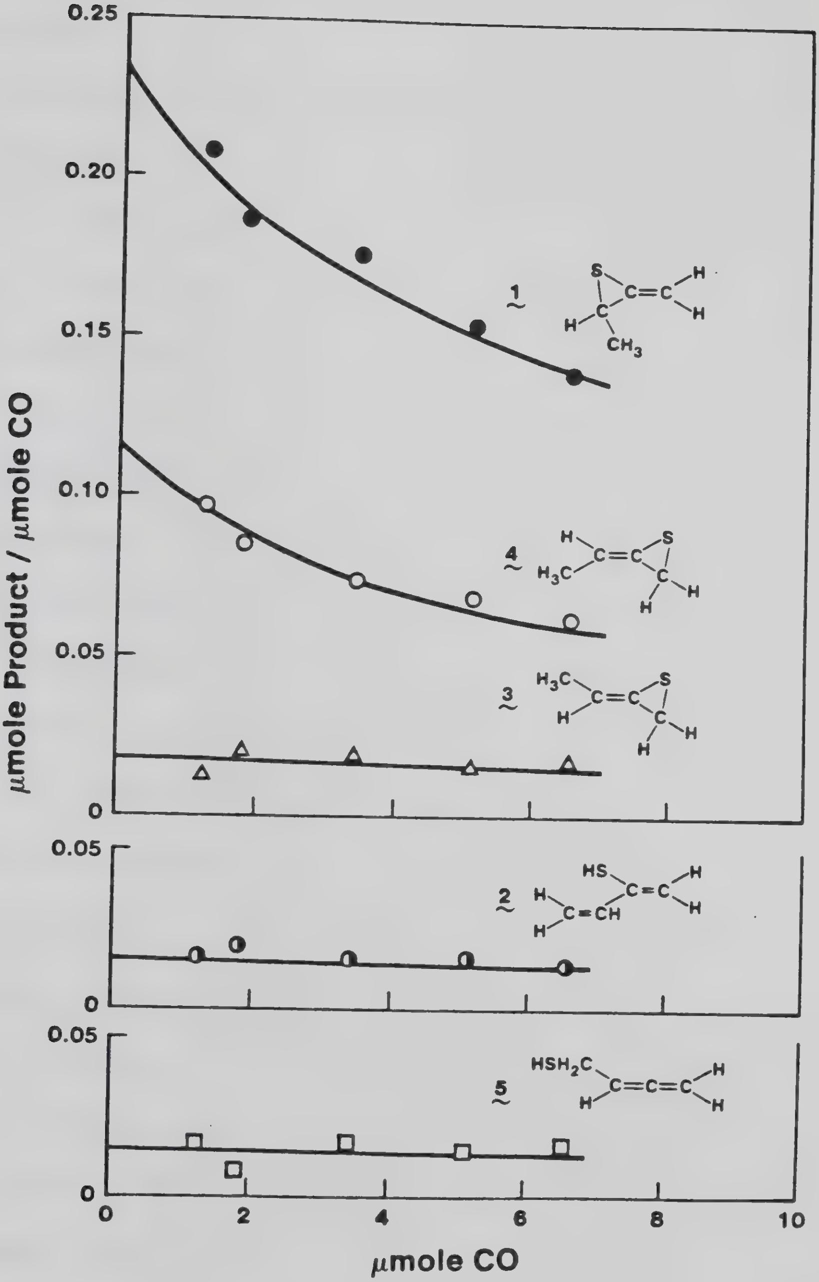

FIGURE III-14: Rates of S product formation versus CO yield in the COS - 1,2-C_4H_6 system, P(COS) = 200 torr, P(1,2-C_4H_6) = 50 torr; Rate($\underset{\sim}{1}$)$_{t=0}$ ≃ 0.235 μmole/μmole CO, Rate($\underset{\sim}{4}$)$_{t=0}$ ≃ 0.115 μmole/μmole CO.

4 decrease with time, whereas those of **2**, **3**, and **5** are apparently constant.

The rates of product formation as a function of total pressure are listed in Table III-3 and illustrated in Figure III-15 (To minimize the effect of the strong time dependence of the rates of **1** and **4** on the pressure study, the same conversion was employed for all runs, and the rates in Figure III-15 were corrected to zero time using Figure III - 14.). There was a dramatic increase in product recoveries at high pressures (45%), and this was entirely due to the increase in the rates of formation of the thiiranes: that of **1** showed a sharp initial increase, levelling off at high pressures, while those of **3** and **4** showed a moderate steady rise. On the other hand, the rates of formation of thiols **2** and **5** were not affected.

The addition of ∿1200 torr CO_2 to a $COS/1,2\text{-}C_4H_6$ = 100/50 mixture suppressed the thiol formation and caused a concomitant rise in the thiirane yields. The production of CH_4 was also suppressed. The total product recovery increased slightly (∿11%). Table III-4 shows the product distributions in the absence and in the presence of 1200 torr CO_2. Values corrected to zero time are also listed.

3. Relative Rate Parameters

For a COS pressure of 100 torr, and a CO_2/COS ratio of ≃ 12-13, it was found that >90% of the S atoms produced are

TABLE III-3

Effect of Total Pressure on Product Yield in the COS-1,2-C_4H_6 System

Pressure (torr)		Time	Products, μmoles; (Rates, μmoles/μmole CO)							% Recovery[a]
1,2-C_4H_6	COS	(min.)	CO	$\underset{\sim}{1}^{b}$	$\underset{\sim}{2}$	$\underset{\sim}{3}$	$\underset{\sim}{4}^{c}$	$\underset{\sim}{5}$	CH_4	
30	120	20.9	5.13	0.615 (0.120)	0.075 (0.015)	0.0076 (0.015)	0.277 (0.054)	0.082 (0.016)	0.051 (0.010)	42.6
50	200	15.0	5.13	0.788 (0.154)	0.083 (0.016)	0.081 (0.016)	0.350 (0.068)	0.075 (0.015)	0.037 (0.007)	41.6
100	400	9.8	5.28	1.050 (0.199)	0.078 (0.015)	0.116 (0.022)	0.421 (0.080)	0.078 (0.015)	0.020 (0.004)	54.0
150	600	8.3	5.40	1.144 (0.212)	0.063 (0.012)	0.171 (0.032)	0.457 (0.085)	0.078 (0.014)	0.012 (0.002)	62.2

[a] % Recovery = $R(\underset{\sim}{1} + \underset{\sim}{2} + \underset{\sim}{3} + \underset{\sim}{4} + \underset{\sim}{5} + CH_4)/R(CO°-CO)$, where R°_{CO} = 0.378, 0.569, 0.873 and 1.024 μmoles min^{-1} for P(COS) = 120, 200, 400 and 600 torr,respectively.

[b] Corrected zero time rates are 0.197, 0.235, 0.275 and 0.283 μmole/μmole CO for P_{total} = 150, 250, 500 and 750 torr, respectively.

[c] Corrected zero time rates are 0.103, 0.115, 0.123 and 0.122 μmole/μmole CO for P_{total} = 150, 250, 500 and 750 torr respectively.

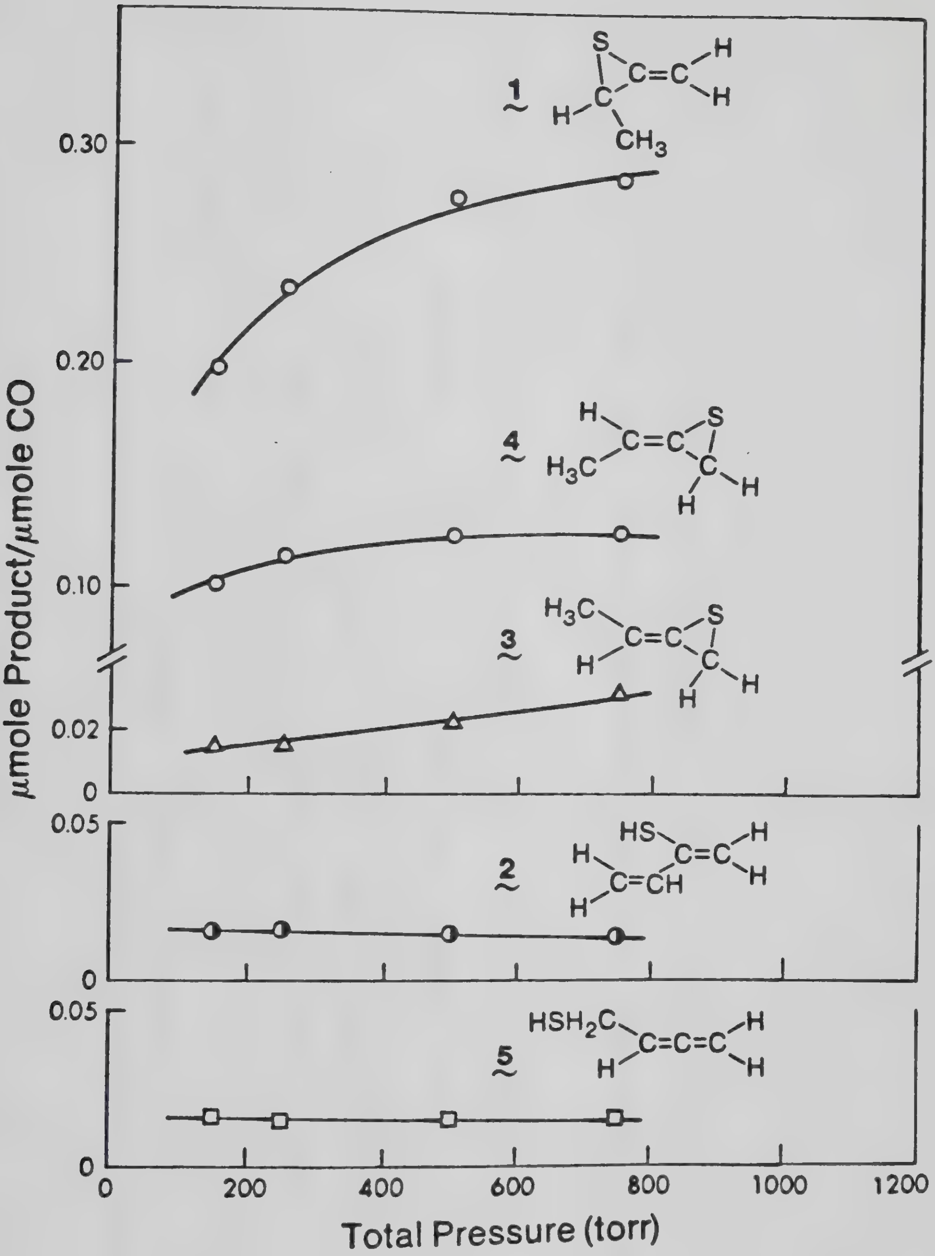

FIGURE III-15: Rates of product formation versus total pressure in the COS - 1,2-C_4H_6 system; P(COS)/P(1,2-C_4H_6) = 4. Rates of 1 and 4 are corrected zero time values. The extrapolated zero time rates at P = 1200 torr for 1, 3, and 4 are 0.290, 0.042 and 0.123 μmole/μmole CO, respectively.

TABLE III-4

Effect of Added CO_2 on the Distribution of 1,2-C_4H_6S Isomers[a]

$P(CO_2)$ (torr)	Products (μmoles)							% Recovery[b]
	CO	**1**	**2**	**3**	**4**	**5**	CH_4	
0	2.36	0.358	0.061	0.057	0.160	0.058	0.038	55.7
1216	1.92	0.731[c]	0.005	0.070	0.275[c]	0	0.006	62

[a] Exposure time = 11 min, P(COS) = 100 torr, P(1,2-C_4H_6) = 50 torr.

[b] % Recovery = R(**1** + **2** + **3** + **4** + **5** + CH_4)/R(CO°−CO), where R°_{CO} = 0.334 μmoles min^{-1}.

[c] Corrected zero time yields are 1.041 and 0.436 μmoles for **1** and **4**, respectively, assuming a similar time dependence for $S(^1D_2)$ and $S(^3P)$ products.

in the triplet ground state. Thus this CO_2/COS ratio is sufficient for the study of $S(^3P)$ reactions.

The relative rates of reaction of $S(^3P)$ atoms with two alkenes, I and II, may be determined from the relative yields of the thiiranes (E) produced. The two competing reactions are:

$$S(^3P) + I \xrightarrow{k_1} E_I \qquad [1]$$

$$S(^3P) + II \xrightarrow{k_2} E_{II} \qquad [2]$$

If $A = E_I/CO$ in the presence of II, and $B = E_{II}/CO$, then the relative rate expression is:

$$\frac{B}{A} = \frac{k_2}{k_1} \cdot \frac{[II]}{[I]} \qquad [3]$$

Therefore, a plot of B/A versus [II]/[I] will give a straight line with a slope k_2/k_1. Thus the absolute rate constant, k_2, of reaction [2] can be obtained if k_1 is known. In cases where the thiirane(s) formed in [2] is/are unstable, then the relative rate can be obtained by monitoring the rate of decrease of thiirane (E_I) formed in [1]. Hence if $A_o = E_I/CO$ in the absence of (II), then [3] becomes:

$$\frac{A_o - A}{A} = \frac{k_2}{k_1} \cdot \frac{[II]}{[I]} \qquad [4]$$

and a plot of $(A_o-A)/A$ versus [II]/[I] will yield k_2/k_1.

$1\text{-}C_4H_8$ was chosen as the reference substrate (I) since its vapour pressure is similar to that of $1,2\text{-}C_4H_6$ (II), allowing low temperature distillation of the reactants. Also, the $S(^3P) + 1\text{-}C_4H_8$ reaction produces $1\text{-}C_4H_8S$ (ethylthiirane)

quantitatively, and the absolute Arrhenius parameters have been measured.

Product yields for mixtures consisting of 100 torr COS, >1200 torr CO_2 and fixed pressures of $1\text{-}C_4H_8$ in the presence of increasing amounts of $1,2\text{-}C_4H_6$ at five different temperatures are summarized in Tables III-5 to III-9. It is seen that the $1\text{-}C_4H_8S/CO$ ratio decreases with increasing pressure of $1,2\text{-}C_4H_6$, owing to the competitive scavenging of $S(^3P)$ atoms by $1,2\text{-}C_4H_6$. It is apparent that the rate constant ratios, $k_{1,2\text{-}C_4H_6}/k_{1\text{-}C_4H_8}$, obtained by monitoring the decrease in the $1\text{-}C_4H_8S/CO$ ratio (A) are consistently higher than those obtained from the $C_4H_6S/1\text{-}C_4H_8S$ ratio, (B/A); this is not unexpected since the product recoveries from the $S + 1,2\text{-}C_4H_6$ reaction are not quantitative. Consequently, the relative rate constants obtained from plots of $(A_o\text{-}A)/A$ versus $[1,2\text{-}C_4H_6]/[1\text{-}C_4H_8]$ were used to calculate $k_{1,2\text{-}C_4H_6}$. These plots are illustrated in Figure III-16, and the slopes and intercepts obtained by least mean squares analysis of these plots are tabulated in Table III-10. The slopes are plotted in the Arrhenius form in Figure III-17. The weighted least squares fit of the Arrhenius plot gives:

$$A_{1,2\text{-}C_4H_6}/A_{1\text{-}C_4H_8} = 5.31 \pm 0.26, \text{ and}$$

$$E_{1\text{-}C_4H_8} - E_{1,2\text{-}C_4H_6} = -(1.17 \pm 0.03) \text{ kcal mole}^{-1}.$$

TABLE III-5

Product Yields as a Function of the $[1,2\text{-}C_4H_6]/[1\text{-}C_4H_8]$ Ratio at 300 K[a]

$P(1,2\text{-}C_4H_6)$	$\frac{[1,2\text{-}C_4H_6]}{[1\text{-}C_4H_8]}$[b]	Products (μmoles)			$\frac{1\text{-}C_4H_8S}{CO}$	$\frac{A_o-A}{A}$[c]	$\frac{A_o-A}{A} \cdot \frac{[1\text{-}C_4H_8]}{[1,2\text{-}C_4H_6]}$[e]	$\frac{B}{A}$[d]	$\frac{B}{A} \cdot \frac{[1\text{-}C_4H_8]}{[1,2\text{-}C_4H_6]}$[e]
		CO	$1\text{-}C_4H_8S$	$\Sigma 1,2\text{-}C_4H_6S$ (**1**, **3**, **4**)					
0	0	1.61	1.122	0	0.697	-	-	-	-
10.81	0.165	1.60	0.993	0.0759	0.621	0.122	0.742	0.0765	0.464
21.53	0.328	1.60	0.895	0.164	0.561	0.242	0.737	0.183	0.558
32.01	0.489	1.55	0.790	0.229	0.510	0.366	0.748	0.289	0.591
42.29	0.647	1.51	0.708	0.259	0.470	0.484	0.748	0.366	0.565

[a] $P(COS) = 100$ torr, $P(1\text{-}C_4H_8) = 65.7$ torr, $P(CO_2) = 1271$ torr. $R^{\circ}_{CO} = 0.349$ μmoles min^{-1}. Exposure time = 500 sec.

[b] $P(1\text{-}C_4H_8)$ values have been corrected for depletion.

[c] $A_o = 1\text{-}C_4H_8S/CO$ in the absence of $1,2\text{-}C_4H_6 = 0.697$.

$A = 1\text{-}C_4H_8S/CO$ in the presence of $1,2\text{-}C_4H_6$.

[d] $B = \Sigma 1,2\text{-}C_4H_6S/CO$

[e] $= k_{1,2\text{-}C_4H_6}/k_{1\text{-}C_4H_8}$

TABLE III-6

Product Yields as a Function of the $[1,2\text{-}C_4H_6]/[1\text{-}C_4H_8]$ ratio at 333 K[a]

$P(1,2\text{-}C_4H_6)$	$\frac{[1,2\text{-}C_4H_6]}{[1\text{-}C_4H_8]}$[b]	Products (μmoles)			$\frac{1\text{-}C_4H_8S}{CO}$	$\frac{A_o-A}{A}$[c]	$\frac{A_o-A}{A}\cdot\frac{[1\text{-}C_4H_8]}{[1,2\text{-}C_4H_6]}$[e]	$\frac{B}{A}$[d]	$\frac{B}{A}\cdot\frac{[1\text{-}C_4H_8]}{[1,2\text{-}C_4H_6]}$[e]
		CO	$1\text{-}C_4H_8S$	$\Sigma 1,2\text{-}C_4H_6S$ (**1**, **3**, **4**)					
0	0	1.63	1.163	-	0.713	-	-	-	-
14.70	0.212	1.62	0.977	0.127	0.602	0.184	0.868	0.130	0.611
22.41	0.324	1.64	0.907	0.177	0.553	0.288	0.890	0.195	0.603
29.74	0.430	1.61	0.831	0.228	0.517	0.379	0.880	0.275	0.639
38.55	0.558	1.59	0.755	0.264	0.476	0.497	0.889	0.350	0.628

[a] $P(COS) = 100$ torr, $P(1\text{-}C_4H_8) = 69.4$ torr, $P(CO_2) = 1248$ torr. $R^{\circ}_{CO} = 0.384$ μmoles min^{-1}. Exposure time = 470 sec.

[b] $P(1\text{-}C_4H_8)$ values were corrected for depletion.

[c] $A_o = 1\text{-}C_4H_8S/CO$ in the absence of $1,2\text{-}C_4H_6 = 0.713$.

$A = 1\text{-}C_4H_8S/CO$ in the presence of $1,2\text{-}C_4H_6$.

[d] $B = \Sigma 1,2\text{-}C_4H_6S/CO$

[e] $= k_{1,2\text{-}C_4H_6}/k_{1\text{-}C_4H_8}$

TABLE III-7

Product Yield as a Function of the $[1,2\text{-}C_4H_6]/[1\text{-}C_4H_8]$ Ratio at 363 K[a]

$P(1,2\text{-}C_4H_6)$	$\frac{[1,2\text{-}C_4H_6]}{[1\text{-}C_4H_8]}$[b]	Products (μmoles)			$\frac{1\text{-}C_4H_8S}{CO}$	$\frac{A_o-A}{A}$[c]	$\frac{A_o-A}{A}\cdot\frac{[1\text{-}C_4H_8]}{[1,2\text{-}C_4H_6]}$[e]	$\frac{B}{A}$[d]	$\frac{B}{A}\cdot\frac{[1\text{-}C_4H_8]}{[1,2\text{-}C_4H_6]}$[e]
		CO	$1\text{-}C_4H_8S$	$\Sigma 1,2\text{-}C_4H_6S$ (**1**, **2**, **3**)					
0	0	1.69	1.208	-	0.714	-	-	-	-
14.62	0.214	1.68	0.979	0.138	0.584	0.223	1.04	0.141	0.661
21.98	0.322	1.72	0.919	0.194	0.533	0.340	1.06	0.211	0.655
29.28	0.429	1.68	0.831	0.239	0.495	0.444	1.03	0.287	0.669
37.37	0.549	1.68	0.764	0.273	0.454	0.573	1.04	0.357	0.655

[a] $P(COS) = 100$ torr, $P(1\text{-}C_4H_8) = 68.5$ torr, $P(CO_2) = 1285$ torr. $R^{\circ}_{CO} = 0.414$ μmoles min^{-1}. Exposure time = 435 sec.

[b] $P(1\text{-}C_4H_8)$ values were corrected for depletion.

[c] $A_o = 1\text{-}C_4H_8S/CO$ in the absence of $1,2\text{-}C_4H_6 = 0.714$.

$A = 1\text{-}C_4H_8S/CO$ in the presence of $1,2\text{-}C_4H_6$.

[d] $B = \Sigma 1,2\text{-}C_4H_6S/CO$

[e] $k_{1,2\text{-}C_4H_6}/k_{1\text{-}C_4H_8}$

TABLE III-8

Product Yield as a Function of the $[1,2\text{-}C_4H_6]/[1\text{-}C_4H_8]$ Ratio at 393 K[a]

$P(1,2\text{-}C_4H_6)$	$\frac{[1,2\text{-}C_4H_6]}{[1\text{-}C_4H_8]}$ [b]	Products (μmoles)			$\frac{1\text{-}C_4H_8S}{CO}$	$\frac{A_o-A}{A}$ [c]	$\frac{A_o-A}{A} \cdot \frac{[1\text{-}C_4H_8]}{[1,2\text{-}C_4H_6]}$ [e]	$\frac{B}{A}$ [d]	$\frac{B}{A} \cdot \frac{[1\text{-}C_4H_8]}{[1,2\text{-}C_4H_6]}$ [e]
		CO	$1\text{-}C_4H_8S$	$\Sigma 1,2\text{-}C_4H_6S$ $(\underset{\sim}{1}, \underset{\sim}{3}, \underset{\sim}{4})$					
0	0	1.69	1.301	-	0.717	-	-	-	-
14.46	0.209	1.80	0.037	0.158	0.577	0.245	1.18	0.152	0.730
22.11	0.320	1.76	0.914	0.196	0.519	0.387	1.21	0.215	0.671
29.85	0.433	1.76	0.834	0.264	0.474	0.517	1.19	0.317	0.732
37.83	0.549	1.72	0.750	0.307	0.436	0.648	1.18	0.409	0.745

[a] $P(COS)$ = 100 torr, $P(1\text{-}C_4H_8)$ = 69.4 torr, $P(CO_2)$ = 1270 torr. R^{o}_{CO} = 0.432 μmoles min^{-1}. Exposure time = 410 sec.

[b] $P(1\text{-}C_4H_8)$ values were corrected for depletion.

[c] $A_o = 1\text{-}C_4H_8S/CO$ in the absence of $1,2\text{-}C_4H_6$ = 0.717.

$A = 1\text{-}C_4H_8S/CO$ in the presence of $1,2\text{-}C_4H_6$.

[d] $B = \Sigma 1,2\text{-}C_4H_6S/CO$

[e] $k_{1,2\text{-}C_4H_6}/k_{1\text{-}C_4H_8}$

TABLE III-9

Product Yield as a Function of the $[1,2\text{-}C_4H_6]/[1\text{-}C_4H_8]$ Ratio at 423 K[a]

$P(1,2\text{-}C_4H_6)$	$\frac{[1,2\text{-}C_4H_6]}{[1\text{-}C_4H_8]}$[b]	Products (μmoles)			$\frac{1\text{-}C_4H_8S}{CO}$	$\frac{A_o-A}{A}$[c]	$\frac{A_o-A}{A} \cdot \frac{[1\text{-}C_4H_8]}{[1,2\text{-}C_4H_6]}$[e]	$\frac{B}{A}$[d]	$\frac{B}{A} \cdot \frac{[1\text{-}C_4H_8]}{[1,2\text{-}C_4H_6]}$[e]
		CO	$1\text{-}C_4H_8S$	$\Sigma 1,2\text{-}C_4H_6S$ $(\underset{\sim}{1}, \underset{\sim}{3}, \underset{\sim}{4})$					
0	0	1.78	1.244	-	0.700	-	-	-	-
14.46	0.209	1.73	0.945	0.148	0.547	0.281	1.34	0.156	0.746
21.87	0.318	1.76	0.860	0.208	0.489	0.433	1.36	0.242	0.761
29.60	0.432	1.74	0.777	0.268	0.445	0.572	1.33	0.345	0.799
37.32	0.545	1.67	0.680	0.295	0.407	0.722	1.33	0.433	0.795

[a] $P(COS)$ = 100 torr, $P(1\text{-}C_4H_8)$ = 69.4 torr, $P(CO_2)$ = 1302 torr. R°_{CO} = 0.502 μmoles min^{-1}. Exposure time = 350 sec.

[b] $P(1\text{-}C_4H_8)$ values were corrected for depletion.

[c] A_o = $1\text{-}C_4H_8S/CO$ in the absence of $1,2\text{-}C_4H_6$ = 0.700.

A = $1\text{-}C_4H_8S/CO$ in the presence of $1,2\text{-}C_4H_6$.

[d] B = $\Sigma 1,2\text{-}C_4H_6S/CO$

[e] $k_{1,2\text{-}C_4H_6}/k_{1\text{-}C_4H_8}$

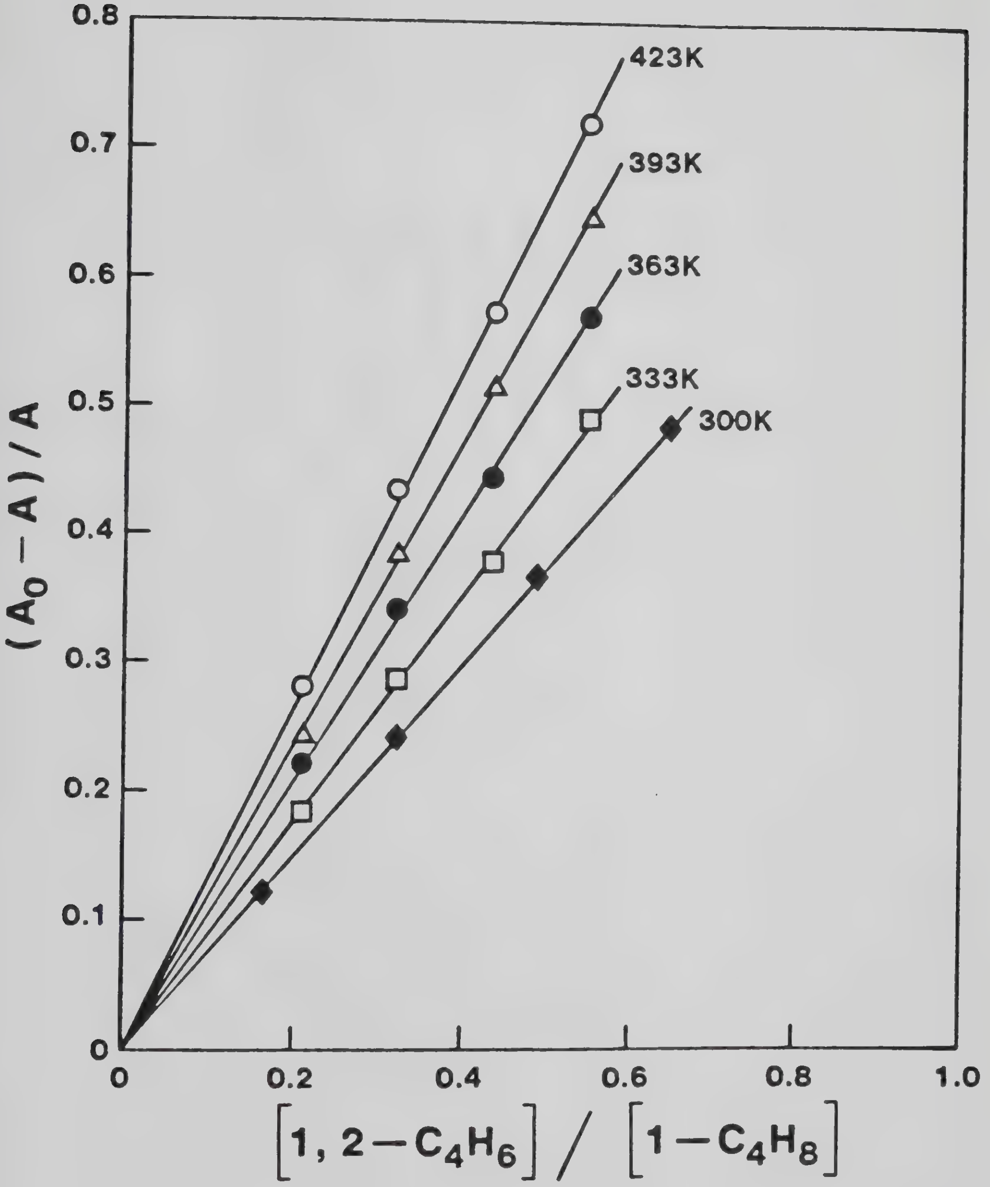

FIGURE III-16: Plots of $(A_0\text{-}A)/A$ versus $[1,2\text{-}C_4H_6]/[1\text{-}C_4H_8]$.

TABLE III-10

Slopes and Intercepts of the Plots in Figure III-16[a]

Temperature (K)	$1/T \times 10^3$ (K^{-1})	Slope ($k_{1,2-C_4H_6}/k_{1-C_4H_8}$)	$Ln(k_{1,2-C_4H_6}/k_{1-C_4H_8})$	Intercept	Correlation Coefficient
300	3.33	0.747 ± 0.019	-0.292 ± 0.003	-0.0037 ± 0.0060	1.000
333	3.00	0.886 ± 0.033	-0.121 ± 0.004	-0.0048 ± 0.0095	1.000
363	2.76	1.042 ± 0.042	0.041 ± 0.004	0.0025 ± 0.0117	1.000
393	2.54	1.188 ± 0.059	0.172 ± 0.005	0.0031 ± 0.0166	0.9999
423	2.36	1.330 ± 0.069	0.285 ± 0.005	0.0098 ± 0.0194	0.9999

[a] The errors are standard deviations.

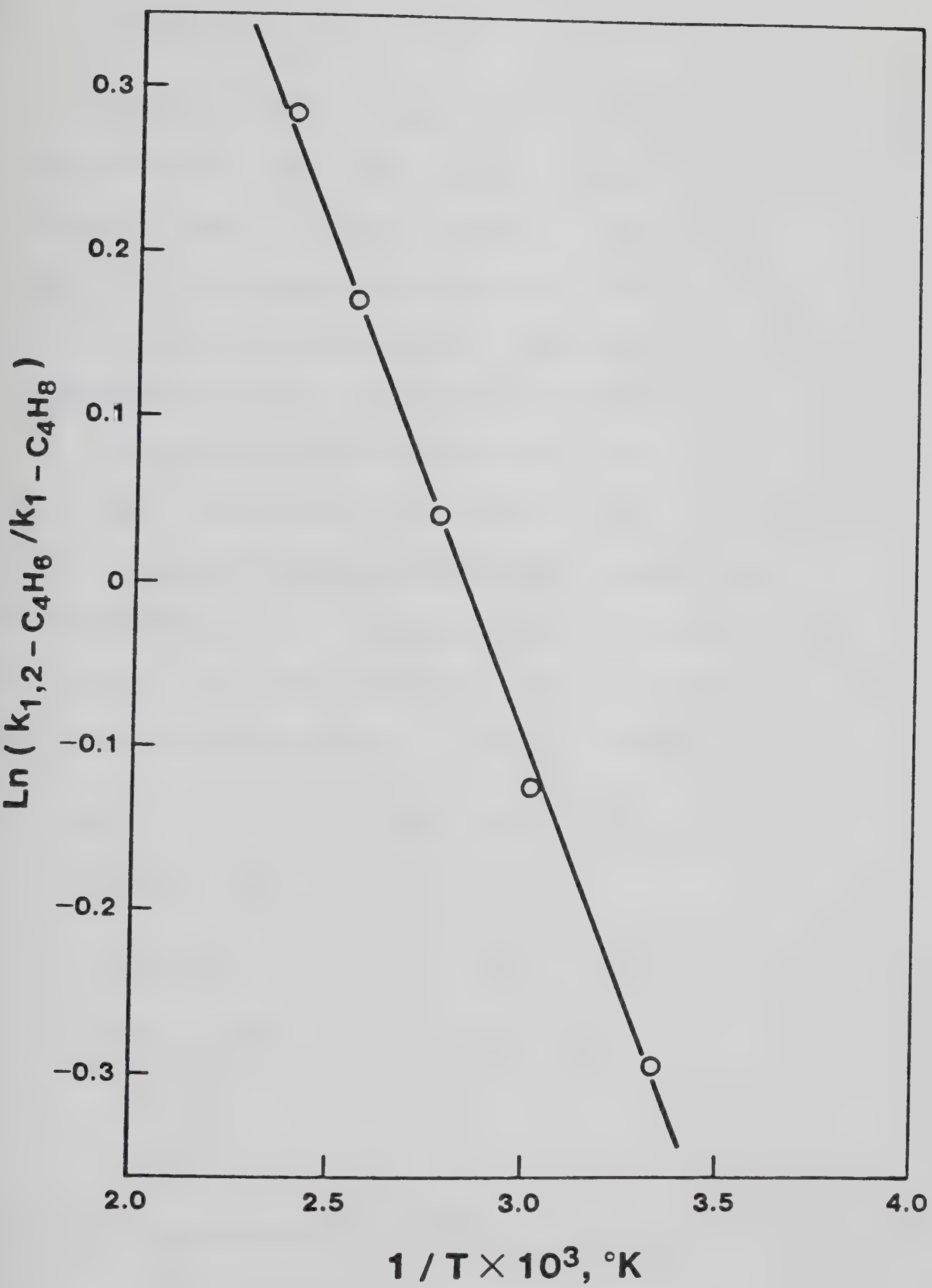

FIGURE III-17: Arrhenius plot for the S(^{3}P) + 1,2-C_4H_6 and 1-C_4H_8 system.

B. Discussion

The cumulated π bonds of 1,2-butadiene are mutually perpendicular, and consequently, there is little interaction between these two bonds. Thus in 1,2-C_4H_6 the π bonds represent two non-equivalent reaction sites. However, there is σ-π overlap between each π bond and the coplanar C-H bonds (hyperconjugation), resulting in stronger C=C bonds.[130]

The products observed in the COS-1,2-C_4H_6 system indicate that the reaction of S atoms with this diene conforms with the general mechanism already established for the reaction with alkenes, i.e. S atoms either add to one of the C=C bonds or insert into the C-H bonds. Thus the following steps may be considered for the S + 1,2-C_4H_6 system:

$$COS + h\nu \longrightarrow CO + S(^1D_2,\ ^3P) \qquad [5]$$

$$S(^1D_2) + COS \longrightarrow CO + S_2 \qquad [6]$$

$$S(^1D_2) + M \longrightarrow S(^3P) + M \qquad [7]$$

$$S(^3P) + COS \longrightarrow CO + S_2 \qquad [8]$$

$S(^1D_2) + CH_3CH{=}C{=}CH_2 \xrightarrow{2,3\text{-addn.}}$

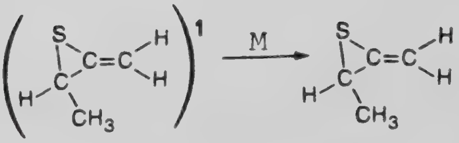

[9]

1

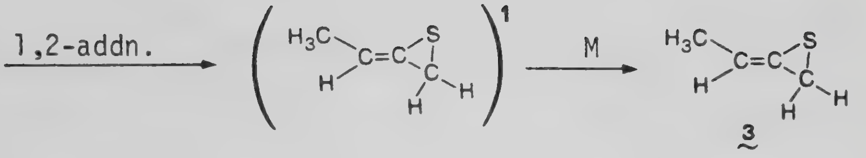

[10]

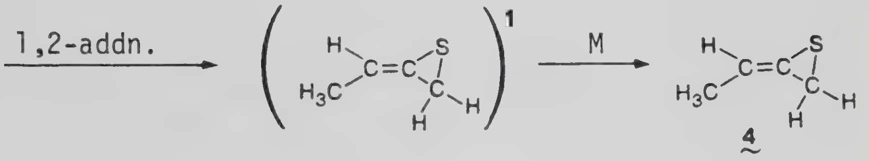

[11]

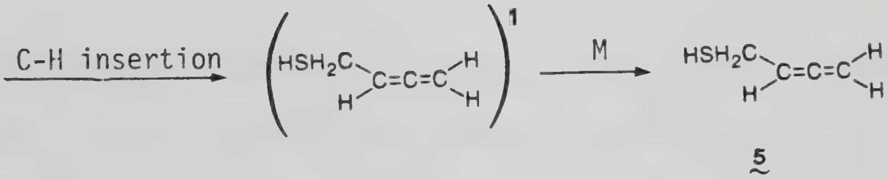
C-H insertion
M
5

[12]

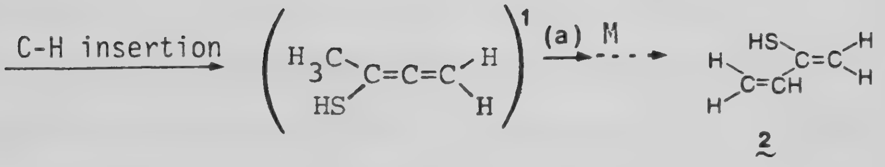
C-H insertion
(a) M
2

[13]

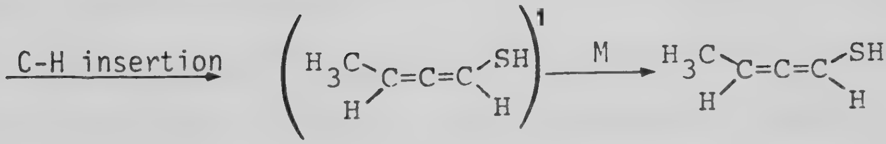
C-H insertion
M

[14]

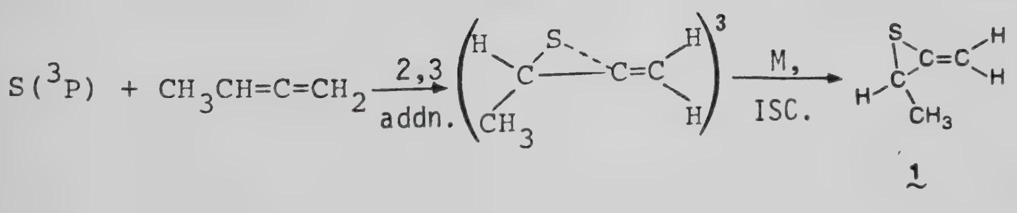
S(3P) + CH3CH=C=CH2
2,3
addn.
M,
ISC.
1

[15]

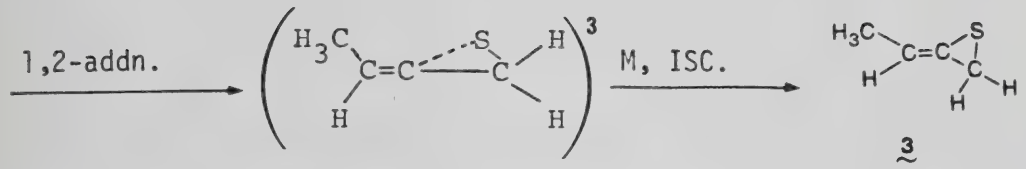

[16]

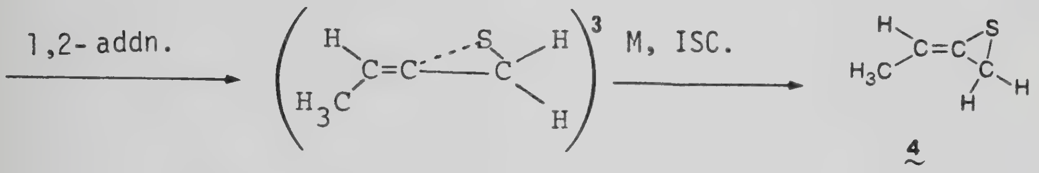

[17]

S addition product recoveries in the present system are relatively low ($\sim$70% at zero time), in contrast to the alkene systems where the yields are quantitative at low conversions. The loss can be ascribed in part to the moderately strong U.V. absorption of the products at longer wavelengths ($\lambda > 250$ nm).

The formation of product 2 presumably could occur via an enethiol-thioketone-enethiol tautomerization. The initial tautomer, $CH_3C(SH)=C=CH_2$ (2,3-butadiene-2-thiol), could be formed from direct insertion of $S(^1D_2)$ into the alkyl substituted vinyl C-H bond (step [13]) or from unimolecular isomerization of the hot thiirane, produced by 2,3-addition of $S(^1D_2)$ (step [9]) via a bicyclic activated complex as shown in scheme (I).

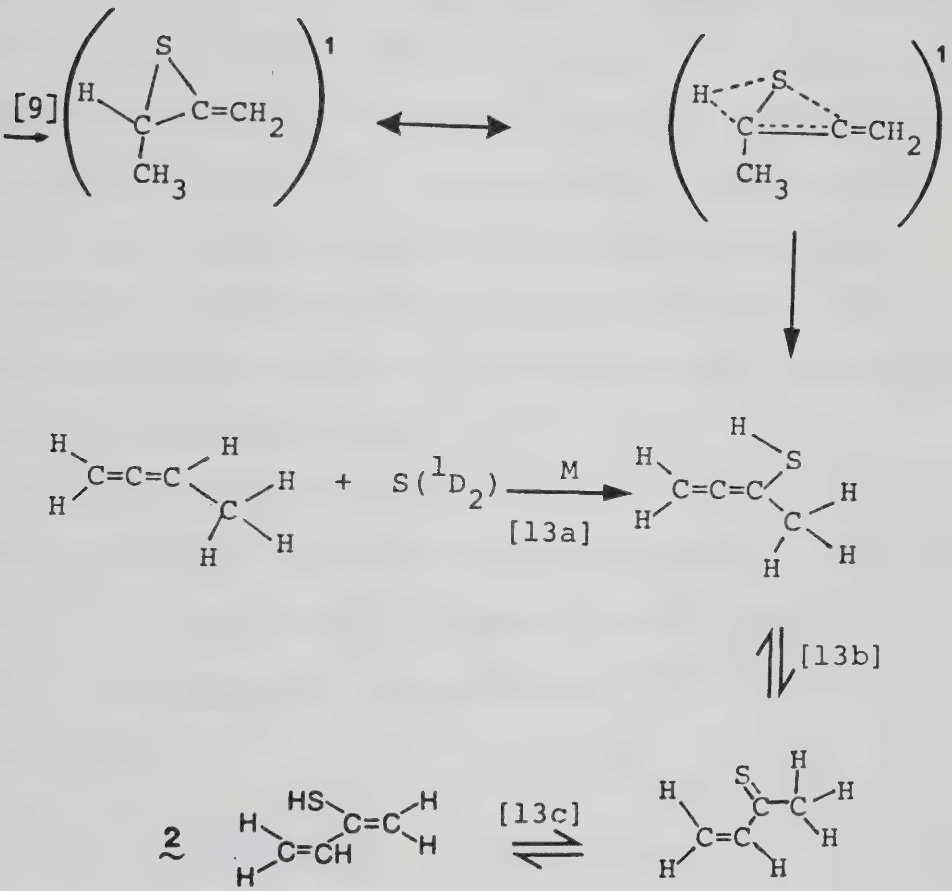

Scheme [I]

The occurrence of a hot thiirane-thiol rearrangement in this system is,however, highly unlikely, since in chemically activated methylthiirane, which has a smaller number of degrees of freedom than the C_4H_6S adducts, this process is of very minor importance.[19] Thus the initial tautomer of 2 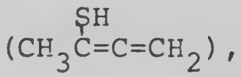 $(CH_3\overset{SH}{C}=C=CH_2)$,

at pressures >2 torr, must result from direct insertion into the C-H bond of C_3. This insertion is a distinct feature of the COS-1,2-C_4H_6 system: the first reported S insertion into the methyl-substituted vinylic C-H bond of an acyclic hydrocarbon system. In fact, 2, the ultimate product of this insertion, is only the second alkyl-substituted enethiol (1-ene-2-thiol) after propene-2-thiol to be reported.[131] Syntheses of enethiols having a terminal vinyl group generally yield only the 1-ene-1-thiol.[42,132]

The existence of enethiol-thioketone rearrangements, which are analogous to enol-keto tautomerisms, is well documented.[133,134] It should be noted that the possibility that product 2 can arise from the addition of $S(^1D_2)$ to any 1,3-butadiene impurity

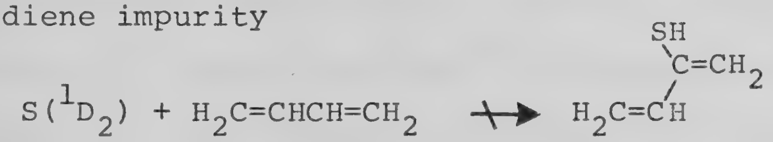

$$S(^1D_2) + H_2C{=}CHCH{=}CH_2 \nrightarrow H_2C{=}CH{-}C(SH){=}CH_2 \quad (2) \qquad [18]$$

can be ruled out for two reasons:

(i) The purity of the substrate was checked chromatographically shortly before use, and no 1,3-butadiene was detected.

(ii) The reaction of S atoms with 1,3-butadiene has been studied and the only major primary product found was vinylthiirane:[25]

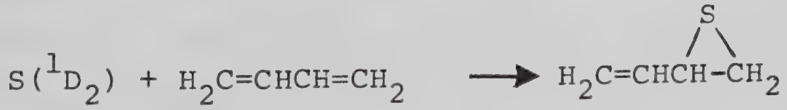

$$S(^1D_2) + H_2C{=}CHCH{=}CH_2 \longrightarrow H_2C{=}CHCH{-}CH_2\ (\text{with S bridging}) \qquad [19]$$

In the present work, no vinylthiirane was observed, even in the presence of high CO_2 pressure (ca. 1200 torr). Thus

1,3-butadiene cannot be responsible for the formation of product **2**.

The thioketone ($CH_2{=}CH\overset{\overset{S}{\|}}{C}CH_3$) formed in step [13b] of Scheme [I], has been synthesized by two research groups using flash thermolysis techniques.[135,136] It was reported to be extremely unstable, dimerizing at -60°[136] and undergoing spontaneous polymerization at room temperature.[135] Neither of these groups reported any observation of the tautomeric enethiols.

The formation of the enethiol (**2**) in the COS-1,2-C_4H_6 system can probably be explained in terms of the experimental conditions employed. In the previous investigations,[135,136] the thioketone produced was immediately condensed at -77 K and allowed to warm up in the condensed state to a temperature at which it either dimerized[136] or polymerized.[135] In the present work, the products were formed in the gas phase at extremely low concentrations ($<10^{-6}$M) diluted by high pressures of COS. Under these conditions, thioketone dimerization or polymerization would occur much less readily than in the condensed phase, thus providing a greater opportunity for tautomerization to take place. Indeed, it has been shown that in the gas phase $CH_2{=}CH\overset{\overset{S}{\|}}{C}CH_3$ dimerizes at high pressures.[136] Furthermore, the higher temperatures ($\geqslant$300 K) employed in this work might be expected to enhance the rate of tautomerization. Additionally, the enethiol-thioketone-enethiol tautomerization could have been photochemically induced, since it has been

demonstrated that enolization of an aliphatic α,β-unsaturated ketone may occur photochemically.[137]

The ultimate fate of any remaining thioketone in this system is uncertain. It could have eventually polymerized in the reaction cell, decomposed during transferral or been lost on the G.C. column. On the other hand, it may have been one of the two unidentified peaks, **6** and **7**, seen in the mass 86 cross-scan (Figure III-1). Bailey and Isogawa[135] could not detect the thioketone by gas chromatography, even when the products of the pyrolysis were fed directly into the GC, but this may have been because their column was made of copper tubing. A related sulfur compound, vinylthiol, has been demonstrated to be quite reactive with copper surfaces,[19] and the thioketone may behave in a similar manner.

Paquer[134] has pointed out that in cases where the tautomerization of a thioketone requires migration of an α-hydrogen belonging to a methyl group, as in step [13c] of scheme (I), the enethiol has not been observed. Since the enethiol can apparently be trapped in chemical reactions, such as the methylation of thiopinacolone,[133]

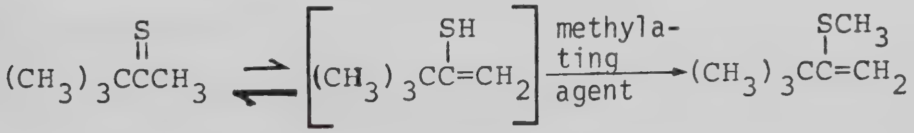

$$(CH_3)_3C\overset{S}{\overset{\|}{C}}CH_3 \rightleftharpoons \left[(CH_3)_3C\overset{SH}{\overset{|}{C}}=CH_2\right] \xrightarrow[\text{agent}]{\text{methylating}} (CH_3)_3C\overset{SCH_3}{\overset{|}{C}}=CH_2 \qquad [20]$$

there is a possibility that the equilibrium lies far to the thioketone side. However it has been pointed out that this observation does not unambiguously prove the real existence of

the enethiol.[134] In the case of product 2, conjugation of the two C=C bonds in the 1-ene-2-thiol form may enhance its stability relative to that of the corresponding thioketone, $CH_2{=}C{-}\overset{S}{\overset{\|}{C}}H_3$, in which the C=C bond is conjugated to the C=S bond. (The initially formed cumulenethiol, $CH_2{=}C{=}\overset{SH}{\overset{|}{C}}{-}CH_3$, which has no conjugation, should be even less stable.) The overall scheme for the production of 2 therefore would appear to be:

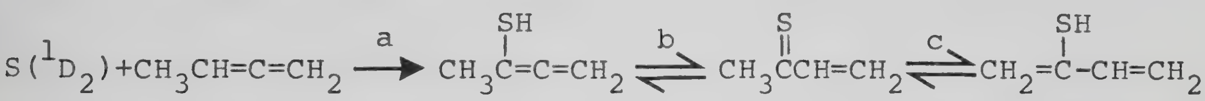

$$S(^1D_2)+CH_3CH{=}C{=}CH_2 \xrightarrow{a} CH_3\overset{SH}{\overset{|}{C}}{=}C{=}CH_2 \overset{b}{\rightleftharpoons} CH_3\overset{S}{\overset{\|}{C}}CH{=}CH_2 \overset{c}{\rightleftharpoons} CH_2{=}\overset{SH}{\overset{|}{C}}{-}CH{=}CH_2$$

(2)

[13]

The fact that no terminal cumulenethiol product ($CH_3CH{=}C{=}C{<}^{SH}_{H}$) was observed in this work can also be explained by a thioketone-enethiol tautomerization process. In the case of the terminal vinyl C-H insertion, the initially formed thiol could tautomerize to a conjugated thioaldehyde:

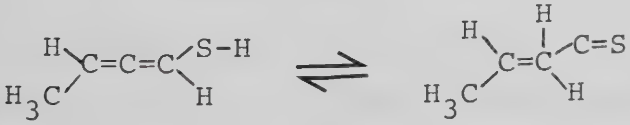

[21]

1,2-butadiene-1-thiol 2-butene-1-thial

However, the only simple conjugated thioaldehyde synthesized to date, thioacrolein ($CH_2{=}CH\overset{S}{\overset{\|}{C}}H$), is so unstable that it decomposes slowly even at 77 K.[138] If the tautomerization (step [21]) equilibrium is reasonably fast, any terminal

cumulenethiol formed may have been lost by rapid reaction, most likely polymerization,of the thioaldehyde tautomer. (There is also a possibility that the terminal cumulenethiol may have been one of the unidentified products, 6 and 7, shown in Figure III-1.)

In the COS-$H_2C=C=CH_2$ system, the corresponding cumulenethiol was also not observed.[63] However, the high methylenethiirane yield,>90%,obtained under low conversion conditions indicates that vinyl C-H insertion can only be of minor importance in this system.

The high yields of thiiranes observed in the present system indicate that for $S(^1D_2)$ atoms, the thiirane formation pathways (steps [9]-[11]) are more important than the insertion reactions (steps [12]-[14]).

The S product distributions listed in Table III-2 are quite different from those for alkenes;[42] thiiranes comprise ∿ 90% of the total C_4H_6S products. As is apparent in Table III-11, the thiirane yield in the S + alkene systems under similar conditions is <70%. These enhanced thiirane yields can be explained in part by the presence of two C=C addition sites and fewer C-H insertion sites. However, since product recoveries were not quantitative, the lower thiol yields may reflect a lower stability of the insertion products in this system.

TABLE III-11

Product Distributions for the COS-Alkene Systems[42]

Alkene	% Distribution		
	Vinyl Type Thiol(s)	Alkenyl Type Thiol(s)	Thiirane
Ethylene	49	..	51
Propylene	19	19	62
Isobutene	12	32	56
2-Butenes	0	32	68
1-Butene	12	29	59
Trimethylethylene	0	42	58
Tetramethylethylene	..	50	50
Vinyl Fluoride	32	..	68
1,1-Difluoroethylene	31	..	69

The increase in thiirane yields with total pressure, as shown in Figure III-15 and Table III-3, provides strong evidence that collisional stabilization of excited precursors, probably hot thiiranes, is important at high pressures (ca. > 150 torr). This pressure enhancing effect cannot be explained on the basis of suppression of isomerization to enethiols since, as mentioned above, such effects are of very minor importance for C_4H_6S. The decrease in CH_4 yield at high pressures suggests the suppression of fragmentation processes. However, the low CH_4 yield indicates that fragmentation leading to formation of this product is of minor importance. An alternative process which would be suppressed at high pressures is fragmentation of the hot thiiranes via a cyclopropanethione intermediate, e.g.[128,139]

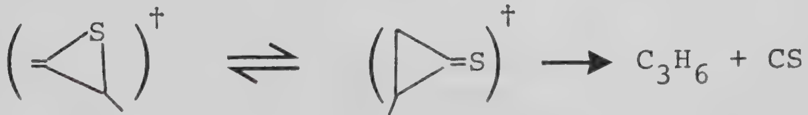

(1)

[22]

The parent cyclopropanethione and methylenethiirane are thought to exist in equilibrium at high temperatures, and it has been suggested that cyclopropanethione can fragment via CS elimination.[128,139] CS may then abstract S from thiiranes yielding the corresponding alkene and CS_2. Indeed, small amounts of CS_2 were observed in the present system and in the COS-allene system.[63]

At high CO_2 pressures (Table III-4), formation of the insertion products **2** and **5** is suppressed and the yields of thiiranes **1**, **3** and **4** are enhanced, as expected. The large increase in the total product yield is a result of pressure stabilization and the increase in concentration of $S(^3P)$ atoms: The greater reactivity of $S(^3P)$ atoms with the substrate relative to COS (vide supra) increases the thiirane yields at the expense of CO formation.

Of the thiiranes, **1** (2,3-addition) is invariably formed in higher yield than **3** + **4** (1,2-addition) for both $S(^3P)$ and $S(^1D_2)$ additions. This preference may be in part due to the electrophilic nature of S atoms: the CH_3 substituted C=C bond is preferred. The intuitive expectation of the greater nucleophilicity of the 2,3 C=C bond is supported by CNDO/S calculations performed on 1,2-C_4H_6,[140]

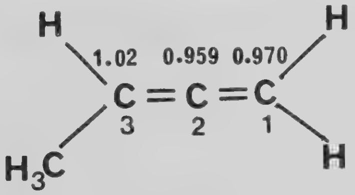

which found that the highest π electron density is at C_3.

Assuming that the yields of **1** and **3** + **4** are proportional to the rates of 2,3 and 1,2-addition respectively, the selectivity of $S(^3P)$ for 2,3 and 1,2-additions may be expressed in terms of the rate constant ratio:

$$\left(k_{2,3}/k_{1,2}\right)^{^3P} \simeq \left(\underset{\sim}{1}/(\underset{\sim}{3} + \underset{\sim}{4})\right)^{^3P}$$

Using the experimental values from Table III-4:

$$\left(k_{2,3}/k_{1,2}\right)^{^3P}_{P=1200\text{ torr, }t=11\text{ min}} \simeq 2.15$$

Alternatively, the values corrected to zero time give:

$$\left(k_{2,3}/k_{1,2}\right)^{^3P}_{P=1200\text{ torr, }t=0} \simeq 2.06$$

Thus the calculated ratio, $(k_{2,3}/k_{1,2})^{^3P}$ is approximately 2.1 and shows essentially no time dependence. Using the zero time values from Table III-4 and the zero time extrapolated thiirane rates at 1200 torr from Figure III-15 reveals that the corresponding selectivity for $S(^1D_2)$ additions in the high pressure limit (Appendix C-1) is:

$$\left(k_{2,3}/k_{1,2}\right)^{^1D}_{P=1200\text{ torr, }t=0} \simeq 1.3$$

Not unexpectedly, $S(^3P)$ is somewhat more selective as a consequence of its lower energy content.

Similarly, assuming that the observed selectivity (2,3 and 1,2-addition) for $S(^3P)$ is pressure independent, the corresponding $S(^1D_2)$ selectivity at zero time and a total pressure of 250 torr is estimated (Appendix C-1) to be:

$$\left(k_{2,3}/k_{1,2}\right)^{^1D}_{P=250\text{ torr, }t=0} \simeq 1.4$$

The apparent similarity in the $k_{2,3}/k_{1,2}$ ratios at 250 and 1200 torr for $S(^1D_2)$ implies that the observed selectivity of $S(^1D_2)$ addition is also pressure independent.

Inspection of the zero time data in Table III-4 reveals that the trans/cis C_4H_6S ratio for $S(^3P)$ addition is

$$\left(\underline{\text{trans}}\ (\underset{\sim}{4})/\underline{\text{cis}}\ (\underset{\sim}{3})\right)^{^3P}_{P=1200\text{ torr, }t=0} \simeq 6.2$$

The high trans/cis product ratio for $S(^3P)$ 1,2-addition is surprising since cis addition does not appear to feature much steric hindrance. However, there is a possibility that the apparent preference for trans addition is a consequence of the relative stabilities of the hot trans and cis adducts.

The trans/cis product ratio for $S(^1D_2)$ addition may be calculated (Appendix C-1) using the zero time values from Table III-4 and the zero time extrapolated thiirane rates at 1200 torr from Figure III-15:

$$\left(\text{trans}(\underset{\sim}{4})/\text{cis}\ (\underset{\sim}{3})\right)^{^1D}_{P=1200\text{ torr, }t=0} \simeq 1.4$$

The much higher trans/cis product ratio for $S(^3P)$ addition ($\sim$6.2) suggests that $S(^3P)$ may be significantly more selective and less reactive than $S(^1D_2)$ in 1,2-addition. Alternatively,

this may reflect a larger difference in stability of the triplet trans and cis adducts.

By analogy with the $S(^1D_2)$ + alkene systems, the addition of $S(^1D_2)$ to 1,2-C_4H_6 most likely follows a single step concerted pathway,[41,46,50,142] e.g.,

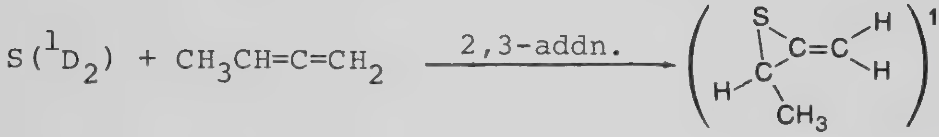
S(¹D₂) + CH₃CH=C=CH₂
2,3-addn.
S
C=C
H
H
H
C
CH₃
1

[9]

For $S(^3P)$ addition, two possible transition states may be considered. One is the ring distorted triplet state thiirane, having a high rotational barrier (∿23 kcal $mole^{-1}$), analogous to that formed in the $S(^3P)$-alkene systems (vide supra), e.g.,

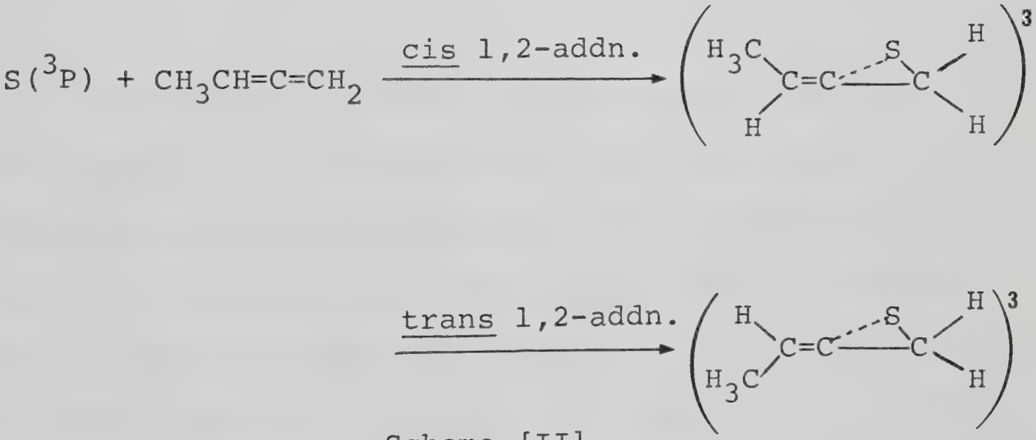
S(³P) + CH₃CH=C=CH₂
cis 1,2-addn.
H₃C
C=C
S
C
H
H
H
3
trans 1,2-addn.
H
C=C
S
C
H
H₃C
H
3

Scheme [II]

On the other hand, the presence of an unsaturated substituent might lower the rotational barrier predicted for the parent thiirane (∿23 kcal $mole^{-1}$)[51] and a freely rotating triplet biradical might be generated, e.g.

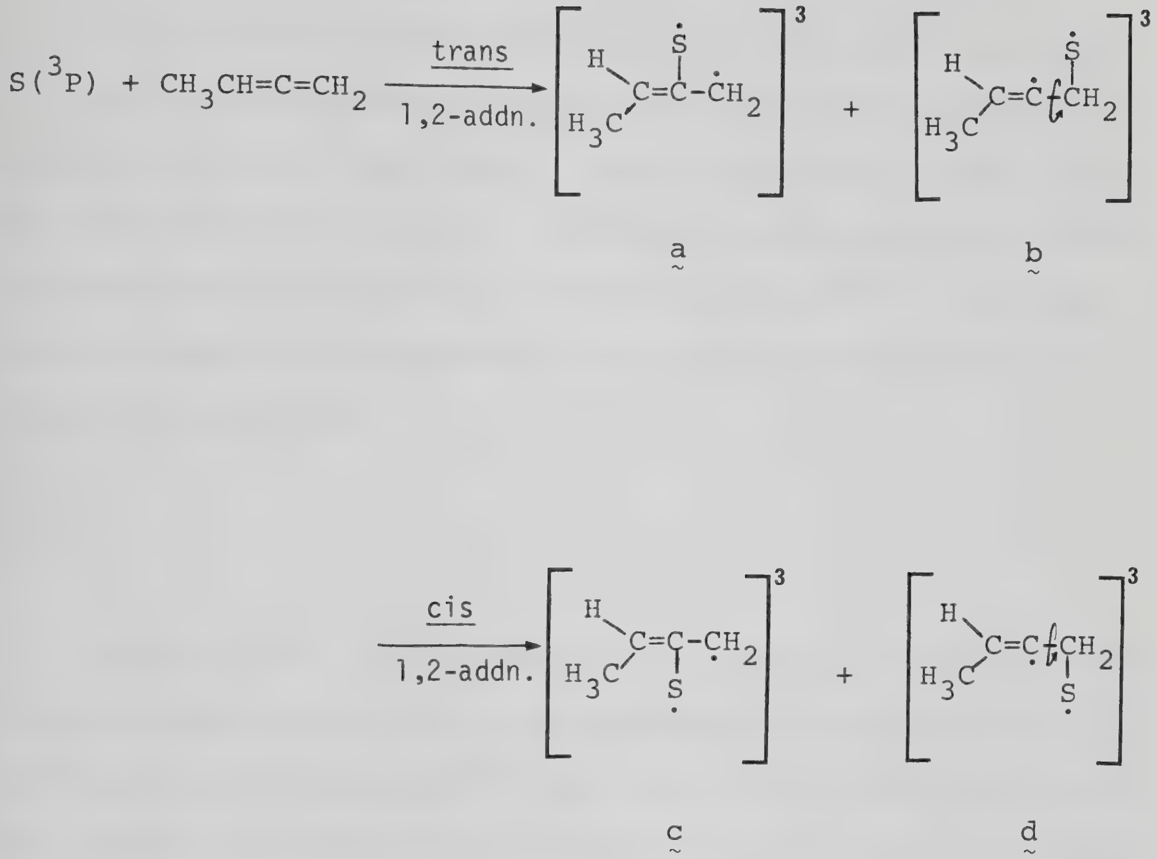

If orientation of S attack is the major influence on the high *trans*/*cis* 1,2-adduct ratio, then biradicals b and d can be ruled out as intermediates since ring closure would lead to a 1:1 mixture of *cis* and *trans* isomers. However, similar to the ring distorted thiirane (scheme [II]),biradicals a and c would evolve to the *trans* and *cis* adducts, respectively, and *cis* S attack may be somewhat hindered by the CH$_3$ group, resulting in a high *trans*/*cis* adduct ratio. Thus an explanation of the observed high *trans*/*cis* ratio based on orientation of attack does not serve to distinguish between the ring distorted thiiranes and biradicals a and c as intermediates.

Nonetheless, the entropies of activation for the $S(^3P)$ 1,2 and 2,3-additions are similar to those of the $S(^3P)$ + alkene reactions (_vide infra_), suggesting that similar transition states are involved. Thus, by analogy with the latter systems, the intermediates involved in the $S(^3P) + 1,2\text{-}C_4H_6$ reaction most likely resemble a ring distorted thiirane as shown in scheme II.

Unlike $S(^3P)$, $O(^3P)$ reacts with $1,2\text{-}C_4H_6$ to yield mainly CO and propylene, with only small amounts of O-containing products being observed.[103] The high CO and propylene yields are thought to result from decomposition of an excited cyclopropanone intermediate:[103]

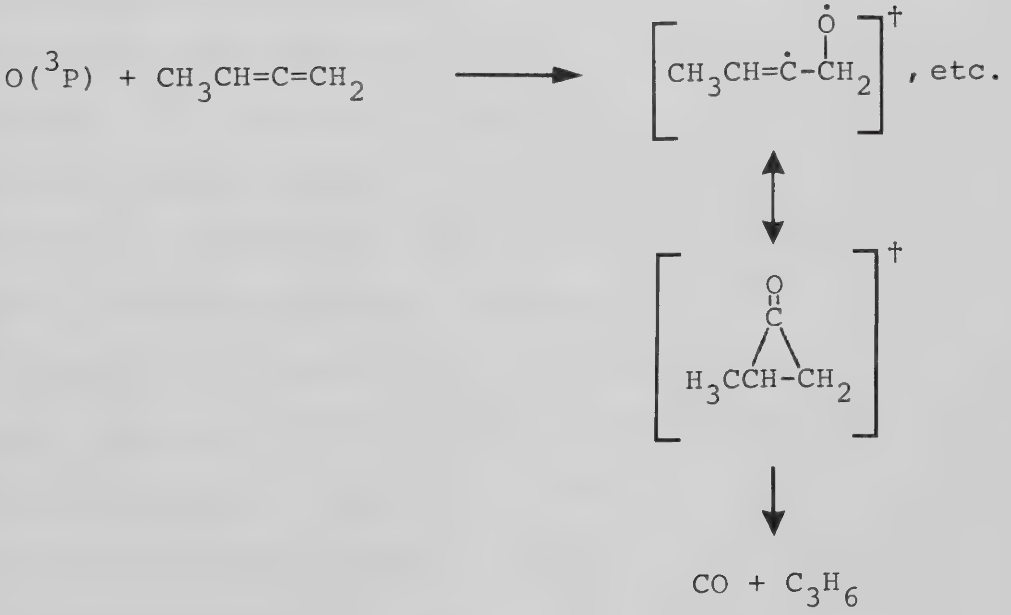

[23]

Although an allene oxide may exist as a transient species, any which is formed would be expected to isomerize to the more stable cyclopropanone.[103,128] The parent cyclopropanone is $\sim$23 kcal mole^{-1} lower in energy than allene oxide,[128,143] but polymerizes rapidly at room temperature.[103] On the other hand, calculations based on bond energies predict the corresponding cyclopropanethione to be $\sim$7 kcal mole^{-1} less stable than methylenethiirane.[128,143] This difference in the order of stability is probably due to the higher bond energy of a C=O bond, 172 kcal mole^{-1}, as compared to that of a C=S bond (129 kcal mole^{-1}). Therefore, a cyclopropanethione intermediate is not likely to be as important in the $S(^3P)$ + 1,2-C_4H_6 reaction. Assuming that the distribution of carbonyl products in the $O(^3P)$ + 1,2-butadiene reaction corresponds to the relative orientations of $O(^3P)$ addition, $O(^3P)$ adds to the allenic carbons in the order: $C_2 > C_1 > C_3$ ($\sim$1.7, $\sim$1.1, $\sim$0.3).[103] This order of affinity for C atom attack implies some preference of $O(^3P)$ for the 1,2 C=C bond and is in contrast to the marked preference of the $S(^3P)$ atom for 2,3-addition. The preference of attack for $O(^3P)$ then depends strongly on the stability of the resulting biradical.

Creary[144,145] recently studied the additions of a series of aryl carbenes to $(CH_3)_2C{=}C{=}CH_2$ and observed that singlet carbenes, $[R_1R_2C:]^1$, add preferentially to the 2,3 C=C bond, whereas the triplet carbenes, $[R_1R_2C:]^3$, reacted to give products corresponding to 1,2-addition. It was postulated that

the initial attack of $[R_1R_2C:]^3$ takes place at the C_2 carbon:

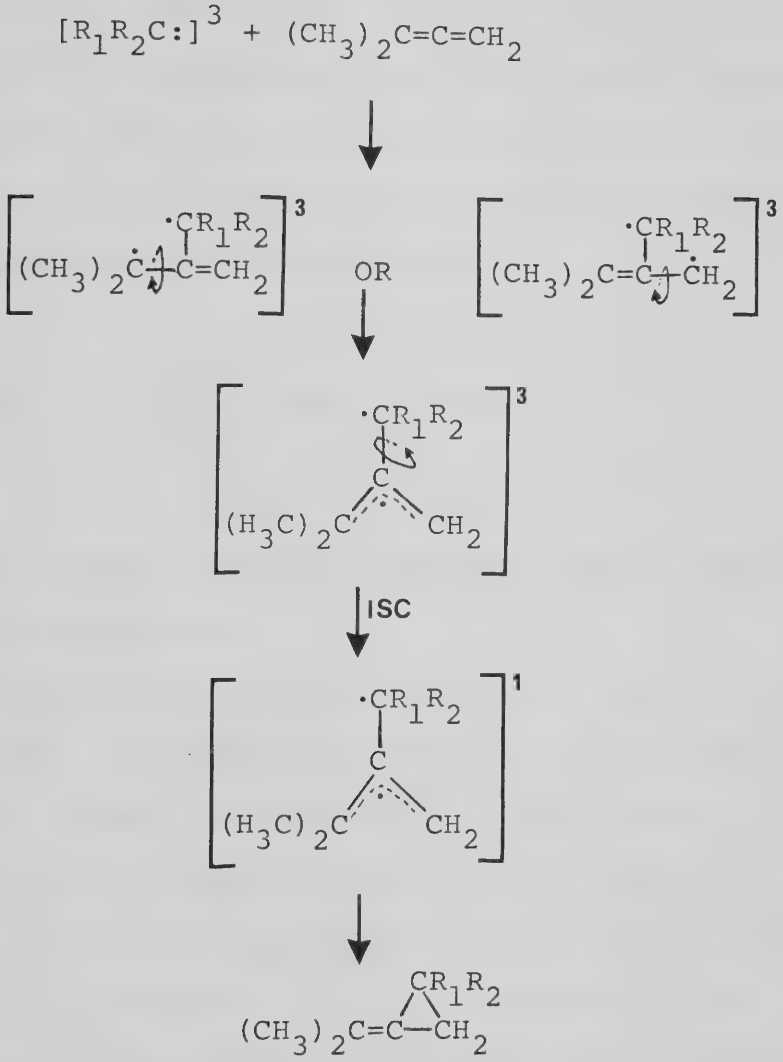

[24]

The initially formed triplet adducts then undergo a 90° internal rotation to form a more stable triplet allyl biradical. The allyl biradical then undergoes intersystem crossing to the singlet state, which leads to the 1,2-addition product via ring closure.

Recent kinetic measurements on the reactions of C_3(:C=C=C:) with a series of allenes indicate that although the rate of reaction is slow ($k \sim 10^7 - 10^9\ M^{-1}s^{-1}$), it increases with increasing alkyl substitution on the allenic carbons.[146] Based on the observed trend in rate constants, it was postulated that C_3 adds electrophilically to one of the allenic bonds to form cyclic intermediates:

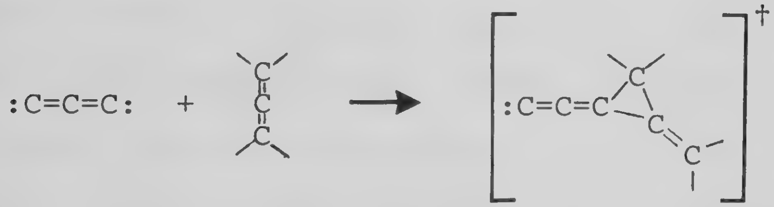

[25]

However, no other evidence supporting the proposed intermediate was obtained.

The reactions of monoradicals with allene have also been studied. The reaction of OH with allene has been investigated by a number of groups.[147,148] The trend in rate parameters for OH + dienes follows similar trends as in the cases of O(^{3}P) and S(^{3}P) (vide infra). This implies that OH also adds electrophilically to dienes. Molecular beam mass spectral studies indicate that the primary step involves the formation of an OH adduct.[150,151] More recent work[148] has shown that abstraction also takes place, but to a very small extent (< 12%). Unfortunately, for the addition reaction, no information is available regarding the preferred site of attack.

Ethylthiyl radical (C_2H_5S) addition to a series of allenes has been studied,[152] and the observed product distributions for

the 1,2-butadiene reaction follow a trend similar to that for O(^{3}P) addition (C_2>C_1>C_3). This product distribution trend is most easily rationalized in terms of the steric hindrance of the CH_3 group and polar effects in stabilizing the radicals involved.[153]

Some reactions of atoms and radicals with allenes are summarized in Table III-12. It is apparent that those singlet species such as S($^1D_2$) and $[R_1R_2C:]^1$, which are expected to form cyclic intermediates, prefer addition to the substituted C=C bond. With the exception of S(^{3}P), the other atomic and radical species listed preferentially add to the unsubstituted C=C bond via acyclic intermediates. These observations also support the postulate that the intermediate for S(^{3}P) addition to 1,2-C_4H_6 is a ring distorted thiirane.

Although 1,2-C_4H_6 possesses two double bonds, the rate of reaction with S(^{3}P) at room temperature, as shown in Table III-5, is slower than that with the reference alkene, 1-C_4H_8. When the relative Arrhenius parameters obtained from the competitive studies with 1-C_4H_8 ($A_{1,2\text{-}C_4H_6}/A_{1\text{-}C_4H_8}$ = 5.31±0.26; $E_{1\text{-}C_4H_8} - E_{1,2\text{-}C_4H_6}$ = -1.17±0.03 kcal mole^{-1}) are calculated on an absolute scale, the following parameters are obtained:

TABLE III-12

Atom and Radical Reactions with Terminal Allenes.

Reagent	Allene	Primary Adduct	Preferred Site of Addition	Reference
$S(^1D)$	$CH_2=C=CH_2$	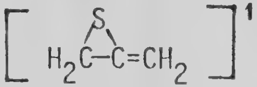	--	63
$S(^3P)$	$CH_2=C=CH_2$	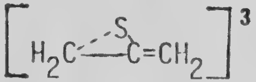	--	63
$S(^1D_2)$	$CH_3CH=C=CH_2$	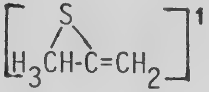 , etc.	2,3-addition	this work
$S(^3P)$	$CH_3CH=C=CH_2$	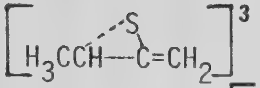 , etc.	2,3-addition	this work
$O(^3P)$	$CH_3CH=C=CH_2$	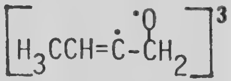 ,etc. ↔ 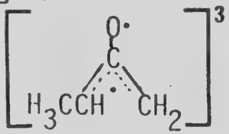	$C_2>C_1>C_3$ (1,2-addition)	103
$[R_1R_2C:]^1$	$(CH_3)C=C=CH_2$	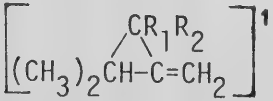	2,3-addition	145
$[R_1R_2C:]^3$	$(CH_3)C=C=CH_2$	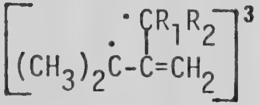 ↔ ,etc. 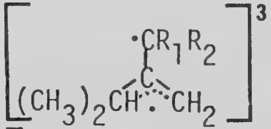	1,2-addition	145
$:C=C=C:$	$CH_2=C=CH_2$	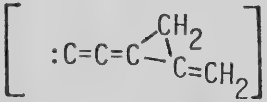	--	146
$C_2H_5S\cdot$	$CH_3CH=C=CH_2$	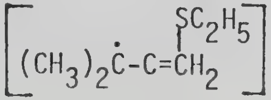 , etc.	$C_2>C_1>C_3$ (1,2-addition)	153

$$A_{1,2\text{-}C_4H_6} = (2.37 \pm 0.38) \times 10^{10}\ M^{-1}s^{-1}, \text{ and}$$

$$E_{1,2\text{-}C_4H_6} = 1.53 \pm 0.10 \text{ kcal mole}^{-1}$$

if the absolute rate parameters for the $S(^3P) + 1\text{-}C_4H_8$ reaction determined by Klemm and Davis[52] are used. However, the values measured by Van Roodselaar[53] lead to:

$$A_{1,2\text{-}C_4H_6} = (6.38 \pm 1.11) \times 10^{10}\ M^{-1}s^{-1}, \text{ and}$$

$$E_{1,2\text{-}C_4H_6} = 1.38 \pm 0.20 \text{ kcal mole}^{-1}.$$

Klemm and Davis[52] measured rate parameters for a number of $S(^3P)$ + alkene reactions using the flash photolysis-resonance fluorescence method, whereas Van Roodselaar[53] employed the flash photolysis-kinetic absorption technique. In general, the E_a's measured by these two methods are in excellent agreement, but the A factors determined by Van Roodselaar[53] are consistently about a factor of 2 to 4 higher than those reported by Klemm and Davis.[52] Since the reason for these discrepancies is not clear, average values will be taken to obtain the absolute rate parameters for $S(^3P)$ + $1,2\text{-}C_4H_6$, which gives:

$$k = (4.38 \pm 1.14) \times 10^{10} \exp[(-1455 \pm 225)/RT]\ M^{-1}s^{-1} \qquad [26]$$

This corresponds to a room temperature rate constant, $k_{298} = 3.8 \times 10^9\ M^{-1}s^{-1}$. Since the two C=C bonds represent two distinct non-equivalent reaction sites (1,2 and 2,3-addition sites), these observed rate parameters are apparent values only. However the rate parameters for the two individual sites can be determined, as will be shown later.

The apparent Arrhenius parameters for the $S(^3P)$ + 1,2-C_4H_6 reactions are compared to those for $O(^3P)$ and OH $(^2\Pi)$ reactions in Table III-13. The A factor for this reaction is somewhat larger than those in the $S(^3P)$ + alkene systems. This is partly a consequence of the presence of the second (orthogonal) C=C bond. A parallel trend is observed in the oxygen systems, where the A factor for the parent allene reaction is approximately twice that for alkenes. The increase in A factor on going from a conjugated to a cumulated diene may be a consequence of the change from a linear reactant molecule to a bent activated complex on addition of an S atom in the latter system.

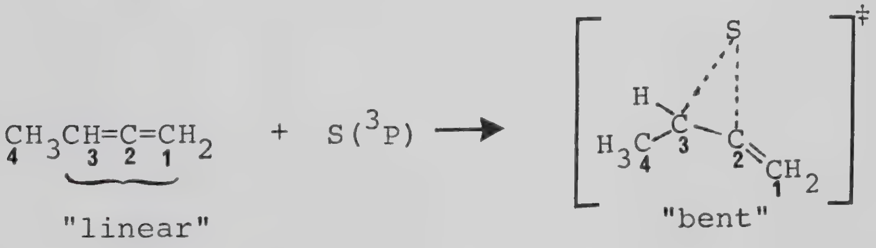

It is apparent from the structure of the transition state that the addition of S results in a large increase in moment of inertia about the C_3-C_2 axis. Consequently, there is a substantial rotational contribution to the entropy of activ-

TABLE III-13

Rate Parameters for $S(^3P)$, $O(^3P)$ and $OH(^2\Pi)$ Reactions with Alkenes and Dienes.

Substrate	$S(^3P)$			$O(^3P)$			$OH(^2\Pi)$		
	$k_{298}\times10^{-9}$ $(M^{-1}s^{-1})$	$A\times10^{-10}$ $(M^{-1}s^{-1})$	E_a $\frac{kcal}{mole}$	$k_{298}\times10^{-9}$ $(M^{-1}s^{-1})$	$A\times10^{-10}$ $(M^{-1}s^{-1})$	E_a $\frac{kcal}{mole}$	$k_{298}\times10^{-9}$ $(M^{-1}s^{-1})$	$A\times10^{-10}$ $(M^{-1}s^{-1})$	E_a $\frac{kcal}{mole}$
$CH_2=C=CH_2$	2-4[a]	..	0-1	0.76[e]	1.8	1.9	2.0[h]	0.34	-0.31
$CH_3CH=C=CH_2$	3.8[b]	4.4	1.5	1.7[f]	..	..	..	..	..
$CH_2=CC=CH_2$	28[c]	2.6	-0.04	12.5[e]	1.2	0	42[h]	0.87	-0.93
$CH_3CH=CH_2$	3.9[d]	0.83	0.44	2.2[g]	0.76	0.70	15.1[h]	0.25	-1.1
$C_2H_5CH=CH_2$	5.1[d]	0.82	0.28	2.4[g]	0.72	0.66	21.1[h]	0.46	-0.93

[a] estimated values from ref. 63.

[b] this work.

[c] calculated from relative rate data in ref. 96, and absolute rate data averaged from ref. 52 and 53.

[d] average values of ref. 52 and 53.

[e] ref. 101.

[f] calculated from relative rate data in ref. 103 and absolute rate data in ref. 101.

[g] ref. 55.

[h] ref. 147.

ation ($\Delta S^{\ddagger}$) and a correspondingly high A factor is observed. On the other hand, in conjugated systems such as 1,3-butadiene, the reactant molecule possesses a bent structure having parallel π bonds, and addition of S has an insignificant effect on the moment of inertia about the C_3-C_2 axis:

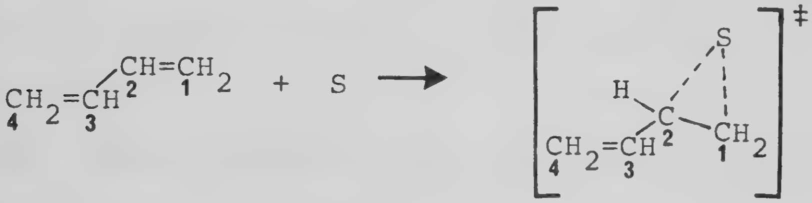

Thus the entropy of activation and A factor are relatively small.

A similar explanation has been invoked to account for the relatively high A factor for the alkyne addition reactions as compared to those of alkenes.[154] For example, the rotational contribution to $\Delta S^{\ddagger}$ in the $S(^3P) + C_2H_2$ system is 3.3 times higher than in the corresponding C_2H_4 case.[76]

The possibility that the larger A-factor for 1,2- as compared to 1,3-butadiene is a consequence of a difference in the transition states (a freely rotating biradical rather than a ring distorted activated complex as suggested for 1,3-C_4H_6) is unlikely. The difference in $\Delta S^{\ddagger}$ for the $S(^3P)$ + 1,2 and 1,3-C_4H_6 is only 1 e.u. ($\Delta S^{\ddagger}_{1,2\text{-}C_4H_6} = -22.1$ e.u., $\Delta S^{\ddagger}_{1,3\text{-}C_4H_6} = -23.1$ e.u.), indicating that the transition states are similar.

The room temperature rate constant measured in this work for the $S(^3P)$ + 1,2-C_4H_6 reaction is approximately twice that for the corresponding reaction of $O(^3P)$. This observation is consistent with the relative rate constants of $S(^3P)$ to $O(^3P)$ in reaction with other substrates (Table III-13), and the higher reactivity of $S(^3P)$ atoms is a consequence of the lower activation energies associated with the addition reactions.

For the OH reactions, the room temperature rate constants also follow a trend similar to that observed for $S(^3P)$. The rate constants are generally greater, due to the negative activation energies for the OH reactions. If abstraction actually occurs, as suggested by Hoyermann and co-workers,[148] the activation energies for addition will be even more negative than those listed in Table III-13. As in the case of $S(^3P)$, the E_a for the OH reactions is highest for the parent allene. The A factors are much smaller than those for the corresponding $S(^3P)$ reactions and show no definite trend.

Despite the larger A factor as compared to the $S(^3P)$ + 1,3-C_4H_6 reaction, the $S(^3P)$ + 1,2-C_4H_6 reaction proceeds at a slower rate. This can be attributed to the higher activation energy ($\sim$1.5 kcal mole^{-1} versus -0.4 kcal mole^{-1}) for the latter reaction. Similarly, in the oxygen systems, the $O(^3P)$ + $CH_2{=}C{=}CH_2$ reaction is much slower than the corresponding 1,3-C_4H_6 reaction (Table III-13) due to its higher E_a.

The lower activation energies observed for the conjugated diene reactions may be ascribed to delocalization of the π electrons.

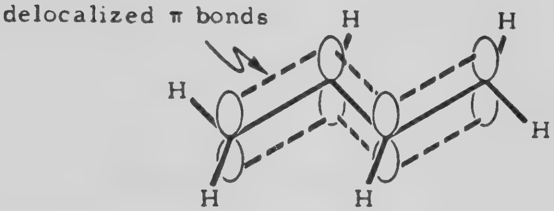

This renders the π orbitals more polarizable than those in non-conjugated systems, resulting in a lower energy requirement for the π complex formation in electrophilic reactions. In cumulated dienes, on the other hand, delocalization of the π electrons is absent due to the orthogonality of the two bonds. Additionally, hyperconjugation (σ-π overlap) between the coplanar C-H and π bonds in 1,2-butadiene imparts partial triple bond character to the C=C bonds, e.g.:[130]

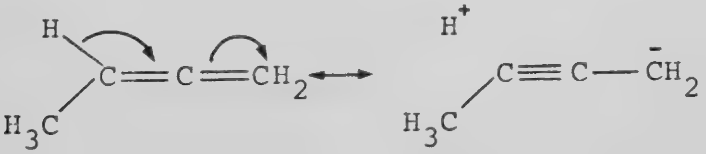

, etc.

This phenomenon raises the energy barrier for π complex formation relative to that for the conjugated and isolated systems.

A plot of E_a versus ionization potential for $S(^3P)$ + alkenes, alkynes, and dienes is given in Figure III-18. It is apparent that the E_a for the $S(^3P) + 1,2\text{-}C_4H_6$ reaction

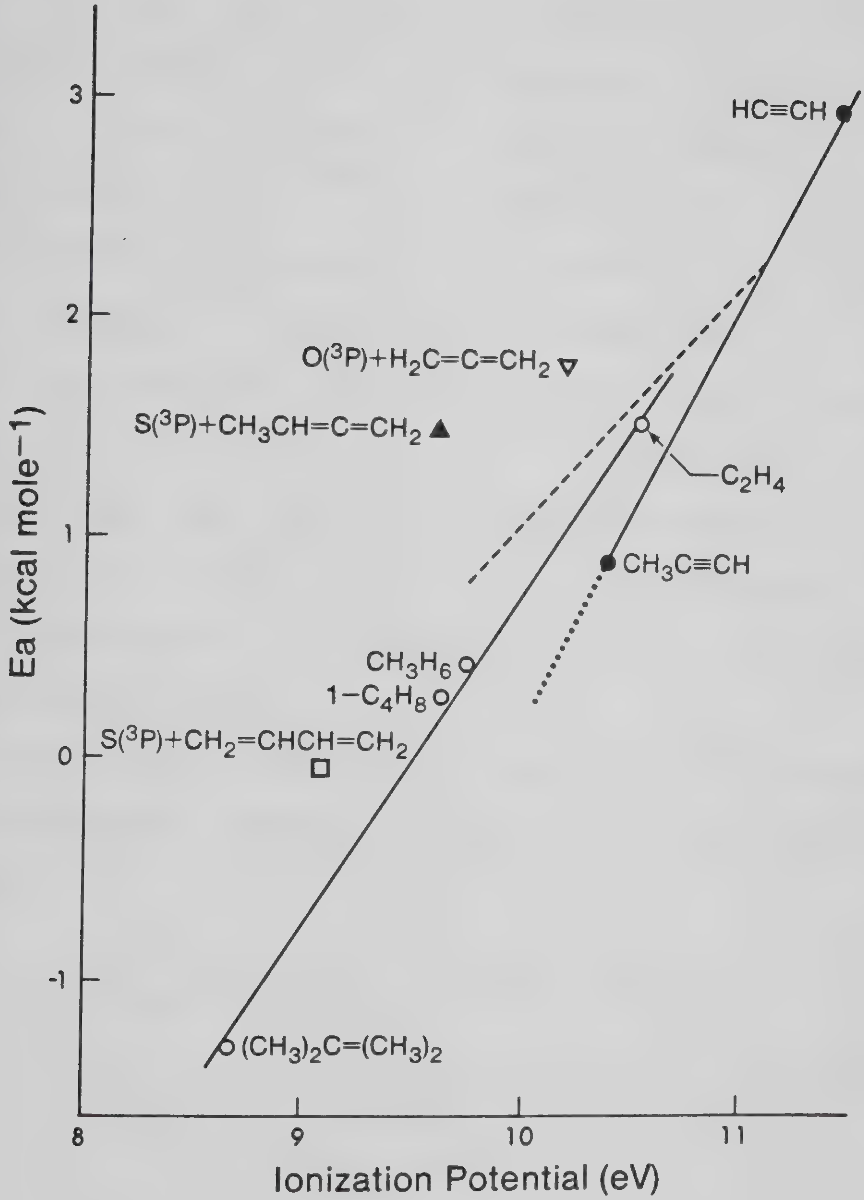

FIGURE III-18: Plots of E_a versus ionization potential for the $S(^3P)$ + alkenes, alkynes and dienes systems, and $O(^3P)$ + alkenes (----).

lies above the correlation line for the $S(^3P)$ + alkene systems. A smaller deviation in E_a is also seen for the conjugated diene, $1,3\text{-}C_4H_6$. Similarly, the E_a for the $O(^3P) + CH_2{=}C{=}CH_2$ reaction[100-1,105] is at least 0.5 kcal mole^{-1} above the correlation line for the $O(^3P)$ + alkene reactions given by Slagle _et_ _al_.[119] Furthermore, although only two substrates have been examined, the E_a-ionization potential correlation for the $S(^3P)$ + alkyne reaction[76] appears to be significantly different from that of the corresponding alkene reactions. Hence, it is likely that the activation energies for the $S(^3P)$ + allene reactions in general lie on a line different from that of the alkenes.

The relative rates of 1,2 and 2,3 $S(^3P)$ addition have been estimated from the isomeric thiirane yields (Table III-4) as:

$$k_{2,3}/k_{1,2} = \underset{\sim}{1}/(\underset{\sim}{3} + \underset{\sim}{4}) \sim 2.1 \text{ at } 300^{\circ}K$$

and since the overall rate of addition is $3.8 \times 10^9\ M^{-1}s^{-1}$,

$$k_{2,3} \simeq 2.6 \times 10^9\ M^{-1}s^{-1}$$

and $$k_{1,2} \simeq 1.2 \times 10^9\ M^{-1}s^{-1}$$

In principle, $k_{2,3}$ and $k_{1,2}$ can have a different temperature dependence. However, the ratios, $\underset{\sim}{1}/(\underset{\sim}{3} + \underset{\sim}{4})$, calculated from the data in Table III-5 - III-9 and listed in Table III-14, are constant over the temperature range studied. Thus, both the 1,2 and 2,3-additions feature equal activation

TABLE III-14

Effect of Temperature on the Yields of 2,3 and 1,2 S(^{3}P)-Addition Products.[a]

Temperature (°K)	Product Yields (μmole)		1/(3+4) = $k_{2,3}/k_{1,2}$
	1	3+4	
300	0.488	0.239	2.05[b]
333	0.548	0.244	2.24
363	0.562	0.281	2.00
393	0.620	0.305	2.03
423	0.649	0.267	2.43

[a] Values at each temperature are sum of four competitive runs where P(COS) = 100 torr, P(CO_2)∿1250 torr, P(1-C_4H_8)∿70 torr and P(1,2-C_4H_6) = 15-40 torr for each temperature; R°_{CO} = 0.349, 0.384, 0.414, 0.432 and 0.502 μmole min^{-1} for temperatures = 300, 333, 363, 393 and 423 °K, respectively, and the corresponding exposure times are 500, 470, 435, 410 and 350 sec.

[b] Average value of 1/(3+4) = 2.15.

energies ($\sim$1.5 kcal mole^{-1}) and the difference between the two rate constants is due to the difference in the A factors. Since $(k_{2,3}/k_{1,2}) \sim 2.1$, the Arrhenius expressions for the two additions are:

$$k_{1,2} = (1.41 \pm 0.38) \times 10^{10} \exp[-(1455 \pm 225)/RT]\ M^{-1}s^{-1} \quad [27]$$

$$k_{2,3} = (2.96 \pm 0.80) \times 10^{10} \exp[-(1455 \pm 225)/RT]\ M^{-1}s^{-1} \quad [28]$$

The A factors calculated for the two addition reactions correspond to entropies of activation,

$$\Delta S^{\ddagger}_{1,2} \simeq -24.4 \text{ e.u.}$$

$$\Delta S^{\ddagger}_{2,3} \simeq -22.9 \text{ e.u.}$$

The values are similar to those for the $S(^3P)$ + alkene reactions, e.g. $\Delta S^{\ddagger}$ for $1\text{-}C_4H_8 \simeq -25.4$ e.u., reflecting a similarity in the transition states for both systems.

The 2,3 and 1,2 C=C bonds of $1,2\text{-}C_4H_6$ share structural similarities with $CH_3CH{=}CH_2$ and $CH_2{=}CH_2$, respectively. The average of the room temperature rate constants obtained by Klemm and Davis[52] and Van Roodselaar[53] for the $S(^3P)$ + $CH_3CH{=}CH_2$ and $CH_2{=}CH_2$ reactions are:

$$k_{C_3H_6} = 3.7 \times 10^{9}\ M^{-1}s^{-1}, \text{ and}$$

$$k_{C_2H_4} = 6.0 \times 10^{8}\ M^{-1}s^{-1}, \text{ respectively.}$$

Surprisingly, the room temperature rate constants for addition to the allenic bonds ($k_{2,3} \simeq 2.6 \times 10^9$, $k_{1,2} \simeq 1.2 \times 10^9$ $M^{-1}s^{-1}$) are within a factor of 2 of those for the corresponding alkenes.

CHAPTER IV

REACTIONS OF SULFUR ATOMS WITH ACYCLIC AND CYCLIC THIOETHERS

A. Results

1) $S(^1D_2, ^3P)$ + Dimethylsulfide - An Acyclic Thioether

(a) UV absorption of dimethysulfide

Dimethylsulfide absorbs significantly in the spectral region used for COS photolysis ($\lambda \simeq 240$-260 nm). Indeed, blank experiments with CH_3SCH_3 indicated that a small amount of decomposition into CH_3SSCH_3, C_2H_6 and CH_4 takes place. For CH_3SCH_3 and COS, the room temperature extinction coefficients at 240 nm are 9.3 and 31.8 l mole^{-1}cm^{-1}, respectively, and at 254 nm, they are 3.6 and 13.6 l mole^{-1}cm^{-1}. Thus for a COS/CH_3SCH_3 ratio of $\sim 10/1$, approximately 97% of the incident radiation is absorbed by COS at these wavelengths.

(b) Reaction Products

Photolysis of COS in the presence of CH_3SCH_3 led to the formation of CH_3SSCH_3 as the major condensable product along with small quantities of C_2H_6 and CH_4. At long exposure times trace amounts of CH_3SH were detected but could not be measured quantitatively, owing to incomplete separation from COS by

GC or distillation. All products were identified by mass spectral analysis and by comparison of their GC retention times with those of authentic samples. C-H insertion products and heavier molecular weight S compounds such as $CH_3S_3CH_3$ and $CH_3S_4CH_3$ were demonstrably absent.

Product recoveries were low, averaging between 20 and 30% (Table IV-1) in terms of the total amount of sulfur atoms reacting with CH_3SCH_3. In order to ascertain whether this product loss could be accounted for in terms of involatile polymer, two sets of high conversion experiments were performed on mixtures consisting of 300 torr COS and 30 torr CH_3SCH_3.

i) Oxidation Experiments

After a 30 minute photolysis, which corresponded to a S product loss of 9.8 μmoles, the cell was evacuated, filled with ∿200 μmole oxygen, and subjected to microwave discharge for two hours. The condensable products, analyzed by GC, consisted solely of SO_2 (∿3 μmoles). Blank experiments with CH_3SCH_3 and O_2 however, showed that CO_2 could be recovered quantitatively but SO_2 recoveries were poor, probably due to reaction with H_2O, one of the other oxidation products. Therefore, these results indicate that the cell residues contained S but not C.

TABLE IV-1

Effect of Exposure Time on the Product Yields in the COS-CH_3SCH_3 System

Time	Pressure (torr)		Products (μmoles)				% Recovery[a]
(min.)	CH_3SCH_3	COS	CO	CH_3SSCH_3	C_2H_6	CH_4	
5	5	100	2.06	0.187	0.027	0.011	27
10	5	100	4.04	0.347	0.047	0.034	24
15	5	100	6.17	0.693	0.069	0.066	33
30	5	100	12.3	1.37	0.123	0.193	33
5	10	100	1.98	0.165	0.035	0.026	25
10	10	100	3.90	0.412	0.068	0.065	29
15	10	100	5.94	0.658	0.093	0.112	31
30	10	100	11.5	1.111	0.161	0.314	27
1.5	30	300	0.682	0.064	0.006	0	18
5	30	300	2.45	0.209	0.024	0.010	22
10	30	300	4.57	0.389	0.040	0.037	18
15	30	300	7.08	0.570	0.071	0.079	20
22	30	300	10.2	0.828	0.080	0.141	19
30	30	300	13.4	1.09	0.101	0.210	18
37	30	300	16.7	1.37	0.118	0.310	14
45	30	300	20.8	1.65	0.151	0.431	15

[a] % Recovery = $R(CH_3SSCH_3 + CH_4 + C_2H_6)/R(CO° - CO)$ where $R^{\circ}_{CO} = 0.58$ μmoles min^{-1} for P(COS) = 100 torr and 0.711 μmole min^{-1} for P(COS) = 300 torr.

ii) Spectroscopic Analysis

High conversion runs corresponding to an S product loss of approximately 19-31 μmoles were carried out. Following each experiment, the cell was evacuated, cut off, and subjected to three 1 ml rinsings with $CHCl_3$. The solvent was evaporated from the combined washings, and the yellowish dry solid was redissolved in $CDCl_3$. No proton NMR (200 MHz) signal from this solution could be detected, even though the minimum detection limit for a single resonance under the conditions used was <0.1 μmole. Finally, the photolysis was repeated using a mixture consisting of $COS/CH_3SCH_3/CO_2 = 300/30/1300$, in which mainly $S(^3P)$ atoms were produced ($>90\%$). NMR samples prepared as above gave no signal. A sample obtained by subsequent rinsings of the cell with CCl_4 was also NMR inactive. These observations indicate the absence of H-containing compounds.

For each NMR sample, the solvent was evaporated and the solid residue was subjected to direct probe MS analysis. The mass spectra obtained were very simple and consisted of peaks at multiples of 32 up to 256, indicating the presence of elemental sulfur only.

Results from the above oxidation and spectroscopic experiments thus demonstrate the absence of hydrocarbons in the cell residue, and indicate that the mass imbalance in the S + CH_3SCH_3 system is due to the formation of elemental sulfur.

(c) Effects of Exposure Time, Total Pressure, and Added CO_2 and NO on Product Yields

The variations in the product yields with time are listed in Table IV-1. The yield of the major product, CH_3SSCH_3, shows little variation when the COS/CH_3SCH_3 ratio decreases from 20:1 to 10:1. CH_4 comprises an increasingly larger fraction of the total yield at longer exposure times. The temporal behaviour of the product yields from the photolysis of 300 torr COS in the presence of 30 torr CH_3SCH_3 is illustrated in Figure IV-1 and the variations in the rates (per μmole CO) are shown in Figure IV-2. The increasing rate of CH_4 formation with increasing conversion clearly indicates that it is a secondary product. The rates of CH_3SSCH_3 and C_2H_6 decrease slightly to apparently constant values at longer exposure times.

The effects of total pressure on the product yields are listed in Table IV-2 and the rates are illustrated in Figure IV-3. At low pressures, the CH_3SSCH_3 rate is relatively high but appears to decrease to a constant limiting value. At high pressures, C_2H_6 and CH_4 exhibit similar behaviour.

The effects of added CO_2 and NO are listed in Table IV-3. Increasing pressures of CO_2 resulted in a marked decrease in the yields of CH_3SSCH_3 and CH_4 and a smaller but still quite significant decrease in that of C_2H_6.

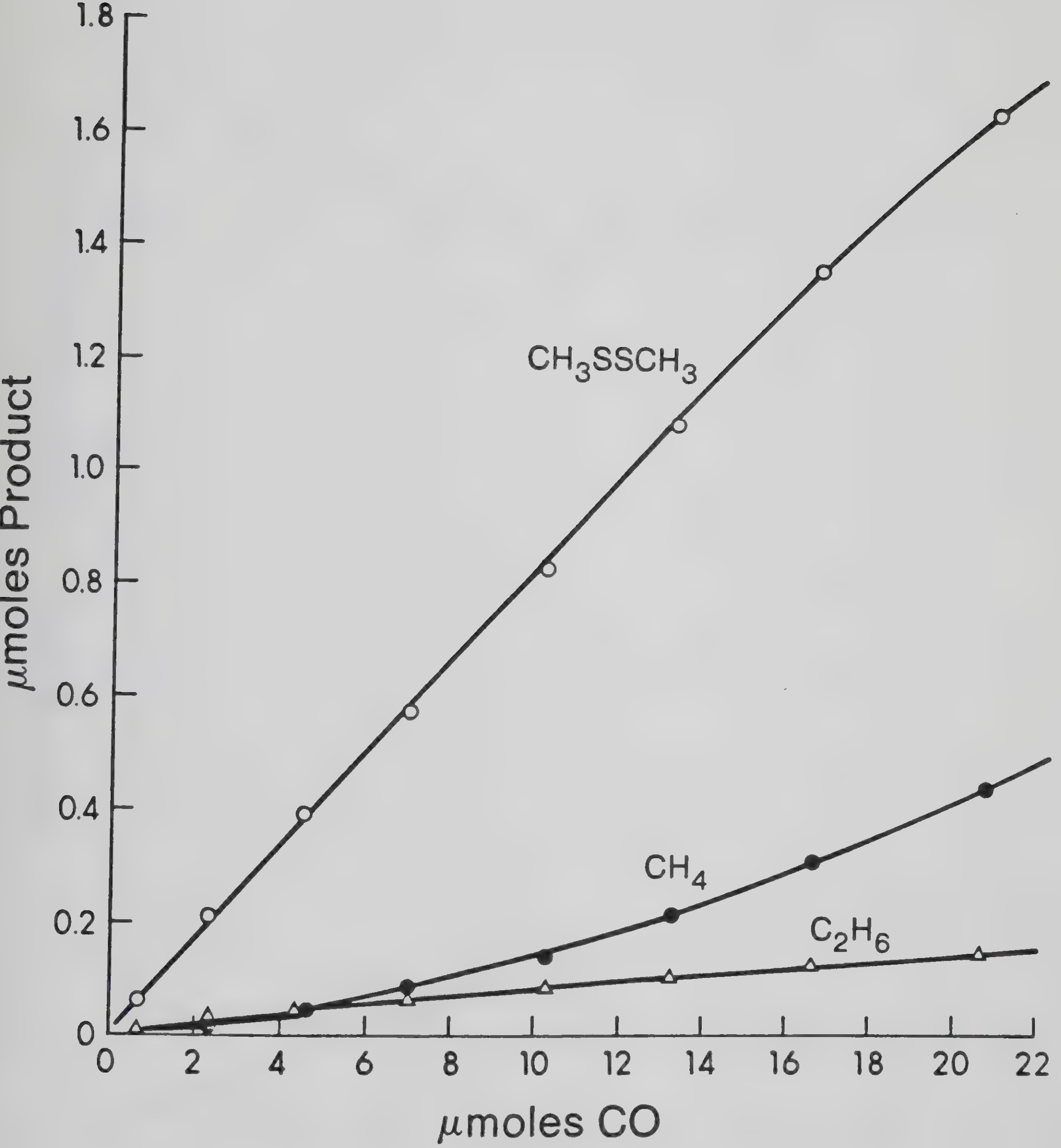

FIGURE IV-1: Product yields as a function of CO yield in the COS - CH_3SCH_3 system.

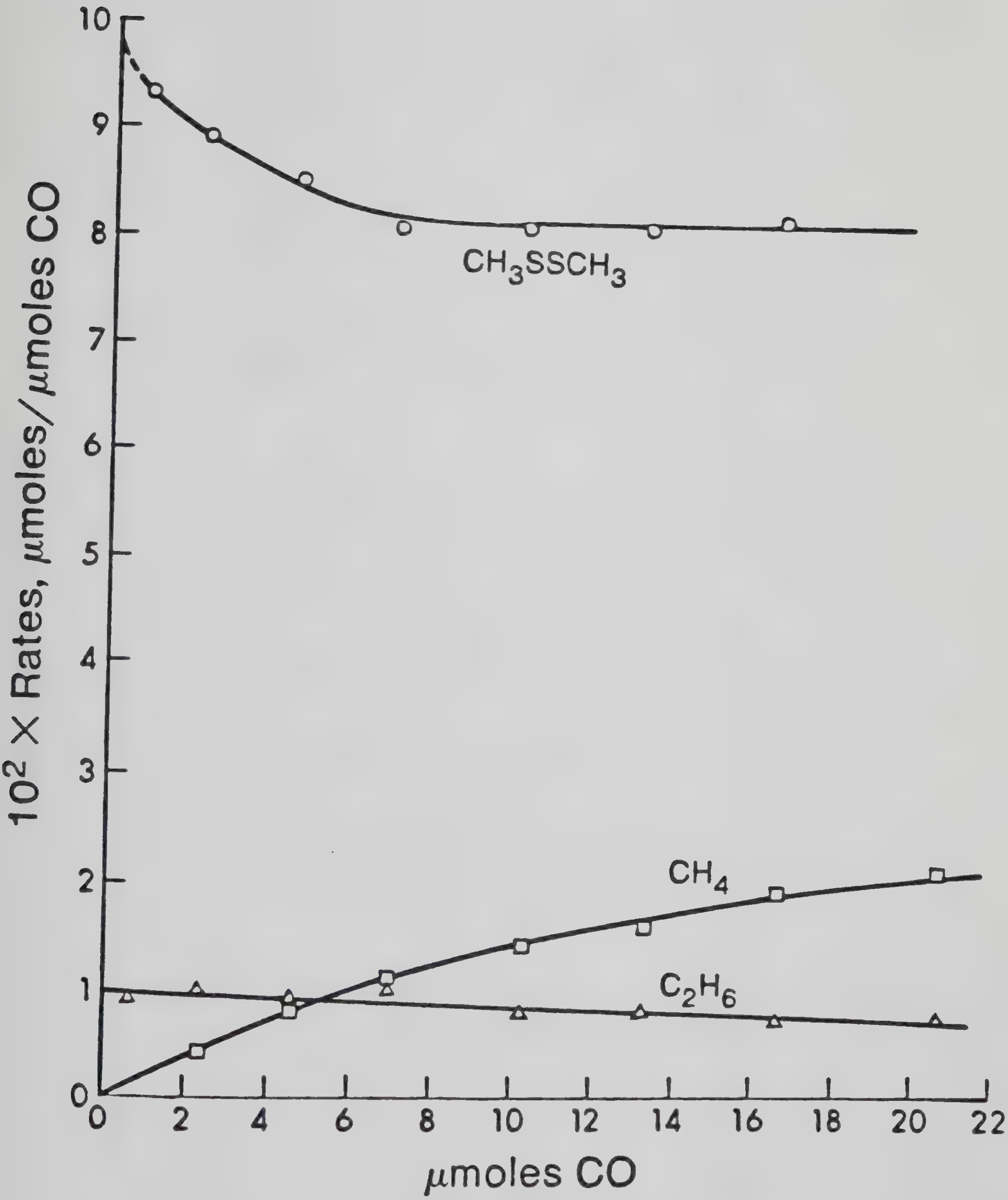

FIGURE IV-2: Rates of product formation _versus_ CO yield in the

COS - CH_3SCH_3 system.

TABLE IV-2

Effect of Total Pressure on the Rates of Product Formation in the COS-CH_3SCH_3 System[a]

Pressure (torr)		Time (min.)	Products (μmoles)				Rates (μmoles/μmole CO)		
CH_3SCH_3	COS		CO	CH_4	C_2H_6	CH_3SSCH_3	CH_4	C_2H_6	CH_3SSCH_3
10	100	15	5.94	.112	.093	.658	0.019	0.016	0.111
10	100	15	5.89	.095	.096	.613	0.016	0.016	0.104
10	100	15	5.80	.076	.085	.622	0.013	0.015	0.107
20	200	9.16	5.74	.058	.064	.489	0.010	0.011	0.085
30	300	7.15	5.82	.063	.055	.500	0.011	0.009	0.086
30	300	7.15	5.76	.062	.057	.501	0.011	0.010	0.087

[a] R°_{CO} = 0.58, 0.94 and 1.21 μmole min^{-1} for P(COS) = 100, 200 and 300 torr, respectively.

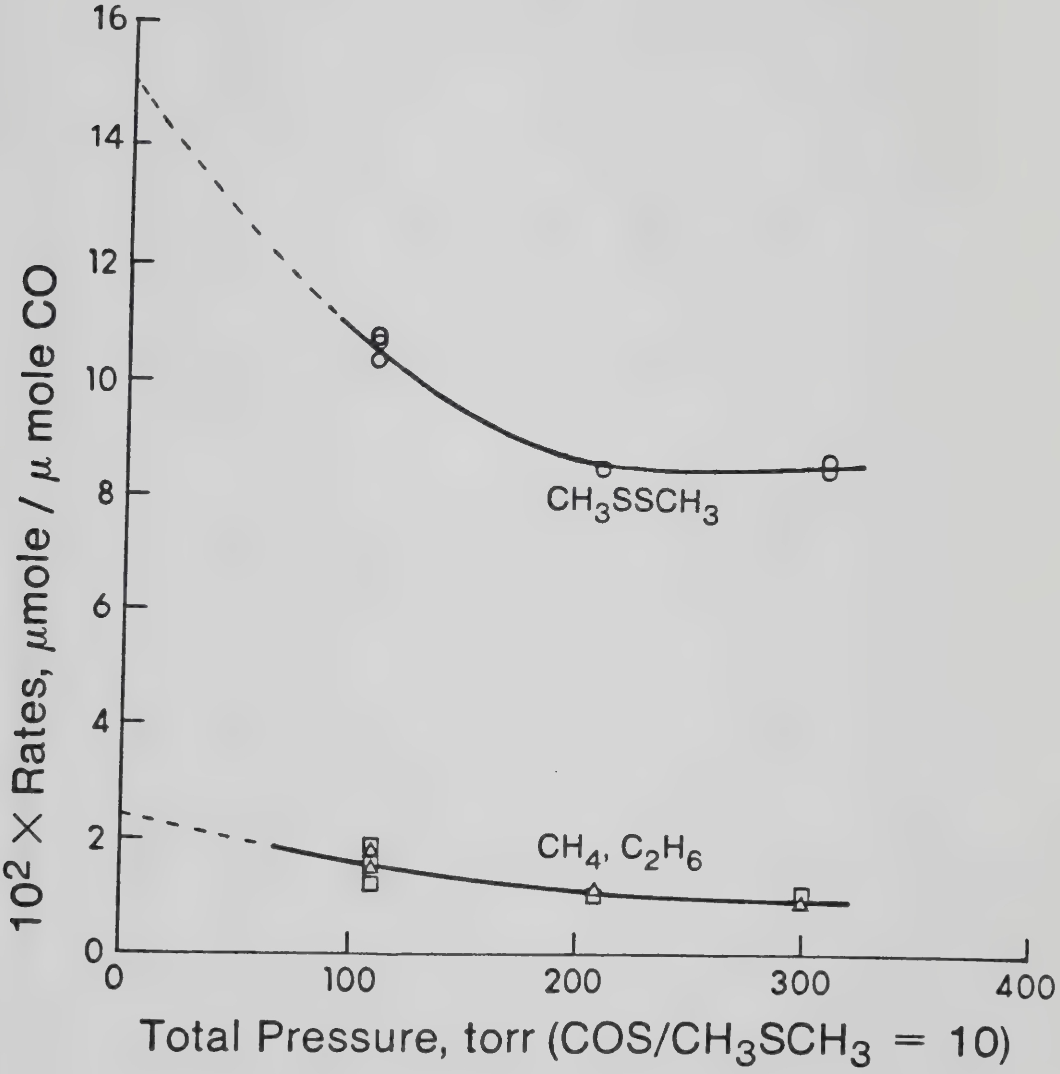

FIGURE IV-3: Rates of product formation *versus* total pressure in the COS - CH_3SCH_3 system. Rate$(CH_3SSCH_3)_{p=0} \simeq$ 0.151 µmole/µmole CO; Rate$(C_2H_6)_{p=0} \simeq$ Rate$(CH_4)_{p=0} \simeq$ 0.024 µmole/µmole CO.

TABLE IV-3

Effects of Added CO_2 and NO on Product Formation in the COS-CH_3SCH_3 System [a]

Pressure (torr)				Time (min.)	Products (μmoles)			
CH_3SCH_3	COS	CO_2	NO		CO	CH_4	C_2H_6	CH_3SSCH_3
-	100	-	-	30	17.3	-	-	-
-	100	770	-	30	16.1	-	-	-
10	100	-	-	30	11.5	.314	.161	1.111
10	100	770	0	30	9.22	.062	.118	.667
10	100	1300	-	30	8.94	.073	.110	.596
10	100	-	<0.1	15	5.77	.013	.032	.370
10	100	-	1.86	15	5.63	-	-	.139
30	300	-	-	7.15	5.76	.062	.057	.501
30	300	-	3.98	7.15	5.60	-	-	.104

[a] R°_{CO} =0.58 and 1.21 μmole min^{-1} for P(COS) = 100 and 300 torr, respectively.

Addition of 2-4 torr NO (Table IV-3) as a radical scavenger completely suppressed the yields of CH_4 and C_2H_6, while a small portion of CH_3SSCH_3 appears to be unscavengeable.

(d) Relative Rate Parameters

In order to determine the rate parameters of the $S(^3P)$ + CH_3SCH_3 reaction, competitive experiments were performed as outlined in Chapter III. Propylene was chosen as the reference substrate since it can be co-distilled with COS from the substrate-product mixture. Competitive studies were carried out on mixtures of $COS/C_3H_6/CO_2 = 100/66/1300$ in the presence of 0-10 torr of CH_3SCH_3. Due to the low recovery of CH_3SSCH_3, the relative rates were measured by monitoring the decrease in methylthiirane (C_3H_6S) yields ($(A_o-A)/A$, cf. eqn. III-[4]). The suppression of the C_3H_6S yields as a function of various concentrations of CH_3SCH_3 at five different temperatures is shown in Tables IV-4 through IV-8, and the plots of $(A_o-A)/A$ versus $[CH_3SCH_3]/[C_3H_6]$ are shown in Figure IV-4. It is apparent that the plots are linear for $[CH_3SCH_3]/[C_3H_6] < 0.11$ but begin to curve down at higher ratios. Slopes and intercepts obtained by least squares analysis of the initial linear portions of these plots with double weighting of the origin are listed in Table IV-9. The slopes are plotted in the Arrhenius form in Figure IV-5. The weighted least squares

TABLE IV-4

Product Yields as a Function of the $[CH_3SCH_3]/[C_3H_6]$ Ratio at 300 K[a]

$P(CH_3SCH_3)$	$\frac{[CH_3SCH_3]}{[C_3H_6]}$ [b]	Products (μmoles)			$\frac{C_3H_6S}{CO}$	$\frac{A_o-A}{A}$ [c]	$\frac{A_o-A}{A} \cdot \frac{[C_3H_6]}{[CH_3SCH_3]}$
		CO	C_3H_6S	CH_3SSCH_3			
0	0	2.93	1.98	0	.675	-	-
2.77	.0418	2.88	0.776	.0247	.270	1.51	36.1
3.49	.0527	2.90	0.670	.0360	.231	1.92	36.5
4.14	.0624	2.88	0.590	.0442	.205	2.30	36.8
4.67	0.706	2.81	0.535	.0496	.191	2.54	36.0
9.61	.145	2.86	0.355	0.125	.124	4.44	30.6

[a] $P(COS) = 100$ torr, $P(C_3H_6) = 66.5$ torr, $P(CO_2) = 1281$ torr, $R^\circ_{CO} = 0.387$ μmoles min^{-1}; exposure time = 14 min.

[b] $P(C_3H_6)$ values have been corrected for depletion.

[c] $A_o = C_3H_6S/CO$ in the absence of $CH_3SCH_3 = 0.675$.

$A = C_3H_6S/CO$ in the presence of CH_3SCH_3.

TABLE IV-5

Product Yields as a Function of the $[CH_3SCH_3]/[C_3H_6]$ Ratio at 330 K[a]

$P(CH_3SCH_3)$	$\frac{[CH_3SCH_3]}{[C_3H_6]}$[b]	Products (μmoles)			$\frac{C_3H_6S}{CO}$	$\frac{A_o-A}{A}$[c]	$\frac{A_o-A}{A} \cdot \frac{[C_3H_6]}{[CH_3SCH_3]}$
		CO	C_3H_6S	CH_3SSCH_3			
0	0	3.18	2.11[b]	-	0.662	-	-
3.01	.0463	3.16	.816	.0240	.258	1.56	33.7
5.05	.0778	3.15	.607	.0475	.193	2.43	31.2
6.49	.100	3.11	.528	.0699	.170	2.90	29.0
7.99	.123	3.12	.473	.0751	.152	3.37	27.4

[a] $P(COS) = 100$ torr, $P(C_3H_6) = 65.2$ torr, $P(CO_2) = 1299$ torr, $R^{\circ}_{CO} = 0.433$ μmoles min^{-1}; exposure time = 13 min.

[b] $P(C_3H_6)$ values have been corrected for depletion.

[c] $A_o = C_3H_6S/CO$ in the absence of $CH_3SCH_3 = 0.662$.

$A = C_3H_6S/CO$ in the presence of CH_3SCH_3.

TABLE IV-6

Product Yields as a Function of the $[CH_3SCH_3]/[C_3H_6]$ Ratio at 300 K[a]

$P(CH_3SCH_3)$	$\frac{[CH_3SCH_3]^b}{[C_3H_6]}$	Products (μmoles)			$\frac{C_3H_6S}{CO}$	$\frac{A_o-A^c}{A}$	$\frac{A_o-A}{A} \cdot \frac{[C_3H_6]}{[CH_3SCH_3]}$
		CO	C_3H_6S	CH_3SSCH_3			
-	-	3.31	2.16[b]	-	.654	-	-
3.08	.0466	3.18	.895	.026	.281	1.32	28.3
3.97	.063	3.19	.797	.057	.248	1.63	27.0
4.89	.0741	3.13	.676	.054	.216	2.02	27.3
9.00	.137	3.24	.438	.090	.135	3.21	23.4
-	-	3.17	2.08	-	.655	-	-
2.69	.0403	3.14	.980	.019	.131	1.09	27.0
6.18	.0932	3.06	.569	.058	.184	2.52	27.0
7.72	.117	3.03	.515	.072	.170	2.85	24.3
9.61	.145	3.05	.472	.129		3.23	22.3

[a] $P(COS)$ = 100 torr, $P(C_3H_6)$ = 66.3 torr, (first five experiments) and 65.9 torr (subsequent experiments), $P(CO_2)$ = 1300 torr, R°_{CO} = 0.473 μmoles min^{-1}; exposure time = 11.5 min.

[b] $P(C_3H_6)$ values have been corrected for depletion.

[c] $A_o = C_3H_6S/CO$ in the absence of CH_3SCH_3 = 0.654 and 0.655 respectively for the two subsequent experiments.

$A = C_3H_6S/CO$ in the presence of CH_3SCH_3.

TABLE IV-7

Product Yields as a Function of the $[CH_3SCH_3]/[C_3H_6]$ Ratio at 392 K[a]

$P(CH_3SCH_3)$	$\frac{[CH_3SCH_3]}{[C_3H_6]}$[c]	Products (μmoles)			$\frac{C_3H_6S}{CO}$	$\frac{A_o-A}{A}$[d]	$\frac{A_o-A}{A}\cdot\frac{[C_3H_6]}{[CH_3SCH_3]}$
		CO	C_3H_6S	CH_3SSCH_3			
-	-	3.14[b]	2.08[b]	-	.662	-	-
3.02	.0465	2.43	.790	.035	.325	1.04	22.4
3.45	.0533	2.44	.728	.036	.298	1.22	22.9
4.00	.0619	2.46	.671	.040	.273	1.43	23.1
4.83	.0745	2.49	.636	.043	.255	1.59	21.4
5.46	.0845	2.44	.579	.055	.237	1.79	21.2
9.37	.145	2.42	.411	.092	.170	2.90	20.0

[a] $P(COS)$ = 100 torr, $P(C_3H_6)$ = 65.0 torr, $P(CO_2)$ = 1301 torr, R°_{CO} = 0.515 μmoles min^{-1}; exposure time = 8 min.

[b] exposure time = 10 min.

[c] $P(C_3H_6)$ values have been corrected for depletion.

[d] A_o = C_3H_6S/CO in the absence of CH_3SCH_3 = 0.675.

A = C_3H_6S/CO in the presence of CH_3SCH_3.

TABLE IV-8

Product Yields as a Function of the $[CH_3SCH_3]/[C_3H_6]$ Ratio at 423 K[a]

$P(CH_3SCH_3)$	$\frac{[CH_3SCH_3]}{[C_3H_6]}$ [c]	Products (μmoles)			$\frac{C_3H_6S}{CO}$	$\frac{A_o-A}{A}$ [d]	$\frac{A_o-A}{A} \cdot \frac{[C_3H_6]}{[CH_3SCH_3]}$
		CO	C_3H_6S	CH_3SSCH_3			
-	-	3.07	2.00[b]	-	.653	-	-
2.89	.0436	2.93	1.07	.031	.367	.780	17.8
3.49	.0529	2.83	.978	.044	.344	.888	16.8
4.02	.0608	2.88	.899	.049	.312	1.09	18.0
4.48	.0680	2.80	.823	.053	.294	1.22	17.9
4.94	.0750	2.77	.775	.067	.281	1.33	17.8
9.79	.149	2.75	.534	.102	.194	2.36	15.9

[a] $P(COS) = 100$ torr, $P(C_3H_6) = 66.5$ torr, $P(CO_2) = 1303$ torr, $R^{\circ}_{CO} = 0.575$ μmoles min^{-1}; exposure time = 8 min.

[b] exposure time = 8.5 min.

[c] $P(C_3H_6)$ values have been corrected for depletion.

[d] $A_o = C_3H_6S/CO$ in the absence of $CH_3SCH_3 = 0.653$.

$A = C_3H_6S/CO$ in the presence of CH_3SCH_3.

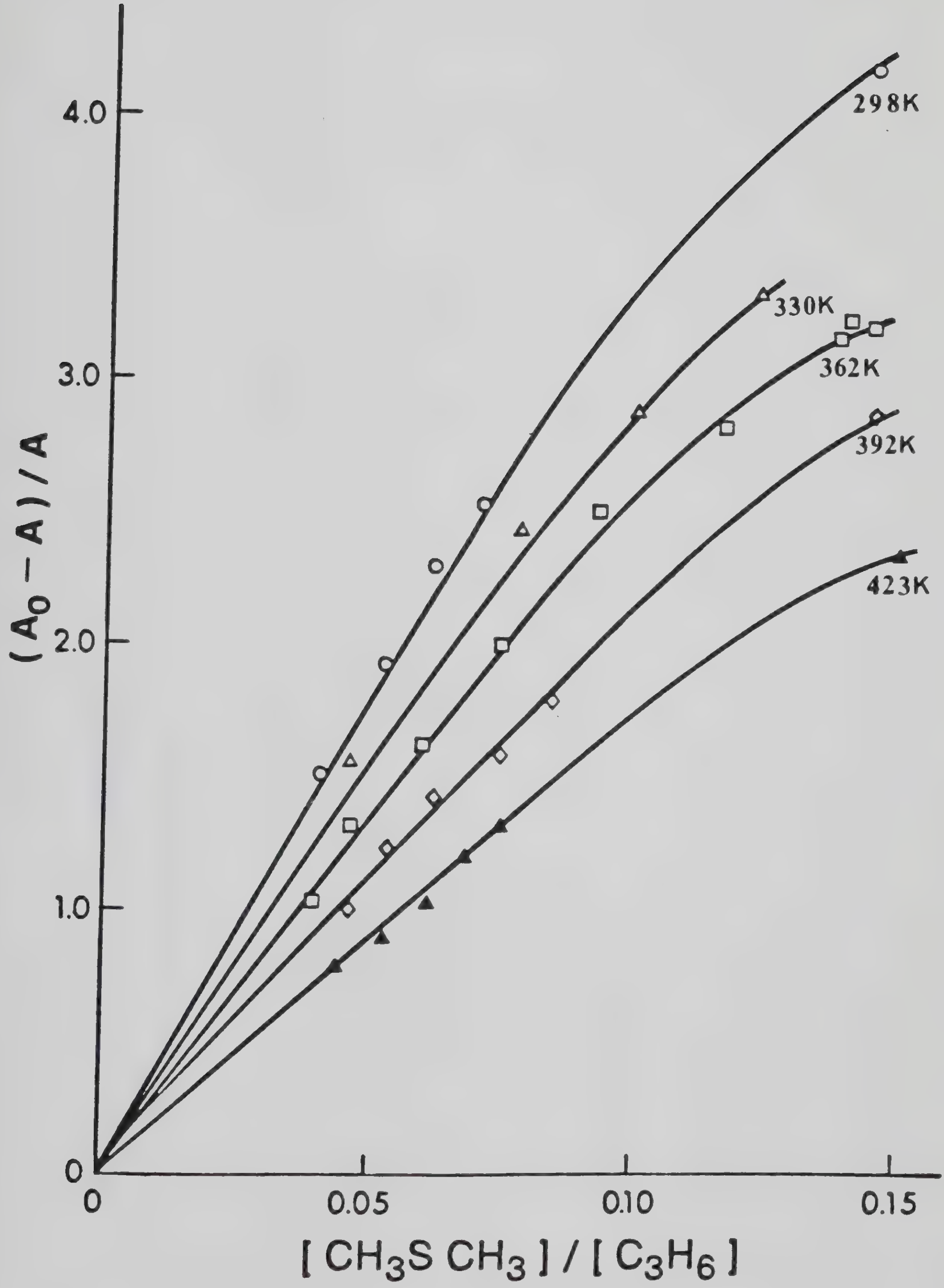

FIGURE IV-4 : Plots of $(A_0-A)/A$ versus $[CH_3SCH_3]/[C_3H_6]$.

TABLE IV-9

Slopes and Intercepts of the Plots in Figure III-4[a]

Temperature (K)	$1/T \times 10^3$ (K^{-1})	Slope ($k_{CH_3SCH_3}/k_{C_3H_6}$)	Log ($k_{CH_3SCH_3}/k_{C_3H_6}$)	Intercept	Correlation Coefficient
300	3.33	36.33 ± 0.44	1.560 ± 0.005	0.0009 ± 0.0230	0.9998
330	3.03	29.30 ± 1.85	1.467 ± 0.028	0.0811 ± 0.1249	0.9960
362	2.76	26.89 ± 0.067	1.430 ± 0.011	0.0085 ± 0.0420	0.9988
392	2.55	21.38 ± 0.085	1.330 ± 0.017	0.0356 ± 0.0508	0.9969
423	2.36	17.79 ± 0.044	1.250 ± 0.011	-0.0055 ± 0.0247	0.9988

[a] The errors are standard deviations.

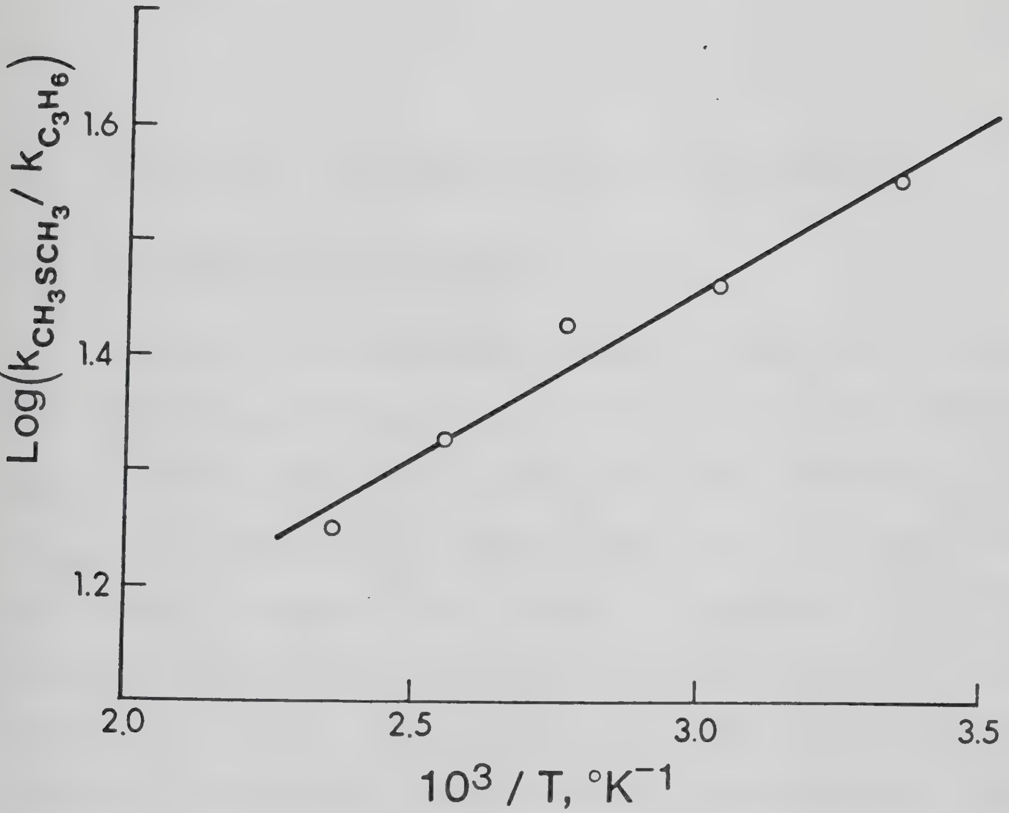

FIGURE IV-5: Arrhenius plot for the $S(^3P)$ + CH_3SCH_3 and C_3H_6 system.

fit of the Arrhenius plot gives

$$A_{CH_3SCH_3}/A_{C_3H_6} = 3.83 \pm 0.17 \quad \text{and}$$

$$E_{C_3H_6} - E_{CH_3SCH_3} = 1.34 \pm 0.06 \text{ kcal mole}^{-1}$$

2) $S(^1D_2, {}^3P)$ + Thietane - A Cyclic Thioether

(a) UV spectrum of thietane

Thietane (trimethylene sulfide) possesses two absorptions in the wavelength region of interest: one at $\lambda < 230$ nm with $\varepsilon_{max} \simeq 2200$ l mole^{-1}cm^{-1}, and the other centered at ∿260 nm with $\varepsilon_{max} \simeq 14$ l mole^{-1}cm^{-1}. The UV spectra of COS and thietane are shown in Figure IV-6, where it can be seen that thietane has a larger extinction coefficient than COS at all wavelengths except in a window around 240 nm. Photolysis of COS with minimal interference from thietane was achieved by using a combination of a 240 nm interference filter and a 1 mm Vycor 791 cut off filter (Figure IV-6), and a high COS/thietane ratio ($\geqslant$ 20:1). Under these conditions the amount of incident light absorbed by COS at 240, 245, 250 and 260 nm is ∿99%, ∿99% ∿97% and ∿95%, respectively. In a blank experiment, a 35 minute photolysis of 5 torr of thietane yielded a small amount of C_2H_4 and a trace quantity of cyclopropane.

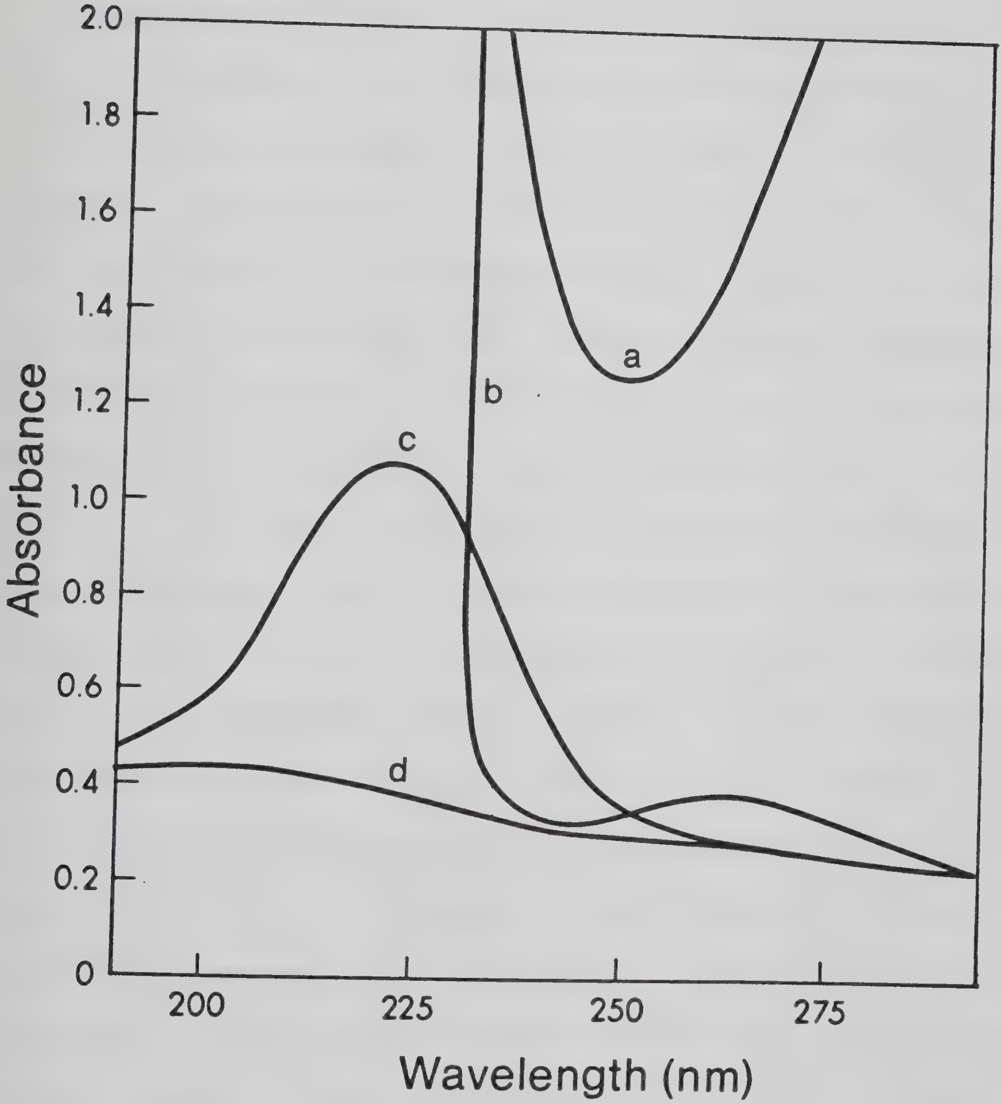

FIGURE IV-6: Absorption spectra of a: 240 nm intereference + Vycor 791 (1 mm) filters, b: 20 torr thietane, c: 23 torr COS, d: base line of 30 ml, 10 cm long quartz UV cell.

(b) Reaction Products

i) Identifications

Photolysis of COS in the presence of thietane resulted in the formation of two major retrievable products, C_2H_4 and a S-containing product, along with trace quantities of a C_3H_6 isomer. Identification of the C_3H_6 isomer was hindered by its similarity in vapour pressure and GC retention time with those of COS (C_3H_6 was observed only as a m/e = 42 peak co-eluting with COS in a GC/MS cross scan). The mass spectrum of the S-containing product (Appendix A-2) indicates that it is of molecular weight 106, corresponding to the molecular formula $C_3H_6S_2$. The NMR spectrum of this product (Figure IV-7) shows two resonances of relative intensities 2:1 in the methylene region, shifted to lower field by sulfur. The first resonance, due to proton H_A, and centered at $\delta = 3.19$ is a triplet; and the second resonance, due to proton H_B, at $\delta = 2.35$ is a quintet. The coupling constant between protons H_A and H_B, J_{AB}, is 7.5 Hz. This relatively large coupling constant implies that the four H_A protons are on the carbon atoms adjacent to the H_B carbon atom as shown.

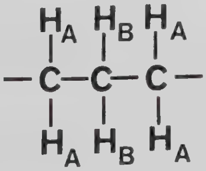

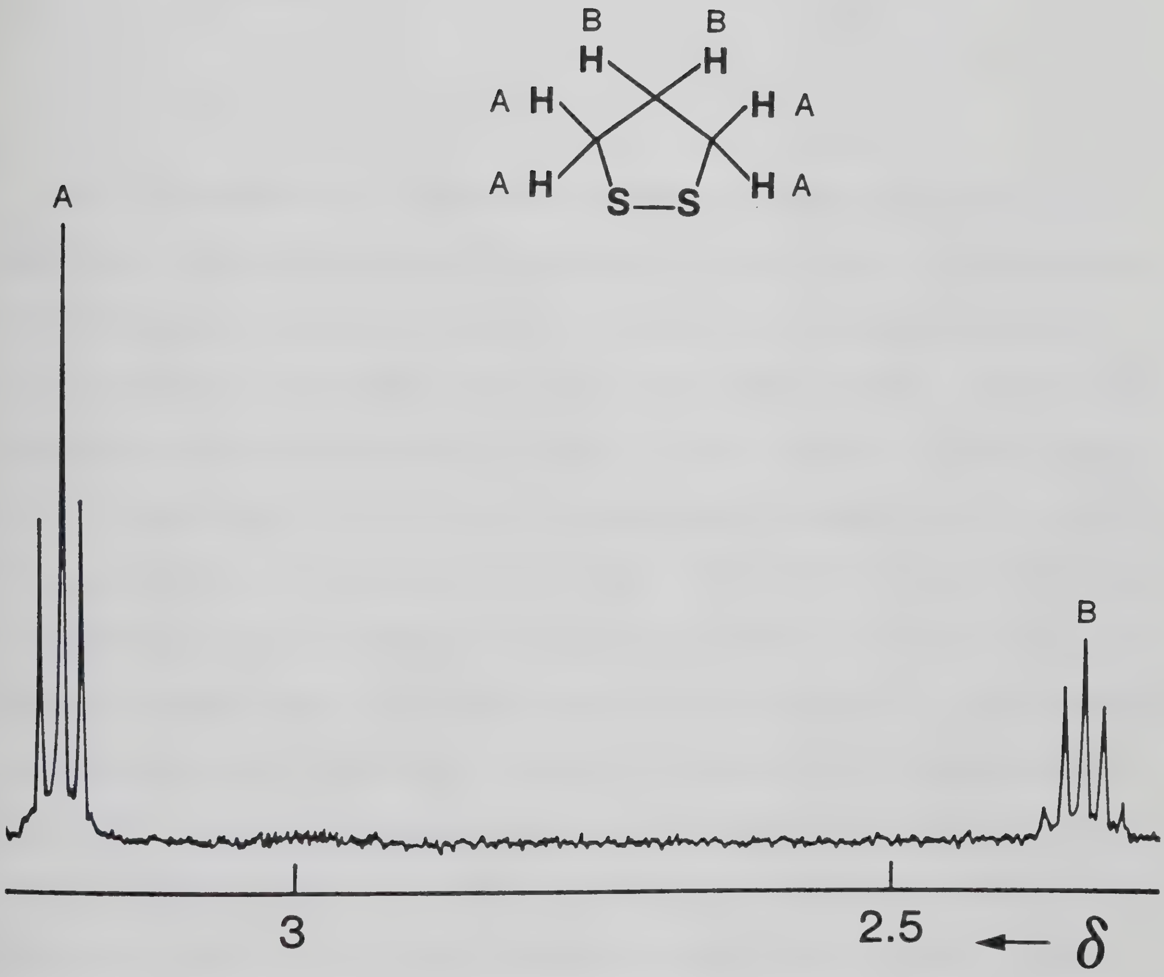

FIGURE IV-7: NMR spectrum of 1,2-dithiolane.

The only structures of molecular formula $C_3H_6S_2$ in which the H_A protons are equivalent are the cyclic compounds:

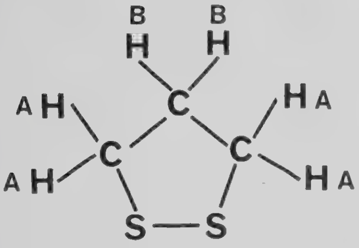

(I)

and

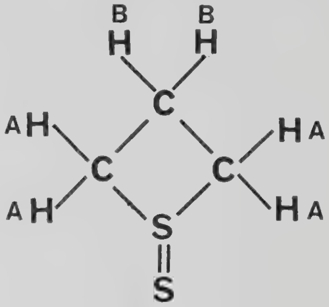

(II)

The question of which structure corresponds to the NMR spectrum observed may be determined on the basis of comparison of this spectrum with that of thietane, a 4-membered ring, (Figure IV-8) recorded under the same conditions. The latter spectrum is quite similar to that of the product, consisting of a triplet at $\delta = 3.29$ and an apparent quintet at $\delta = 2.97$ with a coupling constant of 6.5 Hz. The upfield shift of the resonances of the product spectrum relative to those of thietane is suggestive of ring expansion, analogous to the chemical shift generally observed on going from four to five membered rings.[155] The proton resonances of structure II would not be expected to show an upfield shift, and in fact might occur to low field of the thietane peaks due to the effect of the additional S atom on the ring. Therefore, the observed NMR spectrum strongly suggests that the product is the five-membered ring, 1,2-dithiolane (structure I).

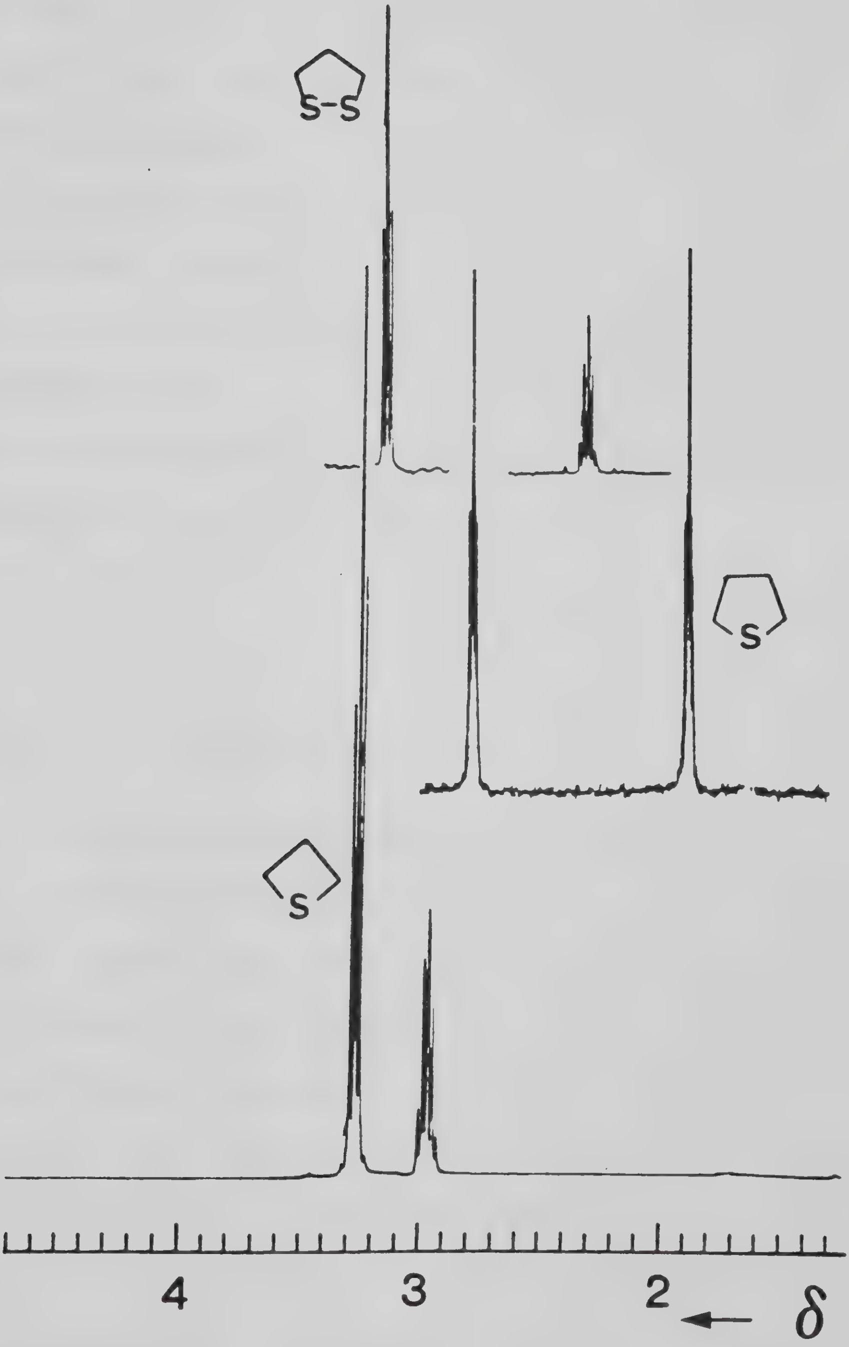

FIGURE IV-8: Comparison NMR spectra of thietane, 1,2-thiolane, and tetramethylenesulfide.

In further support of this assignment, the NMR spectrum of tetramethylene sulfide, a five membered ring, obtained under identical conditions, shows a substantial ring expansion shift, with resonances centered at $\delta = 2.80$ and $\delta = 1.90$. The much smaller ring expansion effect observed for the product, $C_3H_6S_2$, is probably a result of a shift to lower field caused by the second S atom and of the different geometry of the two five membered rings. A comparison of the NMR chemical shifts due to ring expansion for thietane, tetramethylenesulfide and 1,2-dithiolane is shown in Figure IV-8.

ii) Properties of 1,2-dithiolane

Attempts to obtain gas and solution (CH_3OH) phase UV spectra of 1,2-dithiolane were unsuccessful. In the gas phase experiment, the product was observed to polymerize as a brown film on the cell walls upon warming from -196° to room temperature. Insufficient sample size and air oxidation of the product prevented the acquisition of a solution phase spectrum. In this connection, it may be noted that 1,2-dithiolane has been synthesized previously by several workers, and has been shown to be extremely unstable with respect to polymerization, especially in the pure state.[156,157] The UV spectrum of 1,2-dithiolane in CH_3OH has been shown to feature

very strong absorption at wavelengths below 250 nm and to possess a weaker long wavelength absorption (λ_{max} ∿ 334 nm) having an extinction coefficient of ∿150 l $mole^{-1}cm^{-1}$.[154] The strong short wavelength absorption explains the photochemical instability of 1,2-dithiolane: less than 50% of a sample (∿ 0.7 μmole) was recovered after a 15 minute photolysis (λ ∿250 nm). It was also observed that 1,2-dithiolane is extremely sensitive to mercury: the product recovery declined significantly when mercury was allowed to accummulate in the distillation train. Interestingly, mercury has been shown to add to the S-S bond of the cyclic disulfide, $CF_3\overline{C{=}C(CF_3)SS}$,[158]

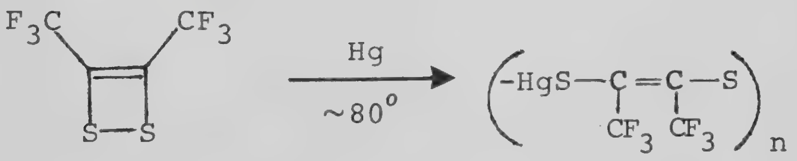

[1]

thus initiating polymerization.

(c) Effects of Exposure Time, Total Pressure and Added CO_2 in the COS-$\overline{CH_2(CH_2)_2S}$ System.

The variations in product yields with time for a mixture consisting of 100 torr COS and 5 torr $\overline{CH_3(CH_2)_2S}$ are listed in Table IV-10 and illustrated in Figure IV-9. It is seen that similar amounts of C_2H_4 and 1,2-dithiolane are produced at

TABLE IV-10

Effect of Exposure Time on Product Formation in the COS-$\overline{CH_2(CH_2)_2S}$ System[a]

Time	Products (μmoles)			Rates (μmoles/μmole CO)		% Recovery[b]
(min.)	CO	$\overline{CH_2(CH_2)_2SS}$	C_2H_4	$\overline{CH_2(CH_2)_2SS}$	C_2H_4	
15	1.50	0.344	0.320	0.229	0.213	80.5
25	2.47	–[c]	0.576	–[c]	0.233	
35	3.35	0.624	0.800	0.186	0.239	68.6
60	6.14	0.775	–[d]	0.126	–[d]	
60[e]	5.48	–[c]	1.08	–[c]	0.198	

[a] $P(CH_2(CH_2)_2S)$ = 5 torr, P(COS) = 100 torr.

[b] % Recovery = $R(\overline{CH_2(CH_2)_2SS} + C_2H_4)/R(CO°-CO)$ where $R°_{CO} = 0.155$ μmoles min^{-1}.

[c] Product accidentally lost.

[d] Not measured.

[e] $R^\circ_{CO} = 0.144$ μmoles min^{-1}.

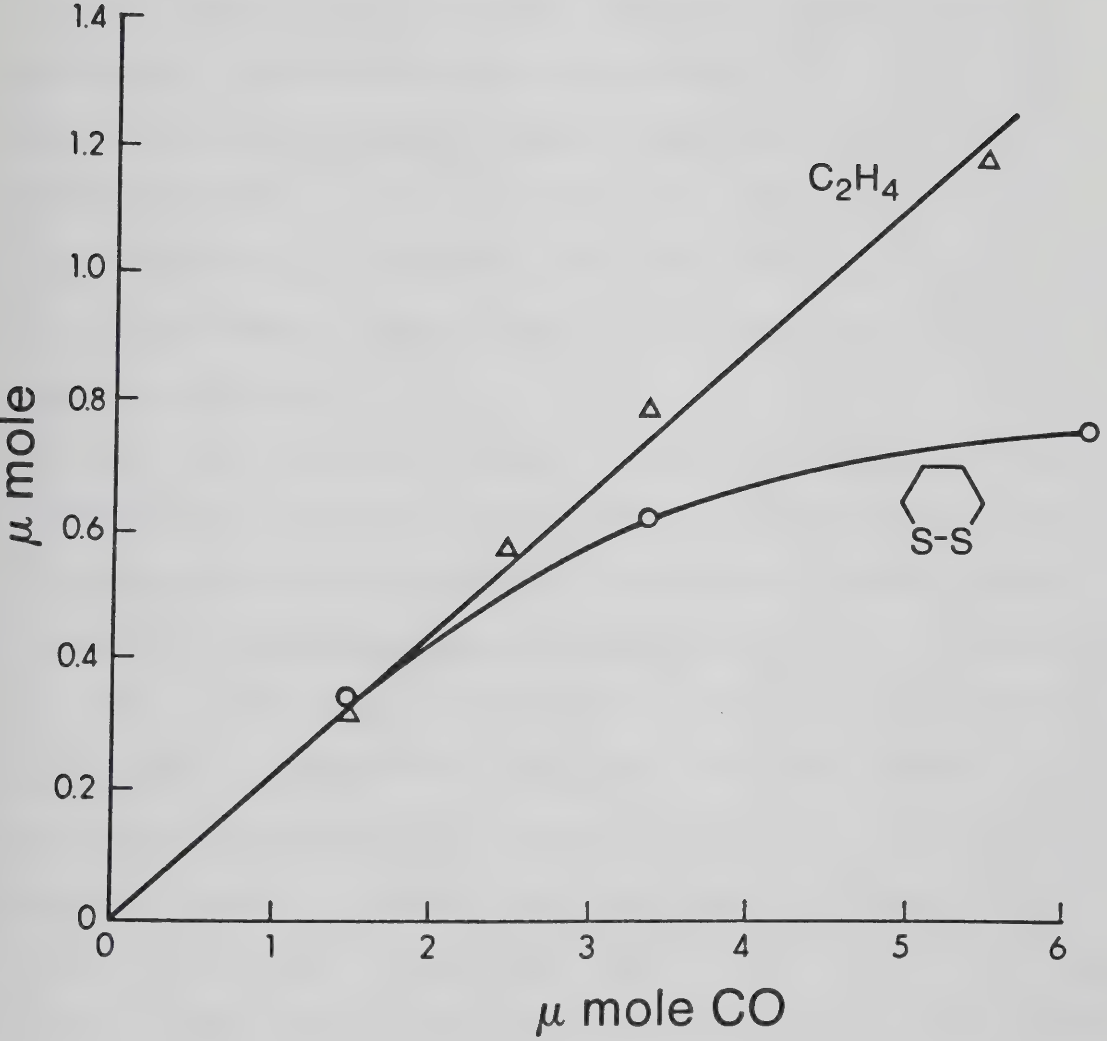

FIGURE IV-9: Product yields as function of CO yield in the COS - Thietane system.

short exposure times, with an estimated total recovery of ∿ 85% at zero time. However, at longer exposure times, the 1,2-dithiolane yield decreases relative to that of C_2H_4, suggesting photodecomposition and/or polymerization. The dependence of the product rates (per μmole CO) on time is shown in Figure IV-10. It is apparent that the rate of C_2H_4 production is constant, but that of 1,2-dithiolane formation decreases linearly with time, indicating that both are primary products.

The variations in product rates with respect to total pressure are listed in Table IV-11. A plot of the rates as a function of total pressure (Figure IV-11) reveals the absence of pressure effects for either C_2H_4 or 1,2-dithiolane.

The yields of the products as a function of added CO_2 are listed in Table IV-12 and shown in Figure IV-12. It is seen that increasing CO_2 pressure results in a slow and steady rise in the dithiolane yield, but a drastic decrease in the C_2H_4 yield, which apparently levels off at high pressures (> 600 torr). The overall product recovery decreases with increasing CO_2 pressure.

(d) Relative Rate Parameters

As in the case of CH_3SCH_3, relative rate parameters were determined using C_3H_6 as a reference substrate. Due to the low stability and poor recovery of 1,2-dithiolane, the relative

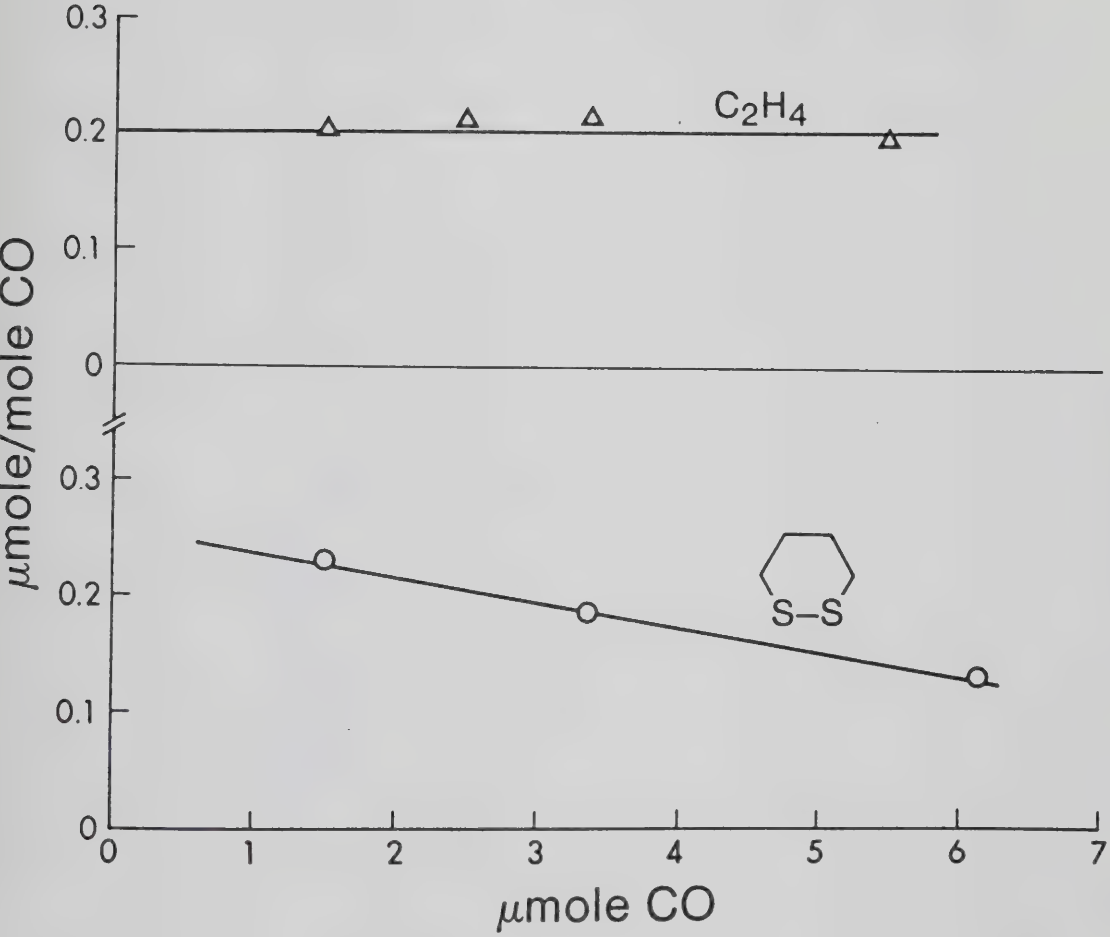

FIGURE IV-10: Rates of product formation _versus_ CO in the COS - $\overline{CH_2(CH_2)_2S}$ system.

TABLE IV-11

Effect of Total Pressure on Product Yields in the COS-$\overline{CH_2(CH_2)_2S}$ System[a]

Pressure (torr)		Exposure	Products (μmoles)			Rates (μmoles/μmole CO)	
$\overline{CH_2(CH_2)_2S}$	COS	time (min.)	CO	$\overline{CH_2(CH_2)_2S}S$	C_2H_4	$\overline{CH_2(CH_2)_2S}S$	C_2H_4
2.90	100	25.0	2.52	0.587	0.365	0.232	0.144
2.90	100	25.0	2.52	0.433	0.371	0.172	0.147
2.90	100	25.0	2.34	0.298	0.381	0.128	0.164
2.90	100	25.0	2.33	0.360	–[b]	0.155	–[b]
2.90	100	25.0	2.32	0.301	0.369	0.130	0.159
4.35	150	20.80	2.42	0.355	0.395	0.146	0.162
5.80	200	17.15	2.53	0.385	0.403	0.152	0.159
8.70	300	13.84	2.54	0.396	0.428	0.156	0.168
11.60	400	12.34	2.54	0.459	0.433	0.181	0.171
14.4	494	11.60	2.34	0.399	0.338	0.170	0.144

[a] $R°_{CO}$ = 0.155 and 0.145, 0.185, 0.226, 0.280, 0.314 and 0.333 μmole min^{-1} for P(COS) = 100, 150, 200, 300, 400 and 494 torr respectively.

[b] Not measured.

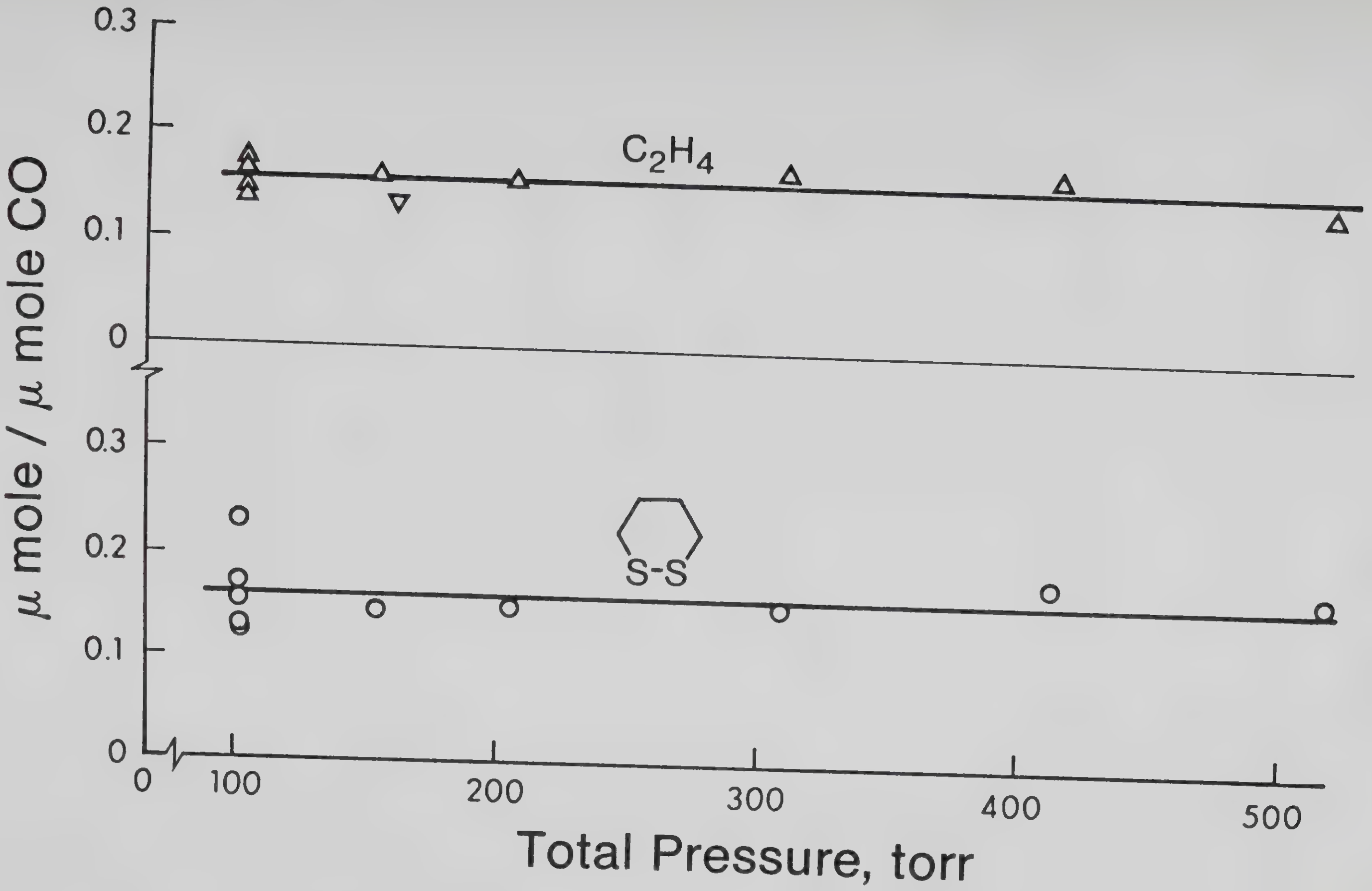

FIGURE IV-11: Rates of product formation versus total pressure in the COS - Thietane system.

TABLE IV-12

Effect of CO_2 Pressure on Product Yield in the $COS-\overline{CH_2(CH_2)_2S}$ System[a]

Pressure (torr)	Products (μmoles)			% Recovery[b]
CO_2	CO	$\overline{CH_2(CH_2)_2SS}$	C_2H_4	
0	2.77	0.620	0.383	62.5
600	2.33	0.717	0.064	38.2
1,200	2.22	0.801	0.107	42.1

[a] P(COS) = 100 torr, $P(\overline{CH_2(CH_2)_2S}) = 2.8 \pm 0.03$ torr, exposure time = 35 min.

[b] % Recovery = $R(\overline{CH_2(CH_2)_2SS} + C_2H_4)/R(CO°-CO)$, where $R°_{CO} = 0.125\ \mu mole\ min^{-1}$.

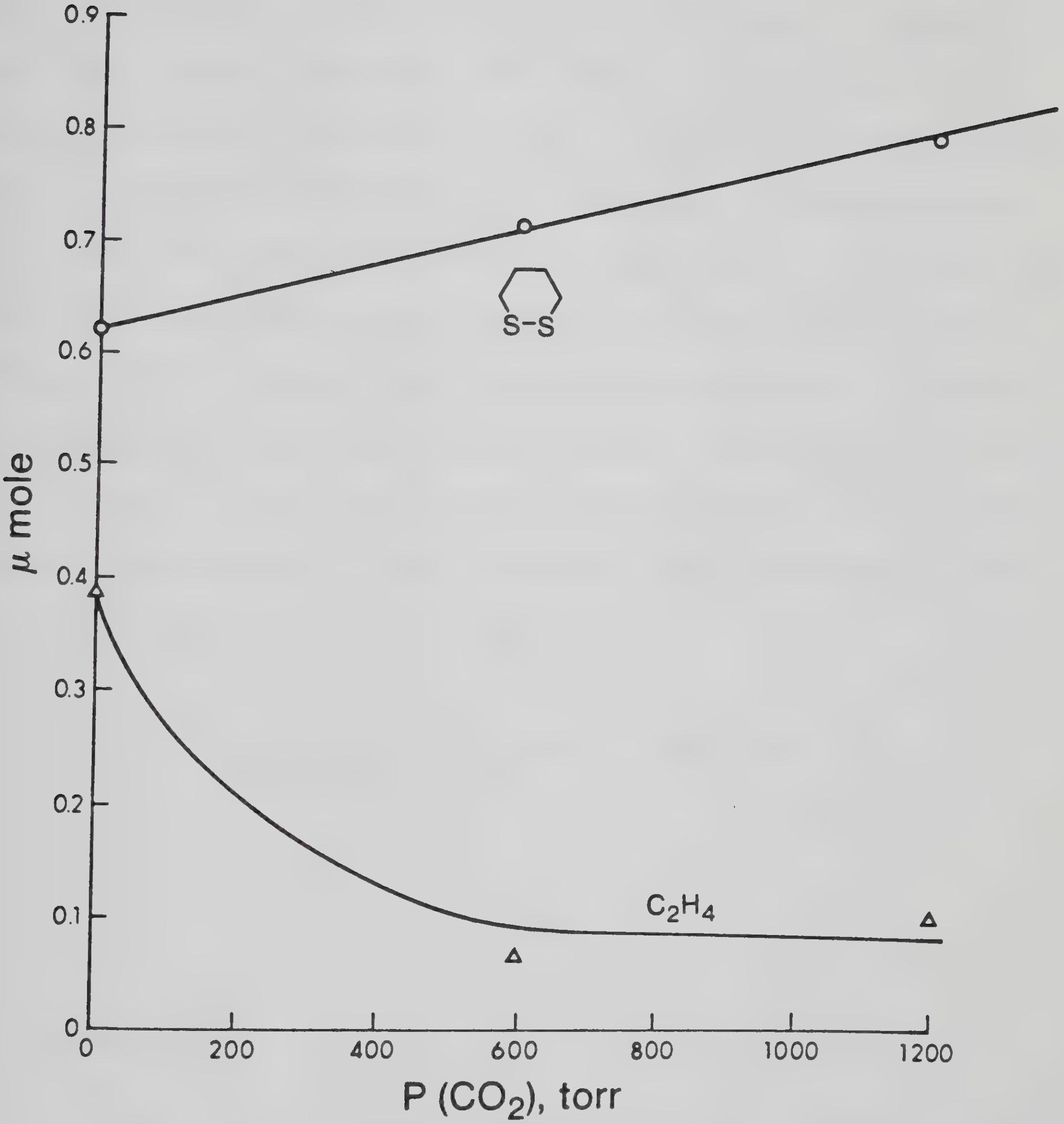

FIGURE IV-12: Product yields as a function of CO_2 pressure.

rates were measured by monitoring the decrease in methylthiirane (C_3H_6S) yields (A_o-A). The suppressions of the C_3H_6S yields as a function of the $[\overline{CH_2(CH_2)_2S}]/[C_3H_6]$ ratio at five different temperatures are listed in Tables IV-13 to IV-17. The corresponding plots are shown in Figure IV-13. The plots are linear over the range of the $[\overline{CH_2(CH_2)_2S}]/[C_3H_6]$ ratio studied. The slopes and intercepts of these plots obtained from least mean squares analysis are presented in Table IV-18. The slopes are plotted in the Arrhenius form in Figure IV-14. The weighted least squares fit gives

$$A_{\overline{CH_2(CH_2)_2S}}/A_{C_3H_6} = 1.84 \pm 0.04 \quad \text{and}$$

$$E_{C_3H_6} - E_{\overline{CH_2(CH_2)_2S}} = 1.25 \pm 0.03 \text{ kcal mole}^{-1}.$$

B. Discussion

S atoms react with dimethylsulfide and thietane, yielding in both cases a single S addition product, the corresponding disulfide. Although the basic mechanism of formation of the disulfide is probably the same in both cases, there appear to be some subtle differences in the reactions involving the primary adduct, and therefore mechanistic and kinetic details concerning the two systems will be considered separately.

TABLE IV-13

Product Yields as a Function of the $[\overline{CH_2(CH_2)_2S}]/[C_3H_6]$ Ratio at 303 K[a]

$P(\overline{CH_2)CH_2)_2S})$ (torr)	$\frac{[\overline{CH_2(CH_2)_2S}]}{[C_3H_6]}$[b]	Products (μmoles)		$\frac{C_3H_6S}{CO}$	$\frac{A_o-A}{A}$[c]	$\frac{A_o-A}{A} \cdot \frac{[C_3H_6]}{[\overline{CH_2(CH_2)_2S}]}$
		CO	C_3H_6S			
0	0	2.46	1.78	0.725	-	-
1.70	0.0261	2.43	0.767	0.316	1.30	49.7
2.56	0.0392	2.38	0.584	0.245	1.95	49.9
3.14	0.0481	2.44	0.522	0.214	2.39	49.7
3.78	0.0580	2.39	0.467	0.196	2.71	46.7

[a] P(COS) = 100 torr, $P(C_3H_6)$ = 65.5 torr, $P(CO_2)$ = 1275 torr, $R°_{CO}$ = 0.145 μmoles min^{-1}, exposure time = 35 min.

[b] $P(C_3H_6)$ values have been corrected for depletion.

[c] $A_o = C_3H_6S/CO$ in the absence of $\overline{CH_2(CH_2)_2S}$ = 0.725.

$A = C_3H_6S/CO$ in the presence of $\overline{CH_2(CH_2)_2S}$.

TABLE IV-14

Product Yields as a Function of the $[CH_2(CH_2)_2S]/[C_3H_6]$ Ratio at 333 K[a]

$P(CH_2)CH_2)_2S)$ (torr)	$\frac{[CH_2(CH_2)_2S]}{[C_3H_6]}$[b]	Products (µmoles)		$\frac{C_3H_6S}{CO}$	$\frac{A_o-A}{A}$[c]	$\frac{A_o-A}{A} \cdot \frac{[C_3H_6]}{[CH_2(CH_2)_2S]}$
		CO	C_3H_6S			
0	0	2.71	1.95	0.720	-	-
1.16	0.0176	2.64	1.09	0.414	0.739	41.9
1.87	0.0284	2.62	0.863	0.329	1.19	41.8
2.33	0.0356	2.60	0.752	0.289	1.47	41.9
3.11	0.0475	2.61	0.633	0.243	1.97	41.5

[a] $P(COS) = 100$ torr, $P(C_3H_6) = 65.9$ torr, $P(CO_2) = 1274$ torr, $R°_{CO} = 0.149$ µmoles min^{-1}, exposure time = 35 min.

[b] $P(C_3H_6)$ values have been corrected for depletion.

[c] $A_o = C_3H_6S/CO$ in the absence of $CH_2(CH_2)_2S = 0.720$.

$A = C_3H_6S/CO$ in the presence of $CH_2(CH_2)_2S$.

TABLE IV-15

Product Yields as a Function of the $[\overline{CH_2(CH_2)_2S}]/[C_3H_6]$ Ratio at 363 K[a]

$P(\overline{CH_2)CH_2)_2S})$ (torr)	$\frac{[\overline{CH_2(CH_2)_2S}]}{[C_3H_6]}$[b]	Products (μmoles)		$\frac{C_3H_6S}{CO}$	$\frac{A_o-A}{A}$[c]	$\frac{A_o-A}{A} \cdot \frac{[C_3H_6]}{[\overline{CH_2(CH_2)_2S}]}$
		CO	C_3H_6S			
0	0	2.98	2.11	0.708	-	-
1.10	0.0165	2.83	1.26	0.445	0.590	35.8
1.69	0.0253	2.76	1.04	0.376	0.882	34.9
2.30	0.0345	2.78	0.890	0.321	1.20	34.9
3.18	0.0478	2.73	0.716	0.262	1.70	35.6

[a] $P(COS) = 100$ torr, $P(C_3H_6) = 67.1$ torr, $P(CO_2) = 1300$ torr, $R°_{CO} = 0.154$ μmoles min^{-1}, exposure time = 35 min.

[b] $P(C_3H_6)$ values have been corrected for depletion.

[c] $A_o = C_3H_6S/CO$ in the absence of $\overline{CH_2(CH_2)_2S} = 0.708$.

$A = C_3H_6S/CO$ in the presence of $\overline{CH_2(CH_2)_2S}$.

TABLE IV-16

Product Yields as a Function of the $[\overline{CH_2(CH_2)_2S}]/[C_3H_6]$ Ratio at 393 K[a]

$P(\overline{CH_2)CH_2)_2S})$ (torr)	$\frac{[\overline{CH_2(CH_2)_2S}]}{[C_3H_6]}$[b]	Products (μmoles)		$\frac{C_3H_6S}{CO}$	$\frac{A_o-A}{A}$[c]	$\frac{A_o-A}{A} \cdot \frac{[C_3H_6]}{[\overline{CH_2(CH_2)_2S}]}$
		CO	C_3H_6S			
0	0	2.93	2.05	0.703	-	-
1.21	0.0180	2.73	1.22	0.448	0.566	31.4
1.61	0.0245	2.76	1.09	0.394	0.782	31.9
2.22	0.0331	2.73	0.937	0.343	1.05	31.6
2.96	0.0442	2.76	0.816	0.296	1.38	31.1

[a] $P(COS) = 100$ torr, $P(C_3H_6) = 67.4$ torr, $P(CO_2) = 1296$ torr, $R°_{CO} = 0.153$ μmoles min^{-1}, exposure time = 32.5 min.

[b] $P(C_3H_6)$ values have been corrected for depletion.

[c] $A_o = C_3H_6S/CO$ in the absence of $\overline{CH_2(CH_2)_2S} = 0.703$.

$A = C_3H_6S/CO$ in the presence of $\overline{CH_2(CH_2)_2S}$.

TABLE IV-17

Product Yields as a Function of the $[\overline{CH_2(CH_2)_2S}]/[C_3H_6]$ Ratio at 423 K[a]

$P(\overline{CH_2)CH_2)_2S})$ (torr)	$\frac{[\overline{CH_2(CH_2)_2S}]}{[C_3H_6]}$[b]	Products (μmoles)		$\frac{C_3H_6S}{CO}$	$\frac{A_o-A}{A}$[c]	$\frac{A_o-A}{A} \cdot \frac{[C_3H_6]}{[\overline{CH_2(CH_2)_2S}]}$
		CO	C_3H_6S			
0	0	2.98	2.04	0.685	-	-
1.50	0.0227	2.78	1.15	0.414	0.629	27.7
2.07	0.0316	2.80	1.02	0.365	0.878	27.8
2.42	0.0367	2.70	0.913	0.338	1.02	27.9
3.03	0.0462	2.72	0.816	0.300	1.28	27.7

[a] $P(COS) = 100$ torr, $P(C_3H_6 = 66.2$ torr, $P(CO_2) = 1248$ torr, $R°_{CO} = 0.169$ μmoles min^{-1}, exposure time = 30 min.

[b] $P(C_3H_6)$ values have been corrected for depletion.

[c] $A_o = C_3H_6S/CO$ in the absence of $\overline{CH_2(CH_2)_2S} = 0.685$.

$A = C_3H_6S/CO$ in the presence of $\overline{CH_2(CH_2)_2S}$.

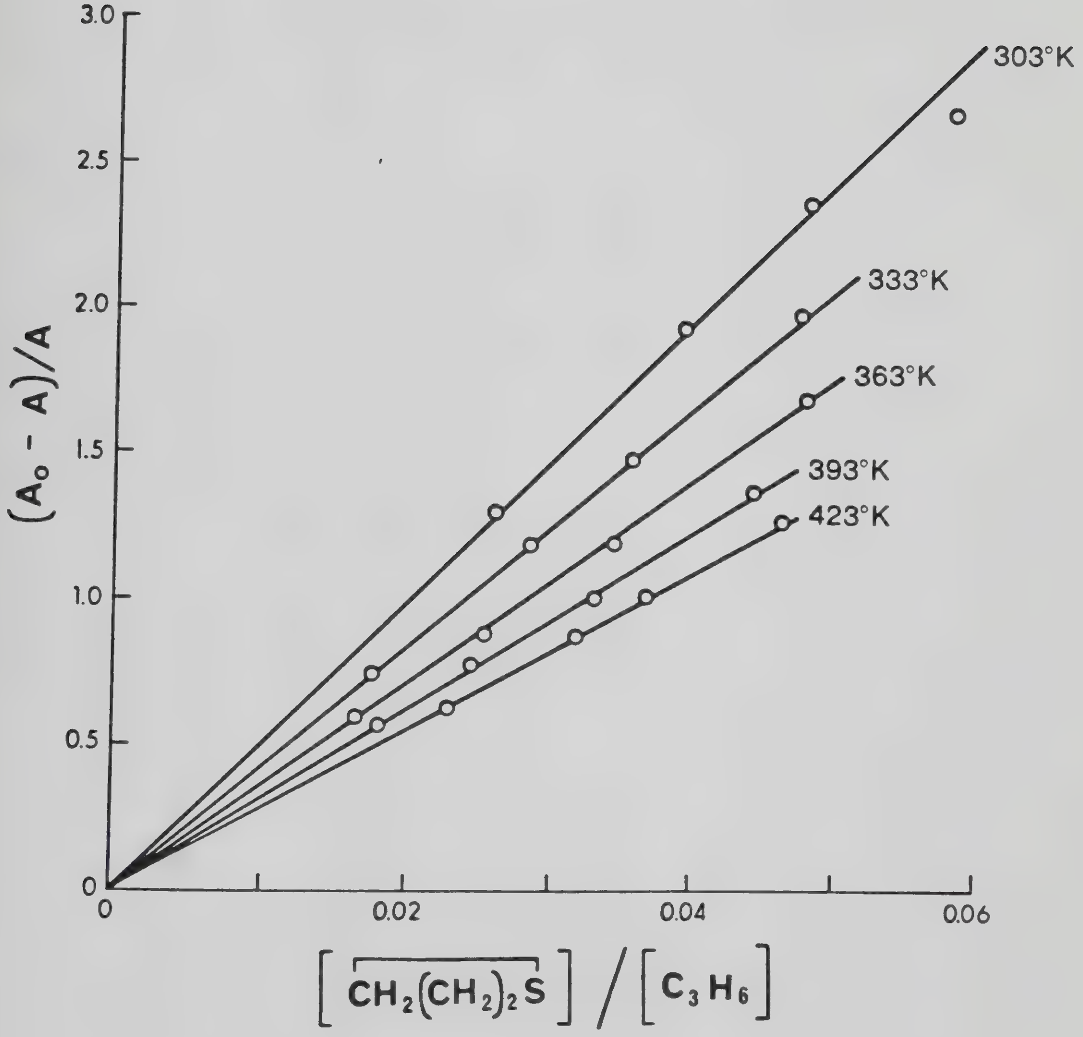

FIGURE IV-13: Plots of $(A_0\text{-}A)/A$ versus $[\overline{CH_2(CH_2)_2S}]/[C_3H_6]$.

TABLE IV-18

Slopes and Intercepts of the Plots in Figure IV-13 [a]

Temperature (K)	1/T × 10^3 (K^{-1})	Slope ($k_{\overline{CH_2(CH_2)_2S}}/k_{C_3H_6}$)	Ln($k_{\overline{CH_2(CH_2)_2S}}/k_{C_3H_6}$)	Intercept	Correlation Coefficient
303	3.30	48.01 ± 1.17	3.871 ± 0.024	0.0203 ± 0.0425	0.9998
333	3.00	41.60 ± 0.16	3.728 ± 0.008	-0.0161 ± 0.0805	1.000
363	2.76	353.31 ± 0.30	3.564 ± 0.008	-0.0161 ± 0.0805	1.000
393	2.54	31.40 ± 0.22	3.447 ± 0.007	0.0265 ± 0.0554	0.9991
423	2.36	27.77 ± 0.07	3.324 ± 0.002	0.0014 ± 0.0196	1.000

[a] The errors are standard deviations.

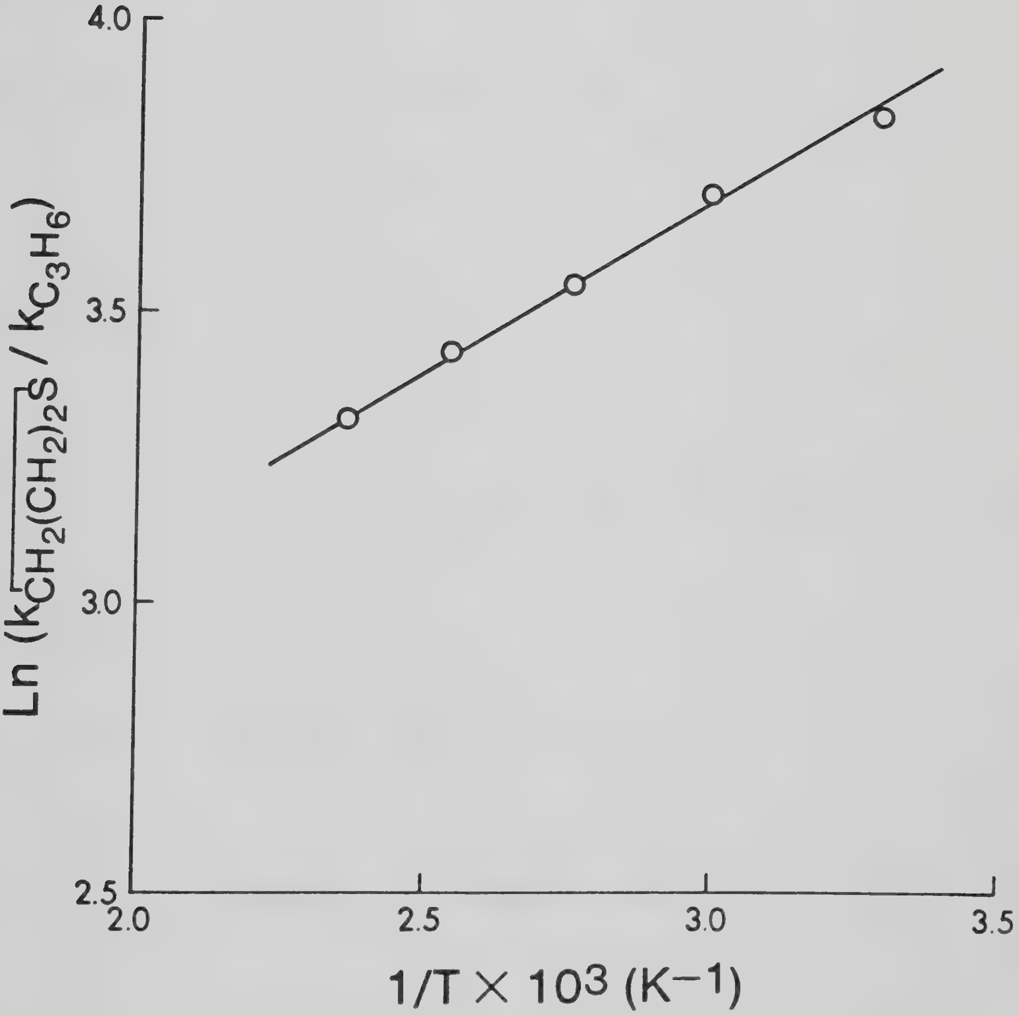

FIGURE IV-14: Arrhenius plot for the $S(^3P)$ + $\overline{CH_2(CH_2)_2S}$ and C_3H_6 system.

1) $S(^1D_2,\ ^3P) + CH_3SCH_3$ Reactions

The $S(^1D_2,\ ^3P)$ atoms produced by the photolysis of COS,

$$COS + h\nu \longrightarrow CO + S(^1D_2,\ ^3P) \qquad [1]$$

$$S(^1D_2) + COS \rightarrow CO + S_2(^1\Delta_g) \qquad [2]$$

$$S(^1D_2) + M \longrightarrow S(^3P) + M \qquad [3]$$

$$S(^3P) + COS \rightarrow CO + S_2(\tilde{X}\,^3\Sigma_g^-) \qquad [4]$$

may react in a number of ways. For $S(^1D)$ atoms, the following steps may be considered:

H abstraction,

$$S(^1D_2) + CH_3SCH_3 \longrightarrow CH_2SCH_3 + SH\cdot \qquad [5]$$

C-H insertion

$$S(^1D_2) + CH_3SCH_3 \longrightarrow CH_3SCH_2SH(S_0)^\dagger \qquad [6]$$

C-S insertion

$$S(^1D_2) + CH_3SCH_3 \longrightarrow CH_3SSCH_3(S_0)^\dagger \qquad [7]$$

or addition to the sulfur site

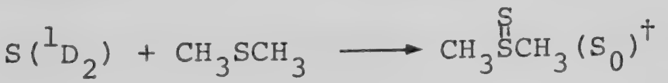

$$S(^1D_2) + CH_3SCH_3 \longrightarrow CH_3\overset{\overset{\displaystyle S}{\|}}{S}CH_3(S_0)^\dagger \qquad [8]$$

$S(^3P)$ atoms, on the other hand, being incapable of insertion, can only react with the sulfur moiety:

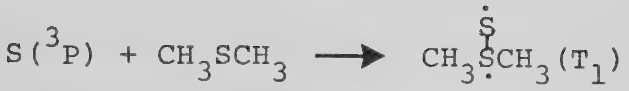

$$S(^3P) + CH_3SCH_3 \longrightarrow CH_3\overset{\dot{S}}{\underset{\cdot}{S}}CH_3(T_1) \qquad [9]$$

Step [5] can be discounted since this process is unknown in S + hydrocarbon reactions (vide infra). Although C-H insertion is known to occur in $S(^1D_2)$ + alkene and alkane systems, the absence of any insertion products in this system indicates that reaction [6] does not occur.

The exclusive occurrence of C-S insertion (reaction [7]) can be ruled out for the following reasons: C-H insertion reactions are extremely rapid and, with the exception of CH_4, are essentially quantitative. C-S insertion should be equally efficient, and yet the CH_3SSCH_3 yields at zero pressure never exceeded 50% (Figure III-3). Furthermore, the $S(^3P)$ + CH_3SCH_3 reaction also leads to the formation of CH_3SSCH_3, indicating the existence of an alternative route for disulfide formation. Additionally, the electron rich S non-bonding 3p orbitals of the substrate should provide a more attractive site for electrophilic attack than the C-S bonds, thus rendering reaction [8] more favourable.

It is therefore proposed that $S(^1D)$ and $S(^3P)$ atoms react with CH_3SCH_3 to yield excited singlet and triplet state dimethylthiosulfoxide (DMTSO), respectively. Although

these species were not observed in the present investigation, there is convincing evidence in the literature to the effect that thiosulfoxides can exist as transient intermediates.[159-165]

Before considering the subsequent mechanistic details, it would be instructive at this point to briefly review what has been reported with regard to thiosulfoxides. DMTSO has long been thought to be the unstable by-product in the oxidation of S-containing compounds by $(CH_3)_2S{=}O$:[159]

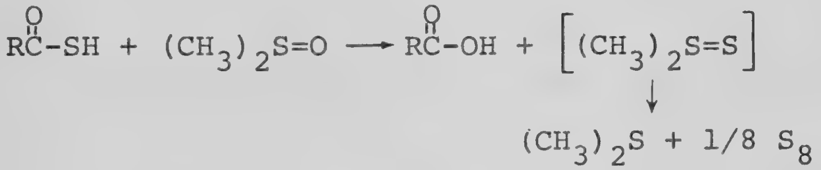

$$\mathrm{R\overset{O}{\overset{\|}{C}}{-}SH + (CH_3)_2S{=}O \longrightarrow R\overset{O}{\overset{\|}{C}}{-}OH + \left[(CH_3)_2S{=}S\right]}$$
$$\downarrow$$
$$\mathrm{(CH_3)_2S + 1/8\ S_8} \qquad [10]$$

The intervention of thiosulfoxide intermediates in the thermal racemization and isomerization of allylic disulfides was postulated by Barnard _et_ _al_. in 1969,[160] and by Höfle and Baldwin in 1971:[161]

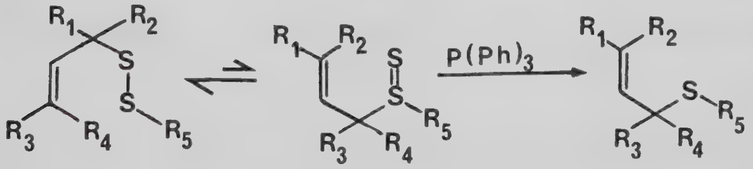

[11]

The latter workers measured the pseudo first order rate constants for interception of the thiosulfoxide intermediate by $P(Ph)_3$ and found, as expected, that increasing the size of R_3, R_4 and R_5 decreases the rate as a result of steric hindrance, but that increasing the size of $R_1 + R_2$ favours

the formation of the thiosulfoxide intermediate. When R_1 through R_4 = H and R_5 = CH_3, the thiosulfoxide loses sulfur spontaneously at 25° to yield the sulfide.

In 1973 Mislow and co-workers[162] reported that allylic sulfides react readily with elemental sulfur to yield the corresponding disulfide, with complete allylic rearrangement. These workers demonstrated the reversible nature of the various elementary processes involving thiosulfoxide intermediates:

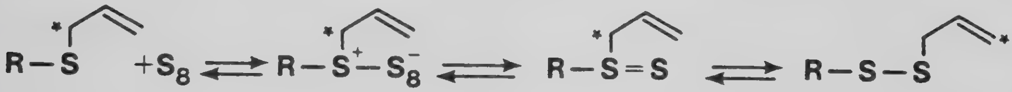

[12]

Still et al.[163] reported that P_4S_{10} is a mild, selective reagent for the reduction of sulfoxides to sulfides and suggested the intervention of a four-centered Wittig-type intermediate, which decomposes to thiosulfoxide:

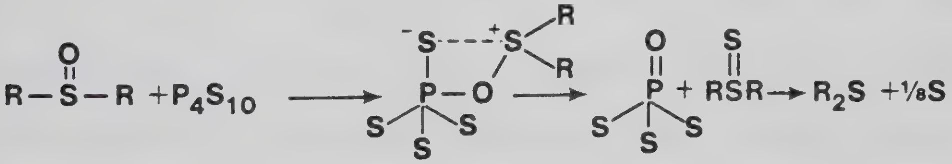

[13]

Baechler and co-workers[164,165] pursued these investigations and discovered that milder reducing agents such as B_2S_3 and SiS_2 effect the conversion of sulfoxides into disulfides, as well as monosulfides.

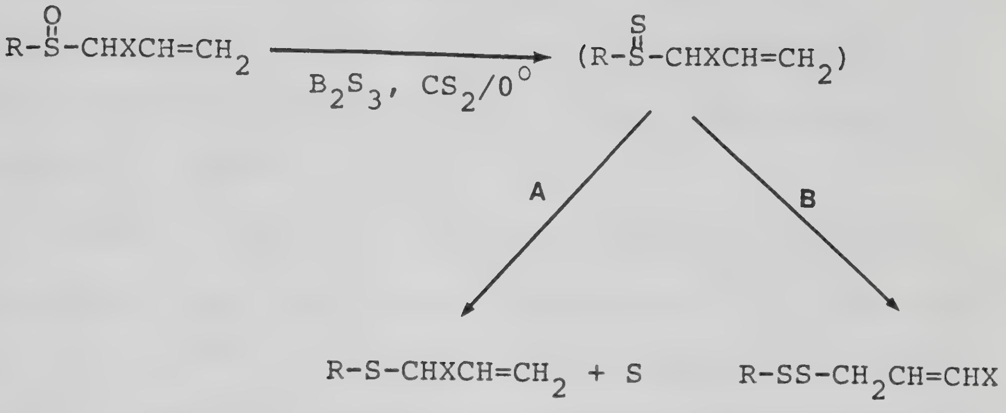

[14]

X = H or D, R = CH_3 or C_6H_5

The fraction of the disulfide formed varied with the choice of reagents, and its presence constitutes compelling evidence for the intermediacy of thiosulfoxides in these systems. Attempts to detect thiosulfoxide intermediates by NMR during low temperature deoxygenation experiments were unsuccessful.

Stepanov _et al._[166] studied the thermal and chemical reactivity of a number of substituted diaryldisulfides, and showed that the presence of strongly electron-withdrawing substituents apparently stabilizes the thiosulfoxide form. Accordingly, the only thiosulfoxides which have been isolated to date are those possessing strongly electronegative groups such as F and O bonded to the S=S moiety:[167]

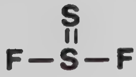

,

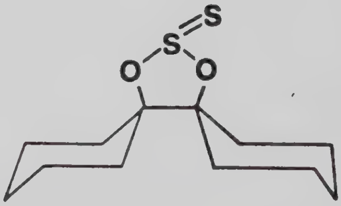

The possible transient existence of thiosulfoxides in some systems, then, is no longer in doubt. In the absence of electron-withdrawing substituents however, they appear to be kinetically unstable species.

In a study of the allyldisulfide-allylthiosulfoxide isomerization, Höfle and Baldwin reported $\Delta H^{\ddagger} \simeq 20$ kcal mole^{-1} and $\Delta S^{\ddagger} \simeq -9$ e.u.[161] Using these values and assuming that the trapping reaction of the thiosulfoxide intermediate by $P(C_6H_5)_3$ has an E_a of 3-4 kcal mole^{-1}, Benson[168] has estimated that ground state thiosulfoxides are at the most 10 kcal mole^{-1} higher in energy than the corresponding disulfides. This suggests that thiosulfoxides are energetically accessible species. However, they are thermodynamically unstable with respect to formation of the corresponding sulfides and elemental sulfur.

The electronic state of the DMTSO formed in step [8] is not known, but is likely to be the ground, vibrationally excited singlet state, $(S_o)^{\dagger}$. Its energy content,

$$E^{*} = \Delta H_f^o(CH_3SCH_3) + \Delta H_f^o(S(^1D_2)) - \Delta H_f^o(DMTSO)$$

can only be estimated, since ΔH_f(DMTSO) is not known. Using

$\Delta H_f^o(CH_3SCH_3) = -8.9$ kcal mole^{-1},[168]

$\Delta H_f^o(S(^1D_2)) = 92.0$ kcal mole^{-1},[19]

and Benson's estimated value of ∿4 kcal $mole^{-1}$ for $\Delta H_f(DMTSO)^{168}$ gives a very approximate value of 79 kcal $mole^{-1}$ for E*.

$DMTSO(S_0)^{\dagger}$ can decay via the following pathways:

fragmentation,

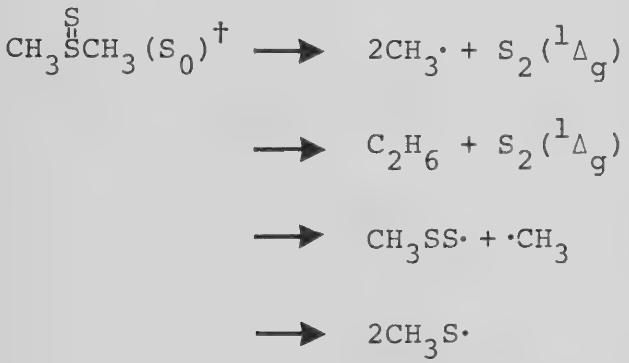

$$CH_3\overset{\overset{S}{\|}}{S}CH_3(S_0)^{\dagger} \longrightarrow 2CH_3\cdot + S_2(^1\Delta_g) \qquad [15a]$$

$$\longrightarrow C_2H_6 + S_2(^1\Delta_g) \qquad [15b]$$

$$\longrightarrow CH_3SS\cdot + \cdot CH_3 \qquad [15c]$$

$$\longrightarrow 2CH_3S\cdot \qquad [15d]$$

collisional deactivation to the thermalized ground state,

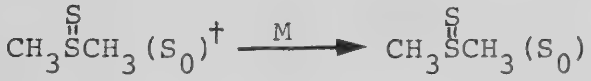

$$CH_3\overset{\overset{S}{\|}}{S}CH_3(S_0)^{\dagger} \xrightarrow{M} CH_3\overset{\overset{S}{\|}}{S}CH_3(S_0) \qquad [16]$$

and isomerization to a vibrationally excited dimethyldisulfide (DMDS) molecule,

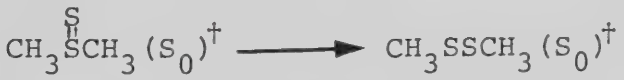

$$CH_3\overset{\overset{S}{\|}}{S}CH_3(S_0)^{\dagger} \longrightarrow CH_3SSCH_3(S_0)^{\dagger} \qquad [17]$$

The heats of formation of the fragment radicals and molecules formed in reactions [15a-d] are, with the exception of CH_3S_2, known with certainty,[169] and since the calculated value for $\Delta H_f(CH_3S_2) = +17.3^{168}$ kcal $mole^{-1}$ is based on reliable kinetic data, the total product enthalpies can be computed accurately. The value of ∿4 kcal $mole^{-1}$

for $\Delta H_f(\mathrm{DMTSO})$, however, is only a very rough approximation. Nonetheless, accurate values of the enthalpies of reactions [15a-d] can be calculated beginning with the two initial reactants, i.e.

	ΔH (kcal mole^{-1})
$S(^1D_2) + CH_3SCH_3 \xrightarrow{[15a]} 2CH_3\cdot + S_2(^1\Delta_g)$	28.3
$\xrightarrow{[15b]} C_2H_6 + S_2(^1\Delta_g)$	-59.3
$\xrightarrow{[15c]} CH_3S_2\cdot + CH_3\cdot$	-32.1
$\xrightarrow{[15d]} 2CH_3S\cdot$	-15.0

Step [15a] can be discounted on energetic grounds. Molecular production of C_2H_6, step [15b], is a distinct possibility in view of the high exothermicity of this reaction. It should be noted that the suppression of the C_2H_6 yields in the presence of NO does not necessarily indicate that C_2H_6 comes from radical precursors: it will be shown later that NO reacts with DMTSO, resulting in a fivefold decrease in the rate of isomerization to CH_3SSCH_3, and thus fragmentation to C_2H_6 should be suppressed as well.

Fragmentation to $CH_3S_2 + CH_3$ is analgous to the de-

composition pathway proposed for triplet state dimethylsulfoxide.[121] In solution, CH_3S_2 radicals are extremely inert and their sole fate appears to be recombination,[170] yet $CH_3S_4CH_3$ was not detected in this system. On the other hand, CH_3 radicals are definitely present (viz. the formation of CH_4), and these can only be formed from step [15c]. One possible explanation for this apparent discrepancy is that CH_3S_2 can disproportionate in the gas, but not in the liquid phase, to yield a variety of products. Although virtually nothing is known concerning the chemistry of CH_3S_2 radicals, it has been demonstrated that the rate of disproportionation of HS_2 radicals in the gas phase is extremely rapid.[171] Finally, dissociation into two CH_3S radicals, step [15d], while energetically possible, is not conceptually inviting. It is therefore concluded that $DMTSO(S_0)^\dagger$ fragments in two ways; a molecular route leading to $C_2H_6 + S_2$ (step [15b]), and a radical one leading to $CH_3S_2 + CH_3$ (step [15c]).

As mentioned above, the ground state thiosulfoxide formed in steps [8] and [9] is unstable with respect to desulfurization; the occurrence of the deactivation step [16] is manifested by the decrease in the CH_3SSCH_3 yields with increasing pressure (Figure IV-3).

The proposed thiosulfoxide-disulfide isomerization, step [17], is analogous to that involved in the 2,3-sigmatropic rearrangements of allyldisulfides as shown in reaction [11], and to the reaction sequence in the B_2S_3 reduction of sulfoxides, step [14]. Senning[172] has proposed the involvement of an equilibrium between the hypothetical dithiirane and thiosulfine molecules in some interconversions:

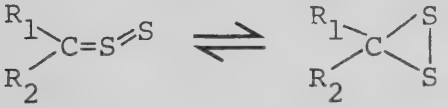

[18]

Although neither species could be chemically trapped, a dithiirane intermediate may be envisioned for the DMTSO$(S_0)^\dagger$ rearrangement,

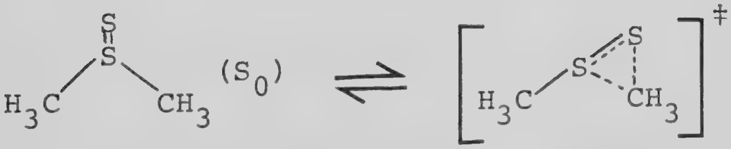

[19a]

followed by cleavage of the original C-S bond,

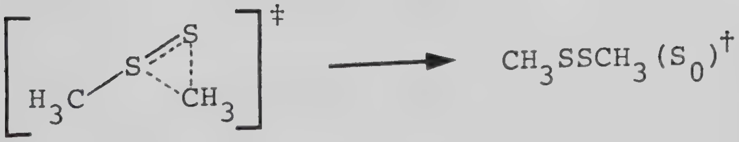

[19b]

to yield $CH_3SSCH_3(S_o)^\dagger$.

The vibrationally excited CH_3SSCH_3 molecule formed in [19b] can fragment to a small extent or be stabilized:

$$CH_3SSCH_3(S_0)^{\dagger} \longrightarrow 2CH_3S\cdot \quad [20a]$$

$$\xrightarrow{M} CH_3SSCH_3 \quad [20b]$$

Since CH_3S, CH_3S_2 and CH_3 radicals are present in the system, the following reactions should be considered:

$$2CH_3\cdot \longrightarrow C_2H_6 \quad [21]$$

$$CH_3S\cdot + CH_3\cdot \longrightarrow CH_3SCH_3 \quad [22a]$$

$$\longrightarrow CH_4 + CH_2S \quad [22b]$$

$$2CH_3S\cdot \longrightarrow CH_3SSCH_3 \quad [23a]$$

$$\longrightarrow CH_2S + CH_3SH \quad [23b]$$

$$CH_3\cdot + CH_3SCH_3 \longrightarrow CH_4 + \cdot CH_2SCH_3 \quad [24]$$

$$CH_3S\cdot + CH_3SCH_3 \longrightarrow CH_3SH + \cdot CH_2SCH_3 \quad [25]$$

$$CH_3\cdot + COS \longrightarrow CH_3S\cdot + CO \quad [26]$$

$$CH_3S_2\cdot + CH_3\cdot \longrightarrow CH_3S_2CH_3 \quad [27a]$$

$$\longrightarrow CH_4 + CH_2S_2 \quad [27b]$$

$$CH_3S_2\cdot + CH_3S\cdot \longrightarrow CH_3S_3CH_3 \quad [28a]$$

$$\longrightarrow CH_3SH + CH_2S_2 \quad [28b]$$

$$2CH_3S_2^{\cdot} \longrightarrow (CH_3S_4CH_3)^{\dagger} \qquad [29a]$$

$$\longrightarrow (CH_3SSCH_3)^{\dagger} + S_2 \qquad [29b]$$

$$\longrightarrow CH_3SH + CH_2S + S_2 \qquad [29c]$$

Thus there are two sources of C_2H_6, steps [15b] (molecular) and [21] (radical). Radical-radical reactions are probably of minor importance owing to their low concentrations. For the self-reactions of CH_3S radicals, steps [23a, 23b], k_d/k_c has been estimated to be ∿0.05,[173] and the value for the cross-reaction, $CH_3 + CH_3S$, steps [22a, 22b], should also be very low. Hence it is not surprising that polymeric thioformaldehyde, the end product of CH_2S formed in the disproportionation reactions [22b] and [23b], was not detected in the cell residues after high conversion experiments. The hypothetical gas phase disproportionation reactions of CH_3S_2 (steps [29b, 29c]) are proposed by analogy with the known chemistry of HS_2[171] and CH_3O_2[174] radicals. The disulfide formed in step [29b] is probably "hot" and may constitute an additional source of CH_3S radicals at low pressures.

For steps [24] and [26], rate parameters have been reported[175,176] and the corresponding room temperature rate constants are:

$k_{24} = 7.8 \times 10^4 \ M^{-1}s^{-1}$

$k_{26} = 1.8 \times 10^3 \ M^{-1}s^{-1}$

These are very low indeed, and thus reactions [24] and [26] are not likely to be important.

Kinetic data for step [25] have not been reported. However, for the $CH_3S + CH_3SSCH_3 \rightarrow CH_3SH + CH_2SSCH_3$ reaction, E_a is 8.5 kcal mole^{-1} [178] and E_a for reaction [25] should be very similar. Although this value is lower than the E_a's associated with steps [24] and [26], 9.4 and 11.4 kcal mole^{-1}, respectively, its magnitude is such that step [25] is probably not important.

Steps [27] and [28] have been included for completeness. Nothing is known with regard to the hypothetical disproportionation reactions.

Abstraction reactions involving CH_3S_2 have not been considered since the product, CH_3S_2H, is a very unstable species.

Since CH_4 is a secondary product, it must be formed as a result of reaction between CH_3 and one of the reaction products. The most likely candidate is CH_3SH,

$$CH_3\cdot + CH_3SH \longrightarrow CH_4 + CH_3S\cdot \qquad [30]$$

which has a readily abstractable H atom: $D(CH_3S{-}H) = 92$ kcal mole^{-1} [168] as compared to $D(CH_3SCH_2{-}H) = 95$ kcal mole^{-1}.[178]

In any event, the total radical reactions taking place in this system are of minor importance, constituting only a few percent of the overall reactions.

As has been demonstrated, the mass imbalance in terms of the S product yield is due to the formation of elemental sulfur. This indicates that reactions involving desulfurization must play a significant role in this system:

ΔH (kcal mole^{-1})

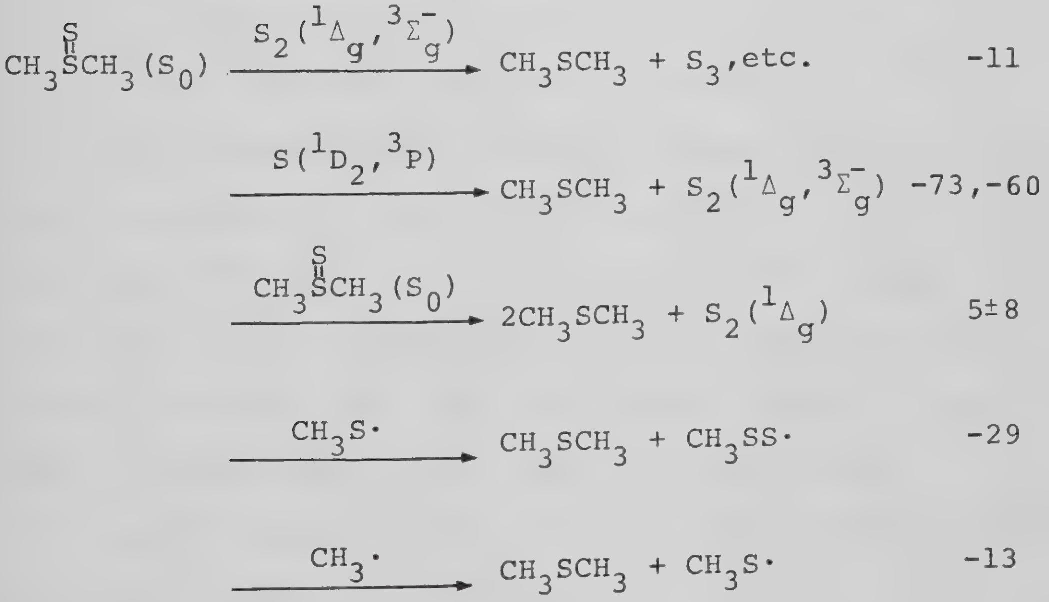

$$CH_3\overset{S}{\overset{\|}{S}}CH_3(S_0) \xrightarrow{S_2(^1\Delta_g,\,^3\Sigma_g^-)} CH_3SCH_3 + S_3,\text{etc.} \qquad -11 \quad [31a]$$

$$\xrightarrow{S(^1D_2,\,^3P)} CH_3SCH_3 + S_2(^1\Delta_g,\,^3\Sigma_g^-) \qquad -73,-60 \quad [31b]$$

$$\xrightarrow{CH_3\overset{S}{\overset{\|}{S}}CH_3(S_0)} 2CH_3SCH_3 + S_2(^1\Delta_g) \qquad 5\pm8 \quad [31c]$$

$$\xrightarrow{CH_3S\cdot} CH_3SCH_3 + CH_3SS\cdot \qquad -29 \quad [31d]$$

$$\xrightarrow{CH_3\cdot} CH_3SCH_3 + CH_3S\cdot \qquad -13 \quad [31e]$$

Since $S(^3P)$ (and presumably $S(^1D_2)$ as well) reacts with CH_3SCH_3 at a rate approaching the collision frequency (vide infra), and $[CH_3SCH_3] >> [(CH_3)_2S{=}S]$, desulfurization by $S(^1D_2,\ ^3P)$ cannot be significant. Desulfurization of DMTSO(S_0) by $S_2(^1\Delta_g)$, formed in step [2], is exothermic by 11 kcal mole^{-1}; although this reaction is thermodynamically feasible, the steady state concentrations of $S_2(^1\Delta_g)$ are extremely low. Ground state S_x species have been shown to be unreactive towards thiirane,[179] and since D(C-S) of thiirane is very similar to D(S=S) in DMTSO (52 and 55 kcal mole^{-1}, respectively), desulfurization of DMTSO by $S_2(^3\Sigma_g^-)$, S_3 etc. should also be of minor importance. Desulfurization by CH_3S or CH_3 radicals (steps [31d] and [31e]) is not likely to be important and moveover, these reactions do not lead to the formation of polymeric sulfur.

Desulfurization via reaction between two ground state DMTSO molecules may be slightly endothermic ($\Delta H \sim 5 \pm 8$ kcal mole^{-1}),[168] but it should be noted that $\Delta H_{DMTSO} \simeq 4 \pm 3$ kcal mole^{-1} is an estimated value only and thus step [31c] may be feasible. Its importance would depend on the transient concentration of the thiosulfoxide species.

Desulfurization could also be envisioned as proceeding via unimolecular S atom extrusion:

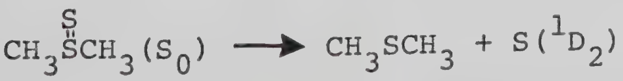

$$CH_3\overset{S}{\overset{\|}{S}}CH_3(S_0) \longrightarrow CH_3SCH_3 + S(^1D_2) \qquad [32]$$

Due to spin conservation, the S atom produced must be in the singlet state, and thus the energy required for the occurrence of reaction [32] is at least equal to the exothermicity of the $S(^1D_2) + CH_3SCH_3$ reaction. Consequently, step [32] may be important only at infinitesimally low pressures. Moreover, its occurrence would not affect the S product recovery. Therefore, it is concluded that desulfurization of DMTSO(S_0) takes place via the bimolecular reaction [31c].

From the mechanism delineated above, it is apparent that three reaction pathways are open to the excited DMTSO adduct. There are two product formation pathways: fragmentation via C-S bond scission, and isomerization. The former leads to $C_2H_6 + S_2$ and to $CH_3S_2 + CH_3$, while the latter leads to CH_3SSCH_3. The other mode of decay, deactivation followed by desulfurization, leads to regeneration of the substrate. The major reactions occurring in the system can thus be summarized as follows:

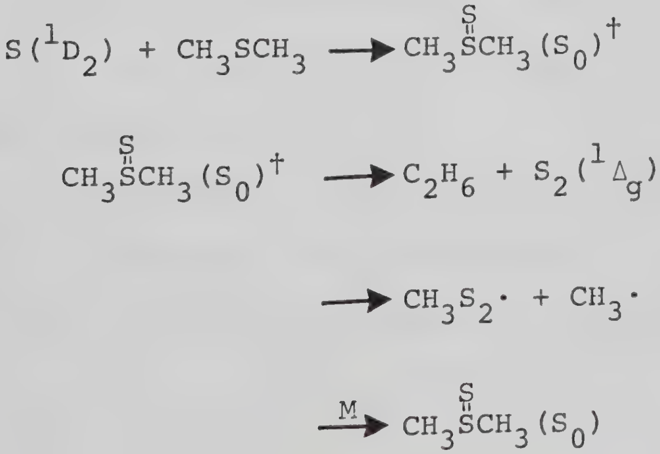

$$S(^1D_2) + CH_3SCH_3 \longrightarrow CH_3\overset{S}{\overset{\|}{S}}CH_3(S_0)^\dagger \qquad [8]$$

$$CH_3\overset{S}{\overset{\|}{S}}CH_3(S_0)^\dagger \longrightarrow C_2H_6 + S_2(^1\Delta_g) \qquad [15b]$$

$$\longrightarrow CH_3S_2\cdot + CH_3\cdot \qquad [15c]$$

$$\xrightarrow{M} CH_3\overset{S}{\overset{\|}{S}}CH_3(S_0) \qquad [16]$$

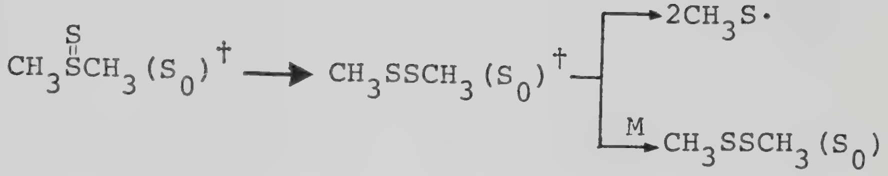

$$CH_3\overset{S}{\overset{\|}{S}}CH_3(S_0)^{\dagger} \longrightarrow CH_3SSCH_3(S_0)^{\dagger} \begin{cases} \longrightarrow 2CH_3S\cdot & [20a] \\ \xrightarrow{M} CH_3SSCH_3(S_0) & [20b] \end{cases}$$

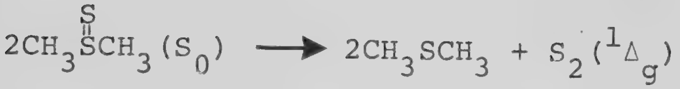

$$2CH_3\overset{S}{\overset{\|}{S}}CH_3(S_0) \longrightarrow 2CH_3SCH_3 + S_2(^1\Delta_g) \qquad [31c]$$

$$2CH_3\cdot \longrightarrow C_2H_6 \qquad [21]$$

$S(^3P)$ atoms also react with CH_3SCH_3 to yield CH_3SSCH_3, CH_4 and C_2H_6 in similar relative proportions and in drastically reduced yields, less than 60% of those obtained from the $S(^1D_2)$ reaction (Table IV-3). The exothermicity of the proposed primary step,

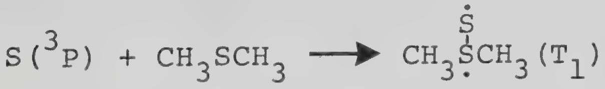

$$S(^3P) + CH_3SCH_3 \longrightarrow CH_3\overset{\dot{S}}{\underset{\cdot}{\overset{|}{S}}}CH_3(T_1) \qquad [9]$$

is approximately 53 kcal $mole^{-1}$, and accordingly, the DMTSO (T_1) is 26 kcal $mole^{-1}$ less energetic than the DMTSO$(S_0)^{\dagger}$ formed in step [8].

If fragmentation reactions analogous to those postulated for DMTSO$(S_0)^{\dagger}$ are considered, i.e. steps [15a-d], only the following are energetically possible for DMTSO(T_1):

ΔH
(kcal $\mathrm{mole^{-1}}$)

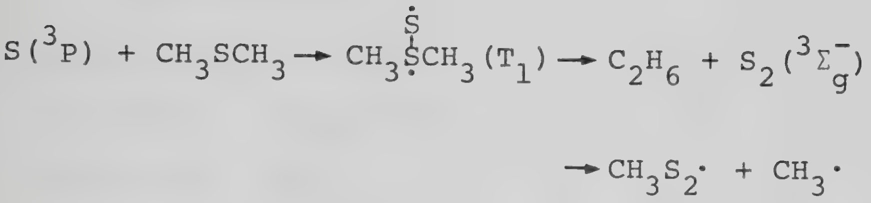

$$\mathrm{S(^3P) + CH_3SCH_3 \rightarrow CH_3\overset{\dot{S}}{\underset{\cdot}{S}}CH_3(T_1) \rightarrow C_2H_6 + S_2(^3\Sigma_g^-)} \qquad -46 \quad [33a]$$

$$\mathrm{\rightarrow CH_3S_2\cdot + CH_3\cdot} \qquad -6.1 \quad [33b]$$

Since the C_2H_6 yields are fivefold less than those of CH_3SSCH_3, it is likely that the bulk of the CH_3SSCH_3 arises from DMTSO(T_1) and not from recombination of the radicals formed in [33b]. One possibility is,

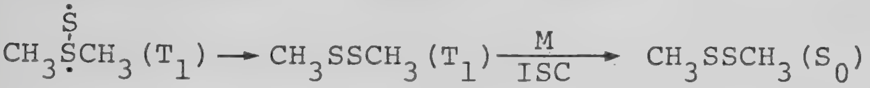

$$\mathrm{CH_3\overset{\dot{S}}{\underset{\cdot}{S}}CH_3(T_1) \rightarrow CH_3SSCH_3(T_1) \xrightarrow[ISC]{M} CH_3SSCH_3(S_0)} \qquad [34]$$

However, $CH_3SSCH_3(T_1)$ has never been observed and is likely to be antibonding in character, dissociating immediately to two CH_3S fragments. A more plausible pathway for the formation of CH_3SSCH_3 from DMTSO(T_1) is:

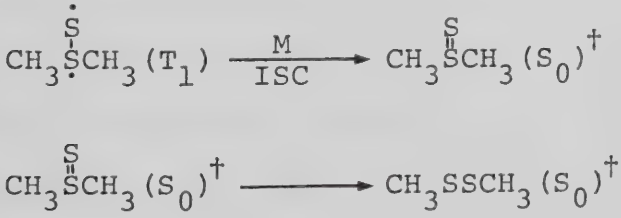

$$\mathrm{CH_3\overset{\dot{S}}{\underset{\cdot}{S}}CH_3(T_1) \xrightarrow[ISC]{M} CH_3\overset{S}{\overset{\|}{S}}CH_3(S_0)^{\dagger}} \qquad [35a]$$

$$\mathrm{CH_3\overset{S}{\overset{\|}{S}}CH_3(S_0)^{\dagger} \longrightarrow CH_3SSCH_3(S_0)^{\dagger}} \qquad [35b]$$

Because of the lower energy content of the DMTSO$(S_0)^{\dagger}$ formed in step [35a], as compared to the $S(^1D_2) + CH_3SCH_3$ adduct, the rates of isomerization to disulfide and of deactivation to the S_0 state are lesser and greater, respectively, resulting in a sharp suppression of the CH_3SSCH_3

yields (Table IV-3).

The increased importance of deactivation in this system may be expressed in a more quantitative manner (Appendix C-2). Comparison of the CH_3SSCH_3 yield in the pressure independent region (> 200 torr), Table IV-2, with those obtained in the presence of CO_2 (Table IV-3) reveals that the CH_3SSCH_3 recovery for $S(^1D_2)$ addition is ∿25%, while that for $S(^3P)$ addition is only ∿7%. It follows that the deactivation/isomerization ratios for the $S(^1D_2)$ and $S(^3P)$ atom reactions are ∿3 and ∿14, respectively, for $COS/CH_3SCH_3 = 300/30$ and at 30 min. exposure time.

The greater importance of deactivation for the triplet DMTSO suggests that the sharp drop in CH_3SSCH_3 yields when the pressure is increased from 100 to 200 torr (Figure IV-3) is mainly due to deactivation of this species.

In the presence of 2-4 torr of NO (Table IV-3), the CH_4 and C_2H_6 yields are completely suppressed, suggesting radical precursors. Interestingly, the CH_3SSCH_3 yield is decreased by only 80%. One possible explanation for the suppression of product yields by NO is the scavenging of S atoms. However, in the presence of NO, the CO yield dropped by only ∿3%, indicating that NO did not react significantly with $S(^1D_2)$. For $S(^3P)$ atoms, $k_{S(^3P)+NO+M} = 1.9 \times 10^{11}\ M^{-2}s^{-1}$ [53] and $k_{S(^3P)} + CH_3SCH_3 = 1.3 \times 10^{11}\ M^{-1}s^{-1}$ (vide infra). Thus for the $COS/CH_3SCH_3/NO = 300/30/4$ mixture

(Table IV-3), M = [COS] + [CH_3SCH_3] + [NO] ∿ 0.018, and it follows that:

$$\frac{\text{Rate}_{S(^3P)+NO+M}}{\text{Rate}_{S(^3P)+CH_3SCH_3}} = 3.5 \times 10^{-3}$$

Thus NO does not react with $S(^3P)$ atoms fast enough to affect the $S(^3P)$ concentration. It may be concluded that scavenging of $S(^1D_2)$ and $S(^3P)$ atoms by NO is not responsible for the decrease in product yields. NO presumably reacts with $DMTSO(S_0)^\dagger,(T_1)$ in competition with the $DMTSO(S_0)^\dagger,(T_1) \rightarrow CH_3SSCH_3$ rearrangements (steps [17] and [35]), most likely via abstraction:

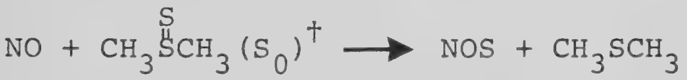

$$NO + CH_3\overset{S}{\underset{}{S}}CH_3(S_0)^\dagger \longrightarrow NOS + CH_3SCH_3 \qquad [36]$$

This reaction is evidently not as efficient as the NO + radical (CH_3 etc.) scavenging reactions. However, this is not unexpected since $DMTSO(S_0)^\dagger$ is a vibrationally excited molecule and not a monoradical. Moreover, the reaction of NO with triplet state thiirane is very slow and a large excess of NO is required to effect even a 30% suppression.[3] In this connection, it is interesting to note that Rao, et al.[173] have reported that 50 torr NO were required to scavenge all the CH_3S radicals in their system, produced at a much higher rate than in the present study.

At this point it would be interesting to compare the present results with the well documented $O(^3P) + CH_3SCH_3$

reaction.[117] The major products are C_2H_6 and $(CH_3)_2S{=}O$ (DMSO) in a ratio ∿3:1, respectively, and their combined yields are ∿35%, in terms of the $O(^3P)$ atoms produced. The overall mechanism is postulated to be:

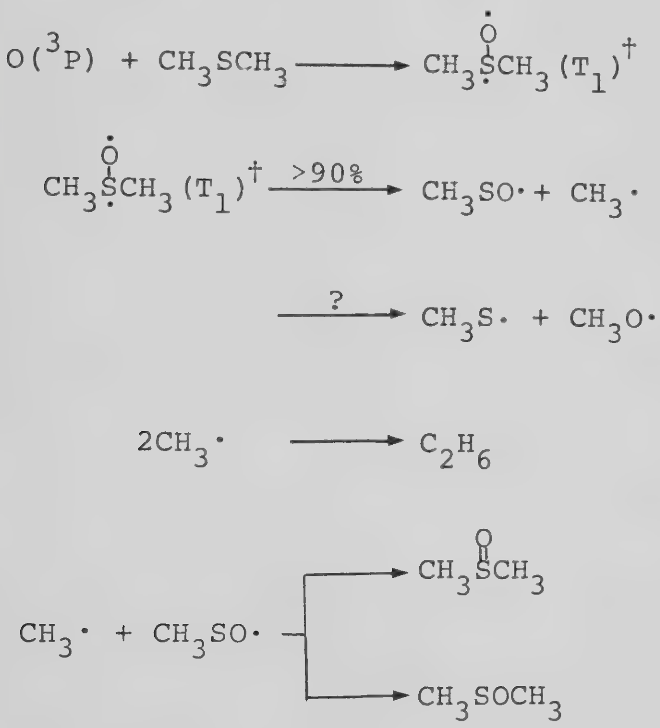

$$O(^3P) + CH_3SCH_3 \longrightarrow CH_3\overset{\dot{O}}{\overset{|}{\underset{\cdot}{S}}}CH_3\,(T_1)^{\dagger} \qquad [37]$$

$$CH_3\overset{\dot{O}}{\overset{|}{\underset{\cdot}{S}}}CH_3\,(T_1)^{\dagger} \xrightarrow{>90\%} CH_3SO\cdot + CH_3\cdot \qquad [38a]$$

$$\xrightarrow{?} CH_3S\cdot + CH_3O\cdot \qquad [38b]$$

$$2CH_3\cdot \longrightarrow C_2H_6 \qquad [39]$$

$$CH_3\cdot + CH_3SO\cdot \longrightarrow CH_3\overset{O}{\overset{\|}{S}}CH_3 \qquad [40a]$$

$$\longrightarrow CH_3SOCH_3 \qquad [40b]$$

In the presence of C_2H_5SH, which has a readily abstractable hydrogen atom, $(CH_3)_2S{=}0$ was completely suppressed, indicating that it arises solely from radical recombination and not from pressure stabilization of the initial adduct.

The structural difference between the final addition products in the $O(^3P)$ and $S(^1D_2, {}^3P)$ systems (branched *versus* linear) is a consequence of the thermodynamic stabilities of the possible products: $(CH_3)_2S{=}S$ is known to be unstable and CH_3SOCH_3 is an unknown entity, hence its

possible formation in this system is purely speculative.

2) $S(^1D_2, {}^3P) + \overline{CH_2(CH_2)_2S}$ Reactions

The methylenic α C-H bonds and possibly the β C-H bonds are expected to be somewhat weaker than the primary C-H bonds in CH_3SCH_3, and insertion into these bonds might take place, leading to the formation of the corresponding thiols.

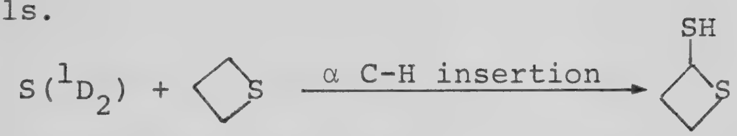

[41a]

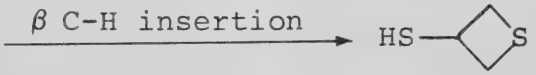

[41b]

Neither thiol was detected however, and the sole retrievable products identified were C_2H_4 and 1,2-dithiolane 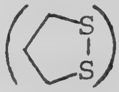 .
Thus, by analogy to the $S(^1D_2) + CH_3SCH_3$ reaction, the primary adduct is believed to be vibrationally excited ground singlet state thietanethiosulfoxide (TTSO):

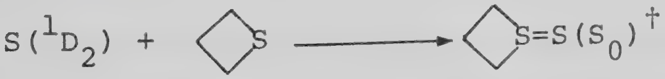

[42]

This adduct may then undergo C-S bond cleavage to form a biradical,

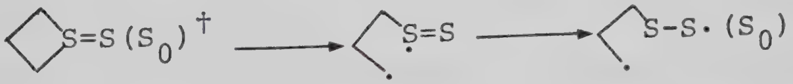

[43a]

which may then undergo ring closure,

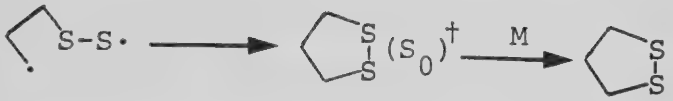

[43b]

fragment via C-C bond cleavage,

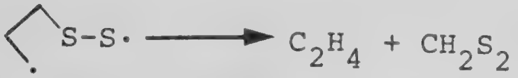

[43c]

or fragment via C-S bond cleavage:

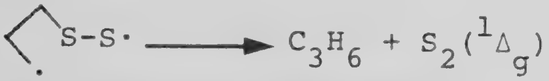

[43d]

Alternatively, the thietanethiosulfoxide may isomerize:

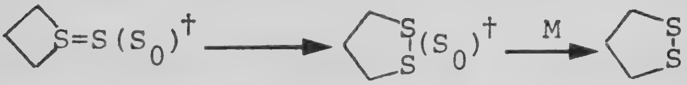

[44]

or be deactivated, followed by desulfurization:

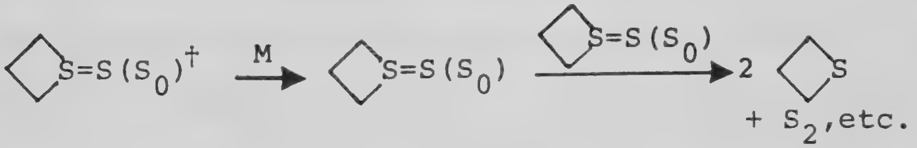

[45]

In sharp contrast to the S+ CH_3SCH_3 reaction, the combined product recovery for this system extrapolated to zero time is ∿85% (Figure IV-10), with a 1,2-dithiolane/ C_2H_4 ratio of ∿1.1. This and the fact that the product yields are independent of pressure (Figure IV-11) is probably indicative of the relative inefficiency of deactivation step [45] or of a much shorter lifetime for the excited TTSO as compared to DMTSO. The recoveries of 1,2-dithiolane for $S(^1D_2)$ and $S(^3P)$ are similar, 44 and 36% respectively, as opposed to the case of CH_3SSCH_3, where the recoveries for $S(^1D_2)$ and $S(^3P)$ are 25 and 7%, respectively (Appendix C-2).

1,2-Dithiolane may form from C-S bond cleavage, steps ([43a] + [43b]), and/or isomerization of TTSO, step [44]. However, the high yield of C_2H_4 suggests that fragmentation is a major decay path for TTSO, and therefore it is suggested that a large portion of 1,2-dithiolane arises from steps ([43a] + [43b]) rather than step [44]. Unfortunately the importance of fragmentation to $C_3H_6 + S_2\ (^1\Delta_g)$, step [43d], cannot be assessed quantitatively. However, the results of the GC/MS cross scan experiment suggest that this path is of minor importance, although it is one of the major processes in the photolysis of trimethylene sulfoxide.[180]

The predominance of fragmentation as the fate of $TTSO(S_0)^{\dagger}$ as compared to $DMTSO(S_0)^{\dagger}$ may be attributed to the relief of ring strain which, for the parent thietane, has been calculated to be 19.4 kcal $mole^{-1}$,[169] since the energy contents for the two adducts are expected to be comparable.

The CH_2S_2 species formed in fragmentation step [43c] may exist in three isomeric forms:

$H_2C{=}S{=}S$,

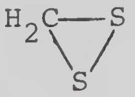

, and

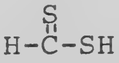

$H{-}\overset{\overset{\displaystyle S}{\|}}{C}{-}SH$

The first two isomers have never been observed, although there is some evidence in support of their transient existence.[172] Dithioformic acid, on the other hand, has been produced by the pyrolysis of $HC(SH)_3$ for microwave spectroscopic structural analysis.[181] Although its stability was

not examined in detail, it could be observed at 25° in a flow system when the pyrolysis was performed between 200° and 900°. Thus, while $H_2C{=}S{=}S$ is logically the most probable structure for the initially formed CH_2S_2 species, it is possible that it might isomerize to form $H\overset{\overset{S}{\|}}{C}SH$, of which the ultimate fate is probably polymerization.

$S(^3P)$ atoms also react with thietane to yield 1,2-dithiolane and C_2H_4. The % recovery of 1,2-dithiolane is similar to the $S(^1D_2)$ case but that of C_2H_4 is drastically reduced (Table IV-12), resulting in a much higher $\overline{CH_2(CH_2)_2SS}/C_2H_4$ ratio (7.5, versus 1.1 for $S(^1D_2)$). The following triplet state analogs of steps [42] to [45] may be considered:

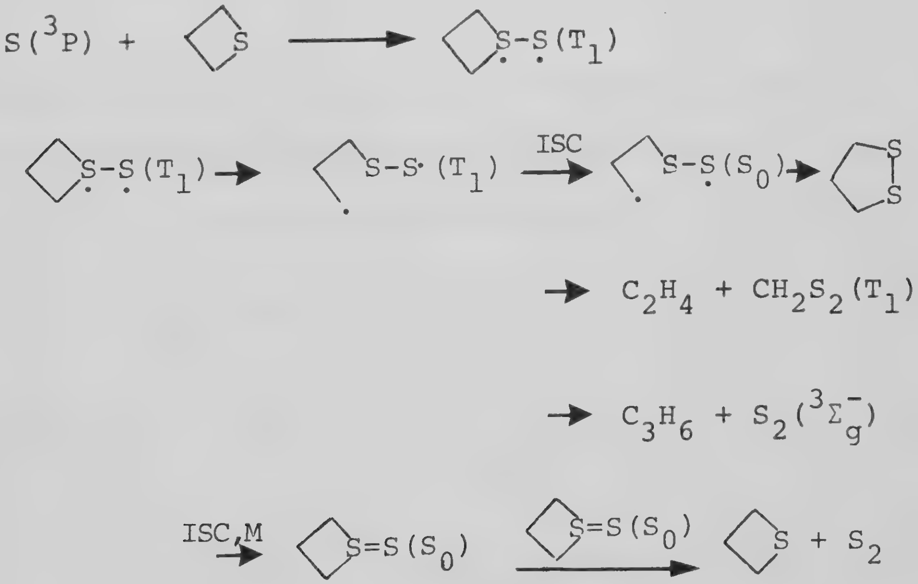

[46]

[47a]

[47b]

[47c]

[47d]

The energy content of $TTSO(T_1)$ is lower than that of $TTSO(S_o)^\dagger$ by 26 kcal mole^{-1}, which explains the much lower

observed yield of the fragmentation product. Moreover, spin conservation requires that the species produced by fragmentation and isomerization must be in triplet states, which may not be energetically accessible. The biradical produced by C-S bond scission (step [47a]) however, should have a low lying triplet state and thus should be formed quite readily. This biradical is postulated to undergo efficient intersystem crossing to the S_o state where ring closure may then take place. The low overall product recovery (∿40%) in the $S(^3P)$ + thietane system (steps [47a] and [47b]) indicates that intersystem crossing followed by deactivation (step [47d]) is one of the major reactions occurring.

$O(^3P)$ atoms also react with thietane to yield C_2H_4; in addition, small quantities of $c\text{-}C_3H_6$ were detected (C_2H_4/$c\text{-}C_3H_6$ = 1/0.3). The following mechanism has been proposed:

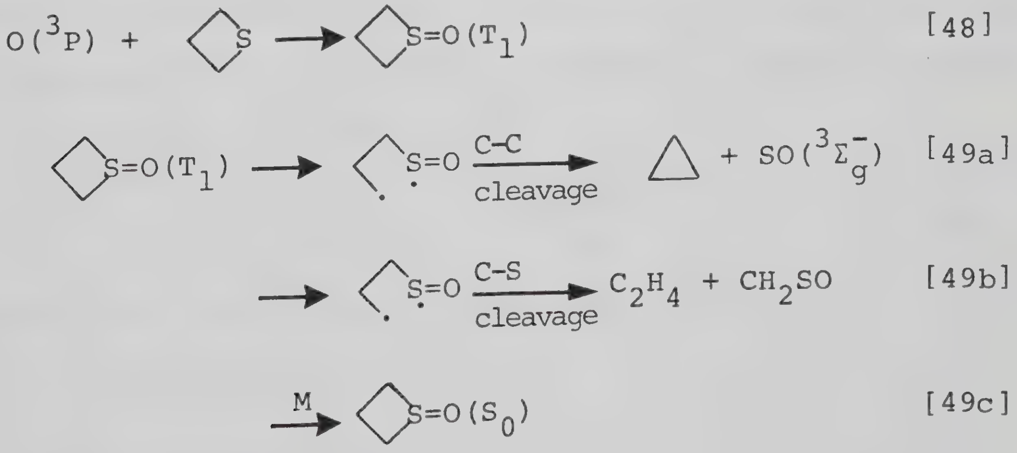

Together, C_2H_4 and c-C_3H_6 account for 90% of the overall reaction. It is noteworthy that the exothermicities of the $O(^3P)$ + $\overline{CH_2CH_2)_2S}$ and $S(^1D_2)$ + $\overline{CH_2(CH_2)_2S}$ reactions exceed the C-S bond dissociation energies of the adducts by nearly identical amounts, yet fragmentation in the latter system is only half as important as in the former. One possible explanation is that rearrangement of 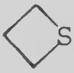$S{=}S(S_0)^\dagger$ (steps ([43a] + [43b]) and [44]) leads to the formation of a relatively stable product, 1,2-dithiolane, whereas the analogous process for 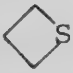$S{=}O(T_1)$ would lead to the formation of 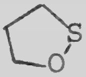, which has never been isolated.

Interestingly, although the $S(^3P)$ + $\overline{CH_2(CH_2)_2S}$ reaction affords mainly the addition product and smaller yields of the fragmentation product, the corresponding three membered ring, thiirane, reacts with $S(^3P)$ atoms to give C_2H_4 as the only retrievable product.[111] Based on the growth of the $S_2(\tilde{X}^3\Sigma_g^-)$ spectrum and the concomitant decay of the $S(^3P)$ absorption observed by flash photolysis-kinetic absorption spectroscopy, it was proposed that the overall reaction is direct abstraction of the S atom from thiirane:[4,53]

$S(^3P)$ + 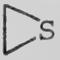 $\longrightarrow C_2H_4 + S_2(X^3\Sigma_g^-)$ [50]

By analogy with the present system, the primary adduct is probably the thiiranethiosulfoxide,

$S(^3P)$ + 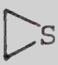 $\longrightarrow$ 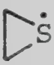$\dot{S}\text{-}\dot{S}(T_1)$ [51]

which may then decay in three ways:

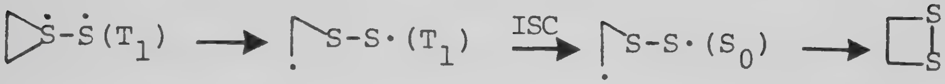
S-S(T1)
S-S·(T1)
ISC
S-S·(S0)
S
S

[52a]

$$\longrightarrow :CH_2(T_1) + CH_2S_2 \qquad [52b]$$

$$\longrightarrow C_2H_4 + S_2(^3\Sigma_g^-) \qquad [52c]$$

Formation of $:CH_2$, step [52b], has not been reported for 3-membered heterocycles.[182] The observation of $S_2(^3\Sigma_g^-)$ is accounted for by step [52c]. The thiosulfoxide-disulfide rearrangement would lead to the formation of the hypothetical 1,2-dithietane, step [52a]. This compound has never been isolated and is expected to be unstable due to strong repulsion of the pπ electrons of the adjoining S atoms. The transient existence of perfluoro-1,2-dithietane has been reported in the pyrolysis of perfluoroethylenedisulfide polymer:[183]

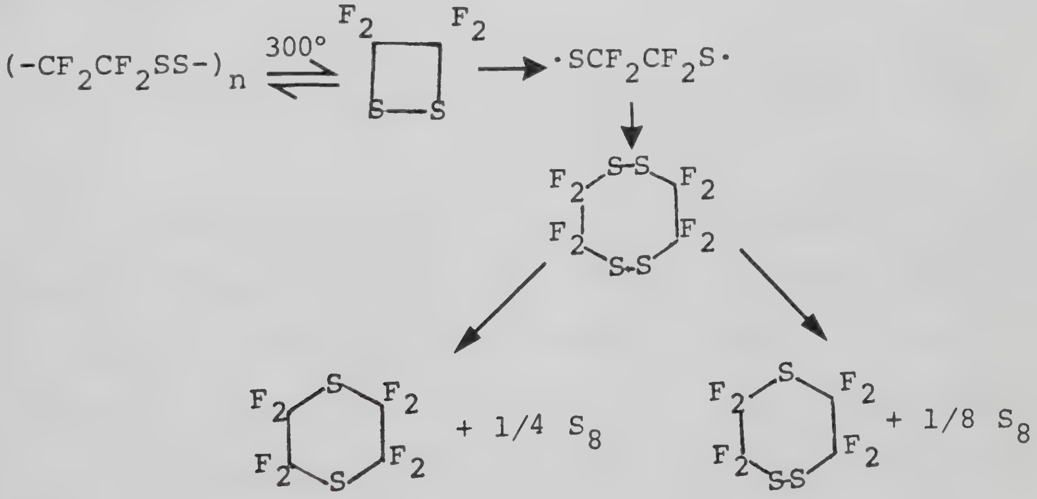
(-CF2CF2SS-)n
300°
F2
F2
S—S
·SCF2CF2S·
S-S
F2
F2
F2
F2
S-S
S
F2
F2
F2
F2
S
+ 1/4 S8
S
F2
F2
F2
F2
S-S
+ 1/8 S8

[53]

However, the dithietane reconverted back to the initial polymer at lower temperatures ($< 300^{o}$).

To date, only one stable 1,2-dithietane, 3,4-diethyl-1,2-dithietane 1,1-dioxide, has been isolated.[184]

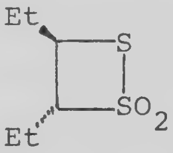

This compound possesses an enhanced stability due to the replacement of the lone pair electrons on one S atom, thus removing the destabilizing effect of the pπ electron repulsion.[183]

It is therefore unlikely that dithietane would be formed in the $S(^3P)$ + reaction. Moreover, the reaction leading to the formation of $S_2(^3\Sigma_g^-)$ is extremely rapid, $k = 2.7 \times 10^{10}\ M^{-1}s^{-1}$, and proceeds with no observable activation energy.[52] $O(^3P)$ atoms also desulfurize thiirane, and the reaction has been described in terms of fragmentation of the sulfoxide adduct:[113]

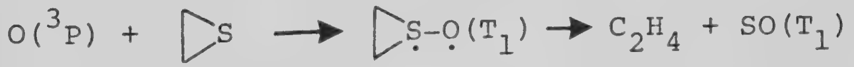

[54]

It is apparent from the foregoing discussions that the reactions of $S(^1D_2, {}^3P)$ atoms with simple thioethers generally feature attack at the sulfur non-bonding 3p orbitals leading to the formation of thiosulfoxides. $O(^3P)$ atoms react similarly to yield the corresponding sulfoxide, and by analogy

the remaining Group VI A atoms, Se and Te, probably form the corresponding unstable adducts. From the few studies reported in the literature, it appears that the high reactivity of the S non-bonding 3p orbitals toward atom and radical attack is not limited only to divalent species: most atoms and radicals also preferentially attack at the sulfur site.

The reactions of H atoms with CH_3SCH_3,[185] thiirane,[186] thiolane,[187] and 3-thiolene[188] have been studied. In all cases, the initial attack is at the S site and the subsequent fate of the adduct is mainly determined by the relative stabilities of the possible products.

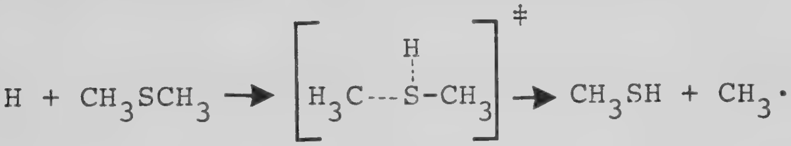
$$H + CH_3SCH_3 \rightarrow \left[H_3C\text{---}\overset{H}{\overset{\vdots}{S}}\text{-}CH_3 \right]^{\ddagger} \rightarrow CH_3SH + CH_3\cdot$$

[55a]

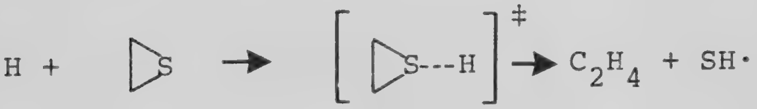

[55b]

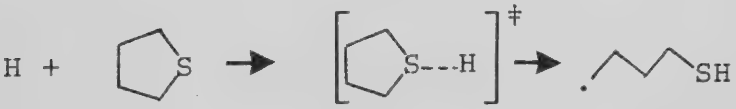

[55c]

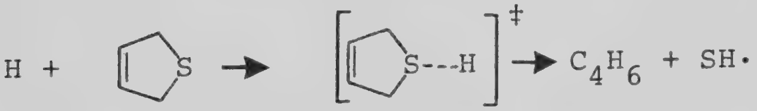

[55d]

A brief study of the C atom reaction with thiirane and thietane[189] revealed that the initial reaction is also addition to the S site, followed by elimination of CS to yield the corresponding hydrocarbons, e.g.

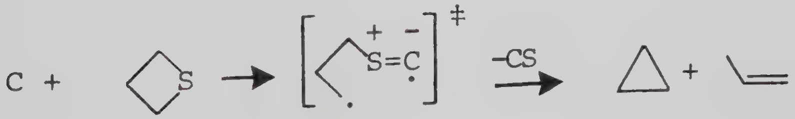

[56]

For the CH_3 + thiirane reaction, S abstraction is the major process although a small amount of H abstraction was observed.[172]

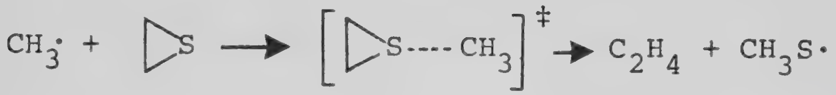

[57]

In this system H abstraction features a significantly higher E_a, resulting in a $R_{S\ abstraction}/R_{H\ abstraction}$ ratio of ∿40. The reactions of CH_3 radicals with CH_3SCH_3 have been investigated by Arthur and Lee,[171] and H abstraction was considered to be the only process occurring:

$$CH_3\cdot + CH_3SCH_3 \longrightarrow CH_4 + \cdot CH_2SCH_3 \qquad [24]$$

Attack at the sulfur site is possible but does not generate any new products:

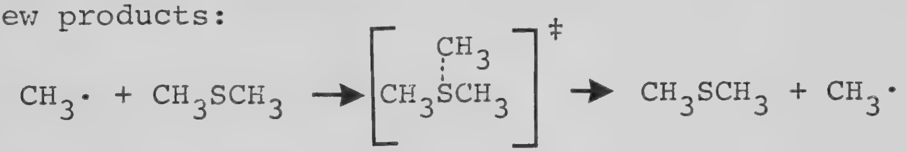

$$CH_3\cdot + CH_3SCH_3 \rightarrow \left[CH_3\overset{CH_3}{\overset{\vdots}{S}}CH_3 \right]^{\ddagger} \rightarrow CH_3SCH_3 + CH_3\cdot \qquad [58]$$

In view of the high reactivity of the sulfur non-bonding p orbitals toward atom and radical attack, it is almost certain that CH_3 radicals also attack at this site; an investigation of the reactions of CD_3 radicals with CH_3SCH_3 would reveal the mechanistic route.

The t-butoxy radical reacts with thietane and thiolane via different mechanisms: addition to the S site of thietane followed by C-S bond scission, and α-H abstraction from thiolane:[190]

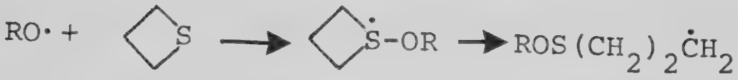

[59a]

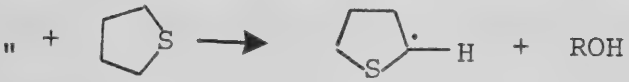

[59b]

This difference has been attributed to the relief of ring strain in the thietane adduct (19.4 kcal mole^{-1} [176]) upon formation of a linear radical. In contrast, C_6F_5 radicals attack the sulfur sites of both thiolane and thietane.

Carbenes and nitrenes have also been shown to add exclusively to the S atom of cyclic and acyclic thioethers in solution to yield the corresponding ylides and sulfimides,[191] with the former reagents exhibiting high selectivity:

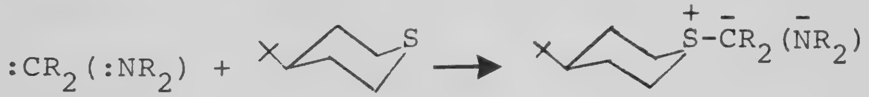

[60a]

$$\text{" " } + CH_3SCH_3 \longrightarrow (CH_3)_2\overset{+}{S}-\overset{-}{C}R_2(\overset{-}{N}R_2) \qquad [60b]$$

3. Rate Parameters for the $S(^3P) + CH_3SCH_3/\overline{CH_2(CH_2)_2S}$ Reactions

As shown in Figure IV-4, plots of $(A_o-A)/A$ *versus* the ratio $[CH_3SCH_3]/[C_3H_6]$ show slight downward curvature at high ratios (>0.11). The reason for this is not readily apparent. However, since for $[CH_3SCH_3]/[C_3H_6] < 0.11$, the plots appear to be linear, it is reasonable to assume that

the data in this region may be used for kinetic evaluation.

As shown in Table IV-4, at room temperature, $S(^3P)$ atoms react with CH_3SCH_3 ∿ 36 times faster than with propylene. The weighted least squares fit of the Arrhenius plot (Figure IV-5) yields,

$$A_{CH_3SCH_3}/A_{C_3H_6} = 3.83 \pm 0.17 \text{ , and}$$

$$E_{C_3H_6} - E_{CH_3SCH_3} = 1.34 \pm 0.06 \text{ kcal mole}^{-1}$$

From the absolute rate parameters for C_3H_6 measured by Klemm and Davis:[52]

$$A_{CH_3SCH_3} = (1.39 \pm 0.18) \times 10^{10} \ M^{-1}s^{-1}$$

$$E_{CH_3SCH_3} = -0.96 \pm 0.11 \text{ kcal mole}^{-1}$$

Alternatively, the data of Van Roodselaar[53] lead to:

$$A_{CH_3SCH_3} = (4.98 \pm 1.20) \times 10^{10} \ M^{-1}s^{-1}$$

$$E_{CH_3SCH_3} = -0.84 \pm 0.24 \text{ kcal mole}^{-1}$$

The average values of these two sets of parameters yield the following Arrhenius expression for the $S(^3P) + CH_3SCH_3$ reaction:

$$k = (3.19 \pm 1.21) \times 10^{10} \exp[(900 \pm 237/RT] \ M^{-1}s^{-1} \qquad [61]$$

This corresponds to a room temperature rate constant,

$$k_{(298)} = 1.35 \times 10^{11} \ M^{-1}s^{-1}$$

Thietane is even more reactive with respect to $S(^3P)$ addition than CH_3SCH_3, having a room temperature rate constant ∿50 times that of C_3H_6 (Table IV-13). The weighted least

squares fit of the Arrhenius plot (Figure IV-14) gives,

$$A_{\overline{CH_2(CH_2)_2S}}/A_{C_3H_6} = 1.84 \pm 0.04$$

$$E_{C_3H_6} - E_{\overline{CH_2(CH_2)_2S}} = 1.25 \pm 0.03 \text{ kcal mole}^{-1}$$

Using the absolute rate parameters for C_3H_6 measured by Klemm and Davis,

$$A_{\overline{CH_2(CH_2)_2S}} = 2.28 \pm 0.28 \times 10^{10} \text{ M}^{-1}\text{s}^{-1}$$

$$E_{\overline{CH_2(CH_2)_2S}} = -0.87 \pm 0.09 \text{ kcal mole}^{-1}$$

and those of Van Roodselaar,

$$A_{\overline{CH_2(CH_2)_2S}} = 8.18 \pm 1.90 \times 10^{10} \text{ M}^{-1}\text{s}^{-1}$$

$$E_{\overline{CH_2(CH_2)_2S}} = -0.75 \pm 0.20 \text{ kcal mole}^{-1}$$

The average values from these two sets of parameters give the following Arrhenius expression for the $S(^3P) + \overline{CH_2(CH_2)_2S}$ reaction:

$$k = (5.23 \pm 1.94) \times 10^{10} \exp[(810 \pm 220)/RT] \text{ M}^{-1}\text{s}^{-1} \qquad [62]$$

This corresponds to a room temperature rate constant,

$$k_{(298)} = 2.0 \times 10^{11} \text{ M}^{-1}\text{s}^{-1}$$

Thus, the reactions of $S(^3P)$ atoms with CH_3SCH_3 and $\overline{CH_2(CH_2)_2S}$ are both extremely fast, occurring at rates approaching the corresponding collision frequencies, 2×10^{11} and 2.5×10^{11} $M^{-1}s^{-1}$, respectively at room temperature, in-

dicating that at least one of every two collisions results in reaction.

It is apparent that at room temperature, thietane is almost twice as reactive as CH_3SCH_3. This is a consequence of the larger A factor for the thietane reaction since the activation energies are fairly similar (-0.90 and -0.81 kcal mole^{-1}). The A factors for the two reactions correspond to entropies of activation,

$$\Delta S^{\ddagger}_{CH_3SCH_3} \simeq -22.7 \text{ e.u.}$$

$$\Delta S^{\ddagger}_{\overline{CH_2(CH_2)_2S}} \simeq -21.8 \text{ e.u.}$$

The small difference in $\Delta S^{\ddagger}$ for the two reactions suggests the involvement of similar transition states, consistent with proposed mechanisms.

Both reactions exhibit negative activation energies, an unusual feature also observed for the $S(^3P)$ + branched alkene reactions. A plot of activation energy versus ionization potential for the reactions of $S(^3P)$ atoms with CH_3SCH_3, $\overline{CH_2(CH_2)_2S}$ and some selected alkenes is illustrated in Figure IV-15. It is apparent that, as in the $O(^3P)$ reactions, the linear correlation of E_a with ionization potential for the $S(^3P)$ + alkene reactions also extends to the above thioethers and this implies that the $S(^3P)$ + organosulfide reactions are basically electrophilic in nature. The $S(^3P)$ + thioether reactions exhibit slightly higher E_a's than

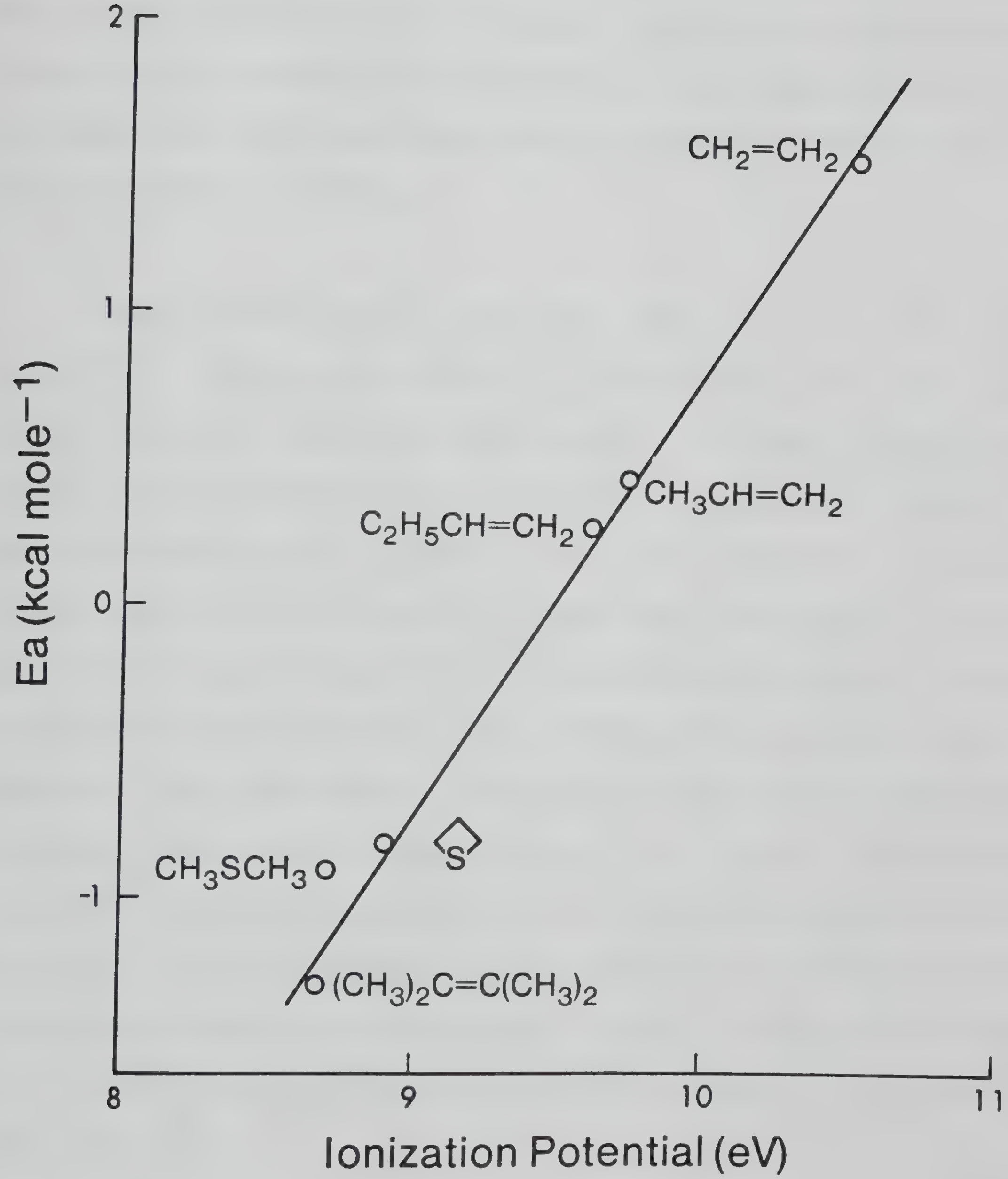

FIGURE IV-15: Plot of E_a versus ionization potential for the $S(^3P)$ + alkenes, CH_3SCH_3 and $\overline{CH_2(CH_2)_2S}$ systems.

that of the $S(^3P)$ + $(CH_3)_2C{=}C(CH_3)_2$ reaction (-1.3 kcal mole^{-1}). However, the overall room temperature rate constants are at least twice as fast, a consequence of the much higher A factors. The larger A factors for the case of thioethers may be ascribed to the greater accessibility of the reaction site: a C=C bond has a van der Waals radius of 1.54 A, whereas that for a sulfur atom is 1.85 A.

Negative activation energies, such as those observed for the $S(^3P)$ + CH_3SCH_3 and $\overline{CH_2(CH_2)_2S}$ reactions, have been reported for other systems (*vide supra*). A number of explanations for the observation of negative temperature dependences in bimolecular reactions have been proposed. In some cases, the observed negative E_a has been ascribed to a near zero actual E_a combined with a temperature dependent A-factor in the Arrhenius equation.[192] However such an explanation appears to be inadequate. Transition state theory does not predict a temperature dependence of the A factor much greater than $T^{-0.5}$ unless some unrealistic assumptions concerning the structure of the transition state are made. Collision theory predicts a temperature dependence of the A factor as high as $T^{-1.5}$ if the reaction cross section is assumed to be energy dependent.[192]

Later models[54,55] have been more successful in providing a rationale for negative activation energies. The

model of Strausz et al.[54] has been proposed to explain the trend to negative E_a's in the $S(^3P)$ + alkene reactions. In the context of this model, the $S(^3P)$ atom and $CH_3SCH_3/\overline{CH_2(CH_2)_2S}$ initially approach each other on a potential energy surface with a shallow minimum corresponding to a loose π complex which intersects the product disulfide surface (on the repulsive part of this curve) at a point below the level of the separate reactants, as illustrated below:

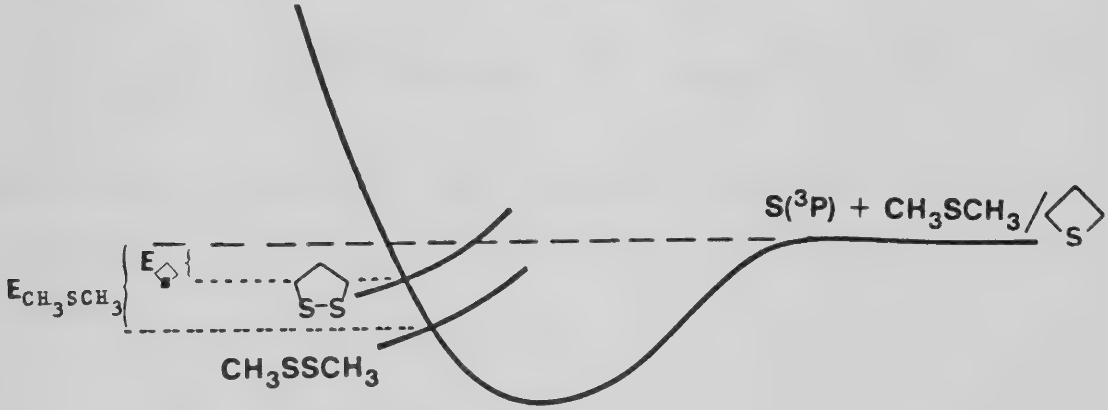

A similar model has been proposed by Cvetanovic et al. to explain the negative E_a's observed for the reactions of $O(^3P)$ with some alkenes.[51,121]

Applying these models to the present system, the addition of $S(^3P)$ to $CH_3SCH_3/\overline{CH_2(CH_2)_2S}$ results in reversible formation of a complex which may either dissociate back to $S(^3P)$ and $CH_3SCH_3/\overline{CH_2(CH_2)_2S}$ or evolve to the corresponding disulfide products as shown:

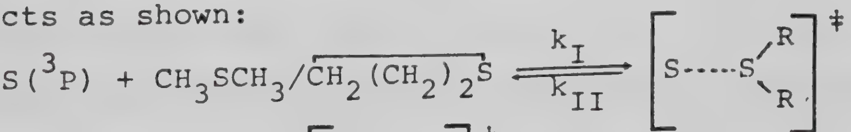

$$S(^3P) + CH_3SCH_3/\overline{CH_2(CH_2)_2S} \underset{k_{II}}{\overset{k_I}{\rightleftharpoons}} \left[S\cdots S\begin{matrix} R \\ R \end{matrix} \right]^{\ddagger} \qquad [63]$$

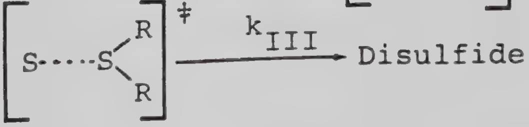

$$\left[S\cdots S\begin{matrix} R \\ R \end{matrix} \right]^{\ddagger} \xrightarrow{k_{III}} \text{Disulfide} \qquad [64]$$

Assuming a steady state concentration of the complex, the rate expression for product formation is:

$$\text{Rate} = \frac{k_I k_{III}}{k_{II}+k_{III}} \cdot [S(^3P)][RSR] \qquad [65]$$

Hence,

$$k_{obs.} = \frac{k_I k_{III}}{k_{II}} \quad \text{when } k_{II} >> k_{III} \qquad [66]$$

Expressing $k_{obs.}$ in the Arrhenius form:

$$k_{obs.} = \frac{A_I A_{III}}{A_{II}} \exp[(E_{II} - E_I - E_{III})/RT] \text{ , and} \qquad [67]$$

assuming no temperature dependence for the initial complex formation ($E_I = 0$), E_a, the activation energy observed, corresponds to,

$$E_a = E_{III} - E_{II} \qquad [68]$$

and will be negative provided $E_{II} > E_{III}$.

The room temperature rate constants and Arrhenius parameters of the $S(^3P) + CH_3SCH_3$ and $\overline{CH_2(CH_2)_2S}$ reactions are compared to those of other related systems in Table IV-19. For the CH_3SCH_3 system, the A factor for $S(^3P)$ addition is substantially larger than that for the $O(^3P)$ addition,[113,119-121] although both reactions exhibit negative E_a's and similar temperature dependences. The larger A-factor could be partly a consequence of the availability of the low-lying 3d orbitals on sulfur, which increases the effective collision diameter

TABLE IV-19

Rate Parameters for the Reactions of Some Atomic and Radical Species with CH_3SCH_3 and $\overline{CH_2(CH_2)_2S}$

Reagent	Substrate	$k_{(298)} \times 10^{-10}$ $M^{-1}s^{-1}$	$A \times 10^{-9}$ $M^{-1}s^{-1}$	E_a kcal $mole^{-1}$	Reference
$S(^3P)$	$\overline{CH_2(CH_2)_2S}$	20	52	-0.81	this work
$O(^3P)$	"	10	--	--	114
$S(^3P)$	CH_3SCH_3	13	32	-0.90	this work
$O(^3P)$	"	3.1	6.7	-0.92	121
"	"	3.3	12	-0.61	119
"	"	2.9	8.6	-0.73	113
"	"	3.0	7.7	-0.80	120
$H(^1S)$	"	0.021	17	2.6	185
"	"	0.015	15	2.7	193
$OH(^2\Pi)$	"	0.60	3.3	-0.36	194
"	"	0.26	4.1	0.27	195
"	"	0.57	3.7	-0.27	196

with respect to attack. In contrast to the $S(^3P)$ and $O(^3P)$ reactions, the $H + CH_3SCH_3$ reaction proceeds at a much slower rate.[185,193] This is a result of the relatively high E_a, reflecting the less electrophilic nature of H atoms. The OH radical is somewhat less reactive than $S(^3P)$ and $O(^3P)$, which is surprising in view of its higher reactivity with alkenes. On the basis of the observed trend in rate constants ($k_{CH_3SH} > k_{C_2H_5SH} > k_{CH_3SCH_3}$), it has been suggested that OH reacts with CH_3SCH_3 via H abstraction.[194] However, a negative E_a is inconsistent with an abstraction mechanism and OH probably reacts with the sulfur site. The lower reactivity as compared to $O(^3P)$ and $S(^3P)$ is probably associated with the nature of the bonding in the transition state.

CHAPTER V

SUMMARY AND CONCLUSIONS

In the gas phase, $S(^1D_2)$ atoms react with 1,2-butadiene to yield unsaturated addition products, thiiranes, 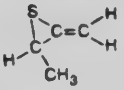 (**1**), 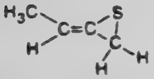 (**3**), and 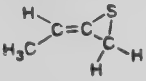 (**4**), and C-H insertion products, thiols, 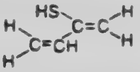 (**2**) and 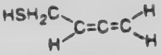 (**5**). Even at low conversion, the overall yields, relative to those of the S + alkene reactions, are low (70% versus 90%). $S(^3P)$ atoms, as expected, afford only the addition products, in yields comparable to those of the $S(^1D_2)$ reaction.

The rates of formation of **1** and **4** decrease drastically with time, but increase with increasing pressure. Thiirane **3**, which is formed at a much slower rate, also requires pressure stabilization, although no time dependence was observed. These observations suggest that photodecomposition is important for thiiranes **1** and **4**, as is apparent from their high UV absorption coefficients (of the order of 10^3 l mole^{-1}cm^{-1} in the region of photolysis). However, the pressure dependence of the thiirane rates indicates collisional stabilization of the hot adducts. One possible decomposition mechanism which is pressure dependent is isomerization of the hot thiirane adducts to unstable thiones followed by CS elimination,[128,139] e.g.

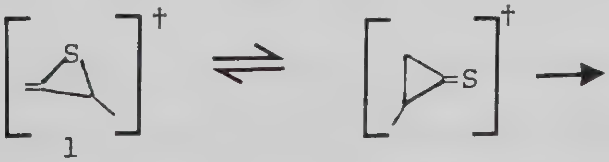

C_3H_6 + CS [1]

1

Due to the low yields of thiols **2** and **5**, no definite trend

in their rate behaviour with respect to time and pressure could be discerned; however, because of the presence of unsaturation, these compounds are expected to be quite unstable.

Although no product indicating insertion into the C-H bond of the alkyl substituted vinylic carbon was observed, the formation of thiol 2 indicates that this process may have taken place, i.e. 2 is postulated to be formed via an enethiol-thioketone-enethiol tautomerization of the initially formed enethiol:

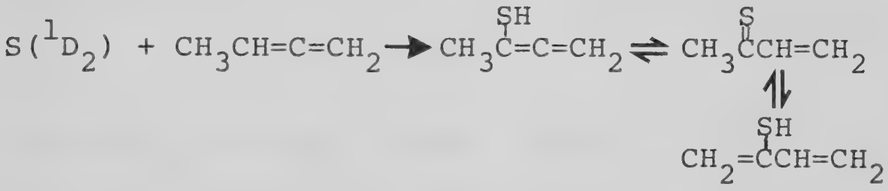

$$S(^1D_2) + CH_3CH{=}C{=}CH_2 \rightarrow CH_3\overset{SH}{C}{=}C{=}CH_2 \rightleftharpoons CH_3\overset{S}{C}CH{=}CH_2 \rightleftharpoons \underset{2}{CH_2{=}\overset{SH}{C}CH{=}CH_2} \quad [2]$$

In contrast to the COS-alkene systems, the combined thiirane yields in this system are very high, comprising 90% of the total S products observed. This is probably due to the presence of two addition sites in 1,2-C_4H_6, and may also be a consequence of lower stabilities of the insertion products in this system.

The relative Arrhenius parameters obtained from competitive rate studies in the presence of 1-C_4H_8 yield the following rate expression for the $S(^3P)$ + 1,2-C_4H_6 reaction:

$$k = (4.38 \pm 1.14) \times 10^{10} \exp[(-1455 \pm 255)/RT]\ M^{-1}s^{-1}$$

The A factor is somewhat larger (by a factor of ∿5) than those of similar $S(^3P)$ + alkene systems. This can be abscribed in part to the presence of two distinct reaction sites

in 1,2-C_4H_6, the two orthogonal π bonds. However, the A factor is also higher than that associated with the isomeric conjugated diene, 1,3-C_4H_6, by a factor of almost 2. This is probably due to a larger rotational contribution to the entropy of activation ($\Delta S^{\ddagger}$) as a result of going from a linear 1,2-C_4H_6 molecule (C_1-C_2-C_3 axis) to a bent transition state as shown,e.g.:

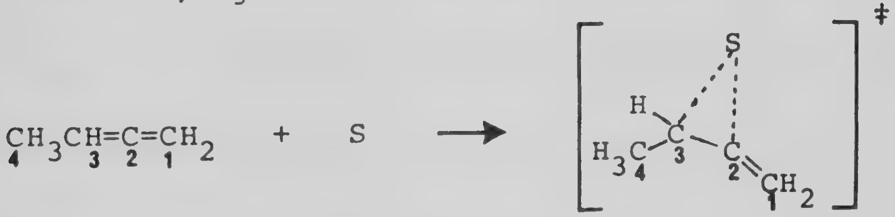

[3]

Despite its high A factor, the $S(^3P)$ + 1,2-C_4H_6 reaction proceeds at a slower rate than the $S(^3P)$ + 1,3-C_4H_6 reaction. This is due to the higher E_a associated with the former reaction, as a consequence of the absence of delocalization of the π electrons, rendering the molecule less polarizable, and the partial triple bond character conferred by hyperconjugation between the co-planar C-H and π bonds of 1,2-C_4H_6 as shown:

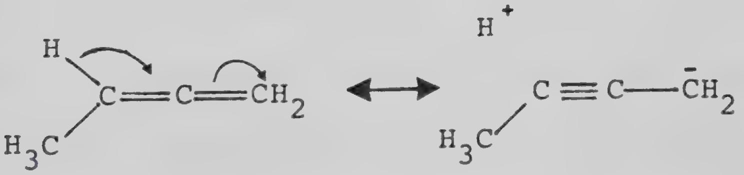

, etc. [4]

Interestingly, although the two π bonds of 1,2-butadiene are non-interacting, their reactions with $S(^3P)$ atoms proceed with similar E_a (∿1.5 kcal $mole^{-1}$). Consequently, the A factors for the 2,3 and 1,2-additions are simply proportional to the rate constants. From the corresponding product yields

(1 and 4) the rate constant ratio for $S(^3P)$ addition is,

$$\left(k_{2,3}/k_{1,2}\right)^{^3P}_{t=0,P=1200\ \text{torr}} \sim 2.1$$

and accordingly, the Arrhenius expressions for the two additions are:

$$k_{1,2} = (1.41\pm0.38) \times 10^{10}\exp[-(1455\pm255)/RT]\ M^{-1}s^{-1}$$

$$k_{2,3} = (2.96\pm0.80) \times 10^{10}\exp[-(1455\pm255)/RT]\ M^{-1}s^{-1}$$

At room temperature, these correspond to:

$$k_{1,2} = 1.2 \times 10^9\ M^{-1}s^{-1}$$

$$k_{2,3} = 2.6 \times 10^9\ M^{-1}s^{-1}$$

Surprisingly, these rate constants are within a factor of 2 of those for the $S(^3P) + C_2H_4$ and C_3H_6 reactions (6.0×10^8 and $3.7 \times 10^9\ M^{-1}s^{-1}$, respectively.). For $S(^1D_2)$ addition, the rate constant ratio for the two additions has been estimated to be:

$$\left(k_{2,3}/k_{1,2}\right)^{^1D}_{t=0,P=1200\ \text{torr}} \sim 1.3$$

The higher ratio observed for $S(^3P)$ addition indicates that the $S(^3P)$ atom is more selective,as a consequence of its lower energy content.

1,2-Addition leads to the formation of thiiranes 4 and 3, the trans and cis isomers, respectively. The trans/cis ratio observed for $S(^3P)$ is:

$$\left(\text{trans}/\text{cis}\right)^{^3P}_{t=0,P=1200\ \text{torr}} \sim 6$$

which is surprisingly high. The lower trans/cis product ratio estimated for $S(^1D_2)$ addition,

$$\left(\underline{\text{trans}}/\underline{\text{cis}}\right)^{1_D}_{t=0,P=1200\ \text{torr}} \sim 1.4,$$

reflects the higher reactivity and lower selectivity of $S(^1D_2)$ atoms.

The gas phase reactions of $S(^1D_2, ^3P)$ atoms with dimethylsulfide and thietane have been examined at room and moderately elevated temperatures.

$S(^1D_2)$ atoms react with dimethylsulfide yielding dimethyldisulfide as the only S addition product along with a small amount of C_2H_6. At high conversions, CH_4 is observed as a secondary product. The overall product recovery is low (<30% in terms of S atoms consumed). The yields of CH_3SSCH_3 and C_2H_6 decrease with pressure up to ∿200 torr, above which they appear to be constant. Analysis of the cell residues after high conversion runs indicates that the S product imbalance observed is due to the formation of polymeric sulfur. In the presence of NO, C_2H_6 and CH_4 are not observed and the yields of CH_3SSCH_3 are suppressed approximately fivefold.

Based on the observed products, the effects of total pressure and added NO, and the well documented high reactivity of the S non-bonding 3p orbitals, it is proposed that the primary step is attack at the S site of the substrate leading to the formation of an unstable dimethylthiosulfoxide(DMTSO) adduct.

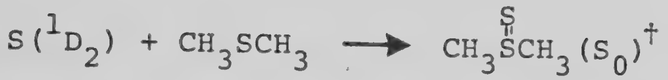

$$S(^1D_2) + CH_3SCH_3 \longrightarrow CH_3\overset{S}{\overset{\|}{S}}CH_3(S_0)^{\dagger} \qquad [5]$$

Three pathways are open to the DMTSO$(S_o)^{\dagger}$:

1) fragmentation via C-S bond scission to yield C_2H_6,

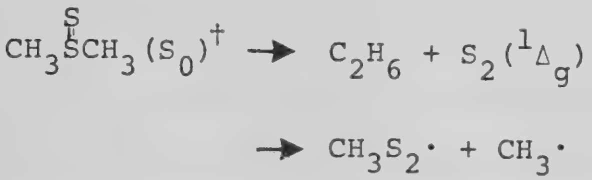

$$CH_3\overset{S}{\overset{\|}{S}}CH_3(S_0)^{\dagger} \rightarrow C_2H_6 + S_2(^1\Delta_g) \qquad [6a]$$

$$\rightarrow CH_3S_2\cdot + CH_3\cdot \qquad [6b]$$

2) isomerization to form the disulfide,

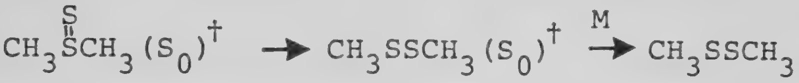

$$CH_3\overset{S}{\overset{\|}{S}}CH_3(S_0)^{\dagger} \rightarrow CH_3SSCH_3(S_0)^{\dagger} \xrightarrow{M} CH_3SSCH_3 \qquad [7]$$

3) deactivation followed by desulfurization,

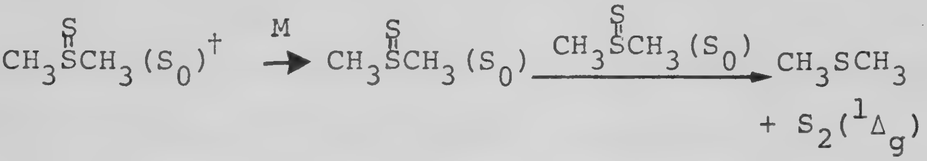

$$CH_3\overset{S}{\overset{\|}{S}}CH_3(S_0)^{\dagger} \xrightarrow{M} CH_3\overset{S}{\overset{\|}{S}}CH_3(S_0) \xrightarrow{CH_3\overset{S}{\overset{\|}{S}}CH_3(S_0)} CH_3SCH_3 + S_2(^1\Delta_g) \qquad [8]$$

Isomerization is the major product-forming step ($R_{CH_3SSCH_3}/R_{C_2H_6} \sim 9$). Desulfurization regenerates the substrate with the concomitant formation of elemental sulfur. Deactivation, the major process (deactivation/isomerization $\sim$ 3), is manifested by a decrease in product yields with an increase in pressure.

$S(^3P)$ atoms also react with CH_3SCH_3 to yield CH_3SSCH_3, C_2H_6 and CH_4 but in drastically reduced yields. The primary step is attack at the S site, yielding triplet state DMTSO, $CH_3\overset{S}{\underset{\cdot}{\dot{S}}}CH_3(T_1)$. DMTSO$(T_1)$ undergoes fragmentation reactions similar to those of DMTSO$(S_0)^{\dagger}$. It is proposed that the CH_3SSCH_3 product arises from isomerization of DMTSO$(S_0)^{\dagger}$ formed by intersystem crossing from the T_1 state. The smaller

yields of CH_3SSCH_3 and the greater importance of deactivation (deactivation/isomerization ∿ 14), as compared to the $S(^1D_2)$ + CH_3SCH_3 system, are attributed to the lower energy content of the $DMTSO(S_0)^\dagger$ formed from the T_1 state.

$S(^1D_2)$ atoms react with thietane, $\overline{CH_2(CH_2)_2S}$, affording a cyclic disulfide, 1,2-dithiolane, as the only retrievable S product. Comparable yields of C_2H_4 were also observed. In contrast to the $S(^1D_2)$ + CH_3SCH_3 reaction, the total product recovery is high (∿85%) and pressure independent, indicating that deactivation is relatively unimportant.

By analogy with the $S(^1D_2)$ + CH_3SCH_3 system, the primary adduct is postulated to be thietanethiosulfoxide (TTSO), 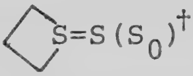 . This adduct undergoes a similar series of reactions:

1) fragmentation via C-S and C-C bond scissions to yield C_2H_4,

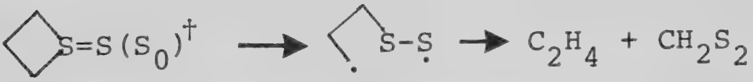

[9]

2) fragmentation via two C-S bond scissions to yield C_3H_6,

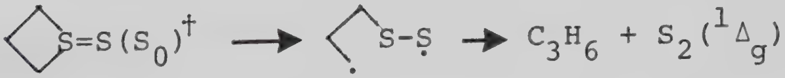

[10]

3) isomerization via C-S bond cleavage to form the disulfide,

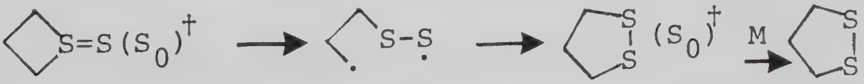

[11]

4) deactivation followed by desulfurization,

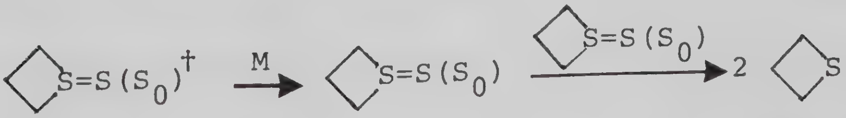

+ S_2, etc. [12]

Although step [10] could not be measured quantitatively, it appears that it is of minor importance.

$S(^3P)$ atoms also react with 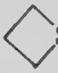S to yield 1,2-dithiolane and C_2H_4,but the yields of the latter are drastically reduced. The primary adduct is postulated to be triplet state thietane-thiosulfoxide (TTSO), 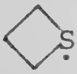$\ddot{S}$-$\ddot{S}(T_1)$. The recoveries of 1,2-dithiolane for the $S(^1D_2)$ and $S(^3P)$ reactions are comparable, 44 and 36%, respectively, in sharp contrast to those of the $S + CH_3SCH_3$ system, where the corresponding recoveries are 25 and 7%:

The relative Arrhenius parameters obtained from competitive rate studies in the presence of C_3H_6 yield the following rate expressions for the $S(^3P) + CH_3SCH_3$ and $\overline{CH_2(CH_2)_2S}$ reactions.

$$k_{CH_3SCH_3} = (3.19\pm1.21) \times 10^{10}\exp[(900\pm237)/RT]\ M^{-1}s^{-1}$$

$$k_{\overline{CH_2(CH_2)_2S}} = (5.23\pm1.94) \times 10^{10}\exp[(810\pm220)/RT]\ M^{-1}s^{-1}$$

These correspond to room temperature rate constants,

$$k_{CH_3SCH_3} = 1.4 \times 10^{11}\ M^{-1}\ s^{-1}\ \text{, and}$$

$$k_{\overline{CH_2(CH_2)_2S}} = 2.0 \times 10^{11}\ M^{-1}s^{-1}$$

which approach the collision frequencies.

Both reactions proceed with negative activation energies, in agreement with those predicted from the E_a - ionization potential correlation established for the $S(^3P)$ + alkene reactions.

The A factors for the two reactions are larger than those of the $S(^3P)$ + alkene systems by a factor of ∿4. This is a consequence of a larger collision cross section resulting from the larger van der Waal radius of the S site.

BIBLIOGRAPHY

1. Candler, C., Atomic Spectra, Hilger and Watts Ltd., London (1964).
2. Strausz. O.P., R.J. Donovan, and M. de Sorgo, Ber. Bun. Physik. Chem., 72, 253 (1968).
3. Lown, E.M., K.S. Sidhu, A.W. Jackson, A. Jodhan, M.Green, and O.P. Strausz, J. Phys. Chem., 85, 1089 (1981), and references therein.
4. Donovan, R.J., D. Hussain, R.W. Fair, O.P. Strausz and H.E. Gunning, Trans. Farad. Soc., 66, 1635 (1970).
5. Addison, M.C., C.D. Byrne and R.J. Donovan, Chem. Phys. Lett., 64,57 (1979).
6. Betteridge, D.R., and J.T. Yardly, Chem. Phys. Lett., 62, 570 (1979).
7. Sidhu, K.S., I.G. Csizmadia, O.P. Strausz, and H.E. Gunning, J.Am. Chem. Soc., 88, 2412 (1966).
8. Black, G., R.L. Sharpless, T.G. Slanger, and D.C. Lorents, J. Chem. Phys., 62, 4274 (1975).
9. Dunn, O.J., S.V. Filseth and R.A. Young, J. Chem. Phys., 59, 2892 (1973).
10. Donovan, R.J., Trans. Farad.Soc., 65, 1419 (1969).
11. Breckenridge, W.H., and H. Taube, J. Chem. Phys., 52, 1750 (1970).
12. Molina, L.T., J.J. Lamb, and M.J. Molina, Geophys. Res. Lett., 8, 1008 (1981).

13. Rudolf, R.N. and E.C.Y. Inn, J. Geophys. Res., 86, 9891 (1981).

14. Strausz, O.P., IUPAC. Suppl. 4, 165 (1971), and references therein.

15. Rao, P.M., and O.P. Strausz, to be published.

16. Gollnick, K., and E. Leppin, J. Am. Chem. Soc., 92, 2217 (1970).

17. Leppin, E., and K. Gollnick, Mol. Photochem., 2, 177 (1970).

18. Donovan, R.J., L.J. Kirsch and D. Hussain, Nature, 222, 1165 (1969).

19. Sherwood, A.G., I. Safarik, B. Verkoczy, G. Almadi, H.A. Wiebe, and O.P. Strausz, J. Am. Chem. Soc., 101,3000 (1979).

20. Addison, M.C., R.J. Donovan and C. Fotokis, Chem. Phys. Lett.,74 , 58 (1980).

21. Klemm, R.B. and D.D. Davis, J. Phys. Chem., 78, 1137 (1974).

22. Gunning, H.E. and O.P. Strausz, Adv. Photochem., 4, 143 (1966).

23. Little, D.J., A. Dalgleish and R.J. Donovan, Farad. Disc. Chem. Soc., 53, 211 (1972).

24. Donovan, R.J., L.J. Kirsch, and D. Hussain, Trans. Farad. Soc., 66, 774 (1970).

25. Lown, E.M., PhD Thesis, University of Alberta, 1966.

26. Rabalais, J.W. J.M. McDonald, V. Sherr, and S.P. McGlynn, Chem. Rev., 71, 73 (1971).

27. Filseth, F.F., Adv. Photochem., 10, 1 (1977).

28. Knight, A.R., O.P. Strausz, and H.E. Gunning, J. Am. Chem. Soc., 85, 2349 (1963).

29. Colussi, A.J., and R.J. Cvetanovic, J. Phys. Chem., 79, 1891 (1975).

30. Paraskevopoulous, G., and R.J. Cvetanovic, J. Am. Chem. Soc., 91, 7572 (1969).

31. Kajimoto, O., H. Yamasaki, and T. Fueno, Chem. Phys. Lett., 349, (1977).

32. Luntz, A.C., J.Chem. Phys., 73, 1143 (1980).

33. Schofield, K., J. Photochem., 9, 55 (1978).

34. Yamasaki, H., and R.J. Cvetanovic, J. Chem. Phys., 41, 3703 (1964).

35. Casavecchia, P., R.J. Buss., S.J. Sibener and Y.T. Lee, J. Chem. Phys., 73, 6351 (1980).

36. Lin, C.L., and W.B. De More, J. Phys. Chem. 77, 863 (1973).

37. Paraskevopoulous, G., and R.J. Cvetanovic, J. Phys, Chem., 81, 2598 (1977).

38. Andreson, P., and A.C. Luntz, J. Chem, Phys., 72, 5842 (1980).

39. Herron, J.T., R.E. Huie, J. Phys. Chem., 73,3327 (1969).

40. Herron, J.T., R.E. Huie, J. Phys. Chem. Ref. Data, 2, 467 (1973), and references therein.

41. Strausz, O.P., Sulfur Research Trends, Adv. Chem. Ser., R.F. Gould, Ed., Am. Chem. Soc., Washington, D.C. (1971).

42. Wiebe, H.A., PhD. Thesis, University of Alberta, 1967.

43. De More, J. Phys. Chem., 73, 391 (1969).

44. Kajimoto, O., H. Yamasaki, and T. Fueno, Chem. Phys. Lett., 68, 127 (1979).

45. Cvetanovic, R.J., Adv. Photochem., 1, 115 (1963).

46. Bader, R.F., M.E. Stephens, and R.A. Gangi, Can. J. Chem. 55, 2755 (1977).

47. Kajimoto, O., and H. Yamasaki, Chem. Phys. Lett., 64, 445 (1979).

48. Wiebe, H.A.,A.R. Knight, O.P. Strausz, and H.E. Gunning, J. Am. Chem. Soc., 87, 1443 (1965).

49. Sidu, K.S., E.M. Lown, O.P. Strausz, and H.E. Gunning, J. Am. Chem. Soc. 82, 259 (1966).

50. Hoffman, R., C.C. Wan, and V. Neagu, Mol. Phys., 19, 113 (1970).

51. Strausz, O.P., H.E. Gunning, A.S. Denes and I.G. Csizmadia, J. Am. Chem. Soc., 94, 8317 (1972).

52. Davis, D.D., and R.B. Klemm, Int. J. Chem. Kint., 5, 841 (1973).

53. Van Roodselaar, A., PhD. Thesis, University of Alberta, 1976.

54. Connor, J., A. Van Roodselaar, R.W. Fair and O.P. Strausz, J.Am. Chem. S0c., 93, 560 (1971).

55. Singleton, D.L., and R.J. Cvetanovic, J. Am. Chem. Soc., 98, 6812 (1976), and references therein.

56. Cvetanovic, R.J. J. Phys. Chem. 74, 2730 (1970).

57. Strausz, O.P., R.K. Gosavi, G.R. DeMare, I.G. Csizmadia, Chem. Phys. Lett., 62, 339 (1979).

58. Yamasaki, K., S. Yabushita, T. Fueno, S. Kato, and K. Morokama, Chem. Phys. Lett. 70, 27 (1980).

59. Dupuis, M., J.J. Wendoloski, T. Takada, and W.A. Lester, Jr., J. Chem. Phys., 76, 481 (1982).

60. DeMare, G.R., M.R. Peterson and I.G. Csizmadia and O.P. Strausz, J. Comp. Chem., 1, 141 (1980).

61. Strausz, O.P., R.K. Gosavi, G.R. DeMare, M.R. Peterson and I.G. Csizmadia, Chem. Phys. Lett., 70, 31 (1980).

62. Hirokami, S., and R.J. Cvetanovic, J. Am. Chem. Soc., 96, 3738 (1974).

63. Verkoczy, B., PhD Thesis, University of Alberta, 1981.

64. Dedio, E.L., PhD Thesis, University of Alberta, 1967.

65. Torres, M., E.M. Lown, O.P. Strausz, Heterocyles, 11,

66. Strausz, O.P., J. Font, E.L. Dedio, P. Kebarle, and H.E. Gunning, J. Am. Chem. Soc. 89,4805 (1967).

67. Torres, M., I. Safarik, A. Clement, J.E. Bertie, and O.P. Strausz, Nouv. J. Chim., 3, 365 (1979).

68. Krantz, A., J. Laureni, J. Am. Chem. Soc., 99, 4842 (1977).

69. Strausz, O.P., R.K. Gosavi, F. Bernardi, P.G. Mezey, J.D. Goddard, and I.G. Csizmadia, Chem. Phys. Lett., 53, 211 (1978).

70. Little, D.J., and R.J. Donovan, J. Photochem., 1, 373 (1972/3).

71. Ogi, K., and O.P. Strausz, to be published.

72. Shaub, W.M., T.L. Burks and M.C. Lin, J. Phys. Chem., 86, 757 (1982).

73. Strausz, O.P., R.K. Gosavi, A.S. Denes, and I.G. Csizmadia, J. Am. Chem., Soc., 98, 4784 (1976).

74. Strausz, O.P., R.K. Gosavi, and H.E. Gunning, Chem. Phys. Lett., 54, 510 (1978).

75. Torres, M., E.M. Lown, H.E. Gunning, and O.P. Strausz, Pure & Appl. Chem., 52, 1623 (1980),and references therein.

76. Van Roodselaar, A., I. Safarik, O.P. Strausz, and H.E. Gunning, J. Am. Chem. Soc., 100,4048 (1978).

77. Avery, H.E., and S.J. Heath, Trans Farad. Soc., 68,512, (1972).

78. Blumenberg, B., K. Hoyermann, and R. Sievert,16th. Symp. on Combustion, P.841, The Combustion Institute, Pittsburg (1977).

79. Brown, J.M. and B.A. Thrush, Trans. Farad. Soc., 63,630 (1967).

80. Shaub, W.N., T.L. Burks, and M.C.Lin, Chem. Phys., 45, 455 (1980).

81. Stiles, D.A., W.J.R. Tyerman, O.P. Strausz, and H.E. Gunning, Can. J. Chem., 44, 2149 (1966).

82. Tyerman, W.J.R., W.B. O'Callaghan, P. Kebarle, O.P. Strausz, and H.E. Gunning, J. Am. Chem. Soc., 88, 4277(1966).

83. Callear, A.B., and W.J.R. Tyerman, Trans. Farad. Soc., 62, 371 and 2760 (1966).

84. Connor, J., G. Greig, and O.P. Strausz, J. Am. Chem. Soc., 91, 5695 (1969).

85. Strausz, O.P., private communication.

86. (a) Boocock, G.,and R.J. Cvetanovic., Can. J. Chem., 39, 2436 (1961).

(b) Jones, G.R.H., and R.J. Cvetanovic, ibid, 2444 (1961).

87. Grobenstein, E., Jr., and A.J. Mosher, J. Am. Chem. Soc., 92, 3810 (1970).

88. Gaffney, J.S., R. Atkinson, and J.N. Pitts, Jr., J. Am. Chem. Soc., 98, 1828 (1976).

89. Nicovich, J.M., C.A. Gump, and A.R. Ravishankara, J. Phys. Chem., 86, 1684 and 1690 (1982).

90. Atkinson, R., and J.N. Pitts, Jr., J. Phys. Chem., 79, 295 (1975).

91. Colussi, A.J., D.L. Singleton, R.S. Irwin, and R.J. Cvetanovic, J. Phys. Chem., 79, 1900 (1975).

92. Atkinson, R., and J.N. Pitts, Jr., Chem. Phys. Lett., 63, 485 (1979).

93. Lee, J.H., and I.N. Tang, J. Chem. Phys., 75, 137 (1981), and references therein.

94. Gaffney, J.S., R. Atkinson, and J.N. Pitts, Jr., J. Am. Chem. Soc., 97, 6481 (1975).

95 Sidhu, K.S., E.M. Lown, O.P. Strausz, and H.E. Gunning, J. Am. Chem. Soc., 88, 254 (1966).

96. Strausz, O.P., W.B. O'Callaghan, E.M. Lown, and H.E. Gunning, J. Am. Chem. Soc., 93, 559 (1971).

97. Davis, D.D., R.B. Klemm, W. Braun, and M. Pilling, Int. J. Chem. Kinet., 4, 383 (1972).

98. Cvetanovic, R.J., and L.C. Doyle, Can. J. Chem., 38, 2187 (1960).

99. Havel, J.T., and K.H. Chan, J. Org. Chem., 39, 2439 (1974).

100. Atkison, R., and J.N. Pitts, Jr., Chem. Phys., 67, 2492 (1977).

101. Nip, W.S., D.L. Singleton, and R.J. Cvetanovic, Can. J. Chem., 57, 949 (1979).

102. Nakamura, K., and S. Koda, Int. J. Chem. Kinet., 9, 67 (1977).

103. Havel, J.J., J. Am. Chem. Soc., 96, 530 (1974).

104. Lin, M.C., R.G. Shortridge, and M.E. Umstead, Chem. Phys. Lett., 37, 279 (1976).

105. Herbrechtsmeier, P., and H.G. Wagner, Ber. Buns. Phys. Chem., 76, 517 (1972).

106. Jones, P.R., and H. Taube, J. Phys. Chem., 77, 1007 (1973).

107. Kriiger, B., and H.G. Wagner, Z. Phys. Chem., 126,1 (1981).

108. Wei, C-N., R.B. Timmons, J. Chem. Phys., 62, 3240 (1975).

109. Krezenski, D.C., R. Simonaites, and J. Heiklein, Int. J. Chem. Kinet., 3, 467 (1971).

110. Westenberg, A.A., and N. de Haas, J. Chem. Phys., 50, 707 (1969).

111. O'Callaghan, W.B., PhD. Thesis, University of Alberta, 1970.

112. Klemm, R.B., and D.D. Davis, Int. J. Chem. Kinet., 5, 149 (1973).

113. Lee, J.H., R.B. Timmons, and L.J. Stief, J. Chem. Phys., 64, 303 (1976).

114. Singleton, D.L. "Comparison of the O(^{3}P) + trimethylenesulfide reaction with the photolysis of trimethylenesulfoxide", presented at the 15th Informal Conference on Photochem., Standford, Ca., U.S.A. June 27-July 1, 1982.

115. Slagle, I.R., and D. Gutman, Int. J. Chem. Kinet., 11, 453 (1979).

116. Slagle, I.R., R.E. Graham, and D. Gutman, Int. J. Chem. Kinet., 8, 451 (1976).

117. Cvetanovic, R.J., D.L. Singleton, and R.S. Irwin, J. Am. Chem. Soc., 103, 3530 (1981).

118. Tevault, D.E., R.L. Mowey, and R.R. Smardzewski, J. Chem. Phys., 74, 4480 (1981).

119. Slagle, I.R., F. Baiocchi, and D. Gutman, J. Phys. Chem., 82, 1333 (1978).

120. Lee, J.H., I.N. Tang, and R.B. Klemm, J. Chem. Phys., 72, 1793 (1980).

121. Nip, W.S., D.L. Singleton, and R.J. Cvetanovic, J. Am. Chem. Soc., 103, 3526 (1981).

122. Lee, J.H., I.N. Tang, and R.B. Klemm, J. Chem. Phys., 72, 1793 (1980).

123. McNair, H.M., and E.J. Bonelli, "Basic Gas Chromatography", 5th Ed., Varian, Pallo Alto, 1969.

124. Pascual, C., J. Meier, and W. Simon, Helv. Chim. Acta., Suppl., 49, 164 (1966).

125. Bellamy, L.J., "The Infra-red Spectra of Complex Molecules", pp. 50-54, Vol. 1, 3rd Ed., Chapman and Hall, London, 1975.

126. Charles, R., V. Beltler, B. Feibush and E. Gil-Av , J. Chromatog., 112, 121 (1975).

127. Bothner-By, A.A., and R.K. Harris, J. Am. Chem. Soc., 87, 3445 (1965).

128. Block, E., R.E. Penn, M.D. Emris, T.A. Owens, S-L. Yu, J. Am. Chem. Soc., 100, 7436 (1978).

129. Noggle, J.H., R.E. Shrimer, "The Nuclear Overhauser Effect", Ch. 1, 2 & 3, Acad. Press, N.Y. 1971.

130. Taylor, D.R., Chem. Rev., 67, 317 (1967).

131. Lipcomb, R.D., and W.H. Sharkey, J. Polymer. Sci., A-1, 8, 2187 (1970).

132. Steacy, F.W., and J.F. Harris, J. Am. Chem. Soc., 85, 963 (1963).

133. Paquer, D., Int. J. Sulfur Chem., B, 7, 269 (1972).

134. Mayer, R. in "Sulfur in Organic and Inorganic Chemistry". Vol. 3, Ed. A. Senning, Dekker, N.Y. (1972).

135. Baily, W.J. and M. Isogawa, A.C.S. Polymer Chem., Poly. Prep., 14, 300 (1973).

136. Beslin, P., D. Lagain, and J. Vialle, Tet. Lett., 2677 (19790.

137. Wan, C.S.K., and A.C. Weedon, J. Chem. Soc., Chem. Comm., 1235 (1981).

138. Giles, H.G., R.A. Marty and P. de Mayo, Can. J. Chem., 54, 547 (1976).

139. Jongejan, E., Th.S.V. Buys, H. Steinberg, and Th.J. de Boer, J. Royal Nerther. Chem. Soc., 97, 214 (1978).

140. Runge, W., W. Kosbahn, and J. Kroner, Ber. Bun. Phys. Chem., 79, 371 (1979).

141. Zandler, M.E., C.E. Choc, and C.K. Johnson, J. Am. Chem. Soc., 96, 3317 (1974).

142. Laufer, A.H., Rev. Chem. Interm., 4, 225 (1981).

143. Stang, P.J., "The Chemistry of Functional Groups". Suppl. E, Part II, Ed. S. Patai, Wiley, N.Y., 1980.

144. Creary, X., J. Org. Chem., 43, 1777 (1978).

145. Creary, X., J. Am. Chem. Soc., 102, 1611 (1980).

146. Nelson, H.H., L. Pasternack, J.R. Eyler, and J.R. McDonald, Chem. Phys., 60, 231 (1981).

147. Atkinson, R., K.R. Darnall, A.C. Lloyd, A.M. Winer, and J.N. Pitts, Jr., Adv. Photochem., 11, 375 (1979), and references therein.

148. Hoyermann, K., R. Sievert, and H.G. Wagner, Oxid. Comm., 1, 145 (1980).

149. Atkinson, R., R.A. Perry, and J.N. Pitts, Jr., J. Chem. Phys., 67, 3170 (1977).

150. Bradley, J.N., W. Hack, K. Hoyermann, and H.G. Wagner, J.C.S. Farad. Trans., 69, 1889 (1973).

151. Slagle, I.R., J.R. Gilbert, R.E. Graham, and D. Gutman, Int. J. Chem. Kinet. Symp., 1, 317 (1975).

152. Jacobs, T.L., and G.E. Illingworth, J. Org. Chem., 28, 2692 (1963).

153. Caserio, M.J., in "Selective Organic Transformations", Ed. B.S. Thyagarajam, Wiley, N.Y., 1970.

154. Owen. G.E., J.M. Pearson and M. Szwarc, Trans. Farad.Soc., 61, 1722 (1965).

155. Chamberlain, N.F., "The Practice of NMR Spectroscopy", pp. 90, Plenum. N.Y., 1974.

156. Vasil'eva, T.P., M.G. Lin'kova and O.V. Kil'disheva, Russian Chem. Rev., 45, 639(1976),and references therein.

157. Barltrop, J.A., P.M. Hayes and M. Calvin, J. Am. Chem. Soc., 76, 4348 (1954).

158. Krespan, C., and B. McKurick, J. Am. Chem. Soc., 50, 844 (1966).

159. Wallace, T.J., and H.A. Weiss, Chem. and Ind., 1558 (1966).

160. Barnard, D., T.H. Houseman, M. Porter, and B.K. Tidd, Chem. Comm. 371 (1969).

161. Hofle, G., and J.E. Baldwin, J. Am. Soc., 92, 6307 (1971).

162. Baechler, R.D., J.P. Hummel, K. Mislow, J. Am. Chem. Soc., 95, 4442 (1973).

163. Still, I.W.J., S.K. Hasan and K. Turnbull, Can. J. Chem., 56, 1423 (1978).

164. Baechler, R.D., S.K. Daley, B. Daly and K. McGlynn, Tet. Lett., 105 (1978).

165. Baechler, R.D., L.J. San Fillippo and A. Schroll, Tet. Lett., 22, 5247 (1981).

166. Stepanov, B.I., V.Ya. Rodionov, and T.A. Chibisova, Z. Org. Khim. 10, 78 (1973).

167. Harpp, D.N., and K. Steliou, J.C.S. Chem. Comm., 825, (1980).

168. Benson, S.W., Chem. Rev., 78, 23 (1978).

169. Benson, S.W., "Thermochemical Kinetics", 2nd Ed., Wiley, N.Y., 1976.

170. Kende, I., T.L. Pickering, and A.V. Tobolsky, J. Am. Soc., 87, 5582 (1965).

171. Strausz, O.P., R.J. Donovan and M. de Sorgo, Ber. Bun. Phys. Chem. 72, 253 (1968).

172. Senning, A., Agnew. Chem. Int. Ed., 18, 941 (1979).

173. Rao, P.M., J.A. Copeck, and A.R. Knight, 45, 1369 (1967).

174. Niki, H., P.D. Maker, C.M. Savage, and L.P. Breitenbach, J. Am. Chem. Soc., 85, 877 (1981).

175. Arthur, N.L., and M-S. Lee, Aust. J. Chem., 29, 1483 (1976).

176. Jakubowski, E., M.G. Ahmed, E.M. Lown, H.S. Sandhu, R.K. Gosavi and O.P. Strausz, J. Am. Chem. Soc., 94, 4094 (1972).

177. Rao, P.M., and A.R. Knight, Can. J. Chem., 50, 844 (1972).

178. Ekwenchi, M.M., PhD. Thesis, University of Alberta, 1980.

179. Vitins, P., PhD. Thesis, University of Alberta, 1973.

180. Dorer, F.H., K.E. Salomon, J. Phys. Chem., 84, 3024 (1980).

181. Bak, B., O.J. Nielsen, and H. Svanholt, J. Molec. Spec., 69, 401 (1978).

182. Brasklavsky, S., and J. Heiklein, Chem. Rev., 77,473 (1977).

183. Krespan, C.G., and W.R. Brasen, J. Org. Chem., 27, 3995 (1962).

184. Block, E., A.A. Bazzi, L.K. Reville, J. Am. Chem. Soc., 102, 2490 (1980).

185. Yokota, T., and O.P. Strausz, J. Phys. Chem., 83, 3196 (1979).

186. Yokota, T., M.G. Ahmed, I. Safarik, O.P. Strausz and H.E. Gunning, J. Phys. Chem., 79, 1758 (1975).

187. Horie, O., K. Onuki and A. Amano, J. Phys. Chem., 81, 1706 (1977).

188. Horie, O., J. Nishino, and A. Amano, J. Org. Chem., 43, 2800 (1978).

189. Skell, P.S., K.J. Klabunde, J.H. Plonka, J.S. Roberts and D.L. William-Smith, J. Am. Chem. Soc., 95, 1547 (1973).

190. Chapman, J.S., J.W. Cooper, and B.P. Roberts, J.C.S. Chem. Comm., 407 (1976), and references therein.

191. Apptelon, D.C., D.C. Bull, J. McKenna, J.M. McKenna and A.R. Wally, J.C.S. Perkin II, 358 (1980).

192. Davis, D.D, R.E. Huie and J.T. Herron, J. Chem Phys., 59, 628 (1973).

193. Lee, J.H., R.C. Machen, D.F. Nava and L.J. Stief, J. Chem. Phys., 74, 2839 (1981).

194. Atkinson, R., R.A. Perry, and J.N. Pitts Jr., Chem. Phys. Lett., 54, 14 (1978).

195. Wine, P.H., N.M. Kreutter, C.A. Gump and A.R. Ravishankara, J. Am. Chem. Soc., 85, 2660 (1981).

196. Kurylo, M.J., Chem. Phys. Lett., 58, 233 (1978).

APPENDIX A-1

Mass Spectral Data of the C_4H_6S Isomers

m/e	Relative Intensity						
	1	**2**	**3**	**4**	**5**	**6**	**7**
86	66.3	100	70.3	71.6	83.7	100	61.8
85	19.6	12.5	23.4	22.9	45.3	18.4	100
71	100	83.1	100	100	100	78.4	19.8
69	5.9	7.6	6.5	6.3	2.7	11.7	7.4
59	14.7	44.6	19.8	15.4	16.1	49.8	10.5
58	26.3	16.8	26.4	24.9	12.4	17.7	6.5
53	14.3	22.3	17.2	15.4	67.2	48.8	65.9
52	4.1	6.0	6.6	3.6	20.3	13.6	14.1
51	9.3	12.5	14.3	9.0	33.6	23.9	23.1
50	9.0	12.2	12.6	8.8	28.4	19.3	19.5
49	2.6	3.7	3.9	2.6	8.0	5.0	6.3
47	3.9	3.6	5.8	4.8	33.0	6.6	2.8
46	10.0	4.8	15.8	17.4	10.8	9.2	3.8
45	33.3	31.5	41.4	37.3	47.6	41.2	33.5
39	12.9	13.0	21.6	15.5	20.3	66.0	15.2

APPENDIX A-2

Mass Spectral Data for $C_3H_6S_2$

m/e	Relative Intensity	m/e	Relative Intensity
106	100	47	5.7
78	26.2	46	7.0
73	6.9	45	28.6
64	39.9	42	10.8
60	8.2	41	89.1
59	10.5	39	17.3

APPENDIX B

Calculations of the Nuclear Overhauser Effect (nOe) for cis and trans Ethylidenethiirane.

The nuclear Overhauser effect (nOe) is a change in the nuclear magnetic resonance (NMR) signal intensity of a nuclear spin when the NMR absorption signal of another spin is saturated by irradiation of the sample at the resonant frequency of the second spin. There will be no effect unless the two spins contribute to each other's magnetic relaxation.

The nOe of proton d in a molecule when proton(s) s in the same molecule are saturated is given by [1][129]:

$$f_d(s) = [\sum_s \rho_{ds}]/2R_d - [\sum_n \rho_{dn} f_n(s)]/2R_d \qquad [1]$$

where n = All spins other than s and d in the same molecule, including those which are magnetically equivalent to d.

ρ_{ds} = the direct dipole - dipole relaxation between spins s and d.

ρ_{dn} = the direct dipole - dipole relaxation between spins n and d.

R_d = the direct relaxation rate for d.

For *cis* and *trans* Ethylidenethiirane:

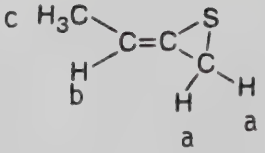

cis

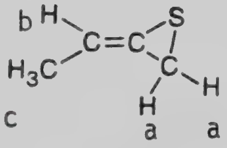

trans

equation [1] may be used to derive six equations relating the six possible nOe's, which can be rearranged to give:

$$f_a(b) = \frac{(1/2)\rho_{ab}R_{cc} - (3/4)\rho_{ac}\rho_{cb}}{R_{aa}R_{cc} - (3/2)\rho_{ca}\rho_{ac}} \qquad [2]$$

$$f_a(c) = \frac{(3/2)\rho_{ac}R_b - (3/4)\rho_{ab}\rho_{bc}}{R_{aa}R_b - (1/2)\rho_{ab}\rho_{ba}} \qquad [3]$$

$$f_c(a) = \frac{\rho_{ca}R_b - (1/2)\rho_{ba}\rho_{cb}}{R_{cc}R_b - (3/4)\rho_{bc}\rho_{cb}} \qquad [4]$$

$$f_c(b) = \frac{(1/2)\rho_{cb}R_{aa} - (1/2)\rho_{ab}\rho_{ca}}{R_{cc}R_{aa} - (3/2)\rho_{ac}\rho_{ca}} \qquad [5]$$

$$f_b(a) = \frac{\rho_{ba}R_{cc} - (3/4)\rho_{ac}\rho_{bc}}{R_bR_{cc} - (3/4)\rho_{bc}\rho_{cb}} \qquad [6]$$

$$f_b(c) = \frac{(3/2)\rho_{bc}R_{aa} - (3/2)\rho_{ac}\rho_{ba}}{R_{aa}R_b - (1/2)\rho_{ab}\rho_{ba}} \qquad [7]$$

R_{aa}, R_b and R_{cc} are the rates of relaxation of the a, b, and c protons. Assuming intramolecular dipolar relaxation is the only relaxation mechanism,

$$R_{aa} = R_a + \rho_{aa}/2 = 3\rho_{ac} + (3/2)\rho_{aa} + \rho_{ab} \qquad [8]$$

$$R_b = 2\rho_{ba} + 3\rho_{bc} \qquad [9]$$

$$R_{cc} = R_c + \rho_{cc} = 2\rho_{ca} + \rho_{cb} + 3\rho_{cc} \qquad [10]$$

For dipolar relaxation between two protons, i and j, $\rho_{ij} = \rho_{ji}$, and

$$\rho_{ij} = (\gamma^4 \hbar^2 T_c)/(r_{ij})^6 \qquad [11]$$

where r_{ij} = proton-proton distance.

T_c = correlation time for the i - j interaction.

If T_c is indentical for all protons in the molecule, then

$$\rho_{ij} \; \alpha \; (1/r_{ij})^6 \qquad [12]$$

Thus, if the geometry of the molecule is known, the relative ρ's may be calculated. The ρ's can then be used to predict the nOe's.

Proton - proton distances in *cis* and *trans* ethylidenethiirane were calculated using the structural parameters for methylenethiirane[128] and literature values for the parameters of the CH_3 group. For the methyl group, which is free to rotate, distances of closest approach were calculated.

The interproton distances for the two isomers are tabulated below, along with the calculated relative ρ's, normalized to ρ_{bc}.

Protons	Interproton Distance (Å)		ρ/ρ_{bc}	
	cis	*trans*	*cis*	*trans*
c,c	1.79	1.79	6.24	6.24
a,a	1.84	1.84	5.25	5.25
a,b	3.88	4.27	0.060	0.034
a,c	4.83	2.80	0.016	0.43
b,c	2.43	2.43	1.00	1.00

Using the calculated relative ρ's and equations [2] - [10], the expected nOe's may be calculated for both isomers.

nOe	Proton(s) saturated	Proton(s) observed	Calculated nOe values	
			cis	trans
$f_a(b)$	CH	CH_2	0.004	0.0001
$f_a(c)$	CH_3	CH_2	0.001	0.069
$f_b(a)$	CH_2	CH	0.019	0.006
$f_b(c)$	CH_3	CH	0.481	0.488
$f_c(a)$	CH_2	CH_3	0.0003	0.047
$f_c(b)$	CH	CH_3	0.023	0.024

It should be emphasized that several assumptions have been made in the above calculations, and so the observed nOe's may differ from the calculated ones. Several factors may affect the observed nOe[129]:

a) Any relaxation caused by species outside the molecule will will increase the total relaxation rate of each proton and so decrease the nOe's observed.

b) The $-CH_3$ group of ethylidenethiirane may spin relativly fast, resulting in shorter T_c's (correlation time) for interactions involving the methyl protons.

c) The rapid spinning of the methyl group may also cause spin rotation relaxation of the $-CH_3$ protons, decreasing the nOe's observed for these protons.

APPENDIX C-1

Estimation of the Ratios, $k_{2,3}/k_{1,2}$ at t=0, P=1200 torr and 250 torr, and trans (4)/cis (3) at t=0, P=1200 torr for $S(^1D_2)$ Addition to $1,2-C_4H_6$

In the photolysis of the COS-$1,2-C_4H_6$ system, the principal reactions are as follows:

$$COS + h\nu \longrightarrow CO + S(^1D_2, ^3P) \qquad [1]$$

$$S(^1D_2) + COS \longrightarrow CO + S_2 \qquad [2]$$

$$S(^1D_2) + M \longrightarrow S(^3P) + M \qquad [3]$$

$$S(^3P) + COS \longrightarrow CO + S_2 \qquad [4]$$

$$S(^1D_2, ^3P) + 1,2-C_4H_6 \longrightarrow \text{Products} \qquad [5]$$

(A) $(k_{2,3}/k_{1,2})^{^1D}_{t=0}$ and $(\text{trans}/\text{cis})^{^1D}_{t=0}$ at P = 1200 torr.

(i) Amount of $S(^3P)$ reacted with $1,2-C_4H_6$:

At 750 torr (Table III-3), the total S atoms ($^1D_2$ and ^3P) produced is:

$$(R^\circ_{CO} \times 8.3)/2 = 4.25 \ \mu\text{moles}$$

Assume equal conversions at P = 1200 and 750 torr, i.e. 4.25 μmoles $S(^1D_2, ^3P)$ atoms and 5.4 μmoles CO are produced.

Since the $S(^1D_2)$ to $S(^3P)$ ratio is ∿ 67:33 in the primary step[19], at P = 1200 torr, the primary yields of $S(^1D_2)$ and $S(^3P)$ atoms are:

$$S(^1D) = 0.67 \times 4.25 = 2.85 \ \mu\text{moles}$$

$$S(^3P) = 0.33 \times 4.25 = 1.40 \ \mu\text{moles}$$

In the present system, $(k_{S(^3P)+1,2-C_4H_6}/k_{S(^3P)+COS}) > 10^3$. Thus at the COS/$1,2-C_4H_6$ ratio of 4/1 used in the pressure

study (Table III-3), the reaction of $S(^3P)$ with COS is insignificant. Therefore, the amount of $S(^1D_2)$ atoms which reacted with COS is:

$$CO - CO°/2 = 1.15\ \mu\text{moles}$$

For the $S(^1D_2)$ + COS reaction, $k_2/k_3 \sim 2$ [19]. It follows that the amount of $S(^1D_2)$ collisionally deactivated to $S(^3P)$ is:

$$1.15\ \mu\text{moles}/2 = 0.575\ \mu\text{moles.}$$

Therefore, the total amount of $S(^3P)$ atoms which reacted with $1,2\text{-}C_4H_6$ is:

$$0.575 + 1.40 = 1.975\ \mu\text{moles.}$$

(ii) $S(^3P)$ products ($\underset{\sim}{1}$,$\underset{\sim}{3}$, and $\underset{\sim}{4}$) recovered at t=0:

Let $(P)^{^3P}$ = amounts of $S(^3P)$ products recovered, and
$(F)^{^3P}$, $(F)^{^1D,^3P}$ = fraction of $S(^3P)$ and $S(^1D_2, {}^3P)$ products recovered, respectively.

Then,

$$(P)^{^3P}_{t=0} = 1.975 \times (F)^{^3P}_{t=0} \qquad [6]$$

Assuming $(F)^{^3P}_{t=0,P=1200\text{ torr}} = (F)^{^1D,^3P}_{t=0,p=1200\text{ torr}}$

$$= \left. \frac{R^{^1D,^3P}(\underset{\sim}{1}+\underset{\sim}{2}+\underset{\sim}{3}+\underset{\sim}{4}+\underset{\sim}{5})}{R^{^1D,^3P}(S+1,2\text{-}C_4H_6)} \right|_{\substack{t=0\\ P=1200\text{ torr}}} \qquad [7]$$

where R = rate

Extrapolation of the zero time thiirane rates in Figure III-15 to P = 1200 torr yields:

$$R^{{}^1D,{}^3P}(\underset{\sim}{1})_{t=o} = 0.290 \ \mu\text{mole}/\mu\text{mole CO}$$

$$R^{{}^1D,{}^3P}(\underset{\sim}{3})_{t=0} = 0.042 \quad '' \quad ''$$

$$R^{{}^1D,{}^3P}(\underset{\sim}{4})_{t=0} = 0.123 \quad '' \quad ''$$

From Table III-3:

$R^{{}^1D}(\underset{\sim}{2}) = 0.014$, and $R^{{}^1D}(\underset{\sim}{5}) = 0.015$ μmole/μmole CO are time and pressure independent (Figs.III-14 and III-15). Thus,

$$R^{{}^1D,{}^3P}(\underset{\sim}{1}+\underset{\sim}{2}+\underset{\sim}{3}+\underset{\sim}{4}+\underset{\sim}{5})_{\substack{t=0,\\ p=1200 \text{ torr}}} = 0.290+0.014+0.043+0.123+0.015$$

$$= 0.485 \ \mu\text{mole}/\mu\text{mole CO} \qquad [8]$$

Expressing eqn. [8] in units of μmole/min:

$$R^{{}^1D,{}^3P}(\underset{\sim}{1}+\underset{\sim}{2}+\underset{\sim}{3}+\underset{\sim}{4}+\underset{\sim}{5})_{\substack{t=0,\\ P=1200 \text{ torr}}} = \frac{0.485 \ \mu\text{mole}}{\mu\text{mole CO} \times (\text{min}/\mu\text{mole CO})}$$

$$= 0.485 \ R_{CO} \qquad [9]$$

Since all S atoms produced react with either COS or 1,2-C_4H_6, the rate of S atom reaction with 1,2-C_4H_6 is:

$$R^{{}^1D,{}^3P}(S + 1,2\text{-}C_4H_6) = R^{\circ}_{CO} - R_{CO} \qquad [10]$$

In order to express eqn. [10] in terms of R_{CO}, R°_{CO}/R_{CO} is obtained by averaging R°_{CO}/R_{CO} values from Table III-3, which gives,

$$R^{\circ}_{CO}/R_{CO} = 1.60 \text{ or } R^{\circ}_{CO} = 1.60 \ R_{CO} \qquad [11]$$

Substitute [11] into [10] to obtain:

$$R^{^1D,^3P}(S + 1,2\text{-}C_4H_6) = 0.60\ R_{CO} \qquad [12]$$

Substitute [9] and [12] into [7] to obtain:

$$(F)^{^3P}_{t=0,p=1200\ \text{torr}} = \frac{0.485\ R_{CO}}{0.60\ R_{CO}} = 0.81 \quad \text{or } 81\%$$

Substitute this value into [6] to obtain:

$$(P)^{^3P}_{t=0,P=1200\ \text{torr}} = 1.975 \times 0.81 = 1.60\ \mu\text{moles} \qquad [13]$$

(iii) Amounts of $\underset{\sim}{1}$ and $(\underset{\sim}{3}+\underset{\sim}{4})$ formed at P = 1200 torr, t = 0:

Using extrapolated $R^{^1D,^3P}(\underset{\sim}{1})$, $R^{^1D,^3P}(\underset{\sim}{3})$ and $R^{^1D,^3P}(\underset{\sim}{4})$ values at 1200 torr (Figure III-15),

$$(\underset{\sim}{1})^{^1D,^3P}_{t=0} = R^{^1D,^3P}(\underset{\sim}{1})_{t=0} \times CO = 0.290 \times 5.4$$
$$= 1.566\ \mu\text{moles} \qquad [14]$$

$$(\underset{\sim}{3}+\underset{\sim}{4})^{^1D,^3P}_{t=0} = R^{^1D,^3P}(\underset{\sim}{1})_{t=0} \times CO = (0{,}042 + 0.123) \times 5.4$$
$$= 0.891\ \mu\text{moles} \qquad [15]$$

(iv) Amounts of $\underset{\sim}{1}$, $\underset{\sim}{3}$ and $\underset{\sim}{4}$ formed from $S(^1D_2)$ at P = 1200 torr and t = 0:

$$(\underset{\sim}{1})^{^1D,^3P} = (\underset{\sim}{1})^{^1D} + (\underset{\sim}{1})^{^3P} \qquad [16]$$

$$(\underset{\sim}{3}+\underset{\sim}{4})^{^1D,^3P} = (\underset{\sim}{3}+\underset{\sim}{4})^{^1D} + (\underset{\sim}{3}+\underset{\sim}{4})^{^3P} \qquad [17]$$

Using [13] and corrected time zero values from Table III-4,

$$(\underset{\sim}{1})^{^3P} = (P)^{^3P} \times (\underset{\sim}{1}/(\underset{\sim}{3}+\underset{\sim}{4}))^{^3P}$$
$$= 1.60 \times 1.041/(1.041+0.07+0.436) = 1.077\ \mu\text{moles.} \qquad [18]$$

Substitute [14] and [18] into [16] to obtain:

$$(\underset{\sim}{1})^{^1D}_{t=0} = 1.566 - 1.077 = 0.489\ \mu\text{mole.} \qquad [19]$$

Similarly,

$$\begin{aligned}(\underset{\sim}{3}+\underset{\sim}{4})^{^3P} &= (P)^{^3P} \times ((\underset{\sim}{3}+\underset{\sim}{4})/(\underset{\sim}{1}+\underset{\sim}{3}+\underset{\sim}{4}))^{^3P} \\ &= 1.60 \times (0.07+0.436)/(1.041+0.07+0.436) = 0.523\ \mu\text{mole} \qquad [20]\end{aligned}$$

Substitute [15] and [20] into [17] to obtain:

$$(\underset{\sim}{3}+\underset{\sim}{4})^{^1D} = 0.891 - 0.523 = 0.368\ \mu\text{mole.} \qquad [21]$$

Therefore,

$$\begin{aligned}(k_{2,3}/k_{1,2})^{^1D}_{t=0,P=1200\text{ torr}} &= (\underset{\sim}{1}/(\underset{\sim}{3}+\underset{\sim}{4}))^{^1D}_{t=0,P=1200\text{ torr.}} \\ &= 0.489/0.368 = \underline{\underline{1.33}}\end{aligned}$$

Using similar procedures, the amounts of $\underset{\sim}{3}$ and $\underset{\sim}{4}$ may be determined and the *trans*/*cis* product ratio at t = 0, and P = 1200 torr is calculated to be,

$$(\underline{\text{trans}}/\underline{\text{cis}})^{^1D} = \underline{\underline{1.4}}$$

B. Evaluation of $(k_{2,3}/k_{1,2})^{^1D}_{t=0,P=250\text{ torr.}}$:

Using zero time data from Tables III-2 and III-4, Figure III-14 and the following assumptions, this value may be calculated.

(i) $(F)^{^3P}_{t=0} = (F)^{^1D}_{t=0} = (F)^{^1D,^3P}_{t=0}$, where $(F)^{^1D,^3P}_{t=0} = 0.62$ (62 %) is obtained from extrapolation of a recovery *versus* time plot.

(ii) the time dependence of $(F)^{^3P}$ is pressure independent.

(iii) the ratio, $(\underset{\sim}{1}/(\underset{\sim}{3}+\underset{\sim}{4}))^{^3P}$ is pressure independent.

Calculations similar to those laid out in Section A give,

$$(k_{2,3}/k_{1,2})^{^1D}_{t=0,P=250\ \text{torr}} = 1.39 \sim \underline{\underline{1.4}}\ .$$

In order to calculate the $(\underline{\text{trans}}/\underline{\text{cis}})^{^1D}_{t=0,P=250\ \text{torr}}$ ratio, it is neccessary to assume $R(\underset{\sim}{1})^{^3P} : R(\underset{\sim}{3})^{^3P} : R(\underset{\sim}{4})^{^3P}$ is pressure independent. However, examination of Figure III-15 reveals that $R(\underset{\sim}{3})^{^1D,\,^3P}$ and $R(\underset{\sim}{4})^{^1D,\,^3P}$ exhibit different pressure dependences. Therefore, the required assumption appears to be invalid, and no attempt was made to calculate the $(\underline{\text{trans}}/\underline{\text{cis}})^{^1D}_{t=0,P=250\ \text{torr}}$ ratio.

APPENDIX C-2

Estimation of the % Recovery of Disulfides and the Deactivation/Isomerization Ratio for $S(^1D_2)$ and $S(^3P)$ Addition to CH_3SCH_3 and $\overline{CH_2(CH_2)_2S}$

(I) The $S(^1D_2, {}^3P) + CH_3SCH_3$ System.

A) Determination of $F = R^1_{add.}/R^1_{abst.}$, the ratio of addition and abstraction for $S(^1D_2)$ atoms.

When COS is photolyzed in the presence of CH_3SCH_3, the only species reacting with COS is $S(^1D_2)$, hence the measured CO yield:

$$CO = \text{total S atoms produced } (CO°/2) + R^1_{abst.} \qquad [1]$$

where $R^1_{abst.}$ is the CO produced by abstraction (CO - CO°/2). Since the ratio of abstraction to deactivation for the $S(^1D_2)$ + COS reaction is ∿ 2,[19] the amount of $S(^1D_2)$ atoms deactivated by COS is (CO -CO°/2)/2.

Assuming that 67% of the S atoms produced in the primary step are in the $^1D_2$ state,[19] the amount of $S(^1D_2)$ atoms reacting with CH_3SCH_3 is given by:

$$\begin{aligned} R^1_{add.} &= 0.67 \times \text{total S atoms produced} - R^1_{abst.} - R^1_{deact.} \\ &= 0.67 \times CO°/2 - (CO - CO°/2) - (CO - CO°/2)/2 \qquad [2] \end{aligned}$$

In order to effect the calculations, data from three mixtures having a constant COS/CH_3SCH_3 ratio (10/1) are used. Thus F in the pressure independent region (P>300 torr) should be the same for these mixtures. Using the data from the 30

minute photolysis of the mixture $COS/CH_3SCH_3 = 300/30$ (Table IV-2), F may be determined as follows:

$CO = 13.4$ μmole

$CO° = 30 \times R^{\circ}_{CO} = 30 \times 0.771 = 21.33$ μmoles

= 2 x total S atoms produced.

Substitution of this value into equations [1] and [2] gives:

$R^{1}_{abst.} = CO - CO°/2 = 13.4 - 21.33/2 = 2.74$ μmoles.

$R^{1}_{add.} = 0.67 \times 21.33/2 - 2.74 - 2.74/2 = 3.04$ μmoles.

There, $(F)^{1} = R^{1}_{add.}/R^{1}_{abst.} = 3.03/2.74 = \underline{1.108}$ [3]

B) Recoveries of CH_3SSCH_3 from $S(^1D_2)$ and $S(^3P)$ atom reactions.

Assuming that the % recoveries of CH_3SCH_3 from the $S(^1D_2)$ and $S(^3P)$ reactions are pressure independent above 300 torr (Figure IV-3 and Table IV-3), these values can be calculated as follows for the three mixtures chosen:

(i) for the 30 minute photolysis of the $COS/CH_3SCH_3/CO_2 = 100/10/1300$ torr mixture,

$CO = 8.94$ μmole and $CO° = 30 \times R^{\circ}_{CO} = 30 \times 0.58 = 17.4$ μmoles.

Since for $CO_2/COS \leqslant 13$, $S(^1D_2)$ atoms are not completely quenched, the extent of participation of $S(^1D_2)$ atoms in abstraction and addition must be determined. Using eqn.[1],

$R^{1}_{abst.} = CO - CO°/2 = 8.94 - 17.4/2 = 0.24$ μmole.

Using eqn.[3],

$R^{1}_{add.} = R^{1}_{abst.} \times 1.108 = 0.24 \times 1.108 = 0.266$ μmole. [4]

Thus $R^3_{add.}$ = total S atoms produced - $R^1_{abst.} - R^1_{add.}$

$$= (CO°/2 - 0.24 - 0.266) = 8.20 \ \mu\text{moles} \qquad [5]$$

If P^1 = recovery of CH_3SSCH_3 from $S(^1D_2)$ atom addition, and

P^3 = " " " " $S(^3P)$ " " ,

and assuming that P^1 and P^3 are pressure independent above 300 torr:

$$CH_3SSCH_3 \text{ observed} = R^1_{add.} \times P^1 + R^3_{add.} \times P^3 \qquad [6]$$

Using Table IV-3 and eqns. [4] and [5], [6] becomes:

$$0.596 = 0.263P^1 + 8.20P^3 \qquad [7]$$

(ii) for the 30 minute photolysis of the mixtures COS/CH_3SCH_3= 300/30 and $COS/CH_3SCH_3/CO_2$ = 100/10/770.

Using similar procedures as above and data from Table IV-1 and IV-3, two equations analogous to [7] can be written for each mixture, respectively:

$$1.09 = 3.05P^1 + 4.89P^3 \qquad [8]$$

$$0.667 = 0.576P^1 + 7.60P^3 \qquad [9]$$

Solving equations [7] and [8] yields,

$$P^1 = 0.255 \text{ and } P^3 = 0.064$$

and from equations [8] and [9], it follows that,

$$P^1 = 0.248 \text{ and } P^3 = 0.069$$

Averaging these values gives,

$$P^1 = \underline{0.252} \text{ and } P^3 = \underline{0.067}$$

Hence the recoveries of CH_3SSCH_3 from $S(^1D_2)$ and $S(^3P)$ atom additions at pressures above 300 torr are:

∿ 25% and ∿ 7%, respectively.

C) Recoveries of C_2H_6 from $S(^1D_2)$ and $S(^3P)$ atom reactions.

Similarly, assuming that each DMTSO produces 1 molecule of C_2H_6, the recoveries of C_2H_6 from $S(^1D_2)$ and $S(^3P)$ additions are calculated to be 1.0% and 1.4%, respectively, for the mixture $COS/CH_3SCH_3 = 300/30$.

D) Deactivation/isomerization ratio for $(S_0)^\dagger$ and T_1 DMTSO.

The data from the $COS/CH_3SCH_3 = 300/30$ mixture (Table IV-1) are used for this calculation and it is assumed that all the CH_3SSCH_3 observed comes from the isomerization of DMTSO. It was shown (see section A above) that:

$$R^1_{add.} = 3.04\ \mu\text{moles}.$$

Since $P^1_{CH_3SSCH_3} \sim 0.25$ and $P^1_{C_2H_6} \sim 0.010$, the isomerization yield is $3.04 \times 0.25 = \underline{0.759\ \mu\text{mole}}$,

and the fragmentation yield is

$$3.04 \times 0.010 = \underline{0.030\ \mu\text{mole}}.$$

Hence the yield of deactivated DMTSO is

$$= 3.04 - 0.759 - 0.030 = \underline{2.25\ \mu\text{moles}}.$$

Therefore, $(\text{deactivation/isomerization})^1 = 2.24/0.759\ \underline{\sim 3}$,

and for $S(^3P)$ addition, similar procedures yield:

$$(\text{deactivation/isomerization})^3\ \underline{\sim 14}.$$

(II) The $S(^1D_2, {}^3P) + \overline{CH_2(CH_2)_2S}$ System.

Using the data from Table IV-12 and the procedures described above, three equations can be written for the three mixtures: $COS/\overline{CH_2(CH_2)_2S} = 100/2.8$, $COS/CH_2(CH_2)_2S/CO_2 = 100/2.8/600; 1200$. Since the $S + \overline{CH_2(CH_2)_2S}$ reaction is pressure independent, the product recoveries from $S(^1D_2)$ and $S(^3P)$ precursors should also be pressure independent.

Thus, let P^3 = recovery of 1,2-dithiolane from $S(^1D_2)$ addition,

P^1 = " " " " $S(^3P)$ "

the three equations are:

$$0.620 = 0.600P^1 + 1.01P^3 \qquad [11]$$

$$0.717 = 0.145P^1 + 1.91P^3 \qquad [12]$$

$$0.801 = 0.031P^1 + 2.13P^3 \qquad [13]$$

Solving [11] and [12] gives $P^1 = 0.459$, $P^3 = 0.342$

" [11] and [13] gives $P^1 = 0.411$, $P^3 = 0.369$

Averaging these two sets of values yields $P^1 = \underline{0.435}$ and $P^3 = \underline{0.356}$. Thus the recoveries of 1,2-dithiolane from $S(^1D_2)$ and $S(^3P)$ additions are:

$\underline{\sim 44\%}$ and $\underline{\sim 36\%}$, respectively.

Similarly, let E^3 = recovery of C_2H_4 from $S(^1D_2)$ addition,

E^1 = " " " $S(^3P)$ "

the three equations for C_2H_4 recoveries are:

$$0.383 = 0.600E^1 + 1.01E^3 \qquad [14]$$

$$0.064 = 0.145E^1 + 1.91E^3 \qquad [15]$$

$$0.107 = 0.031E^1 + 2.13E^3 \qquad [16]$$

Solving [14] and [15] gives $E^1 = 0.667$, $E^3 = -0.019$
As $E^3 < 0$ is clearly unrealistic, these values of E^1 and E^3 are discarded. However, solving [14] and [16] gives:

$$E^1 = 0.566, \; E^3 = 0.043$$

Thus the recoveries of C_2H_4 from $S(^1D_2)$ and $S(^3P)$ additions are:

$\underline{\sim 57\%}$ and $\underline{\sim 4\%}$, respectively.

Assuming that all the 1,2-dithiolane observed comes from isomerization, and that C_2H_4 comes from fragmentation of the TTSO, the deactivation/isomerization ratios are calculated to be(see Section D above):

$$(\text{deactivation/isomerization})^1 \; \underline{\sim 0}$$

$$(\text{deactivation/isomerization})^3 \; \underline{\sim 1.7}$$

It should be emphasized that the above calculations may be subject to considerable uncertainty due to errors in measurement and S product instabilities, and hence the values obtained are approximations only.

APPENDIX D

The Role of CO_2 in the COS-CO_2 System.

It has been observed that when COS is photolyzed in the presence of CO_2, the rate of CO formation (R_{CO}) decreases with increasing CO_2 pressure. The following steps can be postulated:

$$
\begin{array}{lcll}
COS + h\nu & \longrightarrow & COS^{*} & [Ia] \\
COS^{*} & \longrightarrow & CO + S(^{1}D_{2},\ ^{3}P) & [1a] \\
COS^{*} + CO_2 & \longrightarrow & COS + CO_2 & [1b] \\
S(^{1}D_{2}) + CO_2 & \longrightarrow & S(^{3}P) + CO_2 & [2] \\
S(^{3}P) + COS & \longrightarrow & CO + S_2 & [3] \\
S(^{3}P) + S(^{3}P) & \xrightarrow{CO_2} & S_2 + CO_2 & [4]
\end{array}
$$

From this scheme, it is clear that there are two possible ways that CO_2 can decrease the CO yield. It can quench the excited COS formed in the primary step ([1b]), thus decreasing the amount of S atoms formed in step [1a]. Alternatively, CO_2 can act as a third body chaperon for the recombination of $S(^{3}P)$ atoms as shown in step [4].

The relative importance of these two reactions (steps [1b] and [4]) can be determined by measuring the CO yield in the presence of CO_2 and a reactive alkene. The possible occurrence of step [4] does not affect the S atoms produced in the primary step, [1a]. Thus, if it takes place, then in the presence of sufficient quantities of $(CH_3)_2C{=}CH_2$ to

scavenge the $S(^3P)$ atoms, R_{CO} should drop to exactly half the rate obtained when pure COS is photolyzed. On the other hand, if step [1b] is important, the CO yield should drop to half the value when COS is photolyzed in the presence of CO_2.

The CO yields (in μmoles) obtained from 4 minute photolyses of COS (100 torr), COS/CO_2 = 100/1300 and $COS/CO_2/(CH_3)_2C{=}CH_2$ = 100/1300/20 and 50 torr mixtures are shown below. The values in brackets represent the half yields of CO.

COS	COS/CO_2	$COS/CO_2/(CH_3)_2C{=}CH_2$
2.55 (1.28)	2.38 (1.19)	1.36 [a]
2.55 (1.28)	2.49 (1.25)	1.37 [a]
2.56 (1.28)	2.46 (1.23)	1.37 [a]
2.59 (1.30)	2.49 (1.25)	1.30 [b]
2.58 (1.29)	2.48 (1.24)	1.46 [b]
2.49 (1.25)	2.50 (1.25)	1.29 [b]
2.58 (1.29)	2.42 (1.21)	1.25 [b]
2.57 (1.29)	2.41 (1.21)	1.32 [b]
2.49 (1.25)	2.38 (1.19)	1.24 [b]

[a] $P(iso\text{-}C_4H_8)$ = 20 torr.

[b] $P(iso\text{-}C_4H_8)$ = 50 torr.

It is apparent that 50 torr $(CH_3)_2C{=}CH_2$ are required in order to completely scavenge the $S(^3P)$ atoms. Although there is some scatter in the data, the CO yields from the $COS/CO_2/C_4H_8$ mixtures in general , are closer to the half CO values of the pure COS photolyses than to those from the

COS/CO_2 experiments. Thus, it is concluded that the role of CO_2 in decreasing the CO yields from the photolysis of pure COS is to act as a third body energy sink for the recombination of $S(^3P)$ atoms.

The Intermediacy of $S(^3P)$ Atoms in the Photolysis of Thiirane.

In preliminary studies, it was observed that photolysis of thiirane in its first long wavelength absorption band ($\lambda \approx$ 240 nm) led to the formation of C_2H_4 (~90%) along with small amounts of H_2, CH_4 and C_2H_2.[3] $S_2(^3\Sigma_g^-)$ was detected in flash photolysis experiments. Scavenging experiments with added alkenes showed that $S(^1D_2)$ atoms were not formed. The following steps for the photolysis were considered:

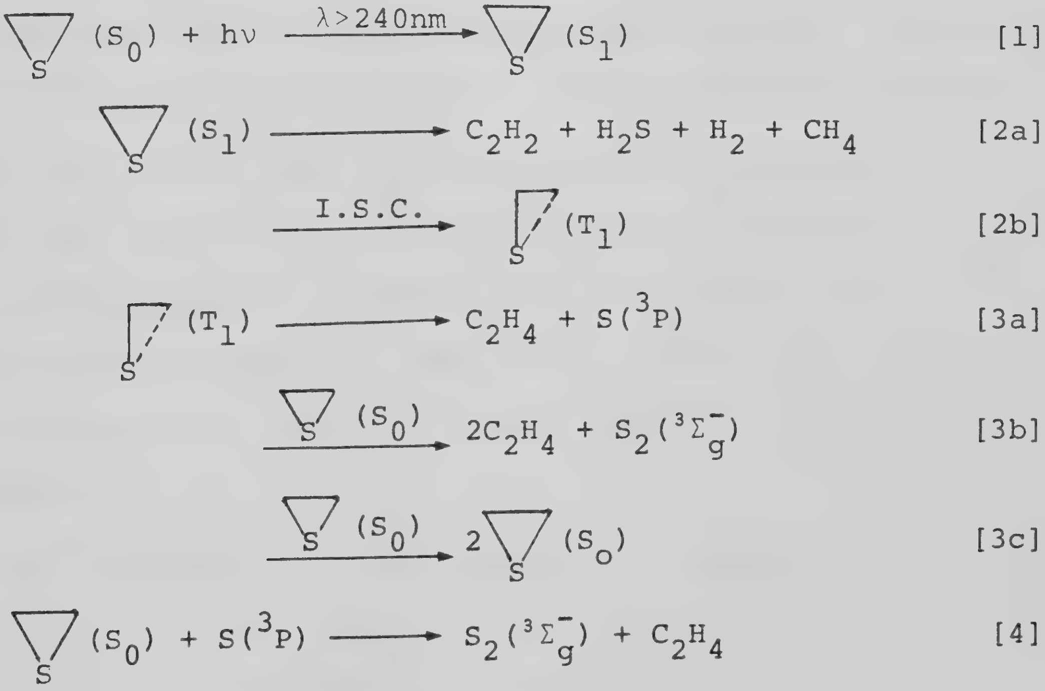
S
(S_0) + hν
λ>240nm
(S_1)
[1]
(S_1)
$C_2H_2 + H_2S + H_2 + CH_4$
[2a]
I.S.C.
(T_1)
[2b]
(T_1)
$C_2H_4 + S(^3P)$
[3a]
(S_0)
$2C_2H_4 + S_2(^3\Sigma_g^-)$
[3b]
(S_0)
2
(S_0)
[3c]
(S_0) + $S(^3P)$
$S_2(^3\Sigma_g^-) + C_2H_4$
[4]

In the presence of alkenes however, the C_2H_4 yields were suppressed and very small quantities of the thiirane analogue of the alkene, along with a terminal alkene corresponding to a C_2H_4 + alkane adduct were detected. These observations can be rationalized in terms of the following reactions, with

the example of 1-butene:

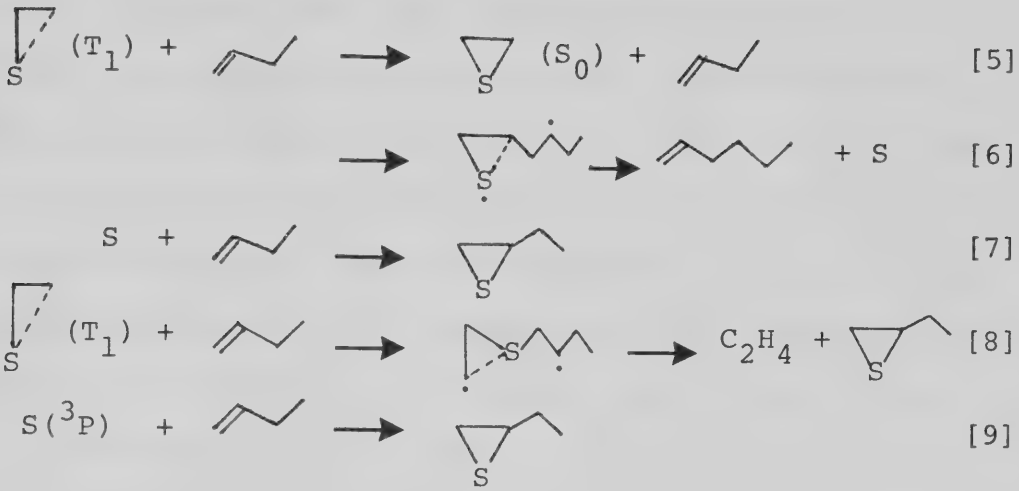

The secondary thiirane yields were several orders of magnitude less than the amount of C_2H_4 suppressed and slowly increased with increasing alkene pressure, up to ~1000 torr. Although kinetic and mechanistic arguments could be presented to the effect that the bulk of the secondary thiirane was formed in a sulfur atom transfer reaction, step [8], and not from $S(^3P)$ precursors via step [3a], more direct evidence was required to prove conclusively that $S(^3P)$ atoms are not produced in the photolysis.

The technique of flash photolysis - vacuum UV absorption spectroscopy has been used to study the kinetics of $S(^3P)$ atom reactions, by monitoring the decay of the $S(^3P_2 \rightarrow {}^3S_1)$ resonance line at 180.7 nm.[53] Thus this technique allows the unambiguous detection of any $S(^3P)$ atoms present in the photolysis of thiirane.

The flash apparatus has been described previously.[53] It consisted of quartz reaction cell (20 cm long and 2.0 cm I.D.)

with LiF and suprasil windows, positioned parallel to the limbs of a U shaped flash lamp inside a thermostated aluminum lined oven housing. An aperture at each end of the housing allowed passage of light from the flash spectroscopic lamp at one end, to the vacuum UV spectrograph at the other. The flash and spectroscopic lamps were operated at 13.5 and 9.5 kV, respectively. 0.7 Torr thiirane was flash photolyzed in the presence of 200 torr CO_2 diluent. Spectra were taken using a spectroscopic slit width of 10 μ.

With a 2mm Vycor 791 filter around the cell body ($\lambda > 230$ nm), the spectra showed no trace of the $S(^3P)$ absorption line. However, in the absence of the filter ($\lambda > 180$ nm), the $S(^3P)$ resonance line was observed, indicating that $S(^3P)$ atoms are produced in the short wavelength photolysis of thiirane.

Based on this observation and the results from conventional studies, it can be concluded that the main process in photolysis of thiirane at long wavelength ($\lambda > 230$ nm) is intersystem crossing of the initially formed (S_1) state thiirane to the lowest excited triplet (T_1) state followed by bimolecular reactions with ground state molecules leading either to deactivation or to the formation of $C_2H_4 + S_2(^3\Sigma_g^-)$, that is, steps [1] - [2] and [3b] - [3c].

The absence of $S(^3P)$ atoms in the long wavelength photolysis may be ascribed to the endothermicity of step [3a] (ΔH $\sim$20 kcal mole^{-1}). Shorter wavelength ($\lambda > 180$ nm) photolysis confers an extra 40 kcal mole^{-1} internal energy to the molecule, thus overcoming the energy requirement of reaction

[3a].

Mechanistic details of the long wavelength photolysis of thiirane are given in the accompanying reprint which follows.

Reprinted from The Journal of Physical Chemistry, **1981**, *85*, 1089.
Copyright © 1981 by the American Chemical Society and reprinted by permission of the copyright owner.

Detection and Properties of Triplet State Thiiranes

E. M. Lown, K. S. Sidhu,[1] A. W. Jackson,[2] A. Jodhan, M. Green, and O. P. Strausz*

Department of Chemistry, University of Alberta, Edmonton, Alberta, Canada T6G 2G2 *(Received: April 11, 1980; In Final Form: September 8, 1980)*

The major primary step in the long wavelength ($\lambda > 240$ nm) photolysis of thiirane is intersystem crossing to the lowest excited triplet (T_1) state with a quantum yield of ~0.86. Triplet thiirane has a long radiative lifetime, is highly resistant to collisional deactivation, and is capable of undergoing reversible addition to alkenes and thereby inducing their geometrical isomerization. Inefficient irreversible addition also occurs. This provides a novel example of an excited triplet molecular sensitization not involving energy transfer. Thiirane T_1 has a cyclic structure which is retained in the alkene adduct and shows strong diradical character.

Triplet state thiiranes have been postulated to be the primary adducts in the addition reactions of ground (^3P) sulfur atoms to alkenes[3] on the basis of MO calculations[4] and by analogy with the $O(^3P)$ + alkene reactions.[5] The T_1 state of thiiranes has also been implicated in the low-temperature thermolysis of thiirane, methylthiirane, and dimethylthiirane.[6] We now report evidence for the involvement of the same T_1 state in the direct and triplet-sensitized photolysis of thiirane as well, and to describe the unusual chemistry of these excited thiirane molecules.

Photolysis in the first long wavelength absorption band of thiirane ($\lambda_{max} \sim 260$ nm)[7] leads to the formation of C_2H_4 (~90%) and small amounts of H_2S, C_2H_2, H_2, and CH_4. $\phi(C_2H_4) = 1.3$ at $\lambda > 240$ nm and is independent of pressure up to 200 torr, but decreases with increasing wavelength of photolysis. In order to test for the intermediacy of sulfur atoms in the decomposition, we flash photolyzed 0.6 torr of thiirane in 200 torr of CO_2. The atomic absorption line at 180.7 nm corresponding to the $S(^3P_2) \rightarrow S(^3S_1)$ resonance absorption was visible when unfiltered ($\lambda > 180$ nm) radiation was used, but was not detected when the photolyzing radiation was limited to $\lambda > 240$ nm. This result corroborated the negative results obtained in chemical-scavenging experiments using an alkane or an alkene to intercept atomic sulfur. It is therefore concluded that sulfur atoms are not involved in

---

[1] Department of Chemistry, Punjabi University, Patiala, India.

[2] Chemical Research Department, Ontario Hydro Research Division, 800 Kipling Ave, Toronto, Ontario, M8Z 5S4.

[3] O. P. Strausz, *Pure Appl. Chem.*, **4**, 165 (1971).

[4] O. P. Strausz, R. K. Gosavi, A. Denes, and I. G. Csizmadia, *Theor. Chim. Acta*, **26**, 367 (1972); O. P. Strausz, H. E. Gunning, A. Denes, and I. G. Csizmadia, *J. Am. Chem. Soc.*, **94**, 8317 (1972); R. Hoffman, C. C. Wan, and V. Neagu, *Mol. Phys.*, **19**, 113 (1970).

[5] R. J. Cvetanovic, *Adv. Photochem.*, 1, 115 (1963).

[6] E. M. Lown, H. S. Sandhu, H. E. Gunning, and O. P. Strausz, *J. Am. Chem. Soc.*, **90**, 7164 (1968).

[7] R. E. Davis, *J. Org. Chem.*, **23**, 1380 (1958).

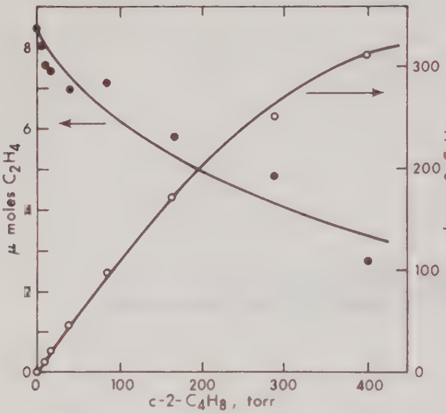

igure 1. Yields of C_2H_4 and *trans*-2-C_4H_8 as a function of *cis*-2-utene pressure from the λ > 240-nm photolysis of 100 torr of thiirane.

he λ > 240-nm photolysis of thiirane.

Added alkanes, e.g., 300 torr of propane to 11 torr of hiirane, have no observable effect on the photolysis. dded alkenes, however, exert a suppressing effect on the ield of C_2H_4 and when *cis*-2-butene is used, geometrical somerization takes place, and *trans*-butene forms in high ields (Figure 1).[8] At 400 torr of *cis*-butene pressure the $_2H_4$ yield decreases by more than half and for each C_2H_4 roduced more than a hundred molecules of *cis*-butene are somerized, giving a quantum yield for *trans*-butene forhation of ~50. Thus it is clear that isomerization does ot take place as a result of energy transfer, but via reersible addition of an intermediate. For this there are nly two candidates, excited triplet thiirane or the sulfur adicals S_2–S_7; however, when triplet thiirane is produced ithout sulfur radicals via the addition of $S(^3P)$ atoms from he photolysis of COS in the presence of CO_2 and *cis*-utene, isomerization of *cis*-butene still occurs with comarable yields. Triplet state thiirane, generated by the riplet benzene or biacetyl sensitization of thiirane, also nduces isomerization of *cis*-butene although the yields of *rans*-butene are smaller in the latter system. Therefore, he agent responsible for isomerization in the direct phoolysis must be triplet state thiirane.

The major steps required for the interpretation of the ong wavelength photolysis of thiirane are as follows:

$$C_2H_4S(S_0) + h\nu \rightarrow C_2H_4S(S_1) \qquad (1)$$

$$C_2H_4S(S_1) \rightarrow C_2H_2,\ H_2S,\ H_2,\ CH_4 \qquad \phi \sim 0.14 \quad (2)$$

$$C_2H_4S(S_1) \rightarrow C_2H_4S(T_1) \qquad \phi \sim 0.86 \qquad (3)$$

$$_2H_4S(T_1) + C_2H_4S(S_0) \rightarrow S_2 + 2C_2H_4 \qquad \phi \sim 0.65 \quad (4)$$

$$_2H_4S(T_1) + C_2H_4S(S_0) \rightarrow 2C_2H_4S(S_0) \qquad \phi \sim 0.21 \quad (5)$$

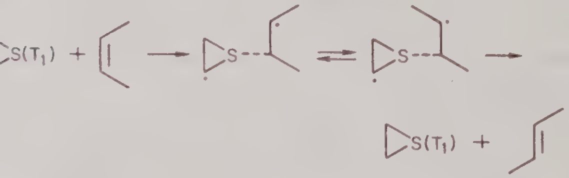

(6)

The effects of added alkenes were examined in detail or the cases of C_3H_6, 1-C_4H_8, and 1-C_5H_{10}. In general, the $_2H_4$ yields decline slowly with increasing alkene pressure nd two additional products are formed in small yields: he thiirane analogue of the alkene, and a terminal alkene corresponding to a C_2H_4 + alkene adduct. The yields of these products are given in Figure 2 for the case of 1-butene. It thus appears that T_1 thiirane can also undergo a nonreversible addition, albeit inefficiently, with the alkene:

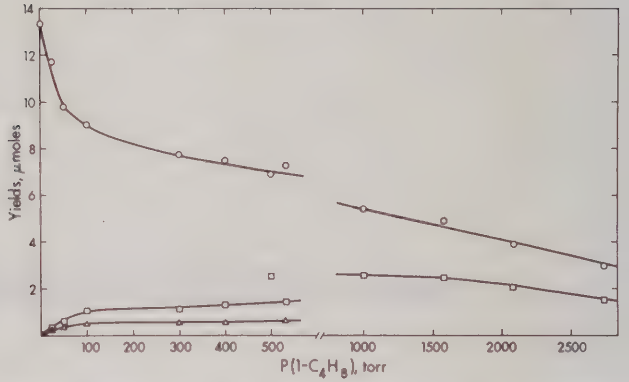

Figure 2. Yields of C_2H_4 (○), C_4H_8S (□), and 1-C_6H_{12} (Δ) as a function of 1-C_4H_8 pressure from the λ > 240-nm photolysis of 12 torr of thiirane.

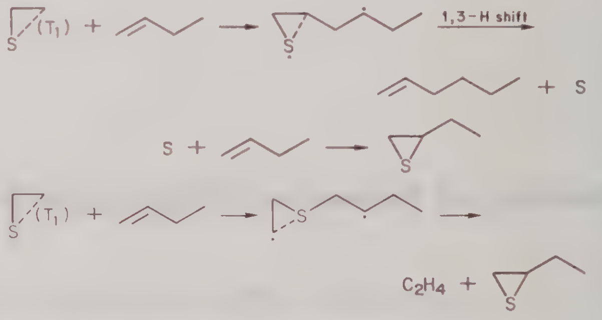

(7)

(8)

(9)

Further evidence in support of the occurrence of steps 7–9 comes from the isotopic distribution of products from the photolysis of C_2D_4S in the presence of 1-C_4H_8, giving C_4H_8S and partially deuterated 1-hexene. The fact that the thiirane yield is about twice that of the alkene indicates that the carbon and sulfur radical sites in $C_2H_4S(T_1)$ are equally reactive.

It has been shown[1] that the addition of $S(^3P)$ atoms to olefins follows a stereoselective reaction path. Moreover, photolysis of *trans*- and *cis*-2,3-dimethylthiirane afforded ~95% *trans*- and *cis*-butene, respectively. Therefore the T_1 state must be cyclic. Indeed, MO calculations[4] predict a ring distorted equilibrium conformation for the T_1 state with a bond strength of ~24 kcal/mol for the stretched C–S bond and a value of ~40 kcal/mol for the excitation energy of the $^3(n,\sigma^*)T_1$ state. From this we conclude that the ring distorted equilibrium conformation of thiirane (T_1) is maintained in the alkene adduct, as indicated in eq 7 and 9. This is also in line with the reversible nature of the addition, since if an open triplet diradical structure $\cdot CH_2$–CH_2–$S\cdot$ were involved the addition would not be expected to be reversible at pressures of several hundred torr.

Small quantities of NO were found to quench efficiently the isomerization of *cis*-butene. Ethylene formation from the photolysis of pure thiirane is also suppressed to a limiting yield of $\phi \sim 0.86$ at a fourfold excess of NO, in agreement with the primary quantum yield of thiirane (T_1) and suggesting the following overall reaction:

$$C_2H_4S(T_1) + NO \xrightarrow{NO} C_2H_4 + SO_2 + N_2$$

---

(8) Isomerization of 2-butene upon photolysis of COS/2-butene mi

The results presented here are of significance for two reasons. First, they shed light on the triplet state chemistry of thiirane for which information is sparse, as is the case with three-membered ring compounds in general. Second, they represent a unique example of geometrical isomerization of an olefin induced by an electronically excited molecule, but without energy transfer. For this type of sensitization the sensitizer should have the following properties: (a) a long radiative lifetime, (b) resistance against collisional deactivation, (c) an excitation energy lower than the nonvertical triplet energy of the olefin, and (d) the ability to form a partial but not a full covalent bond with unsaturated carbon centers. At present, few molecules may be imagined which would fulfill these conditions.

Acknowledgment. We thank the Natural Sciences and Engineering Research Council of Canada for continuing financial support.

B30372